Strål säkerhets myndigheten

2017:30

SSM's external experts' review of SKB's safety assessment SR-PSU – consequence analysis

Main review phase

SSM perspective

Background
The Swedish Radiation Safety Authority (SSM) received an application for the expansion of SKB's final repository for low and intermediate level waste at Forsmark (SFR) on the 19 December 2014. SSM is tasked with the review of the application and will issue a statement to the government who will decide on the matter. An important part of the application is SKB's assessment of the long-term safety of the repository, which is documented in the safety analysis named SR-PSU.

Present report compiles results from SSM's external experts' reviews of SR-PSU during the main review phase. The general objective of these reviews has been to give support to SSM's assessment of the license application. More specifically, the instructions to the external experts have been to make an in depth assessment of the specific issues defined for the different disciplines.

Project information
Contact person SSM: Georg Lindgren

Table of Contents

2017:30

SSM's external experts' review of SKB's safety assessment SR-PSU – consequence analysis

Main review phase

Authors: George Towler and James Penfold[1]
[1]Quintessa Limited, Henley on Thames, UK

SR-PSU Main Review Phase: Radionuclide Transport Modelling

Abstract

The Swedish Radiation Safety Authority (SSM) received an application for the expansion of SKB's final repository for low and intermediate level waste at Forsmark (SFR) on the 19 December 2014. SSM is tasked with the review of the application and will issue a statement to the government who will decide on the matter. An important part of the application is SKB's assessment of the long-term safety of the repository, which is documented in the safety analysis named SR-PSU.

SSM's review is divided into an initial review phase and a main review phase. This assignment contributes to the main review phase. It involves re-implementing SKB's radionuclide transport models for two of SFR's vaults (1BMA and 2BMA), and the geosphere, in a suitable compartmental modelling code; and then comparing the results with the results of SKB's models.

The comparison exercise was undertaken using information and data from SKB's SR-PSU reports; additional information provided by SKB at a meeting between SKB, SSM and supporting consultants held on 28th April 2016; and SKB's model input and data files, which were supplied in October 2016. SKB implemented their models using the ECOLEGO code. The models developed as part of the comparison exercise were implemented using the AMBER code. The findings of the model comparison exercise are summarised as follows.

SKB have built a detailed and complex model of radionuclide transport through the 1 BMA and 2BMA vaults into the geosphere. SKB have put significant effort into representing the detailed geometry of the near-field, spatial variations in near-field flows, and evolution of the system in response to environmental change and barrier degradation. SKB's reports provide a high level description of the models, which enable the configuration to be broadly understood or deduced. However, description of the representation of the different waste package types in the models could be improved, and some aspects of the model configuration are not described, for example how the waste packages and caissons have been discretised.

The models use a large amount of data. Most of these data are provided in SKB's reports, but not all; for example the properties of the waste packages (porosity, density, effective diffusivity, etc) and the detailed flows through the vaults are not presented. (The latter were provided in spreadsheets by SKB). A potentially significant observation is that 2384 steel drums containing cement embedded wastes are planned for disposal in the 2BMA vault, but no inventory is assigned to these drums in SR-PSU. This means that the inventory of 2BMA could be under estimated, and consequently so could the flux of radionuclides released from the vault.

SKB have not described and justified how key aspects of the model have been parameterised, where the parameter values are derived from the underpinning data. This includes important parameters such as cross-sectional areas and distances used to calculate diffusive transfers.

Although SKB's documentation of the model and data could be improved we have built a model in AMBER that broadly reproduces the results of SKB's ECOLEGO model for the 2BMA vault. This helps to build confidence in SKB's assessment calculations for SR-PSU. However, the differences are such that SSM might wish to consider further work to investigate these differences in more detail.

SKB's geosphere model also contains a large number of compartments, but it is less complex than the models of the vaults, and documentation of the model is more complete and transparent. We have built a simpler version of the model which reproduces SKB's results,

with only small differences that can be attributed to the coarser discretisation of the AMBER model compared with the ECOLEGO model.

Due to the complexity of SKB's models, and limitations in their documentation, it was not possible to undertake the high level comparison exercise for 1BMA that was originally planned by SSM. Instead efforts focussed on analysing a range of base case model results, and results from variant cases, to help understand the behaviour of the 2BMA vault model, and the reasons for differences in the fluxes calculated by the AMBER and ECOLEGO models. The key areas for further investigation have been successfully identified and are described in the conclusions section of this report. Once this further investigation has been completed, it should be relatively efficient to use the AMBER model to further explore the radionuclide transport behaviour, including undertaking a high level comparison exercise for 1BMA.

During the initial review phase, we undertook a high-level assessment of SKB's identification of FEPs and their treatment in the assessment. We identified the key FEPs and associated uncertainties that are most significant for potential impacts are the radionuclide inventory and FEPs relating to the performance and degradation of the near-field engineered barriers. It was noted that understanding the coupled processes leading to degradation of the engineered barriers, the rate and timing of degradation, and selection of parameters to represent these processes in models are important. These issues are being considered by other technical areas within this main review phase. Nevertheless, the results of this modelling exercise further highlight the importance of these issues.

Further analysis of SKB's identification and treatment of FEPs, in the context of radionuclide transport, was undertaken as part of this main review phase. Given the knowledge gained during the initial review phase, and during the review of the initial state and process reports, the FEPs represented explicitly in the radionuclide transport models were found to be consistent with expectations. The FEPs represented explicitly are also broadly consistent with safety assessments undertaken for similar facilities, and have been represented using appropriate mathematical models. No omissions of further issues were identified beyond those raised by the initial review and the subsequent further analysis of SKB's identification and treatment of FEPs.

Contents

1 Introduction

The Swedish Radiation Safety Authority (SSM) has received an application for the expansion of SKB's final repository for low and intermediate level waste at Forsmark (SFR) on the 19 December 2014. SSM is tasked with the review of the application and will issue a statement to the government who will decide on the matter. An important part of the application is SKB's assessment of the long-term safety of the repository, which is documented in the safety analysis named SR-PSU.

SSM's review is divided into an initial review phase and a main review phase. This assignment contributes to the main review phase. In the initial review phase, a number of specific topics for further in-depth review have been identified. The scope of those topics has been refined following SKB's provision of complementary information, requested by SSM during the initial review phase and discussed at a meeting between SSM, SKB and supporting consultants on the 28th April 2016.

SSM wish to further understand and build confidence in the radionuclide transport calculations undertaken by SKB. To achieve this, SSM have identified four tasks.

1. To re-implement SKB's radionuclide transport model for the 2BMA vault in a suitable compartmental modelling code. The model should use the same compartmental configuration as SKB's model. The focus should be on review of the configuration of the assessment model to represent the conceptual model, linked to the choice of parameterisation. The model results should be compared to SKB's results to build confidence that they are reasonable and to confirm there are no significantly anomalous behaviours. However, the aim is not to exactly reproduce SKB's results. The model will also be used to test sensitivity of the results to the number of realisations and numerical seed, to build confidence that the number of realisations used by SKB should result in model convergence.

2. The geosphere is to be added to the near-field model developed in (1). Again the focus should be on review of the configuration of the assessment model to represent the conceptual model, linked to the choice of parameterisation. The model results should be compared to SKB's results to build confidence that they are reasonable and to confirm there are no significantly anomalous behaviours. However, the aim is not to exactly reproduce SKB's results. The model will also be used to test sensitivity of the results to the number of realisations and numerical seed, to build confidence that the number of realisations used by SKB should result in model convergence.

3. The model developed in (1) should be used to build confidence in SKB's results for the 1BMA vaults. This will be achieved by changing the inventory and flows for those in 1BMA. SKB's models for 1BMA and 2BMA have different compartmental configurations. Therefore, some pre-processing of the flows may be required and the model is not expected to exactly reproduce SKB's results. However, the model results should still be sufficient to highlight any potential issues for discussion with SKB.

4. The model developed in the previous steps should be used to test sensitivity of the results to any potentially important alternative assumptions that are identified during the course of the review.

Approach

The tasks specified by SSM have been undertaken by re-implementing SKB's models in Version 6.0 of the AMBER code (Quintessa, 2016). The configuration and parameterisation of

the AMBER models is described in Sections 2 and 3 of this report, with reference to the SKB reports that describe the SR-PSU models, which were implemented using the ECOLEGO code. Section 4 describes the calculation cases that have been assessed using the AMBER model, and any calculation case specific data. Section 5 describes SKB's results and compares these to the AMBER model results. Important assumptions and limitations to be noted by SSM are highlighted, as are any differences in the model results that may be important for safety. Section 6 concludes on the overall findings of the work.

During the initial review stage it was identified that some of information required to undertake these tasks is not directly available from SKB's reports. Further information and clarifications were provided by SKB during the meeting of 28th April 2016, and a general information request was also issued to SKB following the meeting. In response, part way through this main review phase, some additional data was provided by SKB including ECOLEGO model files and associated data input files in MS Excel. The ECOLEGO model and input data files have been used to fill some key information gaps. However, due to the size and complexity of the models, it was not practicable to compare and contrast every aspect of the configuration and parameterisation of the AMBER and ECOLEGO models.

2 Near-Field Model for 2BMA Vault

2.1 Model Configuration

2.1.1 Wastes

The 2BMA vault contains the following waste packages:

- Cement solidified wastes in concrete moulds.
- Concrete embedded wastes in concrete moulds.
- Cement solidified wastes in steel moulds.
- Concrete embedded wastes in steel moulds.
- Concrete embedded wastes in steel drums.

The numbers of waste packages associated with each waste stream is described in Appendix A of TR-14-02. This has been used to calculate the number of packages of each type in 2BMA (Table 1). It is noted that tetramoulds are included under steel moulds (p197 in TR-14-09).

Table 1. Number of waste packages in 2BMA

Package Type	Number
Cement solidified wastes in concrete moulds	192
Concrete embedded wastes in concrete moulds	967
Cement solidified wastes in steel moulds	68
Concrete embedded wastes in steel moulds	2225
Concrete embedded wastes in steel drums	2384

Section 9.3.10 in TR-14-09 describes the configuration of the near-field model to represent the different waste packages (Table 2). It is noted that no account is taken of the barrier provided

by the steel containers. This is likely to be a cautious assumption because the containers will be a barrier to release of radionuclides until they become significantly perforated by corrosion.

The associated waste streams have been identified from Appendix A in TR-14-02 and the descriptions of the waste given in Section 9.3.10 in TR-14-01. It is noted that Figure 9-8 in TR-14-09 shows there are no bitumen solidified / embedded wastes in 2BMA.

Table 2. Configuration of the near-field model to represent the different waste packages (Section 9.3.10 in TR-14-09)

Package	Representation	Waste Types
Cement-solidified or concrete embedded waste in concrete moulds	This model waste package is represented using three compartments, two for the interior with cement solidified or concrete embedded waste and one for the concrete mould.	Solidified R.29 Embedded C.23, O.23/O.23:9, S.23, S.23:D
Cement-solidified or concrete embedded waste in steel moulds	This model waste package is represented with two compartments for the interior with cement solidified or concrete embedded waste. The steel casing is not accounted for in the modelling.	Solidified R.15 Embedded B.23:D, B.23:D.sec, C.4K23:D, F.23, F.4K23:D, F.4K23C:D, O.4K23:D, O.4K23C:D, O.4K23S:D, R.23, R.23:D, R.4K23:D, R.4K23C:D, Å.4K23:D, Å.4K23C:D
Cement-solidified or concrete embedded waste in steel drums	This model waste package is represented with two compartments for the interior with cement conditioned waste, the steel casing is not accounted for in the modelling.	Solidified None Embedded S.25D

Figure 1 shows the configuration of the AMBER model to represent the different wastes packages, as described in Table 2. The waste compartments are coloured red. The mould compartment is coloured dark grey, and the compartment representing the grout surrounding the waste packages is coloured light grey. Transfers between the compartments are shown in white. Forwards and backwards transfers are used in each case in order to represent migration of radionuclides by diffusion and advection. (Representation of transport processes is described later).

The 2BMA vault contains 14 caissons. Figure 1 shows the model configuration used to represent the waste packages in one caisson, plus the surrounding grout. The same configuration is used to represent the waste packages in each of the other thirteen caissons. Therefore, a total of 6 x 14 = 84 compartments are required to represent the waste packages.

7
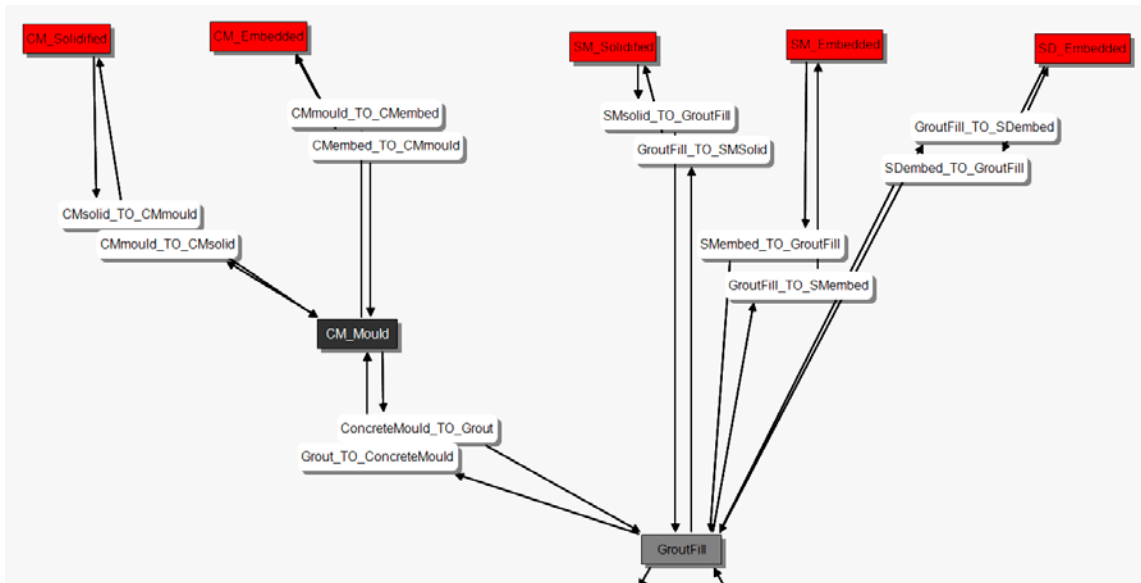
Figure 1. Configuration of the AMBER model to represent the different waste package types

During inspection of the ECOLEGO model files, it was identified that the configuration of the compartments used to represent the waste packages had been misunderstood from the description given in Section 9.3.1 of TR-14-09. In the ECOLEGO model, each package type is represented by two compartments: an inner waste compartment and an outer waste compartment. The concrete moulds associated with cement solidified waste and cement embedded wastes are represented separately. This is illustrated in Figure 2. Therefore, for each of the 14 caissons there are the following additional waste package compartments compared with the AMBER model:

- An additional waste compartment for each of the 5 package types.
- An additional compartment to represent the moulds associated with cement solidified and concrete embedded wastes separately.

Therefore there are an additional 6 x 14 = 84 waste package compartments compared with the AMBER model. It was decided not to include these additional compartments in the AMBER model, but instead test sensitivity of the calculated fluxes to the discretisation of the waste packages for one caisson as a variant calculation.
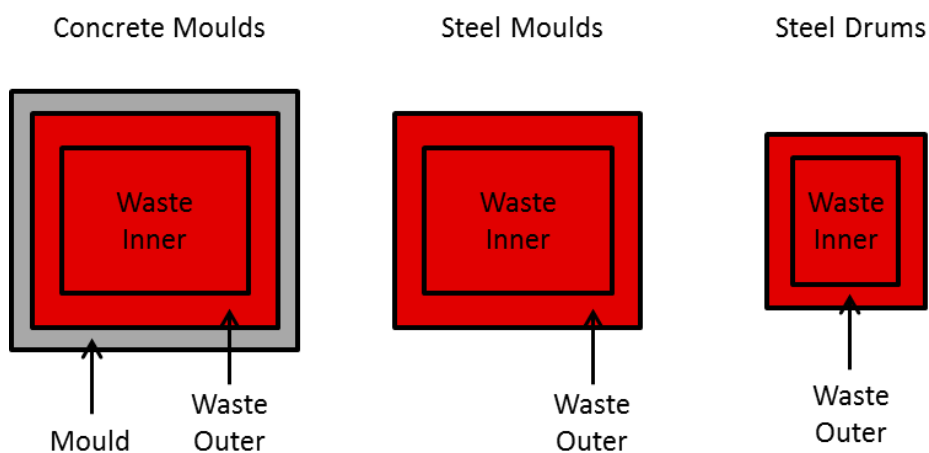
Figure 2. Configuration of compartments used to represent waste packages in ECOLEGO

8

2.1.2 Barriers

The 14 concrete caissons in the 2BMA vault are illustrated in Figure 3. Each caisson is surrounded by crushed rock backfill (macadam), including between the caissons. Macadam is also used to backfill the loading area (the right hand end of the vault in Figure 3) and the far end of vault (the left hand end of the vault in Figure 3). The waste packages are cement grouted into each concrete caisson.
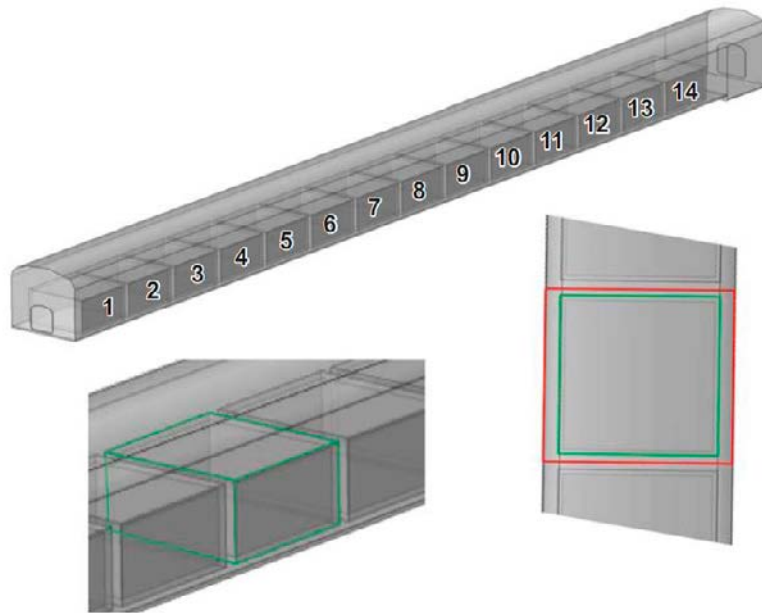
Figure 9-7. The division of 2BMA into control volumes in the hydrological model (Abarca et al. 2013). The green wire frame marks one of the cassions. The red wire frame in the plan view delimits one cassion and surrounding backfill as one of the 14 sections modelled in the RNT model.

Figure 3. 2BMA Vault (Figure 9-7 in TR-14-09)

Figure 4 shows the conceptual model for a single caisson. Radionuclides are transported out of the waste packages and through the near-field barriers by advection and diffusion. Transport from the macadam into fractures in the rock is only by advection.

9
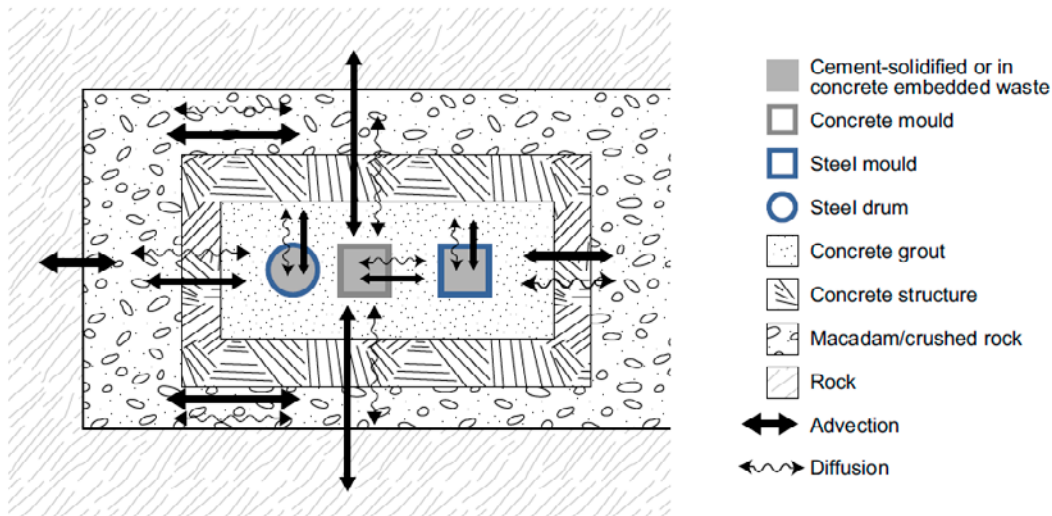
Figure 9-8. Conceptual model of 2BMA(the figure corresponds to one of the 14 modelled sections) in the radionuclide transport model. The figure shows the different types of model-waste packages used in the modelling of radionuclide transport. From the left: cement-solidified or concrete embedded waste in steel drums, cement-solidified or concrete embedded waste in concrete moulds, cement-solidified or concrete embedded waste in steel moulds (figure modified from Lindgren et al. 2001).

Figure 4. Conceptual model of the 2BMA vault (Figure 9-8 in TR-14-09)

Section 9.3.4 in TR-14-09 states that each caisson is represented separately in the radionuclide transport model. For each caisson, the model also includes a compartment for macadam backfill surrounding the caisson. The macadam backfill in the ends of the vaults is also represented by one compartment for each end. Section 9.3.2 in TR-14-09 notes, "*in the radionuclide transport model, all outer walls were represented by five compartments each*".

At the meeting on 28th April 2016, SKB clarified that in the 2BMA vault model the caissons are each represented by 5 radial compartments, whereas in 1BMA vault model, each wall of a caisson is subdivided into 5 compartments (i.e. a total of 30 compartments). The thickness of each of the five radial compartments used to represent the walls of the caisson is not described in the SR-PSU reports, so we have assumed each compartment represents the same thickness of concrete.

At the 28th April meeting SKB also noted that a single compartment is used to represent the rock surrounding the 2BMA vault. Inspection of the ECOLEGO model files clarified that the rock surrounding the vault is represented by the first compartment of the geosphere model for transport through fractures in the rock. There is no compartment representing the specific volume of rock surrounding the vault.

The configuration of the compartments representing the near-field barriers is shown in Figure 5. The implementation in AMBER is shown in Figure 6 for a single caisson. The same configuration is used for all 14 caissons. The colours of the compartments correspond to Figure 5, and transfers are shown in white. Forwards and backwards transfers are used to represent advection and diffusion of radionuclides through the near-field barriers, include transport along the length of the vault into the macadam surrounding adjacent caissons. There is only a single (forwards) transfer into rock, as only advection into the rock is represented in the model.
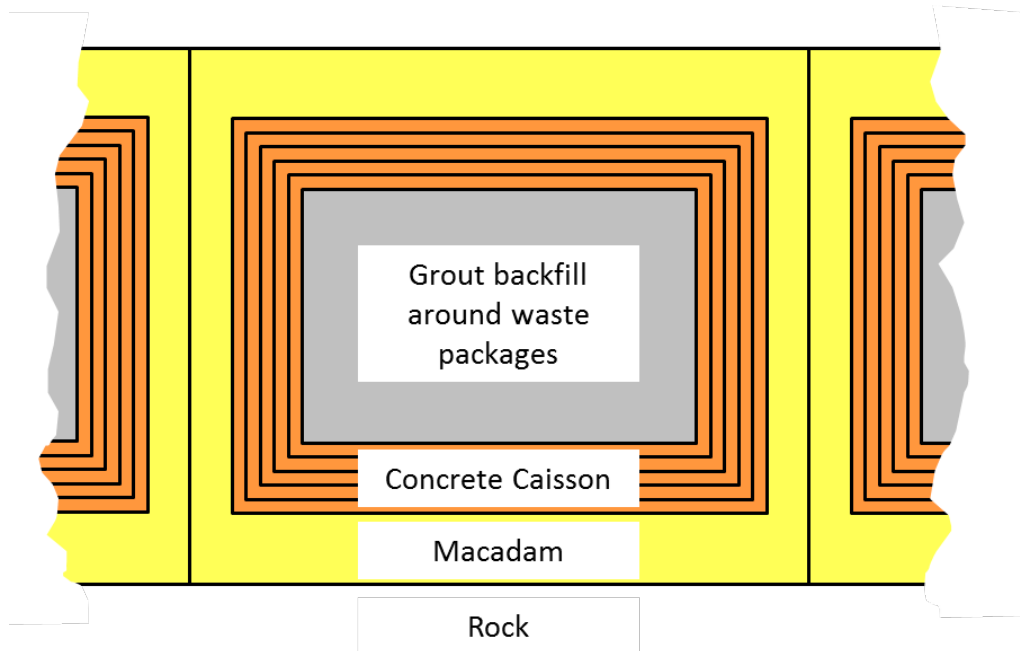
Figure 5. Configuration of compartments representing the near-field barriers
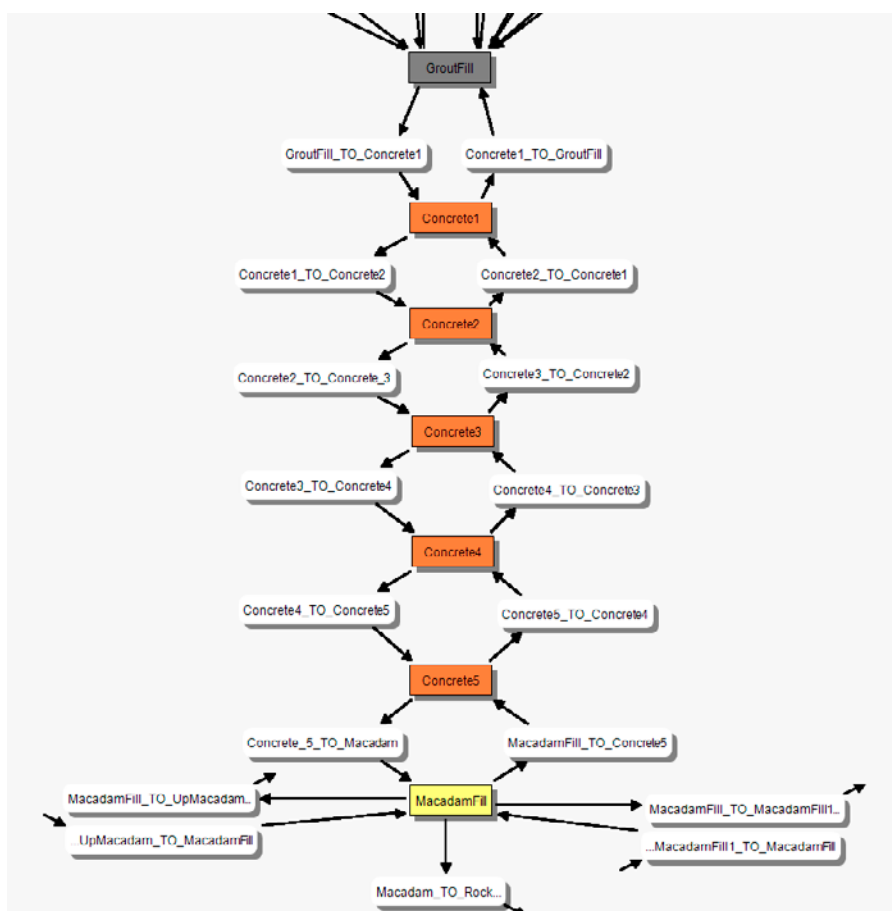
Figure 6. Configuration of the AMBER model to represent a single caisson

Figure 7 shows the configuration of the AMBER model to represent the 14 caissons and the macadam at the ends of the vaults. Transfers are used to represent advection and diffusion of radionuclides along the length of the vault, and advection into the rock. There is advection from the macadam associated with each caisson into the rock, and from the macadam at the ends of the vault into the rock. Therefore the model is able to represent transport parallel and perpendicular to the length of the vault. In total the 2BMA AMBER model comprises 198 compartments. The ECOLEGO model has an additional 84 compartments that provide a more detailed discretisation of the waste packages.

12
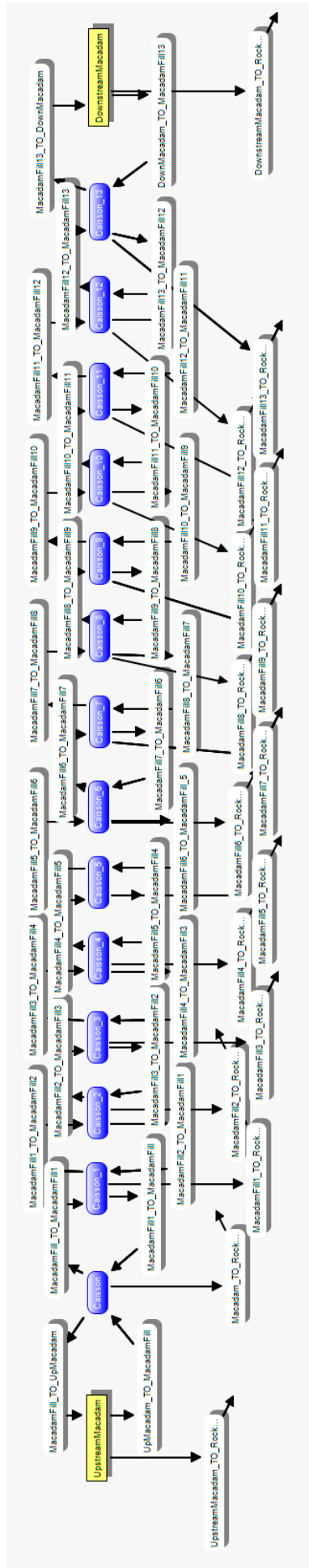
Figure 7. Configuration of the AMBER model to represent the 14 caissons (blue) and macadam at the ends of the vault (yellow)

Conceptually the AMBER model is orientated with the x direction parallel to the long-axis of the vault, and the y direction (sideways) and z direction (vertical) perpendicular to the long-axis of the vault. Given the radial geometry of the compartments used to represent the caissons and macadam, the vault was considered to be symmetrical about the x-z and x-y planes.

Due to the radial configuration, only a single set of transfers is required to represent transport from the waste packages, to the grout, through the caisson and into the backfill, i.e. separate sets of transfers are not required for each of the x, y and z directions. Two sets of transfers are required to represent transport parallel to the long-axis of the vault through the backfill, and perpendicular to the long-axis, from the backfill into the rock.

2.2 Processes

The key processes represented in the near-field model are:
- Decay and ingrowth of radionuclides.
- Advection of radionuclides with groundwater.
- Diffusion of radionuclides in groundwater.
- Sorption of radionuclides.

Section 9.3.1 in TR-14-09 notes that solubility limitation is not considered in the main calculation cases.

Decay and ingrowth of radionuclides was calculated using the in-built functionality in AMBER. Transport of radionuclides, taking into account the effects of sorption, was calculated using the standard mathematical models:

Advection

$$\lambda = \frac{Q}{C}$$

Where
λ is the transfer rate (y^{-1})
Q is the volumetric flow rate (m^3 y^{-1})
C is the element specific capacitance (m^3, Equation 9-6 in TR-14-09).

Diffusion

$$\lambda = \frac{D_e A}{C\Delta}$$

Where
λ is the transfer rate (y^{-1})
D_e is the effective diffusivity (m^2 y^{-1})
C is the element specific capacitance (m^3, Equation 9-6 in TR-14-09).
Δ is the distance from the mid-point of the compartment to the mid-point of the adjacent compartment.

Advection was represented using forwards transfers, while diffusion was represented using pairs of forwards and backwards transfers. This is the standard approach for compartmental models, as used in SKB's models implemented using ECOLEGO. The calculation of distance from the mid-point of a compartment to the outer edge of

a compartment is illustrated in Figure 8 for the different waste types and near-field barriers. For the walls of the concrete moulds (not illustrated) the distance from the mid-point of the compartment to the outer edge of the compartment is equal to half the wall thickness.

Note the distance and cross-sectional area for diffusion are direction dependent and this must be accounted for when calculating the transfer rates. The AMBER model was configured such that different areas and distances can be specified in the x (parallel to the long axis of the vault), y (sideways) and z (up and down) directions. For simplicity, the different thicknesses of macadam above and below the caissons were not represented in the model, as this reduces the number of transfers that have to be included in the model and parameterised. This is not expected to have an important impact on the results, as advection by groundwater is always significant component of radionuclide transport through the macadam.

For radial geometry compartments, such as those used to represent the caissons, the cross-sectional area of the compartment, which is used in the diffusion calculations, was specified based on the dimensions of the outside of the compartment. However, in the transport calculations, the interface area between the compartments was always used. Therefore, while the cross-sectional area of the donor compartment was used for transfers away from the wastes, for backwards diffusive transfers towards the waste, the cross-sectional area of the receptor compartment was used. It is not clear if this distinction was made in SKB's model – see equation 9-9 in TR-14-09.

In the AMBER model, the harmonic mean effective diffusivity was calculated for each diffusive transfer:

$$D_{e,h} = \frac{\Delta_d + \Delta_r}{\dfrac{\Delta_d}{D_{e,d}} + \dfrac{\Delta_r}{D_{e,r}}}$$

Where
D_e is the effective diffusivity (m^2 y^{-1})
Δ is the distance from the mid-point of the compartment to the mid-point of the adjacent compartment (m).
$_h$ is the harmonic mean
$_d$ is the donor compartment
$_r$ is the receptor compartment
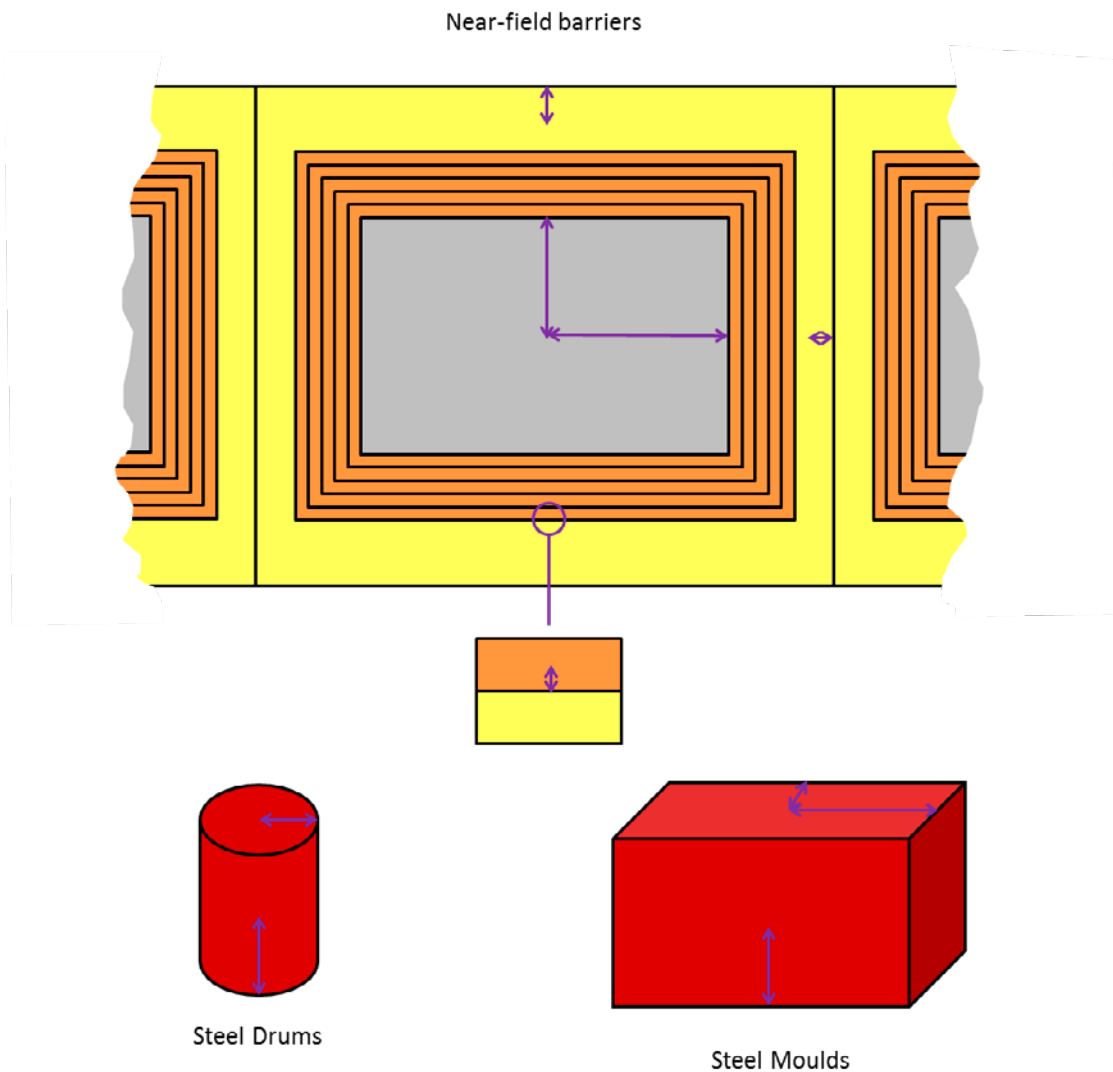
Figure 8. Calculation of the distance from the mid-point of a compartment to the outer edge of a compartment

2.3 Data

2.3.1 Radionuclide Decay Chains and Half-lives

Table 3-1 in TR-14-09 describes the radionuclide decay chains and Tables A-3 and A-4 of the same report describe the half-lives. Only those radionuclides, and their progeny, that lead to the greatest radiotoxicity of releases from the near-field and geosphere have been included in the AMBER model. From Figure 5-1 and 5-2 in TR-14-09 these are:

- ▲ C-14_inorg
- ▲ C-14_org
- ▲ Ni-59
- ▲ Ra-226

- ▲ Mo-93
- ▲ Tc-99
- ▲ Ag-108m
- ▲ I-129
- ▲ Ac-227
- ▲ Pa-231
- ▲ U-235
- ▲ U-238
- ▲ Pu-239
- ▲ Pu-240
- ▲ Am-241
- ▲ Am-243

2.3.2 Inventory

The numbers of packages of each type in 2BMA is given in Table 1. The total inventory in 2BMA is given in Table A-1 in TR-14-09. The inventory associated with each waste type was provided by SKB in an Excel spreadsheet[1]. The inventory associated with each package type was calculated using the mapping between package type and waste type described in Table 2. When the inventory for each package type was summed, the total inventory was found to match that in Table A-1 in TR-14-09, except for Mo-93 where the calculated inventory was slightly higher than given in TR-14-09 and for U-235 where the calculated inventory was slightly lower. The inventory associated with each package type is given in Table 3.

Table 3. Inventory in the different package types (Bq)

	Cement solidified wastes in concrete moulds	Cement embedded wastes in concrete moulds	Cement solidified wastes in steel moulds	Cement embedded wastes in steel moulds	Cement embedded wastes in steel drums
Ac-227	0.00E+00	0.00E+00	0.00E+00	0.00E+00	0
Ag-108m	2.34E+06	9.53E+08	3.26E+08	3.94E+10	0
Am-241	5.01E+06	1.20E+10	7.68E+08	2.85E+10	0
Am-242m	8.97E+03	2.22E+07	1.35E+06	1.60E+08	0
Am-243	3.44E+04	8.70E+07	5.65E+06	5.70E+08	0
Ba-133	1.66E+04	1.36E+07	1.33E+06	1.28E+08	0
C-14-ind	0.00E+00	0.00E+00	0.00E+00	5.09E+09	0
C-14-inorg	0.00E+00	0.00E+00	1.12E+10	3.17E+09	0
C-14-org	0.00E+00	0.00E+00	2.97E+09	9.91E+08	0
Ca-41	0.00E+00	0.00E+00	0.00E+00	1.56E+10	0
Cd-113m	2.71E+05	4.28E+07	3.07E+07	1.94E+07	0
Cl-36	2.53E+04	1.03E+07	3.84E+06	1.88E+08	0

---

[1] "Inventory_2BMA_fromSKB.xlsx" provided by SSM on 7th October 2016. Reference SSM2015-725-32.

Cm-242	0.00E+00	0.00E+00	0.00E+00	0.00E+00	0
Cm-243	6.91E+03	1.87E+07	8.09E+05	8.32E+07	0
Cm-244	5.09E+05	1.48E+09	1.17E+07	9.21E+09	0
Cm-245	3.44E+02	8.32E+05	5.65E+04	9.22E+06	0
Cm-246	9.14E+01	2.22E+05	1.50E+04	3.11E+06	0
Co-60	9.27E+07	3.27E+11	8.02E+09	1.65E+12	0
Cs-135	5.18E+04	8.32E+06	1.93E+07	2.56E+07	0
Cs-137	1.62E+09	2.27E+11	2.24E+11	4.43E+11	0
Eu-152	2.86E+04	4.58E+06	3.22E+06	1.33E+11	0
H-3	2.63E+05	1.82E+08	2.15E+07	3.31E+12	0
Ho-166m	1.64E+05	6.67E+07	2.33E+07	4.32E+08	0
I-129	1.56E+04	3.21E+06	3.08E+06	1.37E+06	0
Mo-93	4.85E+04	3.37E+08	7.23E+06	4.18E+09	0
Nb-93m	4.95E+06	2.85E+09	4.30E+08	1.31E+13	0
Nb-94	4.22E+05	1.71E+08	6.05E+07	9.10E+10	0
Ni-59	4.70E+08	1.69E+10	6.73E+10	8.65E+11	0
Ni-63	4.30E+10	9.78E+11	5.49E+12	8.58E+13	0
Np-237	5.26E+02	1.26E+06	8.98E+04	6.34E+06	0
Pa-231	0.00E+00	0.00E+00	0.00E+00	0.00E+00	0
Pb-210	0.00E+00	0.00E+00	0.00E+00	0.00E+00	0
Pd-107	5.18E+03	7.21E+05	1.00E+06	2.55E+09	0
Po-210	0.00E+00	0.00E+00	0.00E+00	0.00E+00	0
Pu-238	3.07E+06	7.75E+09	1.90E+08	3.62E+10	0
Pu-239	4.80E+05	1.16E+09	7.89E+07	5.54E+09	0
Pu-240	6.76E+05	1.64E+09	1.10E+08	7.46E+09	0
Pu-241	1.26E+07	3.85E+10	1.22E+09	1.26E+11	0
Pu-242	3.46E+03	8.38E+06	5.68E+05	4.13E+07	0
Ra-226	0.00E+00	0.00E+00	0.00E+00	0.00E+00	0
Ra-228	0.00E+00	0.00E+00	0.00E+00	0.00E+00	0
Se-79	2.07E+04	2.88E+06	4.01E+06	3.72E+05	0
Sm-151	1.05E+07	1.44E+09	1.79E+09	3.23E+10	0
Sn-126	2.59E+03	3.61E+05	5.01E+05	1.66E+07	0
Sr-90	1.54E+08	2.06E+10	1.72E+10	3.22E+11	0
Tc-99	6.45E+05	2.08E+08	1.30E+08	1.08E+09	0
Th-228	0.00E+00	0.00E+00	0.00E+00	0.00E+00	0
Th-229	0.00E+00	0.00E+00	0.00E+00	0.00E+00	0
Th-230	0.00E+00	0.00E+00	0.00E+00	0.00E+00	0
Th-232	0.00E+00	0.00E+00	0.00E+00	0.00E+00	0
U-232	2.07E+01	5.25E+04	2.89E+03	9.09E+04	0
U-233	0.00E+00	0.00E+00	0.00E+00	0.00E+00	0
U-234	1.15E+03	2.79E+06	1.90E+05	5.65E+04	0
U-235	2.30E+01	5.60E+04	3.79E+03	1.83E+04	0
U-236	3.48E+02	8.38E+05	5.71E+04	5.11E+06	0
U-238	4.61E+02	1.12E+06	7.55E+04	3.45E+04	0
Zr-93	4.22E+04	1.71E+07	6.06E+06	1.04E+09	0

Importantly, it was found that there is no inventory for the cement embedded wastes in steel drums. There are 2384 of these drums, which accounts for a notable fraction of the total waste volume in 2BMA.

SKB do not describe the distribution of different waste packages, or waste types, between the caissons, so it was assumed the different package and waste types are evenly distributed between the caissons.

18

2.3.3 Waste Package Dimensions

Waste package dimensions are given in Sections 3.6.1 to 3.6.3 in TR-14-02. They are summarised in Table 4.

Table 4. Waste package dimensions

Package	Length (m)	Width (m)	Height (m)	Wall thickness (m)
Concrete mould	1.2	1.2	1.2	0.1
Steel mould	1.2	1.2	1.2	0.005
Steel drum	0.59*	0.59*	0.88	0.0012

* Drum diameter

The volume of each waste package type was calculated in the AMBER model. The areas for diffusion, in three dimensions, were also calculated in AMBER. These values were applied to the compartments that represent each waste package type. (Note that for wastes in concrete moulds, values were calculated for the compartments representing the concrete moulds and the compartments representing the waste inside the moulds). These values (volumes and areas) were then scaled by the number of packages of each type.

For all the compartments in the AMBER model, the area for diffusion was set equal to the calculated outer surface area of the feature represented by the compartment. So, for example, the area for diffusion assigned to each waste package compartment was the calculated external surface area of the package. These surface areas were used in AMBER to calculate the forwards transfer rates from the waste packages into the grout, and the backwards transfer rates from the grout into the waste packages. This is illustrated in Figure 9 for diffusion in a single direction. (Note that diffusion in three dimensions is represented in the AMBER model, e.g. diffusion out of all six faces of a concrete mould).
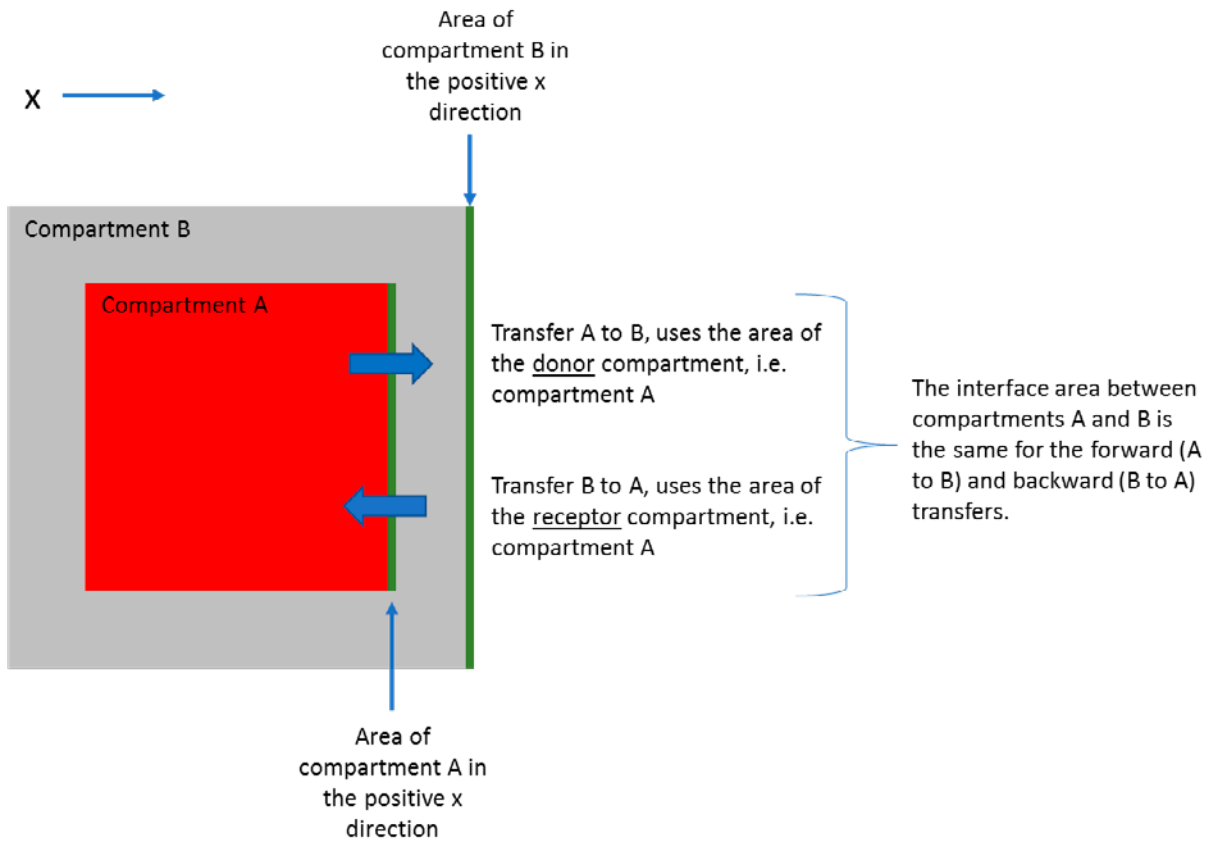
Figure 9. Assignment of surface areas to diffusive transfer fluxes in AMBER. Illustration shows one example direction, but diffusion in all directions is considered in the AMBER model.

2.3.4 Vault and Caisson Dimensions

Vault and caisson dimensions are given in Table 5-1 in TR-14-02. They are reproduced in Table 5. The layout 2.0 dimensions were used in the AMBER model.

The volume of grout in each caisson was calculated in AMBER as the internal volume of the caisson minus the volume of the waste packages in the caisson. The caisson was represented by five radial compartments. The caisson walls are 1 m thick, so each of the five compartments was assumed to be 0.2 m thick.

The surface areas for diffusion were calculated in AMBER for the grout and each of the five radial caisson compartments. The surface area of each compartment was calculated as its external surface area. The areas were assigned to the transfers as shown in Figure 9, so the same interface area was used for the forward and backward transfers between adjacent compartments.

Table 5. Vault and caisson dimensions (Table 5-1 in TR-14-02)

Table 5-1. 2BMA dimensions.

2BMA property	Value (Layout 1.5)	Value (Layout 2.0)	Comment*
Excavated rock cavity			
Total length [m]	275	275	Given in drawing SKBdoc 1391453
Width [m]	19.2	20.4	Layout 1.5, calculated from values (0.3+18.6+0.3) given in drawing SKBdoc 1316398 ver. 2.0
			Layout 2.0, calculated from values (0.3+19.8+0.3) given in drawing SKBdoc 1391456 ver. 1.0
Vertical cross sectional area [m²]	310	322	Layout 1.5 given in drawing SKBdoc 1316398 ver. 2.0
			Layout 2.0, given in drawing SKBdoc 1391456 ver. 1.0
Height max [m]	16.8	16.4	Layout 1.5, calculated from values(16.41+0.4) given in drawing SKBdoc 1316398 ver. 2.0
			Layout 2.0, calculated from values (0.4+15.71+0.3) given in drawing SKBdoc 1391456 ver.1.0
Height average [m]	16.1	15.8	Layout 1.5 calculated 310/19.2
			Layout 2.0 calculated 322/20.4
Excavated volume [m³]	85,250	88,550	Layout 1.5 calculated 275·310
			Layout 2.0 calculated 275·322
Shotcrete thickness [m]	0.05	0.05	From Carlsson and Christiansson 2007, Table 6-2 Un-reinforced 1 or 2 layers: 0.03 or 0.05 m Fibre reinforced: 0.05 or 0.08 m
Inner zone (at tunnel 2TT)			
Length [m]	4.7	4.7	Calculated from values (24,255–19,555) given in drawing SKBdoc 1391802
Waste disposal area			
Concrete structure (14 disposal caissons)			
Length outer [m]	246.3	246.3	Calculated from values (14·16.2+13·1.5) given in drawings SKBdoc 1391802, 139803, 139804
Distance between caissons	1.5	1.5	Given in drawing SKBdoc 1391802
Width outer [m]	16.2	16.2	Given in drawing SKBdoc 1391456 ver. 1.0
Height outer [m]	8.4	8.4	Given in drawing SKBdoc 1391456 ver. 1.0
Concrete lid [m]	0.5	0.5	Given in drawing SKBdoc 1391456 ver. 1.0
Thickness outer walls [m]	0.5	0.5	Given in drawing SKBdoc 1391456 ver. 1.0
Concrete floor [m]	0.5	0.5	Given in drawing SKBdoc 1391456 ver. 1.0
Disposal caissons			
Width inner [m]	15.2	15.2	Calculated from values (16.2–0.5–0.5) given in drawing SKBdoc 1391456 ver. 1.0
Length inner [m]	15.2	15.2	Calculated from values (14·16.2+13·1.5) given in drawing SKBdoc 1391802
Height inner [m]	7.4	7.4	Calculated from values (8.4–0.5–0.5) given in drawing SKBdoc 1391456 ver. 1.0
Bottom			
Macadam/Rock fill thickness [m]	0.4	0.4	Given in drawing SKBdoc 1391456 ver. 1.0
Reloading zone (at tunnel 2BST)			
Length [m]	24	24	Calculated from 275–4.7–246.3

* Drawing numbers in column "Comment" refer to SKB's internal documents.

2.3.5 Time Periods

SKB's conceptual model describes how flows through the repository and conditions in the repository will evolve in response to climate and landform change, and degradation of the wastes and near-field barriers.

Flows through the near-field are calculated for three shoreline positions (at 2000 AD, 3000 AD, and 5000 AD) and for different concrete degradation states (Table 7-

2 in TR-13-08). Evolution of the hydraulic properties of the near-field is shown in Table 4-1 of TR-14-09, which is reproduced below as Table 6.

In the Global Warming Calculation Case, there is assumed to be no radionuclide release or transport during the first 1000 y. This is anticipated by SKB to be a cautious assumption as it ensures radionuclides are not released to the marine biosphere that exists from the present day to 1000 y post-closure. A variant case (the Timing of Releases Calculation Case) is used to explore radionuclide release and transport from time zero. It was found that this is not actually a cautious assumption since the doses were broadly similar to the Global Warming Calculation Case (Section 5.1.2 in TR-14-09).

There is also assumed to be no flow during four periods of permafrost, with the first period starting at 52,000 y AD. Inspection of the ECOLEGO files confirmed that there is also assumed to be no diffusion during the periods of permafrost. This is consistent with the assumption that formation of permafrost results in freezing of the repository and complete degradation of the concrete (Table 6).

Our initial review (SSM, 2016) identified that SFR3 is deeper than SFR1, so it is possible that SFR1 may be frozen during periods of permafrost while SFR3 is not (Figure 7-1 in TR-14-01). In this situation, transport by diffusion would still be possible in SFR3, but complete degradation of the concrete would not occur.

Once the concrete barriers in 2BMA have become severely / completely degraded, radionuclide transport through them is calculated using a fracture flow model, rather than treating them as porous media. This is indicted by '*F*' in Table 6. Appendix D in TR-14-09 explains that in the fracture flow model there is assumed to be no sorption of radionuclides onto fractures in the concrete. However, Section 6.6.3 in TR-14-01 states that when the permafrost melts and the concrete is completely degraded it no longer limits advective flow, but continues to act as a sorption barrier. Therefore SKB's conceptualisation and mathematical model of this transition are unclear.

It is also not clear if this fracture flow models only applies to the construction concrete, or also the grout, concrete moulds and cementitious wasteforms. In the AMBER model, the fracture flow model has been applied to the concrete caissons and concrete moulds, but not to the grout surrounding the waste packages or the cementitious wasteforms.

The time periods for evolution of the material properties and flows are further described in the following sub-sections.

Table 6. Evolution of near-field hydrological cases (Table 4-1 in TR-14-09)

Table 4-1. Progression of hydrological cases in the near-field over time in the *global warming calculation case*. No flow (black), intact concrete K=8.3×10⁻¹⁰ m/s (green), moderately degraded concrete K=10⁻⁷ m/s (blue), severely degraded concrete K=10⁻⁵ m/s (yellow) and completely degraded concrete K=10⁻³ m/s (orange). "F" denotes fracture flow, see further Appendix D.

Time AD	2000–3000	3000–12,000	12,000–22,000	22,000–52,000	52,000–56,000	56,000–67,000	67,000–76,500	76,500–78,000	78,000–81,500	81,500–86,500	86,500–102,000
BMA	black	blue	blue	yellow (F)	black	orange (F)	black	orange (F)	black	orange (F)	black
Silo	black	yellow	yellow	orange	black	orange	black	orange	black	orange	black
BTF	black	yellow	orange	orange	black	orange	black	orange	black	orange	black
Other	black	green	green	green	black	green	black	green	black	green	black

2.3.6 Material Properties

Material properties are given in Section 4.1 in TR-14-09 and are reproduced in Table 7 to Table 9. For effective diffusivity and porosity data, p41 in TR-14-09 notes that, "*the transitions between time periods were modelled as a gradual change over 100 years (but over 10 years for the first transition at 2100 AD)*". Time invariant values are provided for densities.

Effective diffusivities and porosities of construction concrete were specified as probability density functions (PDFs). The values are taken from Table 9-5 and Table 10-4 in TR-14-10. Anion exclusion factors are not specified in TR-14-09, TR-14-10, or TR-14-12 for cementitious materials, so we assumed this is not a relevant process.

The shape of the PDF is not specified for the porosity data range. Section 10.8 in TR-14-10 explains that insufficient data are available to describe the distributions of hydraulic parameters. Therefore, deterministic values are used in the ECOLEGO models. We note that there may be a slight discrepancy between Table 4-2 in TR-14-09 and Table 9-5 in TR-14-10 with the former describing a time period to 52,000 AD and the latter to 54,000 AD. We also note that TR-14-10 states that as far as possible the parameter values are taken from the work of Höglund (2014: R-13-40). Table 10-4 in TR-14-10 gives porosities of 0.5 for construction concrete and moulds beyond 50,000 y, but Table 9-1 in R-13-40 gives values of 0.3. So the audit trail for these long-term values is not transparent.

It is not clear if the densities are grain densities, or bulk densities (i.e. grain density multiplied by (1 – porosity)). In the AMBER model they have been assumed to be bulk densities.

23

Data have not been found in SKB's reports for the cementitious wasteforms. Inspection of the ECOLEGO models files revealed three different materials types that might correspond to the cementitious wasteforms. These are: waste cement; waste wall concrete; and waste concrete. However, without greater familiarity of the ECOLEGO code, it was not possible to deduce how these map to the waste package compartments. In addition, some of the associated properties appear to be effective properties. The logic underpinning these effective properties is not known.

The properties of the cementitious wasteforms (solidified waste and embedded waste) were set to be the same as grout in the AMBER model. Sensitivity to the properties of the wasteforms was then explored as a variant calculation case.

Table 7. Effective diffusivities (De) (m²/s) (Table 4-2 in TR-14-09 and Table 9-5 in TR-14-10)

Time AD		2000 - 2100	2100 – 12,000	12,000 – 22,000	22,000 – 52,000	52,000 – 102,000
Construction concrete	De	3.50E-12	5.00E-12	5.00E-12	1.00E-11	2.00E-10
	PDF	N/A	N/A	N/A	Log triangular Min 8.0E-12 Max 2.0E-11	Log triangular Min 2.0E-11 Max 2.0E-10
Moulds	De	3.50E-12	2.00E-11	5.00E-11	1.00E-10	5.00E-10
	PDF	N/A	N/A	N/A	N/A	N/A
Grout	De	3.50E-10	4.00E-10	4.00E-10	5.00E-10	1.00E-9
	PDF	N/A	N/A	N/A	N/A	N/A
Macadam	De	6E-10	6E-10	6E-10	6E-10	6E-10
	PDF	N/A	N/A	N/A	N/A	N/A

Table 8. Porosities (-) (Table 4-3 in TR-14-09 and Table 10-4 in TR-14-10)

Time AD		2000 - 2100	2100 – 12000	12000 – 22,000	22,000 – 52,000	52,000 – 102,000
Construction concrete	Porosity	0.11	0.14	0.14	0.18	0.5
	PDF	N/A	Range 0.11-0.16	Range 0.11-0.16	Range 0.16-0.20	N/A
Moulds	Porosity	0.11	0.14	0.14	0.18	0.5
	PDF	N/A	Range 0.11-0.16	Range 0.11-0.16	Range 0.16-0.20	N/A
Grout	Porosity	0.3	0.4	0.4	0.5	0.5
	PDF	N/A	N/A	N/A	N/A	N/A
Macadam	Porosity	0.3	0.3	0.3	0.3	0.3
	PDF	N/A	N/A	N/A	N/A	N/A

Table 9. Densities (kg/m³) (Section 4.1 in TR-14-09)

Material	Density (kg/m³)	Notes
Construction concrete	2,529	
Moulds	2,529	Not specified so assumed to be the same as a construction concrete
Grout	2,250	
Macadam	1,890	Rock density 2700 kg/m³ from TR-10-52. Macadam density calculated based on a porosity of 0.3.

2.3.7 Flows

Section 9.3.2 in TR-14-09 describes how, "*the compartments of the RNT near-field model coincide with control volumes of the near-field hydrological model (or sub volumes thereof). The flows from one compartment to another are determined by calculating the flow across the surfaces of the control volumes. The sub-division of control volumes into several compartments for achieving a finer resolution in the radionuclide transport applies particularly to the concrete walls of the models of the BMA vaults and the Silo. The subdivision of the concrete walls is done to avoid the large numerical dispersion that would result from representing the walls with only one compartment each. In the radionuclide transport model, all outer walls were represented by five compartments each*".

The control volumes for 2BMA are illustrated in Figure 3. They are further described in Section 3.3 in TR-13-08:
"*– Each waste compartment is delimited by a concrete barrier on top, bottom, and lateral sides. These outer concrete walls define the waste control volumes. The waste control volumes are numbered from 1 in the south to 14 in the north.*
– There are also 14 control volumes (backfill) surrounding the waste control volumes. Note that unlike the 1BMA there are no concrete walls between the waste storage sections in this case. The limits of the backfill control volumes are chosen exactly in the middle of the two volumes (see Figure 3-16[2]– on the right side). Because of this the size of backfill control volume 14 is slightly bigger."

The same control volumes have been used to parameterise the AMBER model. However, the compartment representing the macadam surrounding caisson 14 was set to be the same size as the other caissons in AMBER, so the diffusion length to the adjacent macadam compartment is the same in either direction. This simplifies implementation of diffusion in the model as diffusive transfers in the different directions do not have to be parameterised with different diffusion lengths.

---

[2] Figure 3 in this report.

Figure 7-7 in R-13-08 is reproduced as Figure 10. It shows the effect of the hydraulic cage provided by the engineering as built (base case), with flows through the macadam being several orders of magnitude greater than flows through the waste. The results also show an approximate order of magnitude change in flow through the wastes along the length of the vault. The different shoreline positions correspond to 2000 AD, 3000 AD and 5000 AD. The shoreline position has limited influence of the total flow through the vault.
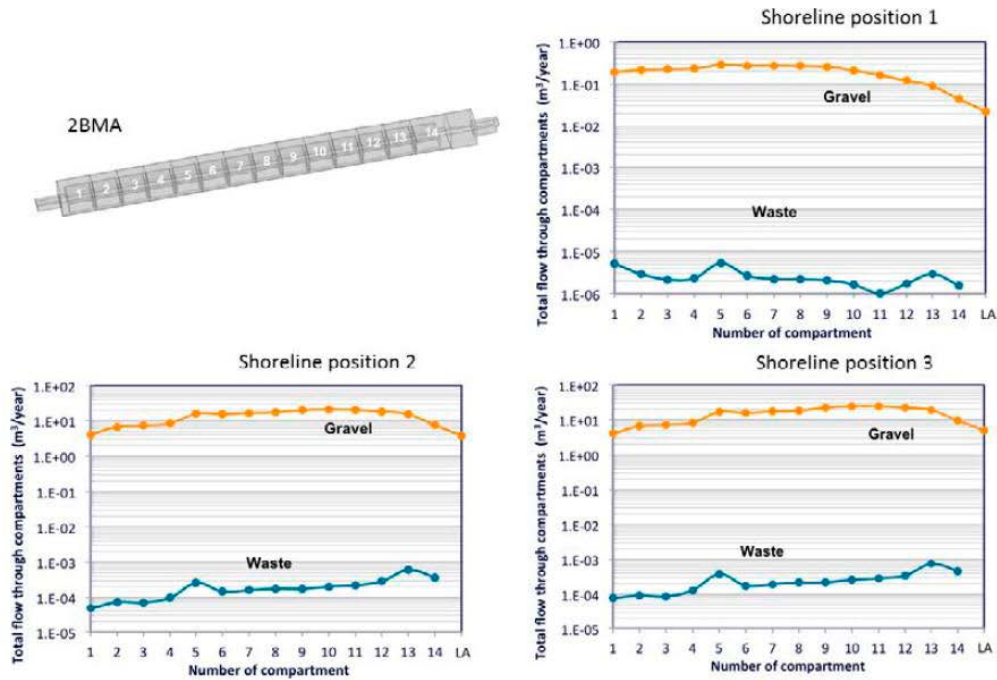
Figure 7-7. Total tunnel (gravel) and waste flow (m3/year) profiles for the 2BMA for the three shoreline positions. The vertical axis is logarithmic.

Figure 10. Flows through the 2BMA vault with as built properties (Figure 7-7 in R-13-08)

Assessment Model Flowchart (AMF) 50 in TR-14-12 describes where the water flow volumes through the different control volumes are stored for input to the radionuclide transport model. However, they are not reported. The complete flow data set was provided by SKB in three Excel spreadsheets. The spreadsheets give the flow out of each of the six sides of each control volume: x-, x+, y-, y+, z-, z+. Interrogation of the ECOLEGO model clarified that the y direction corresponds to the long axis of the vault SKB's model.

All the data from the spreadsheets are read into the ECOLEGO model and are processed inside the model. Negative flows are set to zero, so positive flows must represent flow out of the control volume, and negative flow must represent flow in. The relevant flow is then selected in ECOLEGO depending on the shoreline position and concrete degradation state.

For the AMBER model, the flows were pre-processed in the spreadsheets prior to being entered into the model. The radial representation of the waste packages, grout and caissons, means that flows in different directions do not need to be distinguished for these compartments, so the positive flows can be summed into a single flow

volume. Flow out of the macadam can either be into the adjacent rock or adjacent macadam. Therefore, flows parallel and perpendicular to the long axis of the vault were distinguished. This is illustrated in Figure 11. The flow values used in the AMBER model are given in Table 10.

→ Flow out of caisson to macadam

→ Flow out of macadam to adjacent macadam

→ Flow out of macadam to rock
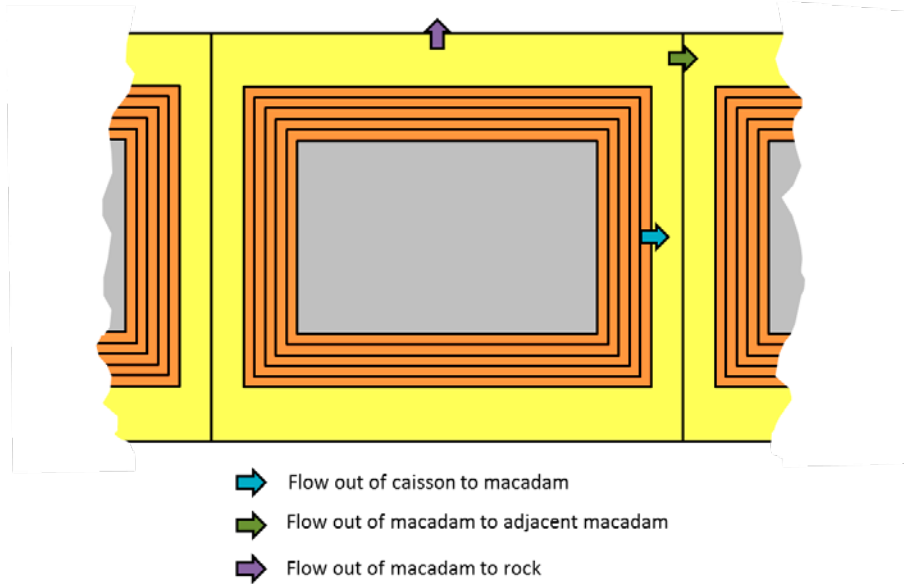
Figure 11. Representation of flows by advective transfers between compartments in AMBER

Table 10. Flows (m³/y) through control volumes in the 2BMA vault pre-processed for the AMBER model, at times corresponding to different shoreline positions (2000, 3000 and 5000 AD) and concrete degradation states (Table 6)

		Time (AD)				
Caisson	**Flow (m³/y)**	**2000**	**3000**	**5000**	**22,000**	**52,000**
1	Macadam parallel	1.77E-01	3.85E+00	3.37E+00	3.38E+00	3.39E+00
1	Macadam perpendicular	0.00E+00	9.25E-02	6.50E-01	6.52E-01	6.54E-01
1	Caisson	3.98E-04	4.81E-03	5.56E-03	3.92E-01	1.91E+00
2	Macadam parallel	2.10E-01	6.59E+00	6.31E+00	6.31E+00	6.33E+00
2	Macadam perpendicular	0.00E+00	8.65E-02	2.50E-01	2.50E-01	2.48E-01
2	Caisson	3.24E-04	7.93E-03	8.21E-03	5.67E-01	2.91E+00
3	Macadam parallel	2.24E-01	7.61E+00	7.25E+00	7.25E+00	7.27E+00
3	Macadam perpendicular	8.18E-03	1.17E-01	1.54E-01	1.55E-01	1.53E-01
3	Caisson	2.93E-04	9.62E-03	9.65E-03	6.65E-01	3.42E+00
4	Macadam parallel	2.28E-01	8.39E+00	7.96E+00	7.96E+00	7.98E+00
4	Macadam perpendicular	1.07E-03	4.89E-02	1.76E-01	1.74E-01	1.70E-01
4	Caisson	2.93E-04	1.19E-02	1.30E-02	8.56E-01	4.15E+00
5	Macadam parallel	2.64E-01	1.46E+01	1.45E+01	1.46E+01	1.46E+01
5	Macadam perpendicular	1.38E-02	1.33E+00	2.36E+00	2.36E+00	2.36E+00
5	Caisson	4.61E-04	2.23E-02	2.71E-02	1.77E+00	7.90E+00
6	Macadam parallel	2.64E-01	1.53E+01	1.54E+01	1.54E+01	1.54E+01
6	Macadam perpendicular	2.64E-03	1.40E-01	2.52E-01	2.50E-01	2.46E-01

6	Caisson	3.62E-04	1.97E-02	2.08E-02	1.40E+00	7.08E+00
7	Macadam parallel	2.60E-01	1.63E+01	1.66E+01	1.67E+01	1.67E+01
7	Macadam perpendicular	9.07E-03	4.56E-01	7.41E-01	7.42E-01	7.36E-01
7	Caisson	3.37E-04	2.19E-02	2.36E-02	1.57E+00	7.91E+00
8	Macadam parallel	2.53E-01	1.69E+01	1.74E+01	1.74E+01	1.74E+01
8	Macadam perpendicular	1.03E-02	5.44E-01	8.49E-01	8.47E-01	8.43E-01
8	Caisson	3.33E-04	2.33E-02	2.55E-02	1.72E+00	8.53E+00
9	Macadam parallel	2.08E-01	1.98E+01	2.21E+01	2.22E+01	2.22E+01
9	Macadam perpendicular	4.49E-02	2.80E-01	3.58E-01	3.55E-01	3.50E-01
9	Caisson	3.06E-04	2.43E-02	2.70E-02	1.87E+00	9.96E+00
10	Macadam parallel	1.59E-01	2.01E+01	2.36E+01	2.37E+01	2.37E+01
10	Macadam perpendicular	4.89E-02	9.29E-01	7.77E-01	7.75E-01	7.68E-01
10	Caisson	2.51E-04	2.81E-02	3.31E-02	2.22E+00	1.12E+01
11	Macadam parallel	1.19E-01	1.84E+01	2.23E+01	2.23E+01	2.24E+01
11	Macadam perpendicular	4.07E-02	1.98E+00	2.19E+00	2.19E+00	2.18E+00
11	Caisson	1.93E-04	2.85E-02	3.42E-02	2.27E+00	1.14E+01
12	Macadam parallel	8.74E-02	1.53E+01	1.91E+01	1.91E+01	1.91E+01
12	Macadam perpendicular	3.12E-02	3.10E+00	3.31E+00	3.30E+00	3.30E+00
12	Caisson	1.99E-04	3.11E-02	3.67E-02	2.35E+00	1.09E+01
13	Macadam parallel	4.32E-02	7.49E+00	9.56E+00	9.60E+00	9.61E+00
13	Macadam perpendicular	4.64E-02	8.28E+00	1.00E+01	1.00E+01	1.00E+01
13	Caisson	2.20E-04	4.17E-02	5.08E-02	3.01E+00	1.11E+01
14	Macadam parallel	2.24E-02	3.84E+00	5.01E+00	5.02E+00	5.02E+00
14	Macadam perpendicular	2.15E-02	3.78E+00	4.71E+00	4.72E+00	4.74E+00
14	Caisson	9.28E-05	1.91E-02	2.45E-02	1.49E+00	5.33E+00
Loading Area	Macadam	2.43E-02	4.20E+00	5.49E+00	5.47E+00	5.48E+00

SKB note that the flow rates given in Table 7-2 in R-13-08 have been normalised per waste package, but do not explain what this means or how it was done. We assume that because each caisson contains a number of different waste package types, not all the flow passes through each package type. In the AMBER model the flow through each package type was set equal to the flow through the caisson scaled by the ratio of the volume of each package type in the caisson, to the internal volume of the caisson, i.e.:

$$F_i = Q_c V_i / V_c$$

Where
F_i is the flow through package type i (m³/y)
Q_c is the flow through the caisson (m³/y)
V_i is the volume of package type i in the caisson (i.e. volume of a single package of type i multiplied by the number of packages if type i) (m³)
V_c is the internal volume of the caisson (m³)

Section 9.3.10 in TR-14-09 notes that, "*Due to the lack of detailed water flow data in the interior of the waste domains a simplified approach is taken to estimate the water flow through the waste packages. For grouted waste packages in 1–2BTF, Silo and 1–2BMA all the water flowing into the waste domain is also assumed to flow through the waste packages*". We assumed this means all the flow through the caisson is considered to flow through the wastes; rather than all the flow through the caisson is assumed to flow through each package type. However, this is not clear.

Section A.2 in TR-14-09 explains that in the radionuclide transport models, flows are linearly interpolated between steady state simulations representing different shoreline positions and concrete degradation states. There is also assumed to be no flow during four periods of permafrost, with the first period starting at 52,000 AD. This is confirmed by the model results, e.g. Figure 5-1 in TR-14-09, and inspection of the ECOLEGO model also confirmed there is assumed to be no diffusion during periods of permafrost, including within the near-field.

The ECOLEGO model results show a step change in radionuclide release from the near-field at 22,000 AD (Figure 5-1 in TR-14-09) and this is ascribed to increases in water fluxes and effective diffusivities as the barriers degrade. This implies there are step changes in the near-field flows as the barriers degrade, or transition over a limited period of time, rather than continuous change. The step change at 22,000 AD also coincides with a change in the degradation state of concrete from moderately to severely degraded, and an associated change from a porous medium model to a fractured medium model (Table 6).

Inspection of the ECOLEGO model confirmed that there are step changes in the near-field flows associated with the changes in concrete degradation state. Therefore, in the AMBER model the flows were linearly interpolated between different shoreline positions (2000 AD, 3000 AD, 5000 AD), but step changes were applied at the changes in concrete degradation state (22,000 AD and 52,000 AD) and at the start and end of periods of permafrost. We were unable to determine if the change to the fracture transport model at 22,000 AD is applied as a step change or is linearly interpolated in ECOLEGO. It was applied as a step change in AMBER.

2.3.8 Sorption and Solubility Limitation

Solubility Limitation

Section 9.3.1 in TR-14-09 notes that solubility limitation is not considered in the main calculation cases.

Sorption onto Cementitious Materials

As cementitious materials degrade, their sorption properties change. Table 11 describes the cement degradation state in the 2BMA vault (from Table 4-4 in TR-14-09). P42 and Table 4-4 in TR-14-09 indicate that the sorption coefficients (Kd) change stepwise with the change in degradation state and are not linearly interpolated between states.

Table 11. Cement degradation state (Table 4-4 in TR-14-09)

Time AD	2000-7000	7000-102000
State	I	II

Kd values for these two states are given in Tables 7-7 and 7-8 in TR-14-10. These are 'base values' that need to be scaled by the fraction of cement paste in the material (Table 4-5 in TR-14-09 or Table 7-12 in TR-14-10). For some elements values are given for different oxidation states. Table 4-10 in TR-14-09 details which oxidation state was chosen for the main scenario. Table 12 gives the sorption distribution coefficients used in the AMBER model, which are then scaled by the fraction of cement paste in each material.

It is noted that Ni-59 is one of the dominant radionuclides contributing to activity released from the near-field. The Kd for Ni increases significantly with the transition from State I to State II. This is a potentially significant parameter choice that we recommend should be considered within the relevant technical area of the SR-PSU review.

Table 12. Distribution coefficients for sorption onto cementitious materials for different cement degradation states used in AMBER

Element (oxidation state)	Kd State I (m^3/kg)	Kd State II (m^3/kg)
U(IV)	30	30
Am	10	10
Pu(IV)	5	30
C_org	0	0
C_inorg	2	5
Ac	10	10
Pa(IV)	30	30
Tc(IV)	3	3
I	0.001	0.001
Ag	0	0
Ni	0.03	0.2
Ra	0.3	0.1
Mo	0.003	0.003
Th	30	30
Pb	0.3	3
Np(IV)	30	30

Table 4-5 of TR-14-09 only gives values for structural concrete and (2BMA) grout. It does not give data for the moulds or cementitious wasteforms. In the AMBER model these have been set to be the same as structural concrete and grout respectively. This approach could overestimate sorption onto the cementitious wasteforms, because the cement waste fraction will be lower for the wasteforms than the grout, because a significant fraction of the volume of the wasteforms is waste.

Sorption is also affected by the presence of complexing agents and this is reflected by applying sorption reduction factors to the Kds. However, these are only applied in the high concentration of complexing agents scenarios (Section 7.11 in TR-14-10), so they are not reported here and are not used in the AMBER model.

Upper and lower limits are specified for the 'base values' in Tables 7-7 and 7-8 in TR-14-10. P104 in TR-14-10 states that these should be applied as a log-triangular distribution with the best estimate as the mode.

Sorption onto Cementitious Materials – Fracture Flow Model

It was previously noted that a fracture flow model is applied to severely and completely degraded concrete. Appendix D in TR-14-09 explains that this is implemented in the model as having zero sorption.

Sorption onto Rock / Macadam

Table 8-6 in TR-14-10 gives rock matrix Kd values. Values are presented for different oxidation states, water types and pH conditions. It states that values less than 1E-5 m^3/kg may be considered to be effectively zero, but it is not clear if they were entered into the ECOLEGO model as zero. The stated value was used in the AMBER model. Table 8-6 in TR-14-10 also gives upper and lower bound values, but does not give the shape of the distribution.

Section 8.11 in TR-14-10 states that the Kd values for macadam/crushed rock will be taken from the rock matrix table, choosing speciation from the assumption of a high pH and redox for the duration of the safety assessment. Table 4-12 in TR-14-09 describes the oxidation state used in the main scenario.

Section 8.10 in TR-14-10 says, "*The suggestion to use equation 1 to estimate the gravel Kd values is accepted, however, without any addition of the porosity and density terms, simplifying the equation*". However, it does not explain or present equation 1. A number of equations are presented in the underpinning report (R-13-38) but there is not an equation 1. This may be referring to the equations in Appendix B of R-13-38, but it is not clear what values were used to calculate the fraction of the gravel mass that can be considered to be equilibrated on the time scale of transport. Therefore in the AMBER model, Kd values for crushed rock were set to those for rock under the relevant conditions (Table 13).

Table 13. Distribution coefficients for sorption onto macadam used in AMBER

Element (oxidation state)	Kd (m³/kg)
U(IV)	0.00011
Am	0.015
Pu(IV)	1.50E-05
Corg	0
Cinorg	0
Ac	0.015
Pa(V)	0.059
Tc(IV)	0.053
I	0
Ag	0
Ni	0.00074
Ra	0.001
Mo	0
Th	0.053
Pb	0.025
Np(IV)	0.00041

3 Geosphere Model

3.1 Model Configuration

The configuration of the geosphere model is described in Section 9.4.1 in TR-14-09, and is illustrated in Figure 12. A single fracture pathway through the geosphere is represented, and is discretised into 20 sections, with each section being represented by a single compartment. Contaminant diffusion from the fracture into the wall rock is then modelled for each of the 20 fracture compartments. There are 20 rock compartments for each fracture compartments giving a total of 420 compartments.

The decision to discretise the geosphere model into 420 compartments was based on comparison of the compartment model results with the semi-analytical model FARF31 (See Appendix B in TR-14-09). This discretisation will minimise any numerical dispersion, and once any dispersive fluxes have been included explicitly in the model, should give similar results to the analytical solution (Appendix F in Quintessa, 2011).

32

Quintessa (2011) shows that discretisation of a transport path into 5 compartments results in a solution that is still close to the analytical solution, and the amount of numerical dispersion is similar to the amount of physical dispersion, i.e. a Peclet number of 10. Given that the geosphere is only a weak barrier to the migration of the key radionuclides, it was decided to discretise the fracture in the AMBER model into 5 equal lengths. The wall rock associated with each fracture length was then discretised into 5 compartments, giving a total of 30 compartments. The configuration of the AMBER geosphere model is shown in Figure 13. The fracture compartments (F1 to F5) are coloured blue. The corresponding matrix compartments are numbered Fi_M1 to Fi_M5. There are pairs of diffusive transfers (i.e. forwards and backwards) between the fracture compartments and the adjacent rock compartments, and between adjacent rock compartments.
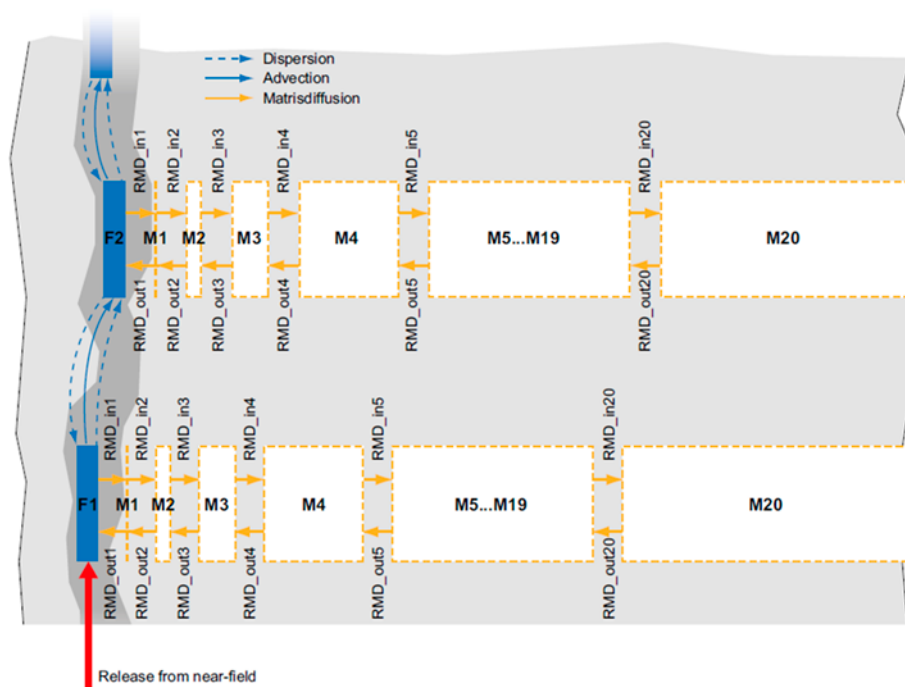
Figure 9-21. Conceptual model of the geosphere. A total of 420 compartments are used in the model. The blue boxes represent the compartments in the model used to represent water-bearing fractures (advection), and the white boxes represent compartments used to represent the rock matrix (diffusion). Solid blue arrows represent advection, dashed blue arrows represent dispersion, and yellow arrows represent diffusion (figure modified from Thomson et al. 2008a).

Figure 12. Configuration of the geosphere model (Figure 9-21 in TR-14-09)

Figure 13. Configuration of the geosphere model in AMBER

3.2 Processes

Section 9.4.2 in TR-14-09 describes the processes modelled in the geosphere. These are:

- Radioactive decay and ingrowth.
- Advection (in the fracture).
- Dispersion (in the fracture).
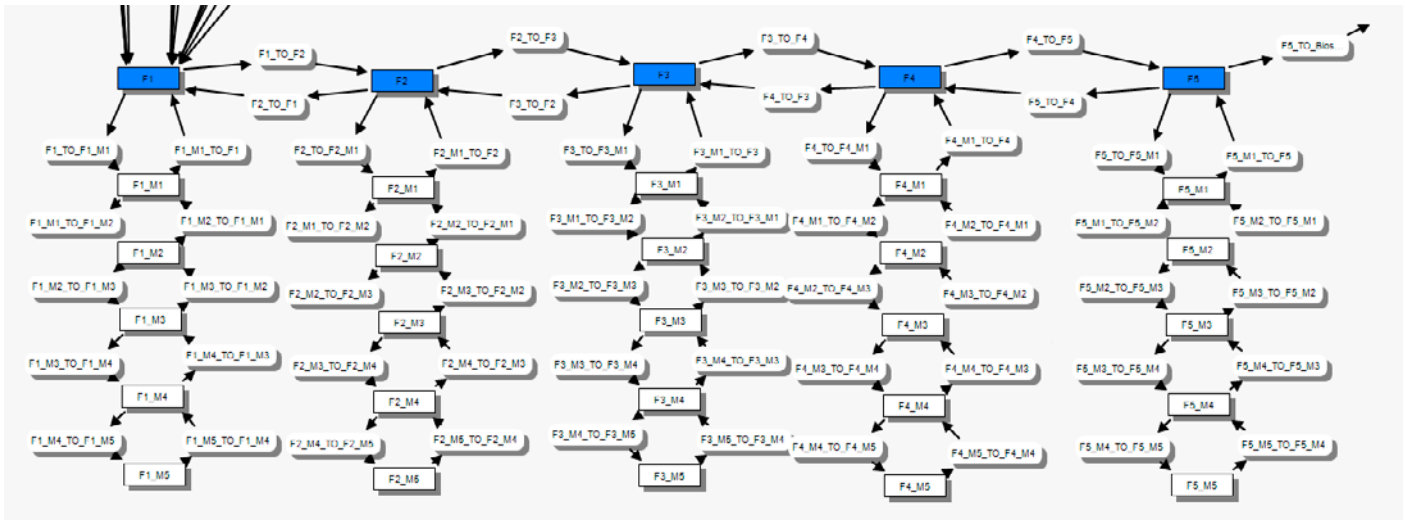- Rock matrix diffusion.
- Sorption.

Cautiously, sorption in the fractures (e.g. onto fracture surface minerals) is ignored.

The mathematical model for transport along the fracture, and diffusion into the rock is described in Sections 9.4.1 and 9.4.2 in TR-14-09. This has been implemented in the AMBER model.

3.3 Data

The following data are used into geosphere model.

- ▲ Advective transport time, t_w, and flow related transport resistance, F.
- ▲ Depth of first matrix compartment, d_o, 1E-4 m.
- ▲ Maximum penetration depth, D_p, 1.4 m.
- ▲ Matrix diffusion coefficient for the rock, D_e.
- ▲ Porosity of the rock, 0.18%.
- ▲ Sorption distribution coefficients.

The depth of the matrix (wall rock) compartments increases away from the fracture. In SKB's model, the first matrix compartment has a depth of 1E-4 m. The depth then increases according to an incremental factor of 1.5667, to give a maximum penetration depth of 1.4 m. The same depth was used for the first matrix

compartment in AMBER. An incremental factor of 10.61 was calculated using Equation 9-25 in TR-14-09 to give a maximum penetration depth of 1.4 m for 5 matrix compartments.

The matrix diffusion coefficient for the rock is referred to in AMF87 in TR-14-12, but the value used in the ECOLEGO models was not found in SKB's reports. Inspection of the ECOLEGO model files showed a value of 3.2E-14 m^2/s was used.

AMF2 in TR-14-12 says that the rock porosity was taken from SR-Site, and cites Table 6-90 in TR-10-52. This gives a rock matrix porosity of 0.18%.

Distribution coefficients for sorption onto rock are given in Table 8-6 in TR-14-10. P226 in TR-14-09 states, "*A cautious approach was taken in the selection of Kd values; In this approach, the minimum of the Kd values for Temperate saline, Early periglacial and Late periglacial ground water types were used in all calculation cases where the geosphere was included (except for some elements that are sensitive to pH and redox...*". Inspection of Table 8-6 in TR-14-10 reveals that for elements sensitive to redox and pH, the minimum Kd value at pH < 10 is always associated with lower oxidation state, which occurs under non-glacial rather than glacial conditions. Therefore the value used by SKB can be deduced. The values used in the AMBER model are given in Table 14.

Table 14. Distribution coefficients for sorption onto rock used in AMBER

Element (oxidation state)	Kd (m^3/kg)
U(IV)	0.053
Am	0.015
Pu(IV)	1.50E-05
C_org	0
C_inorg	0
Ac	0.015
Pa(V)	0.059
Tc(IV)	0.053
I	0
Ag	0
Ni	0.00074
Ra	0.001
Mo	0
Th	0.053
Pb	0.025
Np(IV)	0.053

Advective transport through the fracture is calculated using advective travel times, t_w, flow related transport resistances, F, and a Peclet number applicable to the whole rock volume, which are all derived from hydrogeological calculations for the geosphere performed with the code DarcyTools. The flow wetted surface area is calculated as the flow related transport resistance divided by the travel time. Figures

A-2 (Figure 14) and A-3 in TR-14-09 show the distributions of the travel times and flow wetted surface areas for the different vaults and the silo at different times. The values used in the Global Warming Calculation Case were taken from the ECOLEGO model files. These are reported in Table 15. Dispersion was not modelled explicitly in the AMBER model, but instead was represented implicitly by using a discretisation that results in an amount of numerical dispersion that may be comparable to the amount of dispersion that would be expected in reality. We could not find the Peclet number used by SKB in their reports.
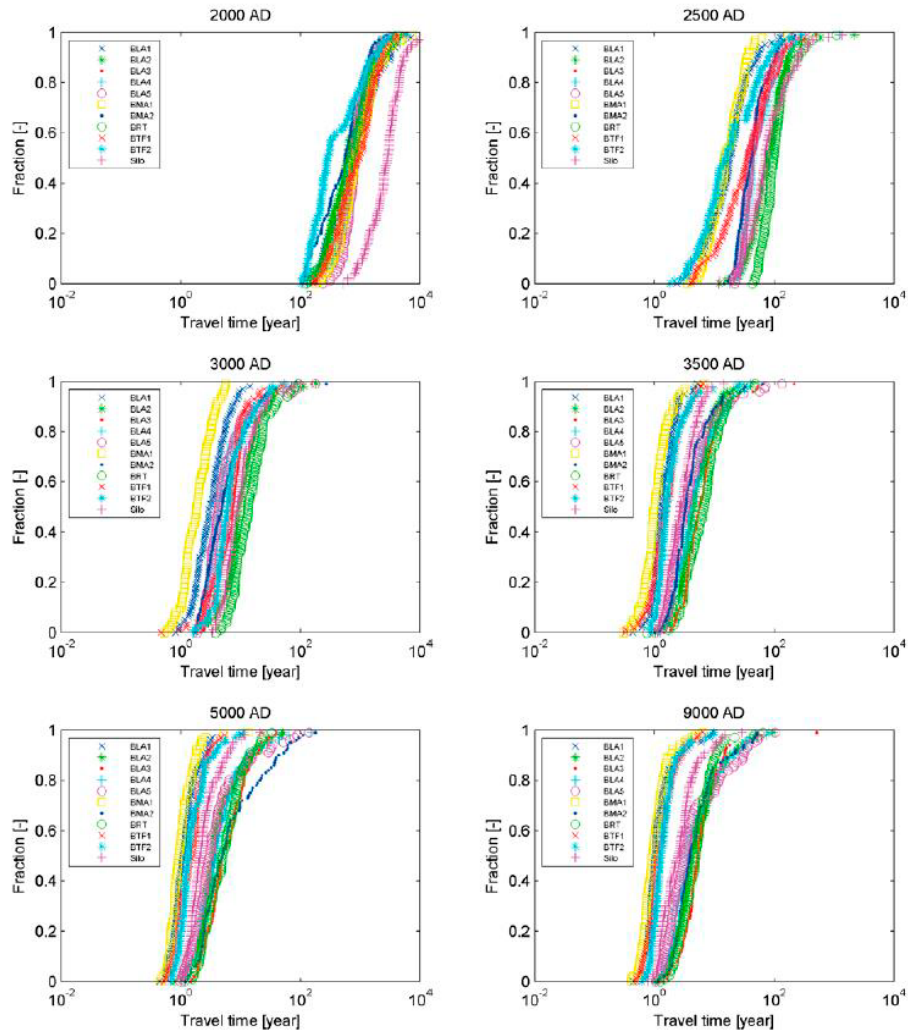

Figure A-2. Subset of 100 travel time samples (used in CCM_GW), selected from bedrock case 1 (Odén et al. 2014).

Figure 14. Distributions of geosphere travel time (Figure A-2 in TR-14-09)

Table 15. Geosphere travel times and flow wetted surface areas from the ECOLEGO model for the global warming calculation case

Time (AD)	Travel time (y)	Flow wetted surface area (m^{-1})
2000	554.7	8981
2500	44.83	7299
3000	4.84	9753
3500	3.79	11191
5000	3.67	11251
9000	3.65	11318

P25 in TR-14-09 states that, during a transitional phase from one stage of landscape development to another, water flow related data are interpolated linearly in time between the data sets representing the initial and the final stage of the transition. Therefore the flow related transport parameters were linearly interpolated in the AMBER model. None of the other geosphere properties are considered to vary over time (i.e. fracture network / spacing, matrix diffusion coefficient for rock, porosity of the rock, sorption distribution coefficients).

4   Calculation Cases

The preceding sections described re-implementation of the ECOLEGO models for the 2BMA vault and geosphere in AMBER. The AMBER model was run deterministically for the Global Warming Calculation Case of the main scenario and the results compared against ECOLEGO. A number of variant calculations cases were then implemented to help explore the behaviour of the AMBER model, but also the differences between the AMBER and ECOLEGO model results. The calculation cases are summarised in Table 16. The logic behind some of the cases requires further explanation, and this is provided subsequently, together with any case specific input data. The results are presented in the next section.

Table 16. Summary of calculation cases

Calculation Case	Description	Objective
Base	Re-implementation of SKB's models for the 2BMA vault and geosphere, as described in Section 2.	Explore, understand and build confidence in SKB's ECOLEGO models.
NF_Var1	Increased discretisation of the wasteform into inner and outer compartments.	Examine the sensitivity of the model results to the increased level of discretisation adopted by SKB.
NF_Var2	Changes in flows associated with degradation of concrete are interpolated linearly rather than step-changes.	Examine sensitivity of the model results to gradual changes in near-field barrier hydraulic properties compared with the assumption of step changes.
NF_Var3	No diffusion. Advection only.	Explore the relative importance of advection and diffusion for radionuclide transport.

NF_Var4	No advection through the caissons, diffusion only. There is still advection within the macadam, and from the macadam into the rock, since the model does not include diffusion into the rock.	Explore the relative importance of advection and diffusion for radionuclide transport.
NF_Var5	Instead of cracking of the caissons and moulds occurring instantaneously at 22,000 AD, cracking is assumed to occur progressively between 22,000 AD and 52,000 AD, with retardation factors linearly decreasing to zero over this period. As in the base case, the grout and cementitious wasteforms are assumed not to crack.	Used to test sensitivity of the model results to different model assumptions as SKB's approach is unclear.
NF_Var6	Fracture model is not applied to cementitious materials.	Used to test sensitivity of the model results to different model assumptions as SKB's approach is unclear.
NF_Var7	The properties of the wastes are varied.	Examine sensitivity of the model results to the properties assumed for the cementitious wasteforms.
NF_Var8	Direction of transport is not accounted for in selection of the cross-sectional areas for diffusive transport.	Used to test sensitivity of the model results to the interface areas used in the calculations since SKB's approach is unclear.
NF_Var9	Simplified model of the 2BMA vault that merges the 14 caissons into a single large caisson.	Explore sensitivity to discretisation. Also, since a simpler model can be checked more easily and with greater confidence than a detailed model, obtaining similar results would build confidence that the detailed geometry and flows have been correctly implemented in the detailed models.
NF_Var10	Simplified model of the 2BMA vault that only represents one caisson, but the radionuclide fluxes are then scaled by a factor of 14 to account for the other caissons.	As NF_Var9, but using a different approach.
NF_Var11	Probabilistic case.	As base case, but for probabilistic calculations.
NF_Var12	Representation of the caisson walls.	To test sensitivity of the radionuclide fluxes to discretisation of the caissons.
NF_Var13	Combination of NF_Var6 and NF_Var12.	Combination of changes to provide a 'best fit' against ECOLEGO.
GEO_Var1	Input of ECOLEGO near-field fluxes to the AMBER geosphere model.	Used to test the AMBER geosphere model independent of the near-field model.

NF_Var1

In the base model the embedded and solidified wastes were each represented using a single compartment. In this variant case, each waste type was sub-divided into an inner waste compartment and an outer waste compartment (Figure 2). Additionally the concrete moulds associated with the cement solidified and concrete embedded wastes were represented by separate compartments, rather than a single

compartment. This mirrors the configuration deduced from the ECOLEGO model files. The objective of this calculation case was to test the sensitivity of the model results to the increased level of discretisation adopted by SKB.

The inner and outer waste compartments were assumed to have the same volume, with the inventory split evenly between them. Table 17 describes the dimensions of the wasteform compartments. Table 18 describes the diffusion distance for each compartment.

The flows through the wastes were scaled relative to the inside of the caissons using the approach previously described for the base case. We assumed that half the flow through the waste package passes through the inner waste compartment, while the full flow through the waste package passes through the outer waste compartment.

This modification was only implemented for Caisson 1. The sensitivity of the model results to the greater discretisation was investigated by comparing the forward flux out of the caisson into the macadam with the base case.

Table 17. Dimensions of the wasteform compartments in calculation case NF_Var1

Container	Dimension	Value (m)	Notes
Mould	Length, width, height of the inner compartment	0.794 m	
Drum	Height of the inner compartment	0.68 m	Assumed to be 0.2 m less than height of the outer compartment
Drum	Diameter of the inner compartment	0.475 m	So the volume of the inner and outer compartments are both equal to half the total

Table 18. Diffusion distances from the mid-point to the outer edge of the compartments in calculation case NF_Var1

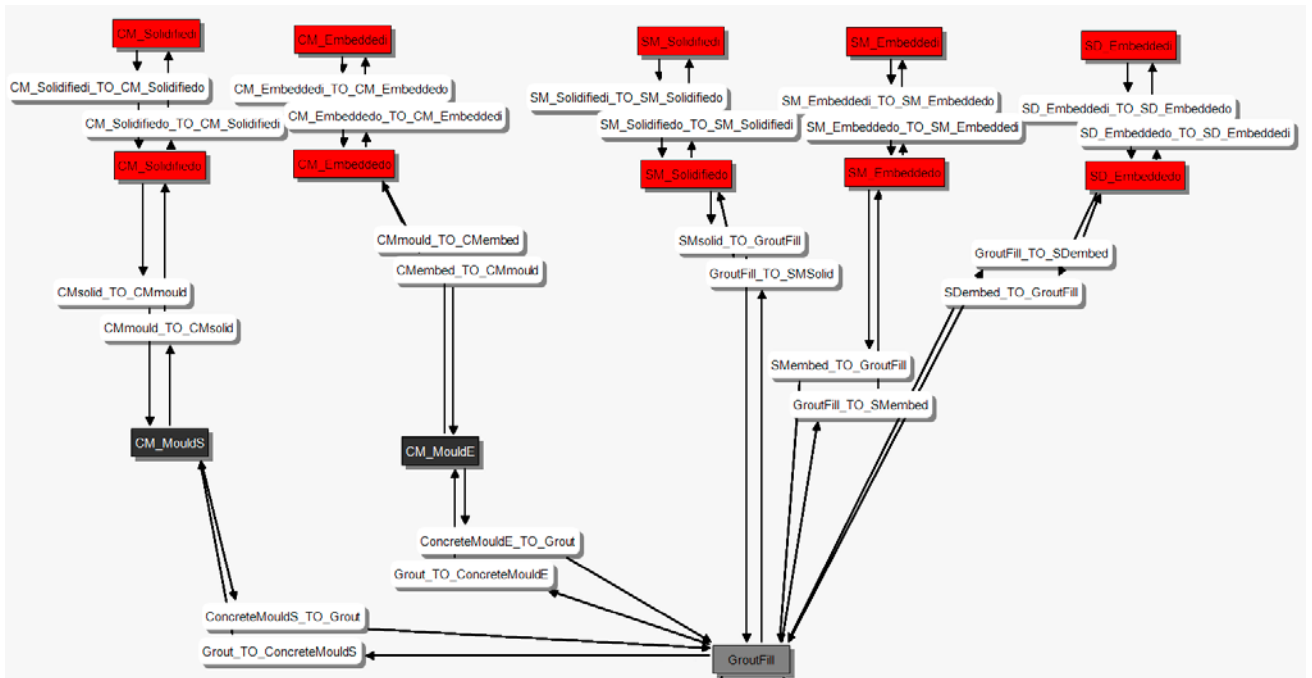| Container	Diffusion Distance	Value (m)
Mould inner	X, Y and Z directions	0.397 m
Mould outer	X, Y and Z directions	0.0515 m
Drum inner	Z direction	0.237 m
Drum inner	Radial (X, Y directions)	0.0289 m
Drum outer	Z direction	0.34 m
Drum outer	Radial (X, Y directions)	0.05 m

Figure 15. Modified configuration of the AMBER model for Caisson 1 (compare with Figure 1)

NF_Var2

The objective of this calculation case was to examine sensitivity of the model results to gradual changes in near-field barrier hydraulic properties compared with the assumption of step changes in the base case. Flows through the near-field in response to changes in the concrete degradation state at 22,000 AD and 52,000 AD were assumes to occur linearly rather than as step changes. Therefore flows through the caissons and macadam were linearly interpolated between values at 3000 AD, 22,000 AD and 52,000 AD. As for the base case there was no further evolution of flow beyond 52,000 AD, except for the cessation of flow under peri-glacial conditions.

NF_Var3, NF_Var4

These are not considered to be realistic cases but are used to explore the relative importance of advection and diffusion for radionuclide transport. Advection within the macadam, and from the macadam into the rock, is retained in the NF_Var4 model because there is only advection from the macadam to the rock. So, if this was not done there would be no transport from the near-field to the geosphere.

NF_Var5, NF_Var6

No additional information required.

NF_Var7

The properties of the cement solidified and cement embedded wastes were set equal to those given in the ECOLEGO model for the material "waste cement". As noted previously we could not deduce the mapping between the different materials specified in ECOLEGO and the compartments that represent the waste packages, so this may be an inappropriate choice of parameter values. Nevertheless, this still remains a useful test of the sensitivity of the model results to the parameter values. The following values were used:

- Density 560 kg/m^3 – this is very low and is presumably an effective value, perhaps accounting for the fraction of the wasteform that is cement, but this may not be the case.
- Porosity 0.33.
- Fraction cement 1.
- Effective diffusivity - Table 19

Table 19. Effective diffusivity for waste cement

Time (AD)	Effective Diffusivity (m^2/s)
2000 – 2100	3.0E-10
2100 – 2500	3.5E-10
2500 – 3000	5.0E-10
3000 – 12000	1.0E-9
12000 – 22,000	1.0E-9
22,000 – 52,000	1.0E-9
52,000 – 100,000	1.0E-9

NF_Var8

In Section 1.2 is was noted that in the AMBER model, for radial compartments, such as used to represent the caissons, the cross-sectional area of the donor compartment was used for transfers away from the wastes, while the cross-sectional area of the receptor compartment was used for backwards diffusive transfers towards the waste. Therefore the same interface area was used for the forwards and backwards transfers. It was not clear if this was done in SKB's ECOLEGO model. In this variant case, the cross-sectional area of the donor compartment was used for all transfers.

NF_Var9

The objective of this case was to explore sensitivity to discretisation. Also, because a simpler model can be checked more easily and with greater confidence than a detailed model, obtaining similar results would build confidence that the detailed geometry and flows have been correctly implemented in the base case AMBER model. Since the base case AMBER results are broadly similar to the ECOLEGO model results, this could also build confidence in the ECOLEGO models.

The model was simplified by merging the 14 caissons into a single large caisson. Therefore the macadam backfill between the caissons was not represented in the

model. The representation of the macadam backfill in the loading area and at the other end of the vault was not changed. The arithmetic mean of the flows through the 14 caissons and associated macadam backfill was used in the model (Table 20).

Table 20. Arithmetic mean of flows through the caissons and associated macadam backfill (m³/y) at times corresponding to different shoreline positions (2000, 3000 and 5000 AD) and concrete degradation states (Table 6)

Flow (m³/y)	Time (AD)				
	2000	3000	5000	22,000	52,000
Macadam parallel	1.80E-01	1.25E+01	1.36E+01	1.36E+01	1.37E+01
Macadam perpendicular	1.99E-02	1.51E+00	1.92E+00	1.91E+00	1.91E+00
Caisson	2.90E-04	2.10E-02	2.43E-02	1.58E+00	7.41E+00

NF_Var10

The objective of this case was the same as case NR_Var9, but a different approach was used. In this case a single caisson was represented, and the other 13 caissons were removed from the model. The representation of the macadam backfill in the loading area and at the other end of the vault was not changed. The arithmetic mean of the flows through the 14 caissons and associated macadam backfill was used for the single modelled caisson (Table 20). The calculated fluxes from the near-field to the geosphere were then scaled by a factor of 14. This approach assumes the inventory in each caisson is the same, which is acceptable because the same assumption is also made in the base case.

NF_Var11

Effective diffusivity and sorption distribution coefficient parameter distributions were added to the base case model of the 2BMA vault. Effective diffusivity parameter distributions are given in Table 7. Sorption distribution coefficient parameter distributions are given in Table 21 to Table 23. The data for cements are 'base values' that need to be scaled by the fraction of cement paste in the material (Table 4-5 in TR-14-09 or Table 7-12 in TR-14-10).

The sorption distribution coefficients for cement are log triangular distributions. The minimum value for iodine is zero, so TR-14-10 recommends that a triangular distribution is used for iodine.

The model was run for 100 realisations using Latin Hypercube Sampling. The radionuclide fluxes from the near-field to the geosphere were reported for comparison with the ECOLEGO results. Only the radionuclides that dominate the fluxes from the near-field to the geosphere were included in the model to enable results to be calculated in a reasonably practical run-time.

Table 21. Sorption distribution coefficient parameter distributions for State I cement. Log Triangular distributions, except for I which is a triangular distribution. (Table 7-7 in TR-14-10).

Element	Modal Kd (m³/kg)	Maximum Kd (m³/kg)	Minimum Kd (m³/kg)
C_inorg	2.0E+00	3.0E+00	7.0E-01
C_org	0.0E+00	0.0E+00	0.0E+00
I	1.0E-03	1.0E-02	0.0E+00
Mo	3.0E-03	3.3E-02	3.0E-04
Ni	3.0E-02	4.0E-01	2.0E-02
Tc	3.0E+00	2.0E+01	7.0E-01

Table 22. Sorption distribution coefficient parameter distributions for State II cement. Log Triangular distributions, except for I, which is a triangular distribution. (Table 7-8 in TR-14-10).

Element	Modal Kd (m³/kg)	Maximum Kd (m³/kg)	Minimum Kd (m³/kg)
C_inorg	5.0E+00	2.0E+01	2.0E+00
C_org	0.0E+00	0.0E+00	0.0E+00
I	1.0E-03	1.0E-02	0.0E+00
Mo	3.0E-03	3.3E-02	3.0E-04
Ni	2.0E-01	2.0E+00	8.0E-02
Tc	3.0E+00	2.0E+01	7.0E-01

Table 23. Sorption distribution coefficient parameter distributions for rock. Truncated normal distributions. (Table 8-6 in TR-14-10).

Element	Best Estimate Kd (m³/kg)	μ	σ	Maximum Kd (m³/kg)	Minimum Kd (m³/kg)
C_inorg	0.0E+00	-	-	0.0E+00	0.0E+00
C_org	0.0E+00	-	-	0.0E+00	0.0E+00
I	0.0E+00	-	-	0.0E+00	0.0E+00
Mo	0.0E+00	-	-	0.0E+00	0.0E+00
Ni	7.4E-04	-3.13	0.79	2.1E-05	2.7E-02
Tc	5.3E-02	-1.28	0.65	2.8E-03	9.8E-01

NF_Var12

The objective of this case was to test sensitivity of the radionuclide fluxes from the near-field to the geosphere to representation of the caisson walls. In the base case, each of the five compartments used to represent the caisson was set to have an equal thickness of 0.2 m. A better representation of the diffusive transport process is gained if the compartments gradually increase in thickness.

In this case, the first caisson compartment, which includes the inner surface of the caisson, was set to be 0.01 m thick. The thickness of the compartments was then incrementally increased to give a total wall thickness of 1 m.

Equation 9-25 in TR-14-09 was used to calculate an incremental increase in the thickness of the other compartments. The thickness of the caisson compartments was as follows:

- Caisson compartment 1 (innermost), 1.00E-02 m.
- Caisson compartment 2, 2.84E-02 m.
- Caisson compartment 3, 8.07E-02 m.
- Caisson compartment 4, 2.29E-01 m.
- Caisson compartment 5 (outermost), 6.52E-01 m.

NF_Var5, NF_Var6

No additional information required.

GEO_Var1

The radionuclide fluxes from the ECOLEGO model of the 2BMA vault were input to the AMBER geosphere model. The objective was to compare radionuclide transport behaviour in the two geosphere models independent of the differences in the near-field models.

5 Results

5.1 Base Case

Figure 16 shows the location of activity in the AMBER model with time. The dashed black line is the total activity. The decrease with time reflects radioactive decay, accounting for ingrowth, of the radionuclides included in the AMBER model. There is assumed to be no radionuclide transport during the first 1000 y, so transport begins at 3000 AD, and much of the activity migrates from the wastes (including the concrete moulds) into the grout. The majority of activity is retained in the grout throughout the assessment timeframe. Some activity is sorbed onto the concrete caisson, but this is rapidly released at 22,000 AD, when the caisson fractures and there is no longer considered to be sorption onto the caissons. Significant activity is never retained in the macadam backfill.
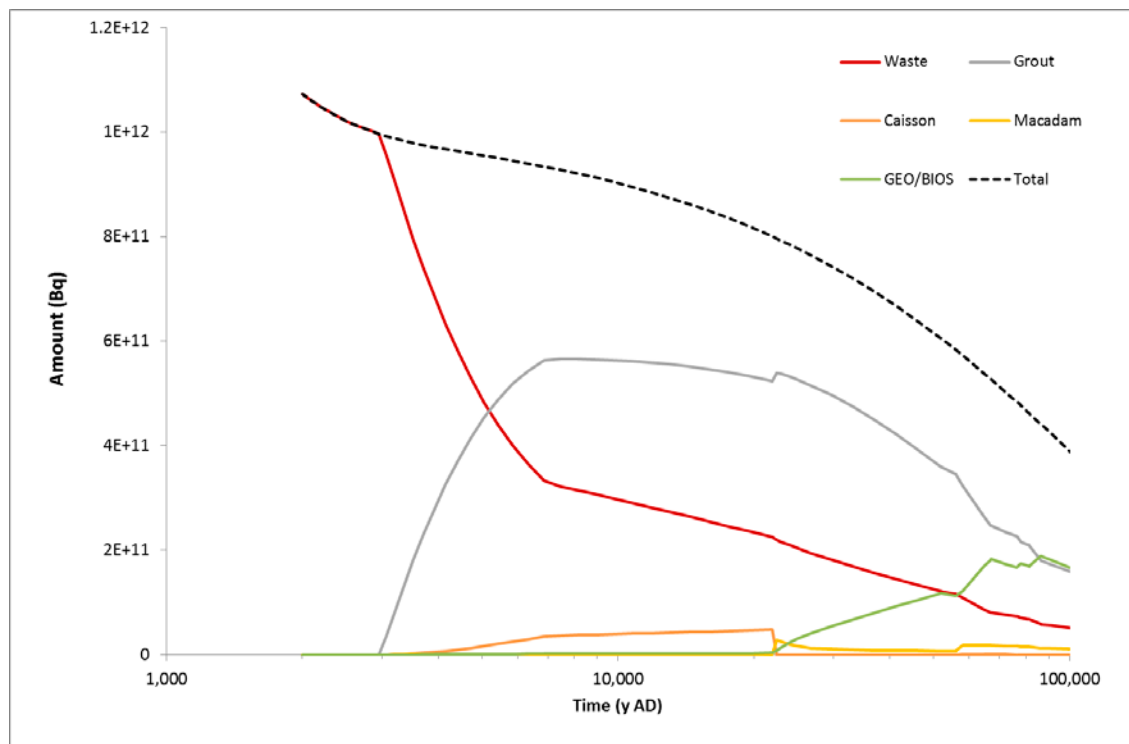
Figure 16. Location of activity in the AMBER model with time

Although Figure 15 shows that the majority of the activity is retained in the waste and grout, the caisson has an important role in providing a barrier to advection / diffusion. It is this physical barrier, in combination with sorption onto the cementitious wasteforms / grout, that retains most of the activity in the wastes and grout. Figure 15 shows that once the caissons become cracked at 22,000 AD releases to the geosphere / biosphere increase

Figure 17 shows the concentration of I-129 in Caisson 1. I-129 is shown due to its very long half-life so decay is not significant over the time period shown. At 3000 AD the concentrations in the wastes decrease significantly, and the concentration in the grout increases, reflecting the location of the activity shown in Figure 16. The concentrations in the waste and grout equilibrate. The concentration in the concrete moulds is lower because they container a lower fraction of cement than the wastes and grout, so I-129 sorbs less strongly onto the moulds.

There is no inventory associated with the wastes embedded in steel drums. However they are represented in the model. At 3000 AD, activity is able to migrate into grout, and then diffuse into the steel drums until the concentrations equilibrate with the other wastes.

The activity in the moulds decreases significantly at 22,000 AD when, consistent with assumptions for the caissons, the moulds are assumed become fractured and there is no longer any sorption onto the moulds. There are also changes in the physical and chemical properties of the near-field barriers at this time, resulting in increased flows through the caissons and reduced retardation through sorption. Therefore the concentrations in wastes and grout decrease more rapidly beyond 22,000 AD, compared with the earlier period of 3000 AD to 22,000 AD.
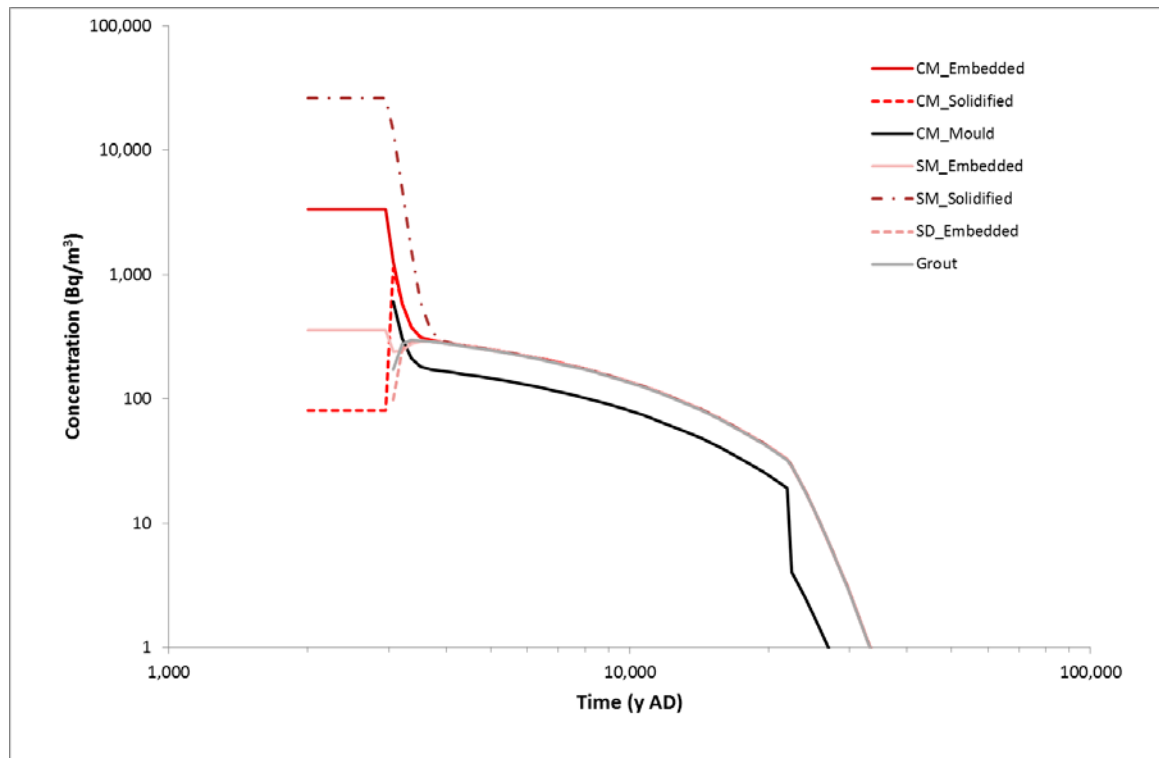
45

Figure 17. Concentration of I-129 in caisson 1 (CM = concrete mould, SD = steel drum, SM = steel mould)

Figure 18 compares the fluxes from the near-field to the geosphere calculated by the ECOLEGO and AMBER models. Results for radionuclides with the highest fluxes are compared. C-14_org is not sorbed, while I-129 and Mo-93 are only weakly sorbed. These three radionuclides exhibit similar behaviour, and the AMBER model results are similar to the ECOLEGO model. However, in all cases the radionuclide release is initially faster in the AMBER model, and the peak flux is higher. The fluxes then decrease more rapidly in the AMBER model because more of the inventory has been released at early times.

At 22,000 AD there is a step increase in flows through the near-field, and a corresponding step decrease in the performance of the near-field barriers. The increases in the fluxes of Mo-93 and I-129 are higher in the AMBER model than ECOLEGO, and the fluxes increase more rapidly. Increasing the number of output times immediately following this transition did not noticeably change the shape of the AMBER results curve, so it is a genuine result and is not down to the choice of output times.

Ni-59 is more strongly sorbed than Mo-93 and I-129. The shape of the AMBER Ni-59 curve is very similar to the ECOLEGO results, until 22,000 AD, but the flux is higher. At 22,000 AD the flux of Ni-59 calculated by AMBER increases markedly. The increase in the flux at 22,000 AD is greater than for Mo-93 and I-129. This shows the decreased sorption associated with degradation of the cementitious materials and cracking of the caissons and moulds has a more significant effect for Ni-59 than Mo-93 and I-129.

The decrease in barrier performance at 22,000 AD is also important for C-14_inorg, Tc-99 and Pu-239, which are all strongly sorbed. These three radionuclides all exhibit significant increases in fluxes at this time, and the increases are greater in the

AMBER model than calculated by ECOLEGO. Tc-99 is more strongly sorbed on the macadam than the other radionuclides presented, so although the fluxes increase significantly at 22,000 AD, Tc-99 does not exhibit the spike shown by the other radionuclides.

Overall, radionuclides are transported more rapidly through the near-field in the AMBER model compared with the ECOLEGO model. The peak near-field fluxes calculated by the ECOLEGO and AMBER models are compared in Table 24. Some of the potential reasons for these differences are explored in the variant calculation cases.

Figure 18. Comparison of radionuclide fluxes from the near-field into the rock calculated by the AMBER (AMB) and ECOLEGO (ECL) models

Table 24. Comparison of peak Near-Field fluxes calculated by the ECOLEGO and AMBER models

Radionuclide	Peak Flux ECOLEGO (Bq/y)	Peak Flux AMBER (Bq/y)	Ratio AMBER/ECOLEGO
C14_inorg	8.9E+00	1.0E+02	11
C14_org	3.4E+05	7.7E+05	2.3
Ni-59	3.5E+06	6.0E+06	1.7
Mo-93	6.4E+04	1.1E+05	1.7
Tc-99	5.1E+02	7.9E+02	1.5
I-129	3.9E+00	8.1E+00	2.1
Pu-239	8.9E+00	2.8E+00	0.3

Comparison of the radionuclide fluxes from the geosphere to the biosphere calculated by ECOLEGO and AMBER shows a similar pattern of differences to the

fluxes from the near-field to the geosphere. This suggests that the two geosphere models give broadly similar results, with the differences primarily arising due to the different fluxes from the near-field into the geosphere.

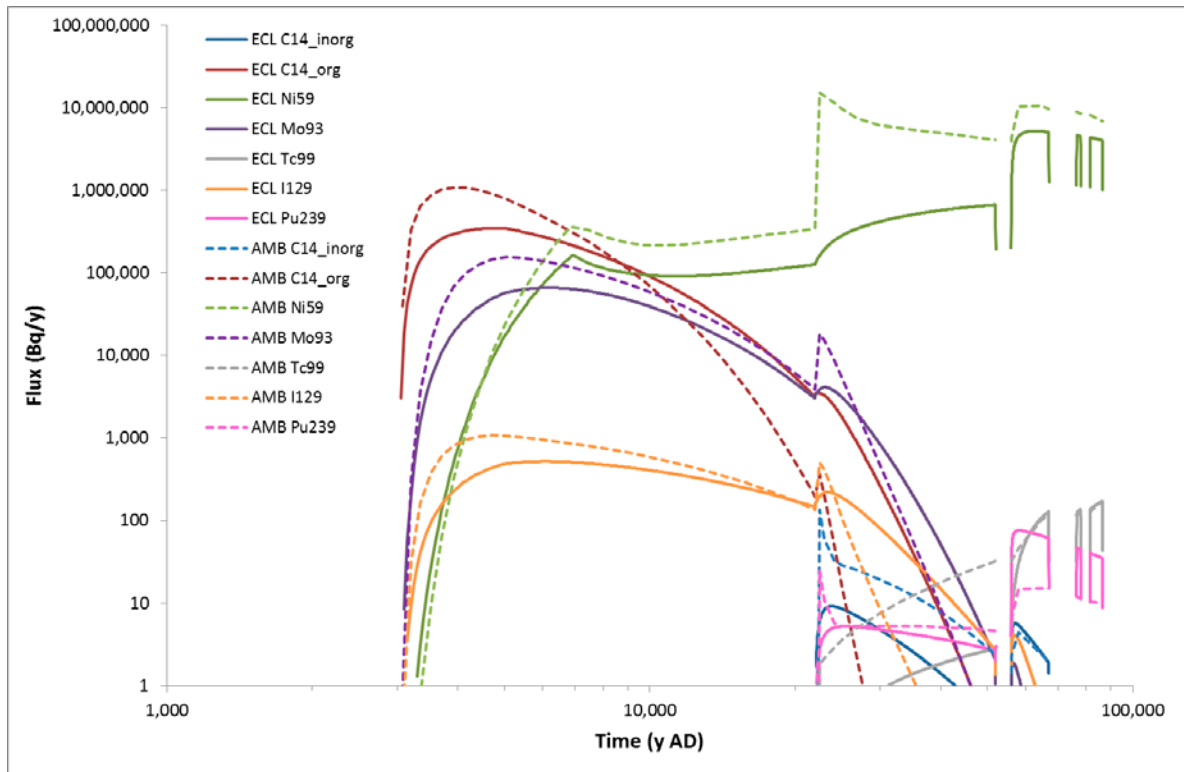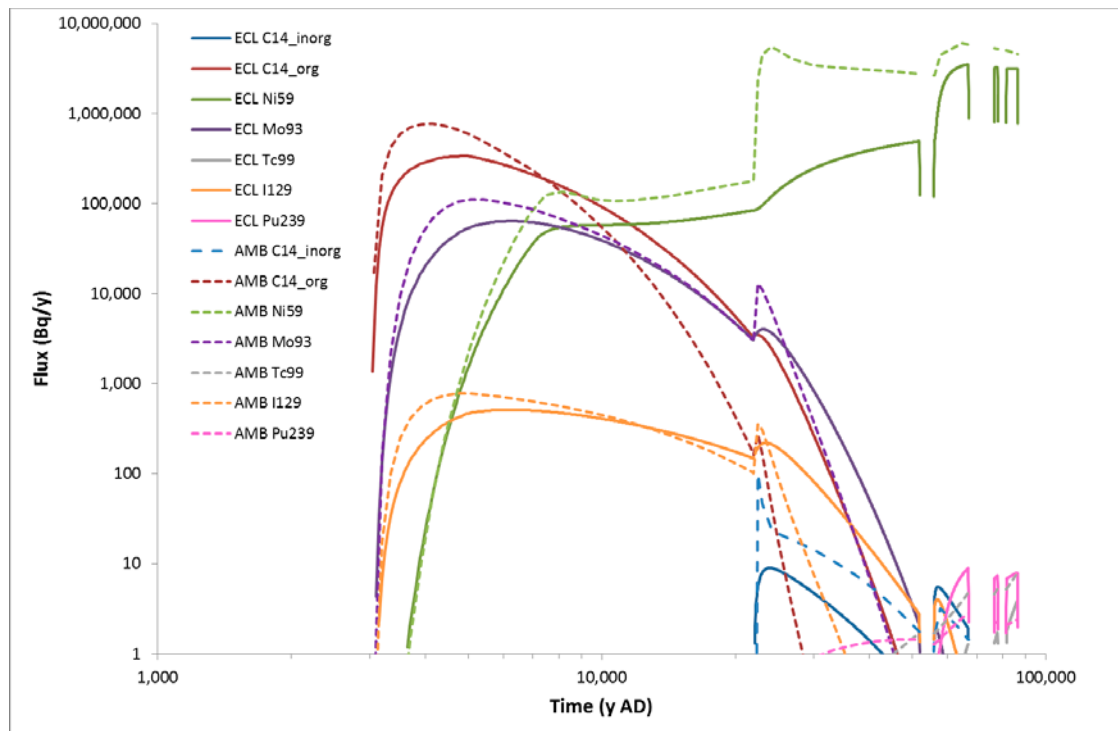**Figure 19. Comparison of radionuclide fluxes from the geosphere into the biosphere calculated by the AMBER (AMB) and ECOLEGO (ECL) models**

5.2 NF_Var1: Increased Discretisation of the Wastes

The discretisation of the cementitious wastes was increased, such that each type was represented by an inner and outer compartment. It was anticipated this would decrease the radionuclide fluxes out of the wastes, as there would be less numerical dispersion associated with calculation of radionuclide release from the wastes. In addition the concrete moulds containing cement solidified wastes and concrete encapsulated wastes were represented by separate compartments.

Figure 20 compares the radionuclide fluxes from Caisson 1 into the backfill to the results for the base case. The fluxes are actually slightly increased compared with the base case. This is because the diffusion distance from the outer waste compartments to the grout compartment is much smaller than the diffusion distance in the base case. This has a bigger effect than reducing the numerical dispersion by increasing the discretisation. It was concluded that the simpler representation of the waste packages in AMBER does not significantly contribute to the difference in the 2BMA model results.
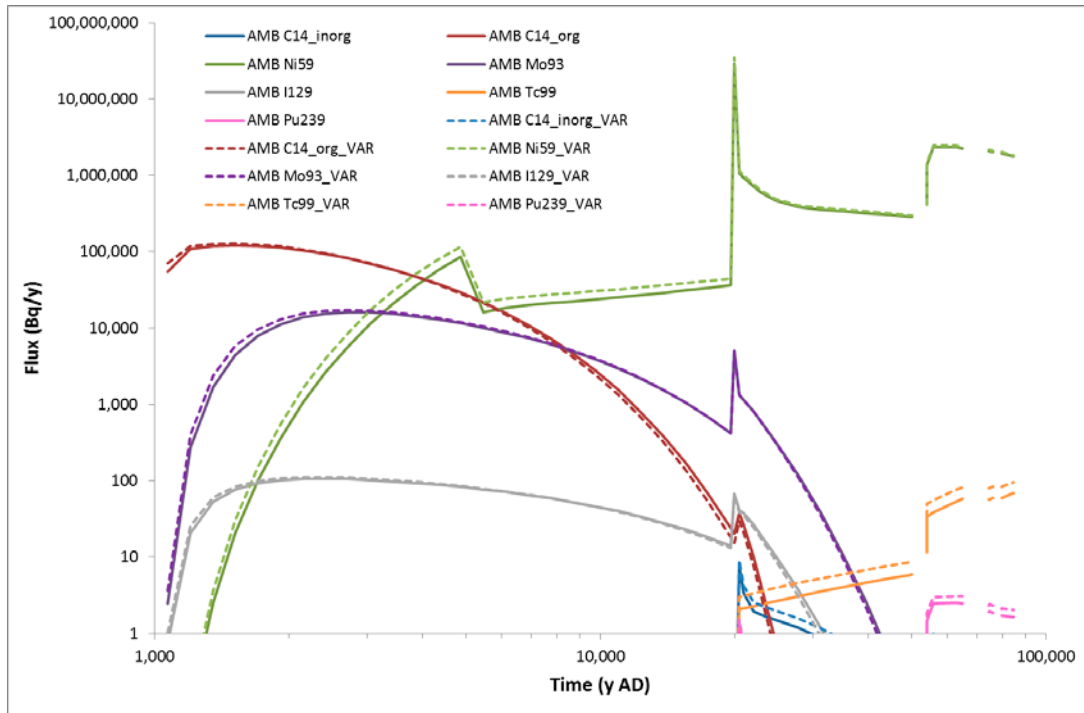
Figure 20. Radionuclide fluxes from Caisson 1 into the backfill in the base case and NF_Var1 case (*radionuclide*_VAR)

5.3 NF_Var2: Linear Interpolation of Flows

Flows through the near-field in response to changes in the concrete degradation state at 22,000 AD and 52,000 AD were assumes to occur linearly rather than as step changes. This change results in flows through the near-field increasing earlier than in the base case, and hence radionuclides being released earlier from the near-field. The peak fluxes are unchanged for C-14_org, Mo-93 and I-129, but are greater for the other radionuclides shown. The results build confidence that changes in near-field flows in response to changes in the concrete degradation state are applied as step-changes in the ECOLEGO model.
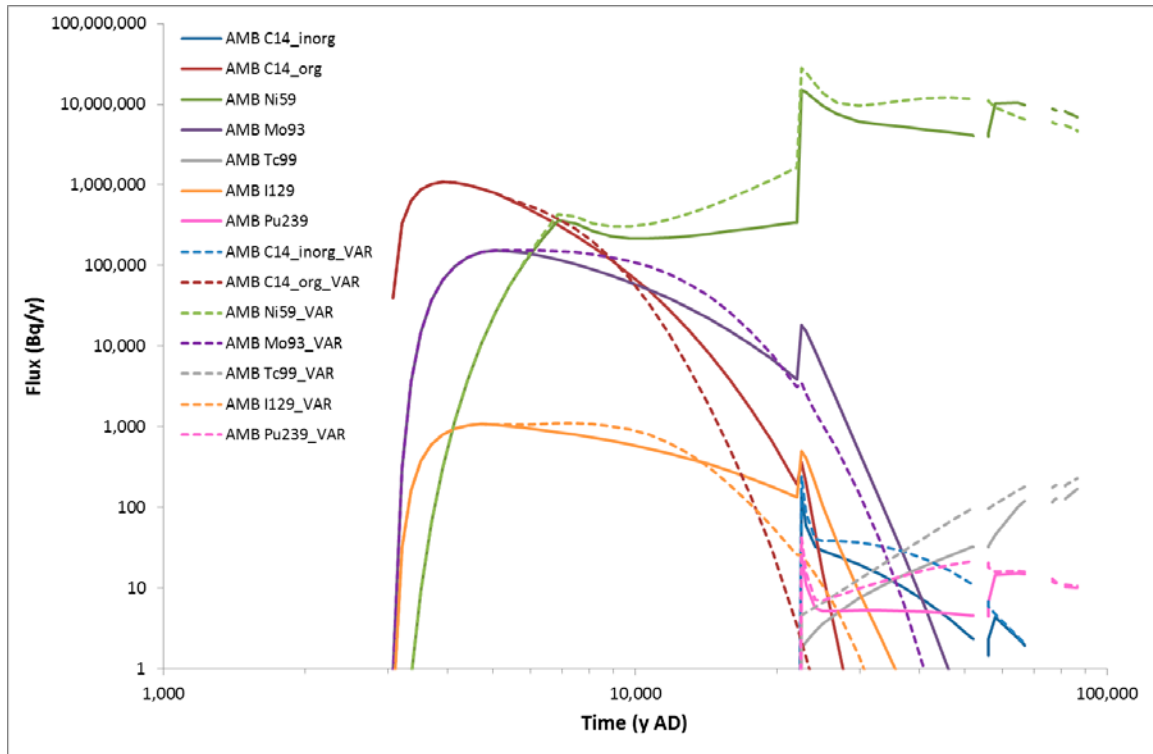
Figure 21. Radionuclide fluxes from the near-field in the base case and NF_Var2 case (*radionuclide*_VAR)

5.4 NF_Var3: No Diffusion, Advection Only

In this variant case there is no diffusion, only advection. The results show that release from the near-field is controlled by diffusion until 22,000 AD. Advection only becomes significant beyond 22,000 AD, when there is a step decrease in the performance of the near-field barriers. The fluxes of C-14_org, Mo-93 and I-129 are greater at this time than in the AMBER base case and ECOLEGO models. This is due to the greater inventories of these radionuclides remaining in the near-field at this time in the variant case.

It is noted that beyond 22,000 AD the flux of Ni-59 is similar to the ECOLEGO model. This suggests the greater fluxes calculated prior to this time in the AMBER base case, when compared to ECOLEGO, are because the diffusive flux is greater in AMBER. It also indicates the higher peak fluxes of C-14_org, Mo-93 and I-129 in the AMBER base case at early times, compared to ECOLEGO, are because the diffusive flux is greater in AMBER. This could be due to differences in the diffusion distances or in the cross-sectional areas for diffusion.

Figure 22. Comparison of radionuclide fluxes from the near-field into the rock calculated by the AMBER (AMB) and ECOLEGO (ECL) models. There is no diffusion in the AMBER model.

5.5 NF_Var4: No Advection, Diffusion Only

In this variant case there is assumed to be transport by diffusion only. Advection within the macadam and from the macadam into the rock is retained in the AMBER model because there is only advection from the macadam to the rock. So, if this was not done there would be no transport from the near-field to the geosphere. Figure 23 confirms the conclusions of the previous variant case, that the diffusive fluxes calculated by AMBER are higher than calculated by ECOLEGO and result in the higher radionuclide fluxes from the near-field to the geosphere before 22,000 AD. The results also show that diffusion from the caissons into the macadam is still an important process beyond 22,000 AD.
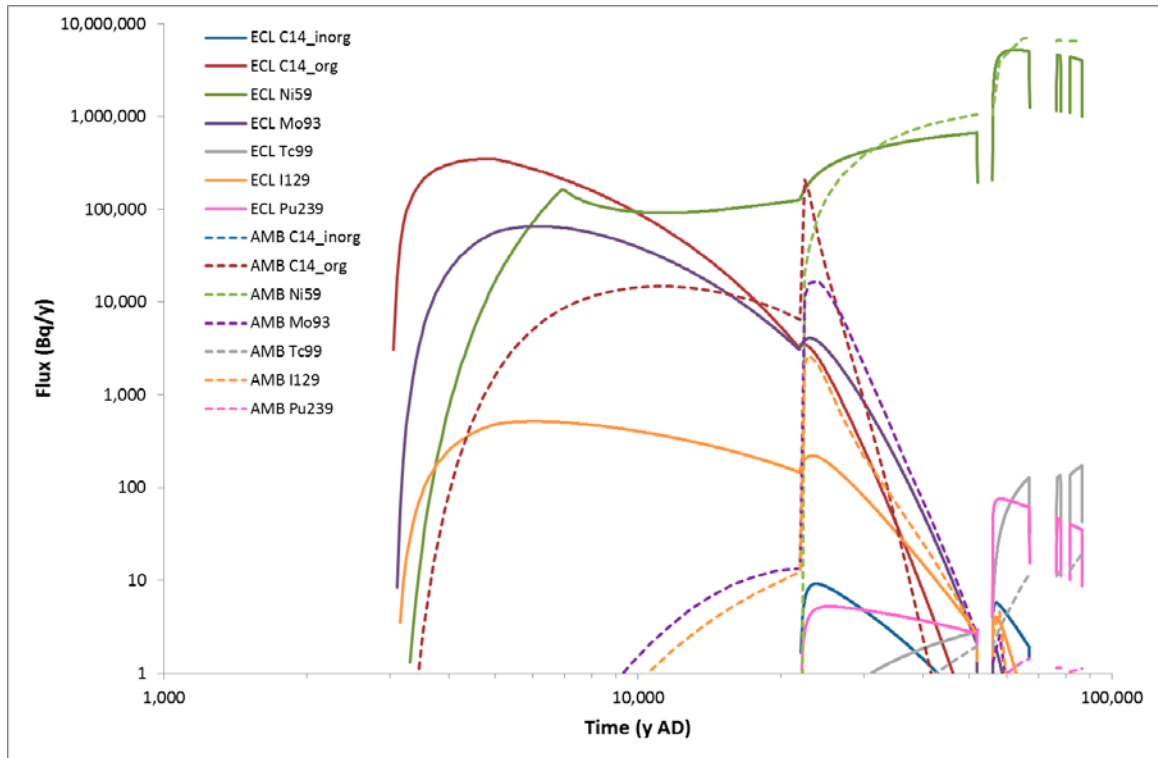
51

Figure 23. Comparison of radionuclide fluxes from the near-field into the rock calculated by the AMBER (AMB) and ECOLEGO (ECL) models. There is no advection through the caissons in the AMBER model.

5.6 NF_Var5: Progressive Fracturing of Structural Concrete

In this case, cracking of the caissons and moulds is assumed to occur progressively between 22,000 AD and 52,000 AD, rather than as a step change at 22,000 AD. Figure 24 shows that the spikes associated with release of radionuclides that were sorbed onto the caissons are removed, although there are significant increases in the fluxes of significantly sorbed radionuclides as the near-field barriers further degrade at 52,000 AD. The shape of the Ni-59 flux is much more similar to that calculated by ECOLEGO, but the flux is still significantly greater than calculated by ECOLEGO (Figure 25). Based on the results of this variant case, it was decided to explore a case in which there is not considered to be any fracturing of the concrete (NF_Var6).

Figure 24. Radionuclide fluxes from the near-field in the base case and NF_Var5 case (*radionuclide*_VAR)

Figure 25. Comparison of radionuclide fluxes from the near-field into the rock calculated by the AMBER (AMB) and ECOLEGO (ECL) models. There is progressive cracking of the caissons and moulds in the AMBER model.

5.7 NF_Var6: No Fracturing of Structural Concrete

In this variant case there was not considered to be fracturing of the caissons or moulds at any time. The shape of the AMBER Ni-59 curve is more similar to the ECOLEGO model, although the fluxes are higher (Figure 26). However, the AMBER model does not produce the significantly increased fluxes of C-14_inorg and Pu-239 at 22,000 AD. These are the most strongly sorbed radionuclides of those presented in the figure, so without the loss of sorption associated with cracking, the peaks in the fluxes of these radionuclides are not reproduced.
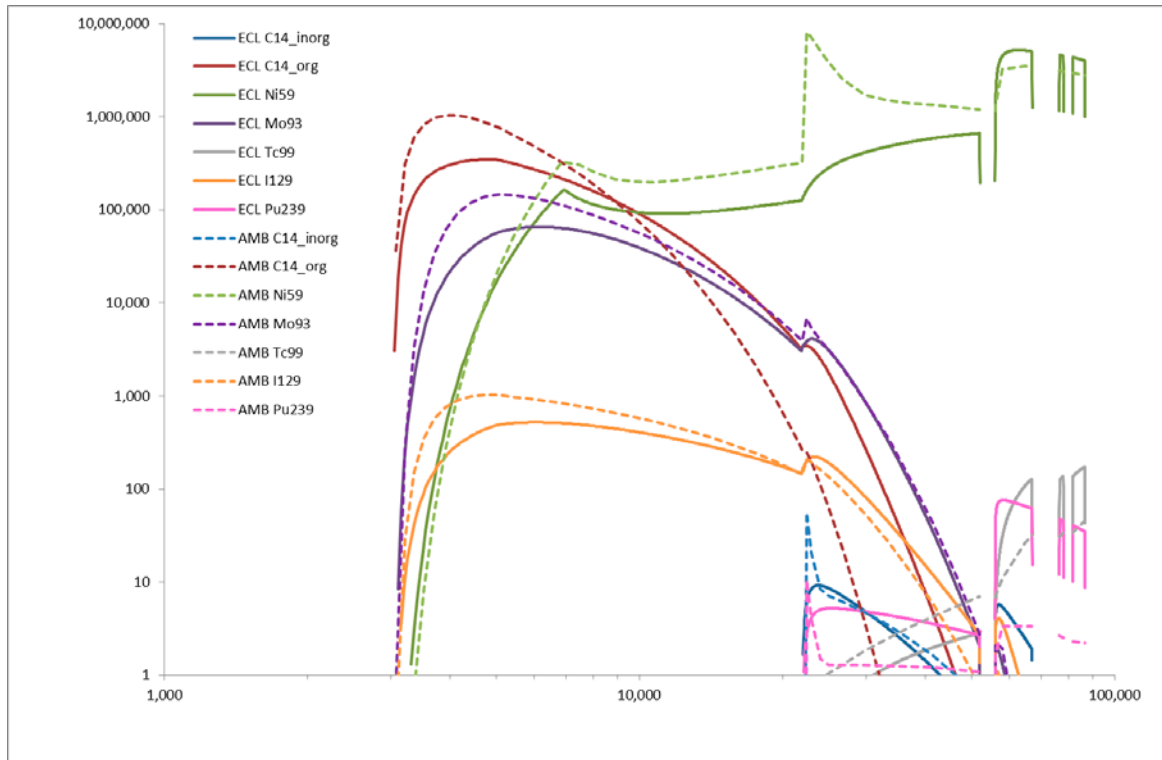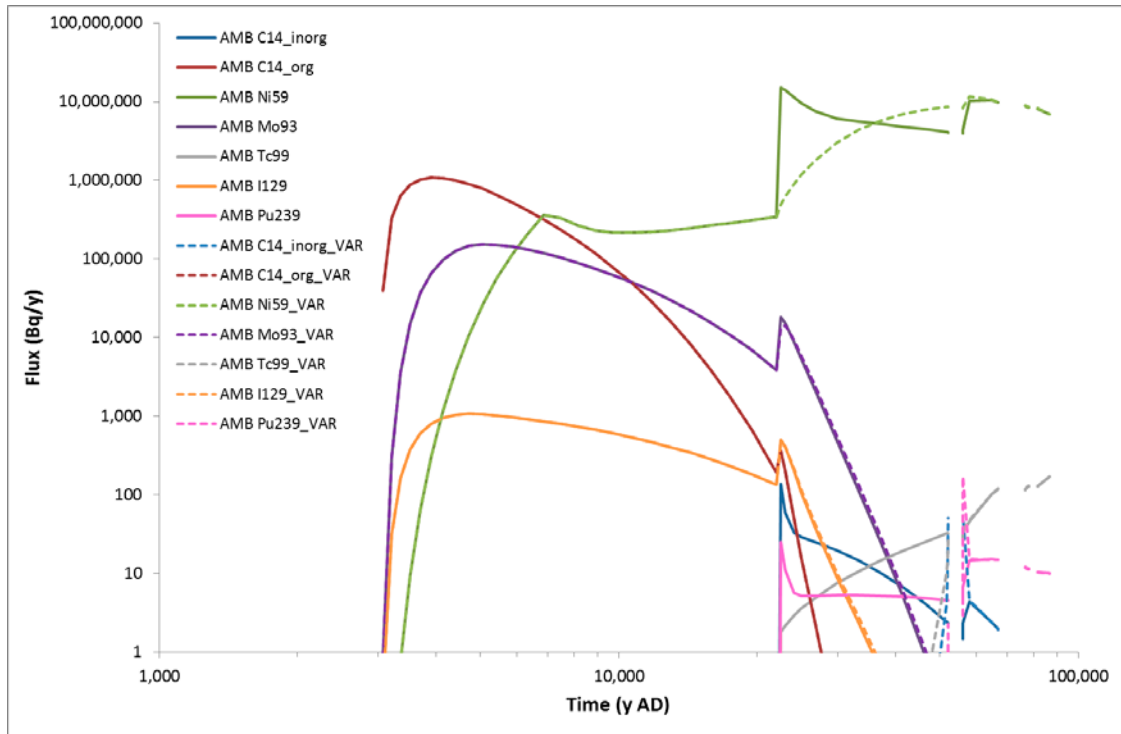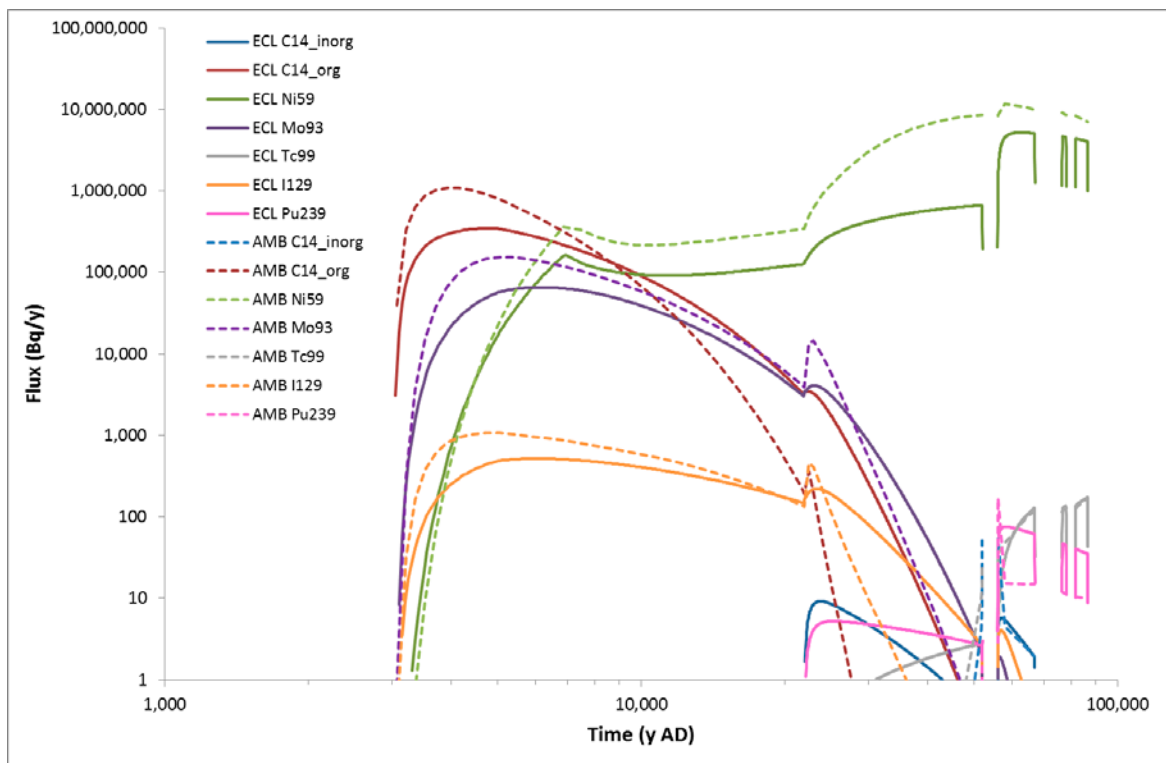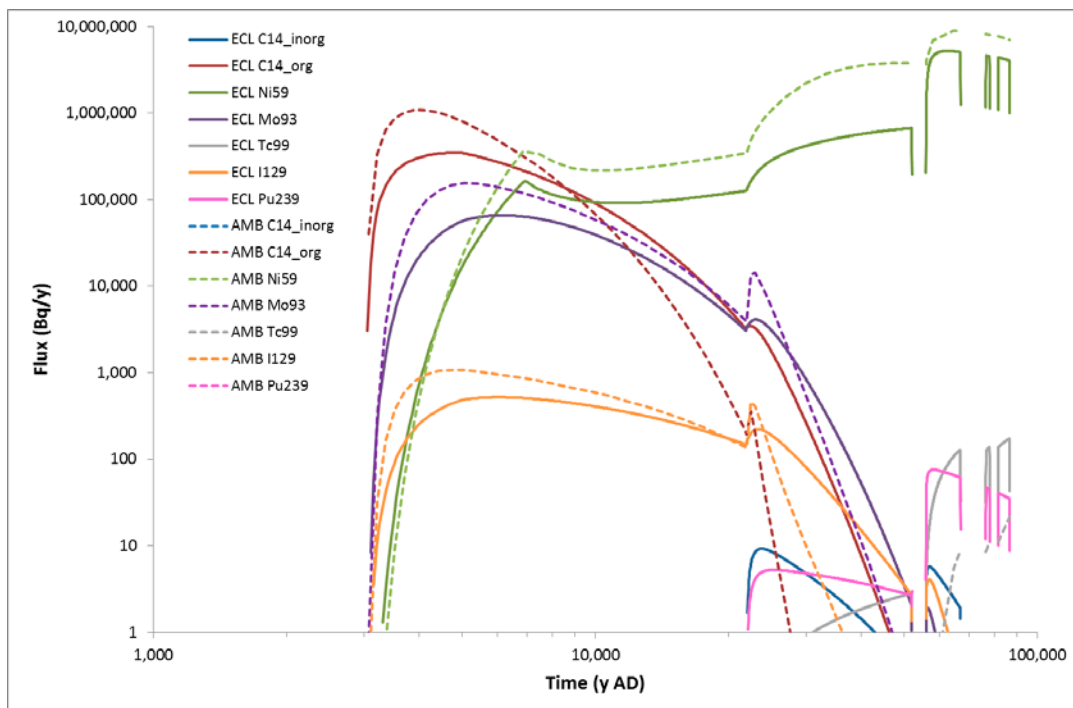

Figure 26. Comparison of radionuclide fluxes from the near-field into the rock calculated by the AMBER (AMB) and ECOLEGO models (ECL). There is no cracking of the caissons and moulds in the AMBER model.

The pattern of changes compared with the base case is different for those radionuclides that are more strongly sorbed, i.e. C-14_inorg and Pu-239, compared with those that are more weakly sorbed, i.e. Ni-59. A potential explanation is that that greater diffusive fluxes exhibited by the AMBER model compared with the ECOLEGO model (see Variant 4) increases the quantities of radionuclides sorbed onto the caisson that are rapidly released when the fracture model is invoked. Hence the AMBER model produces higher spikes in the radionuclides fluxes at 22,000 AD compared with the ECOLEGO model. By not invoking the fracture model, the spikes in the radionuclides fluxes are removed, and the increased fluxes are only due to the other changes to the barrier properties that occur at this time. This gives results more similar to ECOLEGO for the more weakly sorbed radionuclides, but less similar for the more strongly sorbed radionuclides.

5.8 NF_Var7: Properties of the Wastes

Changing the properties of the wastes had little impact on the fluxes calculated by AMBER (Figure 27). This builds confidence that the differences between the AMBER and ECOLEGO models are not due to the properties assumed for the cementitious wasteforms.
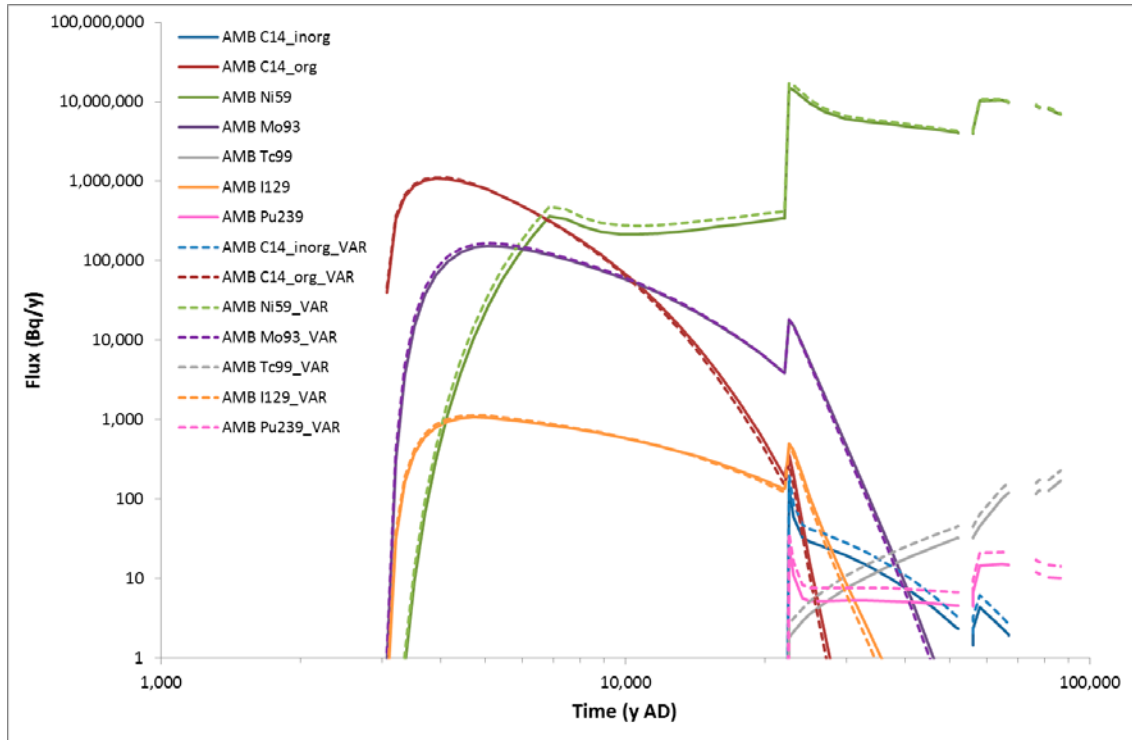
Figure 27. Radionuclide fluxes from the near-field in the base case and NF_Var7 case (*radionuclide*_VAR)

5.9 NF_Var8: Cross-sectional areas for diffusive transport

In the AMBER model, for radial compartments, such as used to represent the caissons, the cross-sectional area of the donor compartment was used for transfers away from the wastes, while the cross-sectional area of the receptor compartment was used for backwards diffusive transfers towards the waste. Therefore the same interface area was used for the forwards and backwards transfers. It was not clear if this was done in SKB's ECOLEGO model. In this variant case, the cross-sectional area of the donor compartment was used for all transfers.

The peak fluxes of C-14_org, Ni-59 Mo-93 and I-129 are more similar to the ECOLEGO model (Figure 28). This is because using the cross-sectional area of the donor compartment for the backwards transfers increases the backwards fluxes. This reduces the net forwards transfer rate, and hence the diffusive flux out of the caissons. However, this is not a correct representation of the system.

Although the AMBER model more accurately reproduces the peak fluxes calculated by ECOLEGO, the fluxes of C-14_org, Mo-93 and I-129 subsequently decrease more rapidly from their peak than calculated by ECOLEGO. The increased fluxes of Mo-93 and I-129 at 22,000 AD are more strongly attenuated than in the AMBER base case, so the shape of the flux curve is more rounded, and more similar to the ECOLEGO model.
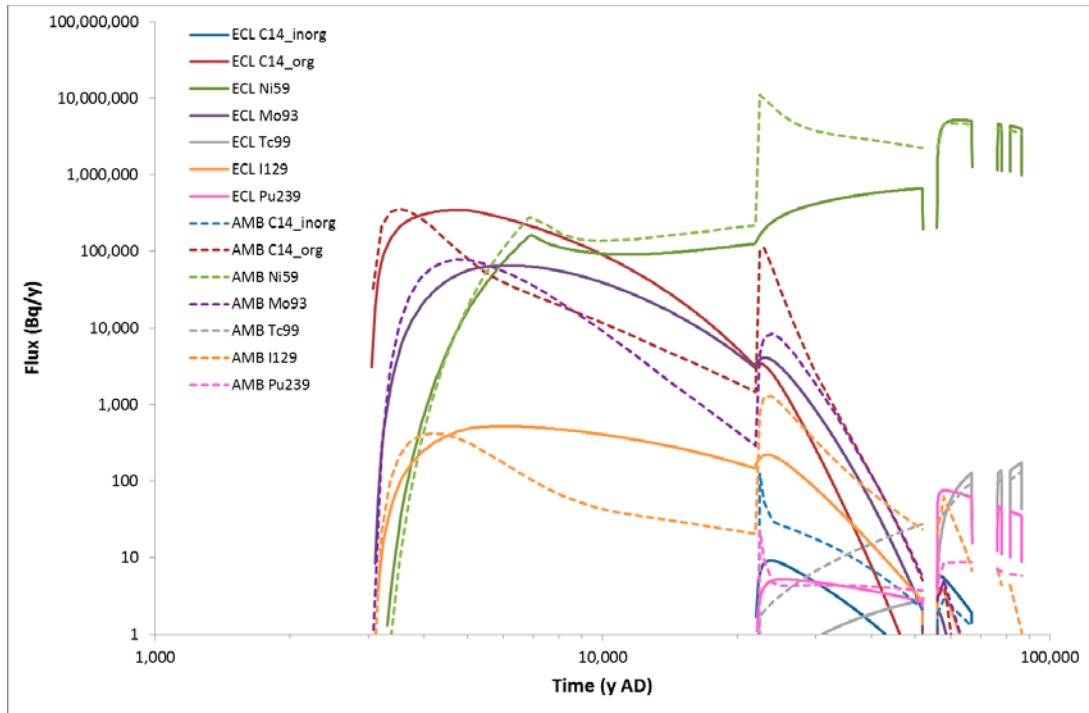
Figure 28. Comparison of radionuclide fluxes from the near-field into the rock calculated by the AMBER (AMB) and ECOLEGO (ECL) models. Cross-sectional areas for backwards diffusive transfers are set equal to the area specified for the donor compartment.

5.10   NF_Var9: Simplified Model

The objective of this case was to explore sensitivity to discretisation. Also, because a simpler model can be checked more easily and with greater confidence than a detailed model, obtaining similar results would build confidence that the detailed geometry and flows have been correctly implemented in the base case AMBER model. Since the base case AMBER results are broadly similar to the ECOLEGO model results, this could also build confidence in the ECOLEGO models.

The model was simplified by merging the 14 caissons into a single large caisson. The calculated radionuclide fluxes from the near-field to the geosphere are compared against the base case in Figure 29.

The fluxes calculated by the simplified model are approximately an order or magnitude lower than in the base case. This is because the advective transfer rate along the length of the vault depends on the ratio of flow velocity to the length. The flow velocity within the caisson has not changed from the base case (except than a average value is used), but the combined caisson is 14 times longer than an

individual caisson. Hence the advective transfer rate has decreased by a factor of approximately 14.

This shows that it is important to represent the individual caissons and the intervening macadam in the model. Two approaches to achieve this are: to represent the individual caissons and macadam explicitly; or to use the effective length of a single caisson to calculate the advective transfer rates in the simplified model. SKB have used the former approach, so this important aspect of the geometry has been represented in the ECOLEGO models.
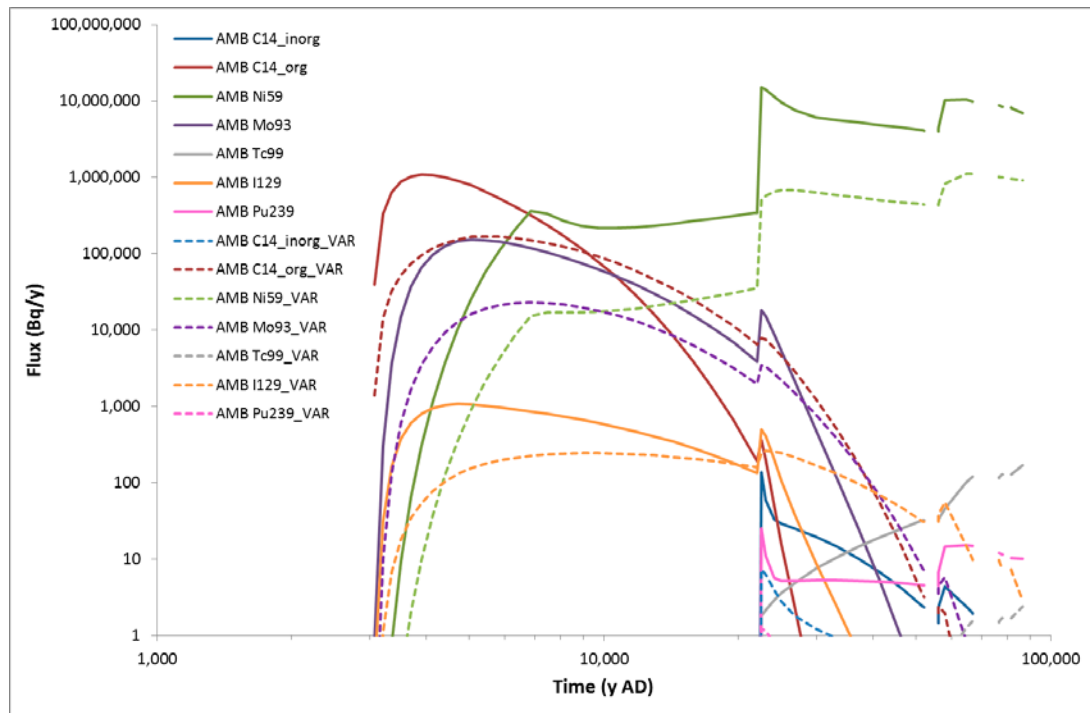
Figure 29. Radionuclide fluxes from the near-field in the base case and NF_Var9 case (*radionuclide*_VAR)

The objectives of this case were the same as case NR_Var9, but a different approach was used. In this case a single caisson was represented, and the other 13 caissons were removed from the model. The calculated fluxes from the near-field to the geosphere were then scaled by a factor of 14. The calculated radionuclide fluxes from the near-field to the geosphere are compared against the base case in Figure 30.

The fluxes are very similar to the base case model. This approach gives very similar results to the base case because the distance for transport along the length of the caisson to the macadam is the same as the base case. The small differences compared with the base case are due to the use of average flows rather than flows specific to each caisson, and also the single caisson is able to interact with the macadam at both ends of the vault, which is not possible in the base case model.

The results of this case confirm that it is important to represent the individual caissons and the intervening macadam in the model (see case NF_Var9). This model builds confidence that the complex geometry and near-field flows have been correctly implemented in the AMBER model and hence the ECOLEGO model.
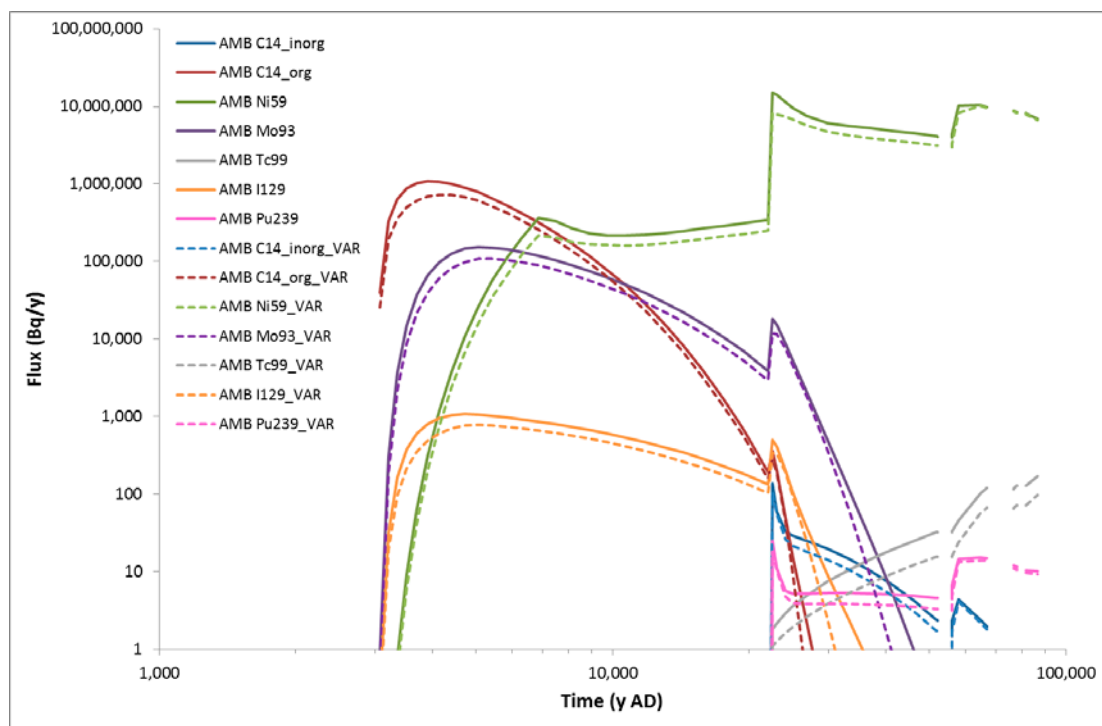
Figure 30. Radionuclide fluxes from the near-field in the base case and NF_Var10 case (*radionuclide*_VAR)

5.11 NF_Var11: Probabilistic Case

The effective diffusivity and sorption distribution coefficient parameter distributions described in Section 3 were added to the base case model of the 2BMA vault. The model was run for 100 realisations, and the radionuclide fluxes from the near-field to the geosphere were reported for comparison with the ECOLEGO results.

Since the base case (deterministic) AMBER results do not exactly match the ECOLEGO results, it was not clear from comparison of the probabilistic ECOLEGO and AMBER case results whether the differences had changed or not. Therefore, the probabilistic ECOLEGO results (Figure 31) were compared against the base case ECOLGEO results, and the probabilistic AMBER results were compared against the base case AMBER results (Figure 32). For both models, the mean radionuclide fluxes from the probabilistic calculations were compared against the deterministic base case result. The differences between the deterministic and probabilistic results are similar for the AMBER and ECOLEGO models. This builds confidence in implementation of the probabilistic calculations in ECOLEGO.

In Section 4 it was noted that a triangular distribution is used for iodine, rather than a log triangular distribution, because the minimum sorption value is zero. A run was also undertaken in which a log triangular distribution was used for iodine, with a minimum Kd of 1E-10 kg/m^3. The results are shown in Figure 33. It is notable that this approach gives a slightly higher peak flux of I-129.
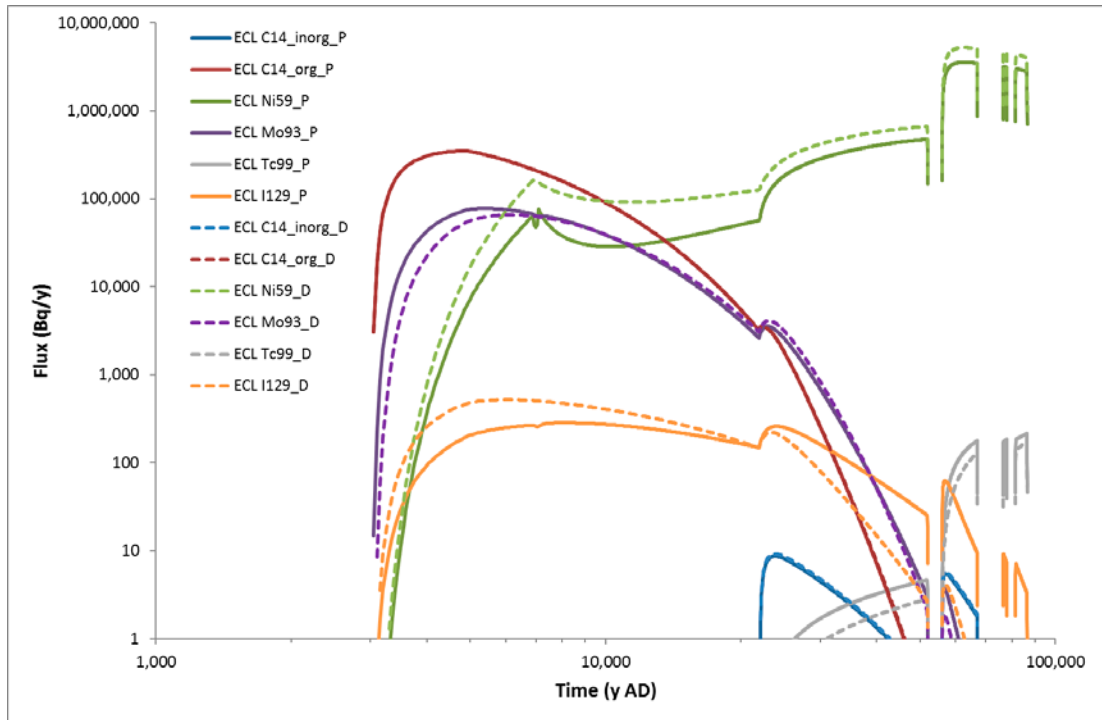
Figure 31. Deterministic radionuclide fluxes from the near-field in the base case (*radionuclide*_D) and probabilistic fluxes in the NF_Var11 case (*radionuclide*_P) calculated by ECOLEGO
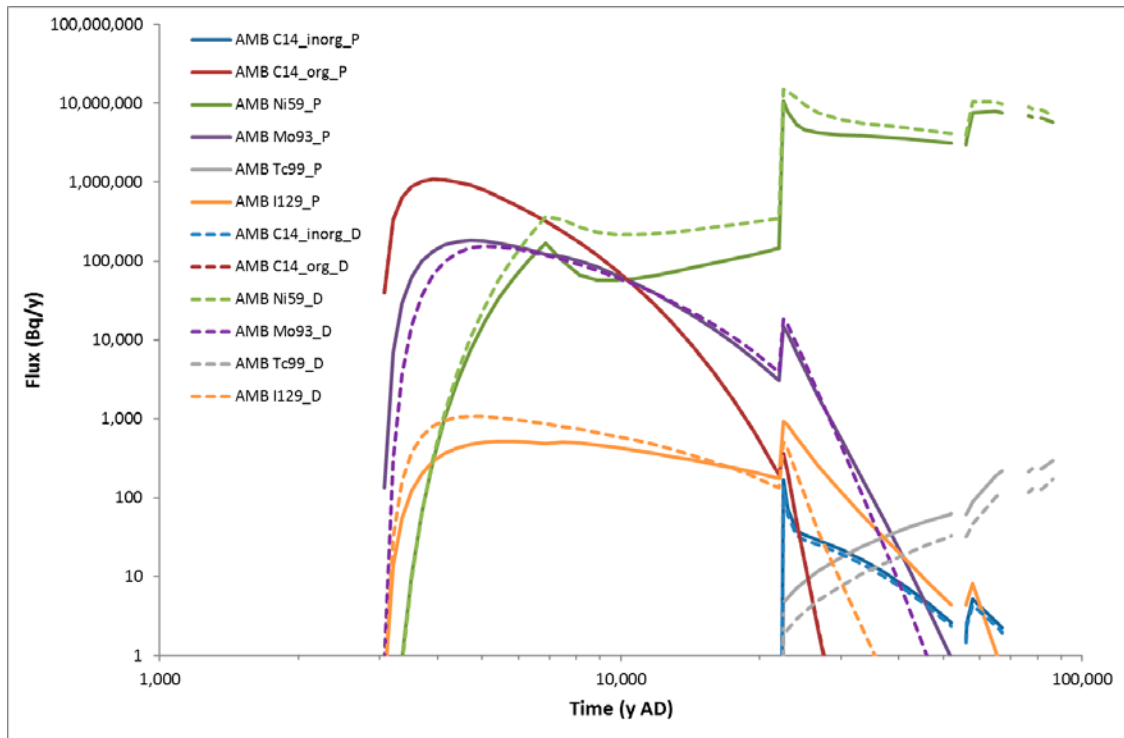
Figure 32. Deterministic radionuclide fluxes from the near-field in the base case (*radionuclide*_D) and probabilistic fluxes in the NF_Var11 case (*radionuclide*_P) calculated by AMBER
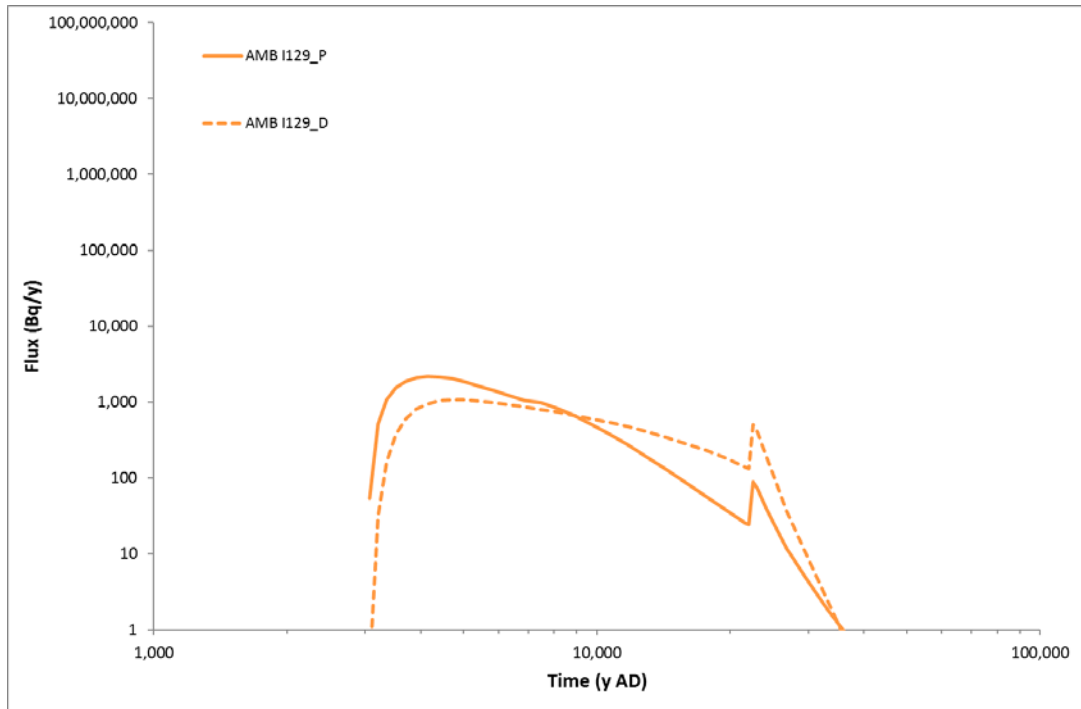
Figure 33. Deterministic I-129 fluxes from the near-field in the base case (*radionuclide*_D) and probabilistic fluxes in the NF_Var11 case (*radionuclide*_P) calculated by AMBER with a log normal parameter distribution for sorption onto cement.

Finally, a run was also undertaken in which the number of realisations was increased from 100 to 200 (Figure 34). This did not have a significant effect on the results, which builds confidence that SKB have used an appropriate number of realisations.
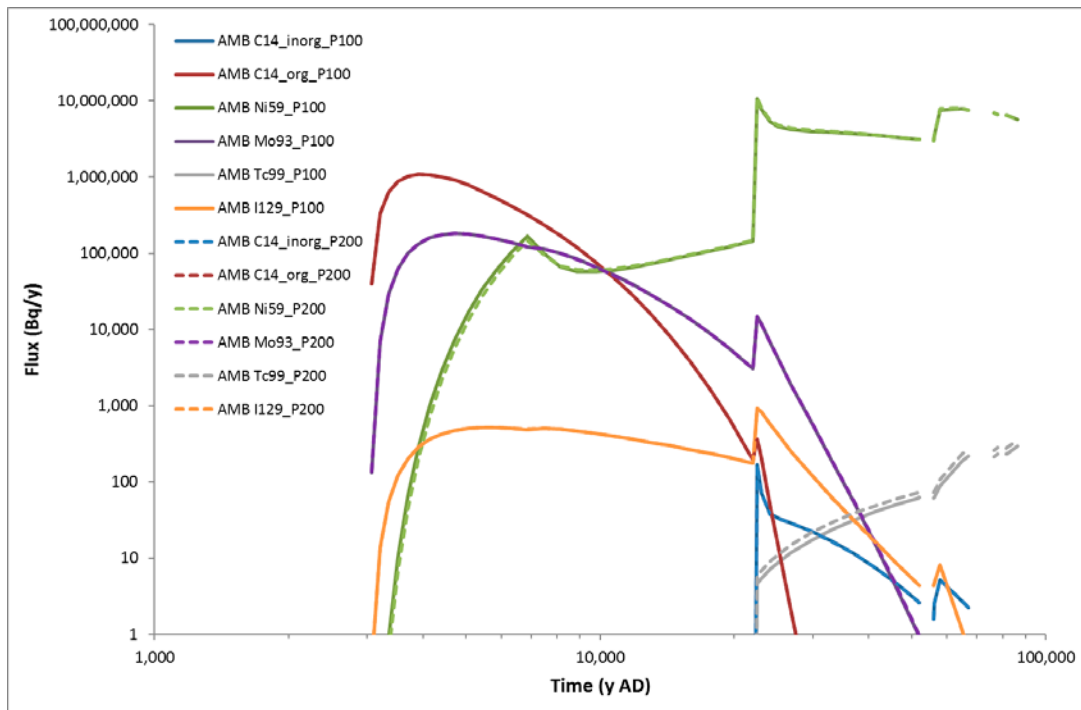
Figure 34. Probabilistic radionuclide fluxes calculated by AMBER for the NF_Var11 case with 100 realisations (*radionuclide*_P100) and 200 realisations (*radionuclide*_P200)

60

5.12   NF_Var12: Representation of the Caisson Walls

The objective of this case was to test sensitivity of the radionuclide fluxes from the near-field to the geosphere to representation of the caisson walls. In the base case, each of the five compartments used to represent the caisson was set to have an equal thickness of 0.2 m. A better representation of the diffusive transport process is gained if the compartments gradually increase in thickness. In this case, the first caisson compartment, which includes the inner surface of the caisson, was set to be 0.01 m thick. The thickness of the compartments was then incrementally increased to give a total wall thickness of 1 m.

The results are shown in Figure 35. The AMBER results are more similar to the ECOLEGO results at early times compared with the base case. However, C-14_org, Ni-59, Mo-93 and I-129 all exhibit slightly greater increased (spikes) in their fluxes at 22,000 AD compared with the base case.

The improved representation of the caisson walls reduces the calculated radionuclide fluxes. Therefore, there is a greater radionuclide inventory remaining in the caissons at 22,000 AD. This results in the larger spikes in radionuclide release at this time compared with the base case. The results before 22,000 AD are more similar to the ECOLEGO model than the AMBER base case, which builds confidence in the ECOLEGO model results. The greater differences at 22,000 AD further confirm the need to better understand how SKB have represented the changes that occur at this time.
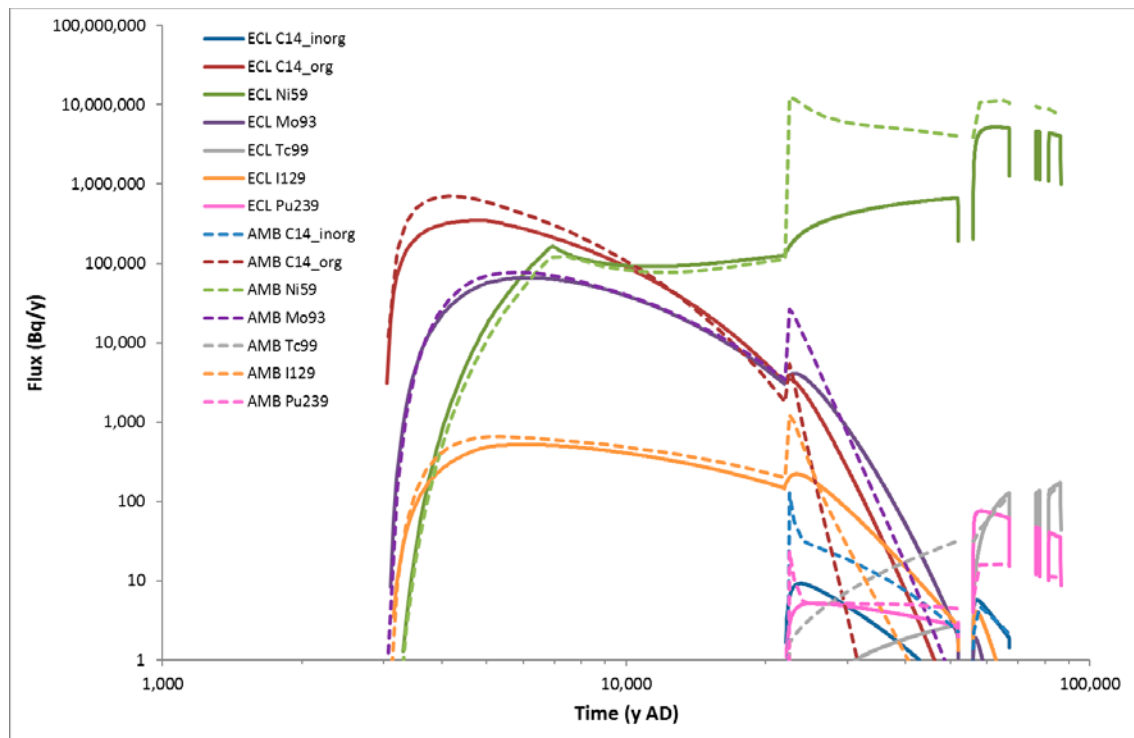
Figure 35. Comparison of radionuclide fluxes from the near-field into the rock calculated by the AMBER (AMB) and ECOLEGO models (ECL), with alternative discretisation of the caissons.

61

5.13   NF_Var13: Combination of Changes

Cases NF_Var6 and NF_Var12 were combined to provide a 'best fit' of the AMBER model results against ECOLEGO. The results are shown in Figure 36. This combination of changes provides the best fit for C-14_org, Ni-59, Mo-93 and I-129. However, it significantly underestimates the fluxes of the more strongly sorbing radionuclides beyond 22,000 AD. This raises the question whether the use of the standard or fracture model (Appendix D in TR-14-09) has been selected on a radionuclide specific basis. Therefore beyond 22,000 AD the standard model is retained for unsorbed and weakly sorbing radionuclides, but the fracture model is used for radionuclides that are significantly sorbed.
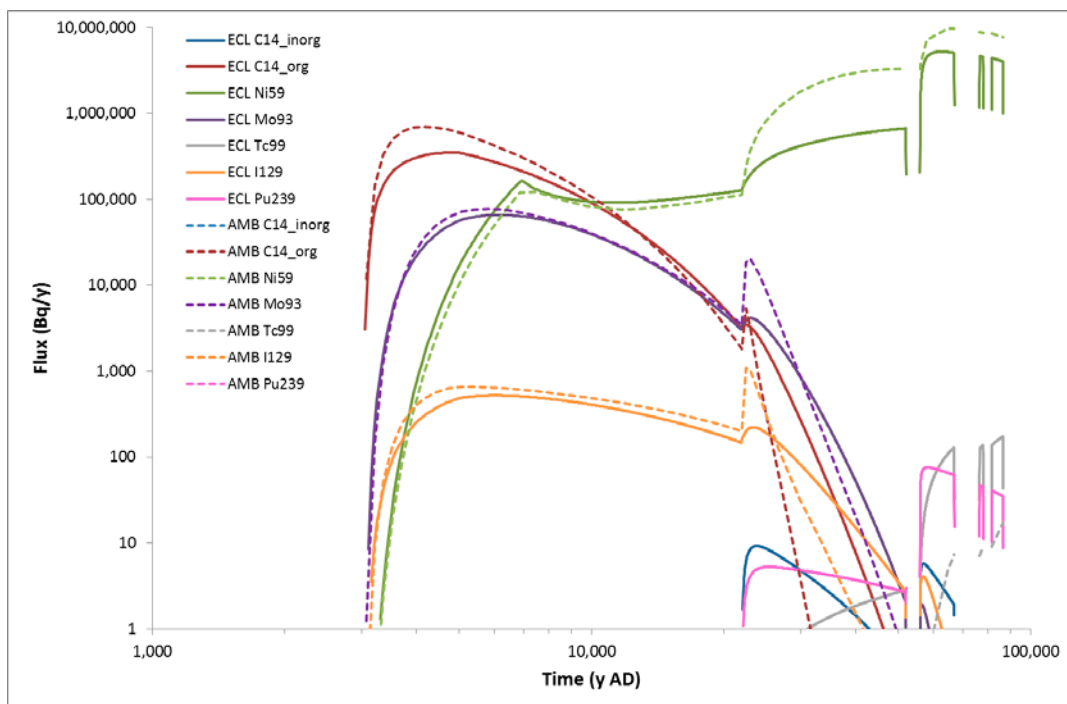
Figure 36. Comparison of radionuclide fluxes from the near-field into the rock calculated by the AMBER (AMB) and ECOLEGO models (ECL), with alternative discretisation of the caissons and no cracking of structural concrete.

5.14   GEO_VAR1: Input of ECOLEGO Near-field Fluxes into AMBER Geosphere

In this variant case the near-field flux calculated by the ECOLEGO model was input to the AMBER geosphere model. The flux to the biosphere calculated by the AMBER geosphere model is compared to the flux calculated by ECOLEGO in Figure 37. The results are very similar. The fluxes of Tc-99 and Pu-239 are slightly higher than calculated by ECOLEGO. These are the most strongly sorbing radionuclides of those presented. The coarser discretisation of the AMBER model

compared with ECOLEGO may result in slightly higher fluxes of these radionuclides due to greater numerical dispersion than ECOLEGO.
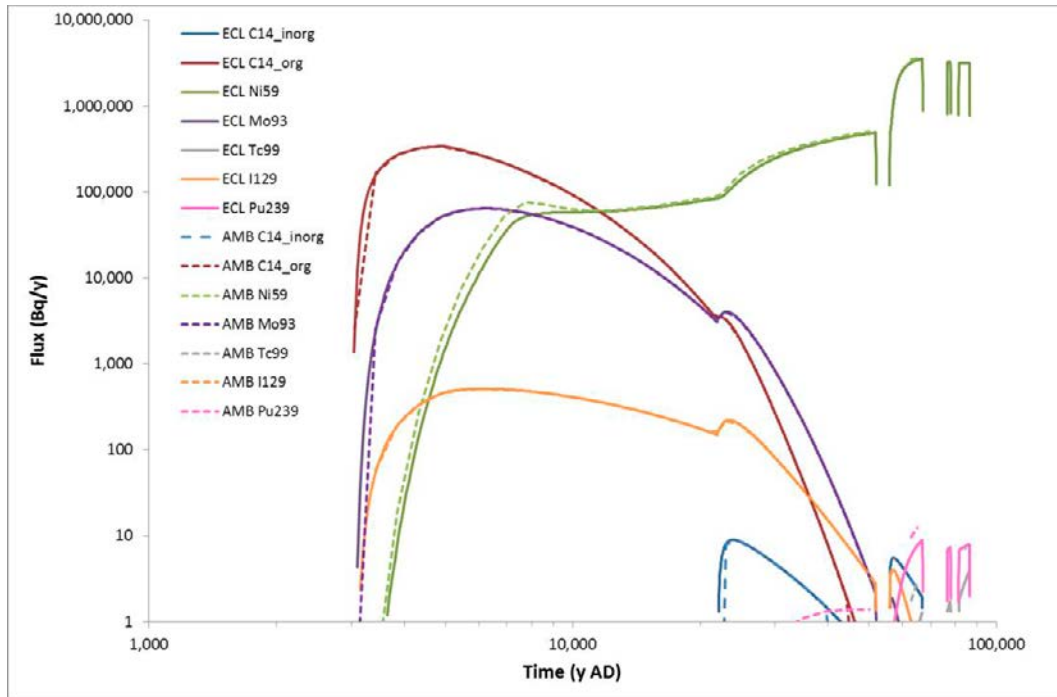
Figure 37. Comparison of radionuclide fluxes from the geosphere into the biosphere calculated by ECOLEGO (ECL), and by AMBER (AMB) using the flux from the near-field calculated by ECOLEGO.

6 Conclusions

SKB have built detailed and complex models of radionuclide transport through the 1BMA and 2BMA vaults into the geosphere. SKB have put significant effort into representing the detailed geometry of the near-field, spatial variations in near-field flows, and evolution of the system in response to environmental change and barrier degradation. SKB's reports provide a high level description of the models, which enable the configuration to be broadly understood or deduced. However, description of the representation of the different waste package types in the models could be improved, and some aspects of the model configuration are not described, for example how the waste packages and caissons have been discretised.

The models use a large amount of data. Most of these data are provided in SKB's reports, but not all; for example the properties of the waste packages (porosity, density, effective diffusivity, etc) and the detailed flows through the vaults are not presented. (The latter were provided in spreadsheets by SKB). A potentially significant observation is that 2384 steel drums containing cement embedded wastes are planned for disposal in the 2BMA vault, but no inventory is assigned to these drums in SR-PSU. This means that the inventory of 2BMA could be under estimated, and consequently so could the flux of radionuclides released from the vault.

63

SKB have not described and justified how key aspects of the model have been parameterised, where the parameter values are derived from the underpinning data. This includes important parameters such as cross-sectional areas and distances used to calculate diffusive transfers.

Although SKB's documentation of the model and data could be improved we have built a model in AMBER that broadly reproduces the results of SKB's ECOLEGO model for the 2BMA vault. This helps to build confidence in SKB's assessment calculations for SR-PSU. However, the differences are such that SSM might wish to consider additional work to investigate these differences in more detail, as further described below.

It would not have been possible to progress the models to the state shown in this report without the ability to interrogate the SKB ECOLEGO model files, and underpinning data files (including flow data) provided by SKB. Although we had access to the ECOLEGO model files, we have not used the files to undertake a detailed review of how the ECOLEGO models were configured and parameterised. We have only used the files to provide information and data that were not available from SKB's reports, insofar as we were able to deduce it from the models, not being trained users of ECOLEGO.

Since the ECOLEGO vault models are complex, in the future SKB could build more confidence in the results by presenting a wider range of model outputs, and the results of variant cases, to show that the model results and behaviours are logical and consistent with expectations. SKB could also build supporting simpler models that can be quality assured with greater confidence and more easily reproduced. These models should give broadly similar results to the more detailed models and would further build confidence. For example, we note that variations in flows through the vault are primarily controlled by evolution of the material properties, not environmental change or location within the vault. Therefore, simplifications to the model flow field should not lead to significant differences in the radionuclide fluxes.

SKB's geosphere model also contains a large number of compartments, but it is less complex than the model of the 2BMA vault, and documentation of the model is more complete and transparent. We have built a simpler version of the model which reproduces SKB's results, with only small differences that can be attributed to the coarser discretisation of the AMBER model compared with the ECOLEGO model. This builds good confidence in SKB's geosphere radionuclide transport model, but also shows that a simpler model may have offered benefits such as increased transparency, simpler to QA, and faster runs time for probabilistic assessment and sensitivity analyses.

Due to the complexity of SKB's models, and limitations in their documentation, it was not possible to undertake the high level comparison exercise for 1BMA that was originally planned by SSM. Instead efforts focussed on analysing a range of base case model results, and results from variant cases, to help understand the behaviour of the 2BMA vault model, and the reasons for differences in the fluxes calculated by the AMBER and ECOLEGO models. The results indicate that key areas for any further investigation in the future are:
- Parameterisation of diffusive transfers (areas and distances).
- Representation of evolution of barrier properties, and in particular the effects of cracking of the caissons.

Further inputs may be required from SKB to help understand these aspects of the ECOLGEO model. Once this has been completed it should be relatively efficient to use the AMBER model to further explore the behaviour of the models, including undertaking a high level comparison exercise for 1BMA.

During the initial review phase, we undertook a high-level assessment of SKB's identification of FEPs and their treatment in the assessment. We identified the key FEPs and associated uncertainties that are most significant for potential impacts are the radionuclide inventory and FEPs relating to the performance and degradation of the near-field engineered barriers (Towler et al., 2015). It was noted that understanding the coupled processes leading to degradation of the engineered barriers, the rate and timing of degradation, and selection of parameters to represent these processes in models are important. These issues are being considered by other technical areas within this main review phase. Nevertheless, the results of this modelling exercise further highlight the importance of these issues.

Further analysis of SKB's identification and treatment of FEPs, in the context of radionuclide transport, was undertaken as part of this main review phase. Metcalfe (2016) reviewed SKB's initial state and process reports and concluded that:

"*The reviewed reports are well structured and clearly describe the system components and the couplings between variables (which are stated to be entities that are represented by parameters within the assessment) and either processes that affect the components of the repository (in the case of TR-14-02, TR-14-03 and TR-14-04), or processes that affect the geosphere (TR-14-05). The treatment of these couplings in the assessment is described, together with the associated uncertainties. It is possible to deduce couplings between processes in different parts of the SFR from the information provided, but such couplings are not presented explicitly. Such an explicit explanation of the couplings would help the reader understand how (or whether) these couplings have been taken into account by the assessment*".

Several areas where the assessment could be strengthened were identified by Metcalfe (2016):
- The relationships between processes in the geosphere, the initial state of the SFR at the time of closure and engineered components of the facility.
- Potential chemical and mechanical interactions between adjacent vaults and the silo.
- Some mechanical processes and associated process couplings that might affect the performance of engineered barriers, particularly in the silo.

Given the knowledge gained during the initial review phase, and during the review of the initial state and process reports, the FEPs represented explicitly in the radionuclide transport models were found to be consistent with expectations. The FEPs represented explicitly are also broadly consistent with safety assessments undertaken for similar facilities, and have been represented using appropriate mathematical models. No omissions of further issues were identified beyond those raised by Towler et al. (2015) and Metcalfe (2016).

7   References

Höglund, L. O. 2014. The impact of concrete degradation on the BMA barrier functions. R-13-40.

Metcalfe, R. 2016. SR-PSU Review Title: Review of Initial State and Process Reports. *In preparation*.

Quintessa. 2011. OPG's Deep Geologic Repository for Low and Intermediate Level Waste. Postclosure Safety Assessment: Analysis of the Normal Evolution Scenario. NWMO DGR-TR-2011-26.

Quintessa. 2016. AMBER Version 6.0.
https://www.quintessa.org/software/AMBER/index.html

SKB. 2010. Data report for the safety assessment SR-Site. TR-10-52.

SKB. 2013a. Flow modelling on the repository scale for the safety assessment SR-PSU. TR-13-08.

SKB. 2013b. Quantification of rock matrix Kd data and uncertainties for SR-PSU. R-13-38.

SKB. 2014a. Safety analysis for SFR. Long-term safety. Main report for the safety assessment SR-PSU. TR-14-01.

SKB. 2014b. Initial state report for the safety assessment SR-PSU. TR-14-02.

SKB. 2014c. Radionuclide transport and dose calculations for the safety assessment SR-PSU. TR-14-09.

SKB. 2014d. Data report for the safety assessment SR-PSU. TR-14-10.

SSM. 2016. SSM's external experts' reviews of SKB's safety assessment SR-PSU – radionuclide transport, dose assessment, and safety analysis methodology. Initial review phase. SSM 2016:09.

Towler, G., Robinson, P., Watson, C. and Penfold, J. 2015. SR-PSU Review. Review of radionuclide transport methodology in SR-PSU. In SSM 2016:09.

Author: Richard Metcalfe [1]

[1]Quintessa Limited, Henley on Thames, UK

Review of Initial State and Process Reports for Waste, Barriers, and Geosphere

Abstract

The Swedish Radiation Safety Authority (SSM) received an application for the expansion of SKB's final repository for low and intermediate level waste at Forsmark (SFR) on the 19 December 2014. SSM is tasked with reviewing the application and will issue a statement to the Swedish government who will decide on the matter. An important part of the application is SKB's assessment of the long-term safety of the repository, which is documented in the safety analysis named SR-PSU.

SSM's review is divided into an initial review phase and a main review phase. This assignment contributes to the main review phase. In the initial review phase several specific topics for further in-depth review were identified. The scope of those topics has been refined following SKB's provision of complementary information, requested by SSM during the initial review phase and discussed at a meeting between SSM, SKB and supporting consultants on the 28th April 2016.
The initial radionuclide transport review identified that the initial state of the repository and a number of coupled processes are potentially very important to the long-term evolution and performance.

The present report reviews SKB's initial state report and process reports for the waste, barriers and geosphere, with a focus on the treatment of the potentially important initial conditions and couplings between hydro-mechanical-chemical processes identified by the initial review.

The review covered the following reports:
- Initial state report for the safety assessment SR-PSU: TR-14-02;
- Waste form and packaging process report for the safety assessment SR-PSU: TR-14-03;
- Engineered barrier process report for the safety assessment SR-PSU: TR-14-04;
- Geosphere process report for the safety assessment SR-PSU: TR-14-05.

The review focussed on sections concerning radionuclide transport and in particular on sections relevant to answering questions posed in the initial review.

The reviewed documents consist of a total of 962 pages, and form only a sub-set of the much larger suite of reports that make-up the SR-PSU safety assessment. It was not possible to review all of them in detail within the few days of time allotted to this review topic. Therefore, only TR-14-02 was reviewed in its entirety. The other reports were reviewed in sufficient detail to understand as far as practicable how couplings between processes had been identified and treated in the assessment. An overview of the wider suite of SR-PSU reports, and important issues for the main review was provided by the outcomes of the initial review phase.

The review considered the extent to which the four reports describe the initial state of the repository; identify Features, Events and Processes (FEPs) and couplings; describe the treatment of FEPs and couplings; and whether the treatment is appropriate. Within this scope of review, three specific questions were considered:

1. Is the process that was used to determine the treatment of the different FEPs and couplings described?
2. Is the treatment of FEPs and couplings described sufficiently, and is the treatment appropriate.

3. Are all the potentially relevant mechanical FEPs included in the FEP catalogue and how are they treated in the assessment? Of particular interest are:
   a. Interactions between adjacent vaults and vaults / the silo.
   b. Waste stack settlement, e.g. due to creep of metal containers and degradation of waste packages, especially within the silo.
   c. In the silo, creep / flow of bitumen out of damaged / ruptured waste containers, in response to expansive stresses and the load from over-stacked packages.

The reviewed reports are well structured and clearly describe the system components and the couplings between variables (which are stated to be entities that are represented by parameters within the assessment) and either processes that affect the components of the repository (in the case of TR-14-02, TR-14-03 and TR-14-04), or processes that affect the geosphere (TR-14-05). The treatment of these couplings in the assessment is described, together with the associated uncertainties. It is possible to deduce couplings between processes in different parts of the SFR from the information provided, but such couplings are not presented explicitly. Such an explicit explanation of the couplings would help the reader understand how (or whether) these couplings have been taken into account by the assessment.

Very little is stated about possible chemical interactions between adjacent vaults and between the silo and adjacent vaults.

Mechanical processes are considered in depth. However, very little is stated about interactions between adjacent vaults and vaults/silo. Based on the processes reported and their relationships with the identified key variables, it is possible to make some general inferences about these interactions. However, TR-14-02, TR-14-03 and TR-14-04 would all have benefited from including an explicit consideration of these interactions.

The relationships between processes in the geosphere (covered by TR-14-05), the initial state of the SFR at the time of closure (covered by TR-14-02) and engineered components of the facility (covered by TR-14-03 and TR-14-04) are not covered clearly. TR-14-02 describes the initial states of the engineered components of the facility and presents very little information about the state of the geosphere at the time of facility closure. Additionally, while the geosphere process report (TR-14-05) covers mechanical processes in the geosphere, it does not explain clearly how these might impact on the vaults, silo and closure engineering.

Very little information could be found in the reviewed reports concerning the possibility of waste stack settlement and its treatment within the assessment. Similarly, none of the reports were found to cover the possibility of bitumen creeping/flowing out of failed containers due to loading by overlying stacks of containers or expansion of the bitumen. This latter process is, however, recognized as being potentially important.

We do not expect these mechanical processes, and the implications for coupled hydro-chemical processes, would markedly change the assessment results, if they were important. Nevertheless, these findings indicate there is scope to further assess the mechanical evolution of the near-field, and the implications of this for barrier performance. The same conclusions are drawn regarding mechanical interactions between the vaults and the vaults/silo. It is noted that the review has not searched through the much wider suite of SR-PSU reports to see if these processes and couplings are further treated elsewhere.

Contents

1. Introduction

The Swedish Radiation Safety Authority (SSM) received an application for the expansion of SKB's final repository for low and intermediate level waste at Forsmark (SFR) on the 19 December 2014. SSM is tasked with reviewing the application and will issue a statement to the Swedish government who will decide on the matter. An important part of the application is SKB's assessment of the long-term safety of the repository, which is documented in the safety analysis named SR-PSU.

SSM's review of the SR-PSU assessment is divided into an initial review phase and a main review phase. The assignment reported here contributes to the main review phase.

The initial review phase included a review of SKB's methodology for modelling radionuclide transport in the SR-PSU (Towler et al, 2015). This initial review task identified several specific topics for further in-depth review. The scope of those topics has been refined following SKB's provision of complementary information, requested by SSM during the initial review phase and discussed at a meeting between SSM, SKB and supporting consultants on the 28th April 2016.
This process identified that the initial state of the repository and a number of coupled processes are potentially very important influences on the long-term evolution and performance of the SFR. To further understand how SKB has treated these aspects in the SR-PSU, the present report therefore reviews SKB's initial state report (TR-14-02) and process reports covering the waste (TR-14-03), engineered barriers (TR-14-04) and geosphere (TR-14-05).

1.1. Objectives of the Main Review

In addition to identifying the potential importance of the initial state of the repository and several key couplings for long-term evolution and performance, the initial review raised three specific questions that fall within this topic area. These questions have been reviewed and updated following the meeting held on 28th April 2016.

It is important that all the relevant Features, Events and Processes (FEPs) and couplings that describe the system have been identified. Some FEPs and couplings will be more important for safety and performance than others, and the magnitude and potential significance of the associated uncertainties will also vary. It is not possible or practical to treat all the FEPs and couplings in the same way within the assessment, and the focus needs to be on those that are most important for safety. Therefore, in addition to ensuring all the relevant FEPs and couplings have been identified it is useful to understand the process by which the treatment of the FEPs and couplings in the assessment was decided, and who undertook the assessment. Relevant questions are:

- Is the process that was used to determine the treatment of the different FEPs and couplings described?
- Is the treatment of FEPs and couplings described sufficiently, and is the treatment appropriate?

The initial review identified that couplings relating to mechanical processes may be of particular interest, due to the potential for some of the wastes to swell, and in

particular in the silo due to large height of the waste stacks, which may be subject to long-term settlement as the packages degrade. Safety assessments often focus on chemically and hydraulically 'driven' coupled processes, rather than mechanically driven processes, so it is of particular interest to understand how these mechanically driven couplings have been treated. An appropriate question to ask is:

- Are all the potentially relevant mechanical FEPs included in the FEP catalogue and how are they treated in the assessment? Of particular interest are:
    - o Interactions between adjacent vaults and vaults / the silo.
    - o Waste stack settlement, e.g. due to creep of metal containers and degradation of waste packages, especially in the silo.
    - o In the silo, creep / flow of bitumen out of damaged / ruptured waste containers, in response to expansive stresses and the load from over-stacked packages.

In summary, the first objective of this main review task is to better understand SKB's identification and treatment of the initial conditions and couplings in SR-PSU, to build confidence they are comprehensive, robustly defined and treated appropriately. The second objective is to answer the specific questions given above.

1.2. Scope of the Review

The review has covered the following SR-PSU reports:

- Initial state report for the safety assessment SR-PSU: TR-14-02;
- Waste form and packaging process report for the safety assessment SR-PSU: TR-14-03;
- Engineered barrier process report for the safety assessment SR-PSU: TR-14-04;
- Geosphere process report for the safety assessment SR-PSU: TR-14-05.

The focus of the review has been on sections concerning radionuclide transport and in particular on sections relevant to answering the questions posed above, which have been developed from the findings of the initial review (Towler et al., 2015).

1.3. Approach

The reviewed documents consist of a total of 962 pages. It was not possible to review all of them in detail within the few days of time allotted to this review topic.

The **initial state report** (TR-14-02) was reviewed in its entirety. The **waste form and packaging process report** (TR-14-03), **engineered barrier process report** (TR-14-04) and **geosphere process report** (TR-14-05) were each reviewed in sufficient detail to understand how SKB had treated couplings between the considered processes in its treatment of radionuclide transport in the SR-PSU safety assessment. Those sections of the reports dealing explicitly with radionuclide transport were therefore reviewed in detail. Additionally, searches were undertaken for key words corresponding to the questions identified by Towler et al. (2015).

Based on these reviews, the reports were assessed against the objectives described in Section 1.1:

- Section 2 presents the findings based on TR-14-02.
- Section 3 presents the findings based on TR-14-03.
- Section 4 presents the findings based on TR-14-04.
- Section 5 presents the findings based on TR-14-05.

An overall assessment of the reviewed documents is given in Section 6.

2. Initial State Report, TR-14-02

The report on the initial state of the repository system TR-14-02 focuses on the wastes and the engineered barriers and gives little information about the initial state of the geological barriers at the time of closure. This focus apparently reflects the fact that safety in the SFR is stated in the first paragraph of Section 2.4 on page 20 to be '*based on a limited quantity of radioactivity in the waste form and, for some vaults, the retardation of radionuclides by the system components e.g. waste packaging and concrete structures in the repository*.' Emphasis is therefore placed on defining waste acceptance criteria that achieve the desired limitation of radioactivity and the characteristics of the engineered barriers that ensure they limit releases of radionuclides.

Aspects of the different repository components that impact upon their safety functions are summarized in Table 2-1.

Table 2-1. Potential aspects that may be considered in the long-term safety assessment for the different system components in some or all the waste vaults (Table 2-2, reproduced from TR-14-02, page 21).

System component	Aspect
Waste form	Level of radioactivity Limited advective transport Mechanical stability Limited dissolution Sorption Favourable water chemistry
Waste packaging	Limited advective transport Mechanical stability Sorption Favourable water chemistry
Grouting surrounding waste packages	Limited advective transport Mechanical stability Sorption Favourable water chemistry
Concrete structures	Limited advective transport Mechanical stability Sorption Favourable water chemistry
Shotcrete	Mechanical stability (during operating phase, together with rock bolts) Sorption Favourable water chemistry
Bentonite and sand/bentonite	Limited advective transport Mechanical stability Sorption
Backfill in waste vaults (crushed rock/ macadam)	Mechanical stability Sorption
Plugs and other closure components (investigation boreholes)	Limited advective transport in the repository Sorption

The safety-relevant aspects given in Table 2-1 depend to some degree on the characteristics of the geosphere, notably upon the flow and chemistry of groundwater. The report recognizes this importance explicitly, for example in the third paragraph of Section 4.2 on page 57, which states that '*The depth of 1BMA (~70 m) results in favourable conditions with respect to mechanical stability, low groundwater flow and redox conditions.*' Similar statements are made in connection with the other vaults. The report also recognizes the rock surrounding the repository and the surface environment near the repository as components of the disposal system (last paragraph of Section 2.3 on page 20). However, it is stated that the initial states of these components are described in the Chapter 4 of the Main report concerning the long-term safety for the SFR repository (SKB, 2015). This separate presentation of the initial states of engineered components of the repository system (in report TR-14-02) and the states of the geosphere and biosphere at the time of repository closure (in SKB, 2015) hinders a clear understanding of the relationship between the two. For example, TR-14-02 does not inform the reader about spatial variations in groundwater chemistry at the time of closure and no details are given of the spatial relationships between the vaults and silo and conductive features in the rock mass. For these reasons, it would have been helpful for the report to provide a more in-depth explanation of the relationship between the condition of the geosphere at the time of repository closure (from the perspective of the safety assessment its 'initial condition') and the initial conditions of the engineered repository components.

The coverage within TR-14-02 of the wastes themselves, their packaging, their allocation to different parts of the SFR, the layout of the SFR and its engineered features are covered logically.

Section 2 of the report provides an overview of the repository's characteristics and the functions of its various components. This section also outlines the legal framework within which the repository has been developed and operated to date and within which it will be further developed in future.

Section 3 of TR-14-02 describes the inventory, the waste and the ways in which the waste is handled, waste packaging and the allocation of the waste to different sections of the SFR.

The report is then structured according to the various major engineered system components, which are:

- The waste forms
- The waste packages
- System components for SFR 1:
  - 1BMA (vault for intermediate-level waste (ILW));
  - 1BTF and 2BTF (vaults for concrete tanks);
  - Silo (for ILW);
  - 1BLA (vault for low-level waste (LLW));
- System components for SFR 3:
  - 2BMA (vault for ILW);
  - 2BLA, 3BLA, 4BLA and 5BLA (vaults for LLW);
  - BRT (vault for reactor pressure vessels);
- Plugs and other closure components.

7

As noted previously, the report recognizes the geosphere as a system component, but it is not described in detail.

Each of Sections 4 to 10 describe a specific type of vault or the silo. For each component, the design, the reasons for it, inspection control measures, its dimensions and the quantities of waste contained are described. Section 11 describes the plugs and other sealing components, again providing similar kinds of information to those given for the vaults and silo, except that rather than volumes of waste, the volumes of the sealing components are presented.

Section 12 then presents the expected state at the time of repository closure (i.e. the initial state) of each 'variable' that is required to describe the properties and condition of each system component in the assessment. These variables are stated to be described by parameters in the assessment. The states of each variable are presented for each system component in turn:

- geometry;
- radiation intensity (waste form only);
- temperature;
- hydrological variables;
- mechanical stresses;
- radionuclide inventory (waste form only);
- material composition;
- water composition;
- gas variables.

The report makes clear that the allocation of waste between the different vaults and the silo is undertaken so as to maximize the barrier function of cementitious barriers and also minimize deleterious effects of waste evolution on these barriers. For example, it is stated that all bituminised waste will be deposited in 1BMA and not in 2BMA, because the latter will not have reinforced concrete barriers. This strategy avoids the potentially negative influence of bitumen swelling on the unreinforced cement barriers in 2BMA (although it is noted in the report that the cementitious barriers in 1BMA will need repair before closure).

The extent to which key questions posed by Towler et al. (2015) can be answered by the information in TR-14-02 is considered below.

Is the process that was used to determine the treatment of the different FEPs and couplings described?
TR-14-02 references the FEP report (SKB, 2014a) as the sources of the FEPs used to represent the initial state of the repository. TR-14-02 itself does not give details of the decision-making process used to decide the treatment of the FEPs. Furthermore, no information is given about the personnel who undertook such a process.

Is the treatment of FEPs and couplings described sufficiently, and is the treatment appropriate?
The focus of TR-14-02 is providing descriptions of the system characteristics, or features of the system, rather than the processes that occur. Hence there is little direct consideration of couplings between the processes and no indication about how these couplings are treated in the assessment.

The couplings between the major identified different system components (wastes, packaging etc. – see above) are mentioned, but not in detail. For example, paragraph

7 of Section 5.2 states that in vault 2BMA '*The interaction between the different components, i.e. the caisson, grout and waste, ensures that the water pressure that develops will not lead to significant damage.*'

There is, however, some coverage of couplings between the detailed processes that occur within the identified main system components. For example, the last paragraph of Section 7.2 on page 77 states that: '*In addition, the creation of reducing conditions in the silo shafts that is caused by the consumption of oxygen by aerobic corrosion will favour the sorption of many radionuclides e.g. technetium and some actinides.*'

The structure of the report according to the key variables that need to be considered by a safety assessment (geometry, radiation intensity etc. – see above) does allow some inferences to be made about how couplings between FEPs are treated. For each major component of the repository (waste form, waste packaging, vaults etc. – see above) the features and processes that impact upon the value of each variable are described systematically. Therefore, where the same feature or process impacts upon the values of two different variables it is possible to infer something about the coupling between the variables. For example, Section 12.1.7 concerns the variable 'material composition' and mentions the occurrence of cement within some of the waste packages. Section 12.1.8 concerns the variable 'water composition' and states that the composition of groundwater will affect the composition of the porewater within concrete. Hence, it can be inferred that the composition of the materials in the waste packages, porewater composition and groundwater composition are coupled.

Are all the potentially relevant mechanical FEPs included in the FEP catalogue and how are they treated in the assessment? Of particular interest are: a) Interactions between adjacent vaults and vaults / the silo; b) Waste stack settlement, e.g. due to creep of metal containers and degradation of waste packages, especially in the silo; c)In the silo, creep / flow of bitumen out of damaged / ruptured waste containers, in response to expansive stresses and the load from over-stacked packages.

Interactions between the adjacent vaults and between the vaults and the silo are not explained explicitly by TR-14-02. However, Section 12 of the report concerns the system variables (see above) and these are described separately for each of the major system components (waste forms, waste packages, vaults etc). Because the same variables are used to describe each component it is possible to make some general inferences about possible interactions (or lack of them) between the different components. For example, the variable 'water composition' for each of the system components is stated to depend upon groundwater composition. The composition of the groundwater is conditioned within each component by interactions with the materials present (e.g. cement). However, there is no explicit statement of the extent to which water conditioned in one component (e.g. the vault) may be able to interact with another component (e.g. the silo).

TR-14-02 says little about waste stack settlement. Section 7.3 concerns the inspection and control of the silo and covers settlement of the *silo*, which is concluded to be insignificant. No information is given about the settlement of waste stacks as such, either within the silo or within the vaults, however this is not expected to be significant while the waste packages are in good condition. The section on 'robustness against external influences' on page 28 states that '*Waste packages allocated to the silo shall withstand stacking of 42 moulds or 56 drums grouted with concrete*'. The implication is that, SKB consider that, provided the

facility is implemented correctly, settlement will not be an issue. However, no explicit statement that such settlement has been excluded was identified in the report.

While settlement may indeed not be an issue at the time of closure, a question is whether the potential exists for settlement to become important in the post-closure period. This is a topic that would be appropriately covered in the waste form and packaging process report (TR-14-03 – see Section 3 below). However, the likelihood that such settlement will occur will depend partly on how much open voidage is left at the time of closure, which is a topic that is appropriate for TR-14-02. Information about voidage in each of the vaults and the silo at the time of closure is given in Appendix A. The implications of this voidage for settling should be assessed, although it is not clear from report TR-14-02 whether that has been done.

The report says nothing about creep or swelling of bitumen, except that the allocation of bitumen-bearing waste to the vaults partly reflects consideration of its swelling properties. Bitumenized waste is placed in vault 1BMA, which contains reinforced concrete that will not be damaged by swelling bitumen, rather than 2BMA, which does not contain reinforced concrete (although it is noted that the concrete in 1BMA will need to be repaired before closure).

3. Waste Form and Packaging Process Report, TR-14-03

TR-14-03 describes processes that are expected to occur in the waste forms and packaging of the SFR during a period of 100,000 years following closure. The report explains the significance and handling of each process within SR-PSU.

For each process considered, a table is used to identify how the process is influenced by the specified set of physical variables and how the process influences the variables. The handling of each influence in SR-PSU is also indicated in the table, and a more extensive description of the influences and handling are given in the text. The variables considered are:

- geometry;
- temperature;
- hydrological variables;
- mechanical stresses;
- material composition;
- water composition; and
- gas variables.

The extent to which key questions posed by Towler et al. (2015) can be answered by the information in TR-14-03 is considered below.

Is the process that was used to determine the treatment of the different FEPs and couplings described?
It is stated in TR-14-03 that '*The purpose of this process report is to document the scientific knowledge and handling of the processes in the waste form and the packaging that has been identified to be relevant for the long term safety in a previous assessment step, Step 1 – Handling of FEP's (features, events and*

processes)'. In other words, this process report itself does not identify the FEPs. However, Section 1.4 of TR-14-04 does summarize the process by which FEPs were identified. Key aspects of this process are stated to be:

- The original FEP analysis for SFR was carried out within the SAFE project and addressed the first 10,000 years post closure.
- FEPs and interactions between processes that will affect the future evolution of the repository were identified with the aid of an interaction matrix.
- The matrix was cross-checked against the NEA FEP database version 1.0 (NEA, 1997).
- The resulting FEP list was later used as the basis for the FEP analysis in the SAR-08 safety assessment, during which the FEPs were revisited and checked for their validity and the possible need of updates due to new information and/ or changed conditions.
- For SR-PSU, a renewed FEP processing was implemented using all project FEPs in the international NEA FEP database (version 2.1).
- Additionally, preliminary, unpublished FEP lists from two additional projects for L/ILW waste were evaluated:
  - Olkiluoto L/ILW Hall in Finland; and
  - Rokkasho 3 in Japan (both in preliminary unpublished versions).
- The resulting FEP lists were checked in order to ensure that all relevant aspects of a process are addressed in the process descriptions and handled appropriately in the SR-PSU assessment. The handling of each FEP has been documented in tables given in the SR-PSU FEP report (SKB, 2014a).

The experts involved in the decision-making process are given in Section 1.4.3 and Table 1-1 of TR-14-03. However, details of the actual decision-making process are not presented.

Is the treatment of FEPs and couplings described sufficiently, and is the treatment appropriate?

The report states in the last bullet point on page 13 that it covers: '*Handling of the interactions between the process and the specified waste form variables, and coupling to other processes within the system.*' However, there is no specific format in which these interactions are addressed, except in so far as relationships between the various variables considered in the assessment (geometry, radiation intensity etc. – see Section 2) and the various processes are presented and discussed systematically.

Section 3 of the report describes the various processes that are considered to influence the evolution of the waste form and the packaging:

- radiation-related processes (Section 3.1);
- thermal processes (Section 3.2);
- hydraulic processes (Section 3.3);
- mechanical processes (Section 3.4)
- chemical processes (Section 3.5); and
- radionuclide transport (Section 3.6).

Each of the sub-sections that concerns a group of processes consists of a number of further sub-sections, each one covering a different group of relevant processes. For example, under Section 3.1, which concerns radiation-related processes, there are sub-sections concerning radioactive decay (Section 3.1.1), radiation attenuation and

heat generation (Section 3.1.2), radiolytic decomposition of organic material (Section 3.1.3) and water radiolysis (Section 3.1.4).

Each of the process descriptions in these various sub-sections includes a discussion of relevant couplings. No obvious omissions of discussions of couplings were noticed during the review, although as noted in Section 1.3 a comprehensive review of the report was not possible and hence comprehensive coverage of couplings could not be confirmed.

The influence of each variable (geometry, radiation intensity etc. – see Section 2) on each process, and the influence of the process on each variable is summarized in a table and explained in more detail in the main text. Because for each process, the influences exerted by / on the same variables are evaluated, it is possible to deduce couplings between the different processes.

Each of these sections also explains generally how the process is treated in the assessment and discusses uncertainties. These discussions of uncertainties often cover couplings between different processes and are divided into three categories:

- uncertainties in mechanistic understanding;
- model simplification uncertainties
- input data and data uncertainties

This systematic approach to presenting the uncertainties and their treatment allows readers to compare different processes readily. However, it is less clear how processes in one of the major system components (vaults, silo etc.) may affect the processes in a different major system component.

Are all the potentially relevant mechanical FEPs included in the FEP catalogue and how are they treated in the assessment? Of particular interest are: a) Interactions between adjacent vaults and vaults / the silo; b) Waste stack settlement, e.g. due to creep of metal containers and degradation of waste packages, especially in the silo; c) In the silo, creep / flow of bitumen out of damaged / ruptured waste containers, in response to expansive stresses and the load from over-stacked packages.

TR-14-03 says little about possible interactions between adjacent vaults and vaults / the silo. Mutual influences between component variables and processes are considered systematically for each vault and the silo, but influences between vaults or between vaults and the silos are not considered. An implication is that such interactions are not considered important, but the justification is not clear.

The report covers physical and chemical aspects of bitumen behaviour in the repository environment in some detail. However, creep/flow of bitumen out of damaged/ruptured containers is not considered explicitly.

Section 3.3 briefly reviews the effects of radiolytic decomposition of bitumen and notes that hydrogen gas that could be generated may cause swelling of the bitumen. However, in the assessment, swelling caused by radiolytic decomposition of bitumen is neglected due to the low radioactivity of the waste.

Swelling of bitumen due to water uptake is the process considered explicitly in the safety assessment. Table 5.1 on page 210 states that '*Knowledge of swelling pressure as a function of expansion volume is used to evaluate how much pressure*

structures and barriers surrounding bituminised waste will experience. The effect of water uptake on the subsequent release of radionuclides is handled by assigning appropriate release rates for the radionuclides from the bituminised waste.'

Table 3.3 mentions this effect as influencing the variable 'geometry'. On page 30, the section on handling radioactive decay in the assessment concludes that '*Due to the low radiation levels, radiolysis is not expected to affect the bitumen matrix except in the waste packages receiving the highest absorbed doses, where some swelling of the matrix might occur.*' Section 3.4.1 considers fracturing of bitumen. However, it is pointed out in the section on model and experimental studies on page 54 that few studies have investigated the magnitude of bitumen swelling pressures that could result in fracturing of waste containers or barriers in the repository. Section 3.5.7, which begins on page 131 considers swelling of bitumen. It is stated that the degree of swelling will depend on the mechanical properties of the bitumen, the waste loading and the homogeneity of the waste product. Table 3.17 indicates that this swelling is taken into account in the assessment, by recognizing its possible influence on the system variables. There is a paragraph entitled 'influence on mechanical stresses' on page 134 that recognizes that swelling of the bituminised waste may cause mechanical stresses on the surrounding packaging and barriers.

4. Engineered Barrier Process Report, TR-14-04

TR-14-04 describes the processes that are expected to occur in the engineered barriers of the SFR during a period of 100,000 years following closure. The report explains the significance and handling of each process within the SR-PSU.

The summary of the report erroneously states that the document '*consists of two main chapters describing the waste form processes and the packaging processes respectively*'.

For each process considered, a table is used to identify how the process is influenced by the specified set of physical variables and how the process influences the variables. The handling of each influence in SR-PSU is also indicated in the table, and a more extensive description of the influences and handling are given in the text. The variables considered are the same as those considered by TR-14-03.

The extent to which key questions posed by Towler et al. (2015) can be answered by the information in TR-14-03 is considered below.

Is the process that was used to determine the treatment of the different FEPs and couplings described?
TR-14-04, concerning processes in the engineered barrier reports also does not provide details of the decision-making process use to decide on the treatment of the FEPs and couplings between them. Like TR-14-02 and TR-14-03 the report references the FEP report (SKB, 2014a), but unlike TR-14-03 it does not provide a summary of the approach to FEP list development. Section 1.6 of TR-14-04 simply states that '*The list of processes is developed by the experts in cooperation with the manager of the FEP database*'. It is stated that the list is based on the processes identified in earlier safety assessment of the SFR facility, the FEP work conducted for SR-PSU (FEP report), and in the Buffer, backfill and closure process report

for SR-Site (SKB, 2010a). Additionally, it is stated that for the bentonite, all processes in the Buffer, backfill and closure process report for SR-Site are included, except for the process 'Radiation attenuation/heat generation'. As for TR-14-03, the experts involved in the decision process are identified in Section 1.7.

Is the treatment of FEPs and couplings described sufficiently, and is the treatment appropriate?
The nature of the information provided concerning couplings between the processes that affect system components and their treatments in the assessment is very similar to the presentation of this information in the waste form and packaging process report (TR-14-02; Section 3). Again, a systematic approach is followed in which the influences of the system variables (geometry, radiation intensity etc. – see Section2) on each process and vice versa are discussed. The processes considered are:

- thermal processes;
- hydraulic processes;
- mechanical processes;
- chemical processes; and
- radionuclide transport.

Thus, the same processes are considered as in the case of the waste form and packaging process report (TR-14-02) except for radiation-related processes. This is reasonable in view of the relatively low radioactivity of the waste, a consequence of which is that radiation is not expected to influence the engineered barriers directly.

Unlike TR-14-02, the engineered barrier process report presents the relationships between the system variables and the processes separately for each of the major repository components (each kind of vault, the silo and plugs and other closure components). However, the potential for processes in one major repository component to affect processes in another is not discussed.

Are all the potentially relevant mechanical FEPs included in the FEP catalogue and how are they treated in the assessment? Of particular interest are: a) Interactions between adjacent vaults and vaults / the silo; b) Waste stack settlement, e.g. due to creep of metal containers and degradation of waste packages, especially in the silo; c)In the silo, creep / flow of bitumen out of damaged / ruptured waste containers, in response to expansive stresses and the load from over-stacked packages.

Mechanical processes that may affect each vault, the silo and plugs and other closure components are described explicitly. However, little is said specifically about waste stack settlement. Furthermore, the review identified little information about possible mechanical interactions between adjacent vaults, or between the silo and adjacent vaults.

It is stated in Section 5.3.1 that in the 1BMA and 2BMA vaults stresses due to the weight of the concrete, backfill and waste packages will be neglected prior to degradation, but after degradation these stresses may cause settlement. It is stated that this settlement, and its potential to open the roof of the vault will be analysed in the assessment. Similar statements are made in Section 6.3.1 concerning the 1BTF and 2BTF, in Section 7.3.1 concerning the silo, and in Section 9.3.1 concerning the BRT vault.

In contrast, for the 1-5BLA vaults, the only mechanical process that is stated to be considered is rock fall from the walls and roof, after the shotcrete used has degraded. This process will result in fragments of rock lying on the floor of the vaults and on the waste packages. It is not clear from the report whether the loading and damage of the waste packages by such rock falls has been considered. However, no account is taken of the waste packages in the assessment models (Section 9.3.8 in TR-14-09: SKB, 2014b), so such damage would not lead to poorer performance than calculated in the assessment.

Stresses on the backfill caused by its own weight and settlement of the backfill by wetting are considered in Section 5.3.1 for the 1BMA and 2BMA vaults, in Section 6.3.1 for the 1BTF and 2BTF vaults and in Section 9.3.1 concerning the BRT vault. However, in Sections 5.3.1 and 6.3.1 the backfill is referred to as sand, whereas in Section 9.3.1 it is referred to as Macadam. The statements in Sections 5.3.1 and 6.3.1 that the backfill is sand is confusing since the descriptions in Section 2 state that all these vaults are to be backfilled with Macadam, or with transition material consisting of 30/70 bentonite/crushed rock.

For the silo, Section 7.3.1 considers stresses in the bentonite wall fill caused by its own weight, and deformation caused by stress changes. This section states that the sand and cement-stabilised sand on top of the silo are affected by the stresses caused by their own weight and the weight of overlying materials and by settlement caused by wetting. Line 30 on page 195 states that before cement degradation the cement-stabilised sand will have properties reminding of poor concrete, with a shear strength that is high enough to withstand settlement and rock fall out. However, after cement degradation the filling will completely loose its strength and the remaining sand will settle by its own weight and by the weight of rock pieces that have come loose from the roof. Table 7-7, which presents the dependencies between variables and mechanical processes affecting the silo states that '*The geometry will be changed after concrete degradation, after rock fall out and after settlement of the sand. These cases will be handled*'.

Report TR-14-04 does not say anything about the creep / flow of bitumen out of damaged waste containers.

5. Geosphere Process Report, TR-14-05

TR-14-05 describes the processes that are expected to occur in the geosphere surrounding the SFR during a period of 100,000 years following closure. The report explains the significance and handling of each process within the SR-PSU.

The extent to which key questions posed by Towler et al. (2015) can be answered by the information in TR-14-03 is considered below.

Is the process that was used to determine the treatment of the different FEPs and couplings described?
TR-14-05, concerning the geosphere processes, like the other process reports, does not deal with the identification of the FEPs. It is stated in Section 1.3 that the '*The Geosphere process report is a product of step 4 [of the assessment methodology] – Description of processes, and identified as relevant for the long-term safety in Step 1 – Handling of FEP's (Features, Events and Processes), in the applied methodology for the long-term safety (Main report, Section 2.4)*'. The geosphere FEPs considered in TR-14-05 are based largely on those in the geosphere processes report of the

SR-Site assessment (SKB, 2010b). However, it is also stated, in Section 1.4.1 that the FEPs used in the SR-PSU were audited against the FEPs in the NEA FEP database version 2.1 (NEA, 2006). The resulting FEP list is stated to be presented in the FEP report (SKB, 2014a), but the details of how the FEPs were chosen are not provided.

Is the treatment of FEPs and couplings described sufficiently, and is the treatment appropriate?

The nature of the information provided concerning couplings between the processes that affect system components and their treatments in the assessment is very similar to the presentation of this information in the waste form and packaging process report (TR-14-02; Section 3). Again, a systematic approach is followed in which the influences of the system variables (geometry, radiation intensity etc. – see Section2) on each process and vice versa are discussed. The processes considered are:

- thermal processes;
- hydraulic processes;
- mechanical processes;
- chemical processes; and
- radionuclide transport.

TR-14-05 does not describe the volume of rock around each different major repository component (each kind of vault, the silo and plugs and other closure components). There is no consideration of how the geosphere may vary across the footprint of the SFR or in the area around it. It is therefore unclear whether a given geosphere process may have a greater impact on one system component than on another. Additionally, the report does not discuss how the geosphere might impact upon possible interactions / couplings between processes in different major components of the facility.

The report discusses influences between geosphere variables and the various processes, and vice versa. The geosphere variables have a similar function within the assessment to the system variables that are considered in TR-14-02, TR-14-03 and TR-14-04. Whereas these system variables describe the properties and condition of the major system components (each kind of vault, the silo and plugs and other closure components), the geosphere variables describe the properties and condition of the geosphere. The geosphere variables considered are:

- **temperature in bedrock**;
- **groundwater flow**;
- **groundwater pressure**;
- **gas phase flow;**
- **repository geometry**;
- fracture and pore geometry;
- **rock stresses;**
- matrix minerals;
- fracture minerals;
- **groundwater composition;**
- **gas composition**;
- **structure and stray materials**; and
- saturation.

Each variable in bold can be equated with one or more system variables considered in TR-14-02, TR-14-03 and TR-14-04.

In TR-14-05 separate tables present the influences of these geosphere variables on the considered processes and influences of the considered processes on the geosphere variables.

The main groups of processes considered by the geosphere process report (TR-14-05) are the same as the processes considered by the engineered barrier process report (TR-14-04) and the waste form and packaging process report (TR-14-03) (except for radiation-related processes which are considered only by TR-14-03). Therefore, couplings between processes in the geosphere and the in the engineered parts of the facility can be deduced.

Are all the potentially relevant mechanical FEPs included in the FEP catalogue and how are they treated in the assessment? Of particular interest are: a) Interactions between adjacent vaults and vaults / the silo; b) Waste stack settlement, e.g. due to creep of metal containers and degradation of waste packages, especially in the silo; c) In the silo, creep / flow of bitumen out of damaged / ruptured waste containers, in response to expansive stresses and the load from over-stacked packages.

Report TR-14-05 covers mechanical processes in the geosphere in Section 4. However, the impact of these mechanical processes on the vaults, silo and closure engineering is not explained directly. No explanation was found of the possible heterogeneity of the mechanical properties of the geosphere and the implication of this heterogeneity for the future behaviour of the vaults, silo and closure engineering. Consistent with its purpose to describe geosphere processes, TR-14-05 does not cover the behaviour of the bitumen within the facility.

6. Summary and Conclusions

Overall the reviewed reports are well-structured and thorough accounts of the initial state of the engineered components of the SFR and the processes that are expected to operate within these structures and in the surrounding geosphere during a period of a 100,000 years following closure.

Couplings between the processes that might affect the evolution of each system component are considered in each of the reviewed reports. TR-10-03 considers couplings between processes that will affect the waste and packaging; TR-14-04 considers couplings between processes that will affect the engineered barrier system; and TR-14-05 considers couplings between processes that will affect the geosphere. However, it is less clear how couplings between each category of processes have been addressed. For example, it is unclear how couplings between processes in the waste form and packages (reported in TR-14-03) and processes in the engineered barriers (reported in TR-14-05) have been considered.

Is the process that was used to determine the treatment of the different FEPs and couplings described?
SKB's approach to identifying the key FEPs relevant to the initial state of the SFR at the time of closure and its subsequent evolution during the subsequent 100,000 years is thorough and provides confidence that all relevant FEPs have been identified. The review did not identify any omissions of FEPs. However, the process by which the

treatment of the FEPs and couplings has been decided in the assessment is not reported in detail in the reviewed documents.

Is the treatment of FEPs and couplings described sufficiently, and is the treatment appropriate?
Couplings between variables, which are stated to be represented in the assessment (e.g. geometry; radiation intensity (waste form only); temperature) and processes affecting the repository components and geosphere are described. The treatment in the assessment of these couplings is explained, together with the associated uncertainties. Because the same (or similar) variables and processes are considered for the waste form and packaging (TR-14-03), engineered barriers (TR-14-04) and geosphere (TR-14-05) it is possible to deduce couplings between system components and how these have been treated in the assessment. However, these couplings are not stated explicitly.

The explanations of the relationships between variables and processes and their treatments are clear and systematic. No obvious omissions were identified in the review. However, it would aid clarity for couplings between the system components to be stated explicitly. An additional limitation is that it is not possible for the reader to understand clearly how geosphere processes will impact upon different parts of the repository, or cause different parts of the repository to interact.

Are all the potentially relevant mechanical FEPs included in the FEP catalogue and how are they treated in the assessment? Of particular interest are: a) Interactions between adjacent vaults and vaults / the silo; b) Waste stack settlement, e.g. due to creep of metal containers and degradation of waste packages, especially in the silo; c) In the silo, creep / flow of bitumen out of damaged / ruptured waste containers, in response to expansive stresses and the load from over-stacked packages.

Mechanical processes are considered in depth. However, very little is stated about interactions between adjacent vaults and vaults/silo. Based on the processes reported and their relationships with the identified key variables, it is possible to make some general inferences about these interactions. However, TR-14-02, TR-14-3 and TR-14-04 would all have benefited from including an explicit consideration of these interactions. From the presented information, it would appear that SKB does not consider such interactions to be significant for overall performance and safety. From the presented information, this would appear to be reasonable, but some explicit explanation for the reasons would have been helpful.

Additionally, the geosphere process report (TR-14-05) covers mechanical processes in the geosphere, but does not explain clearly how these might impact on the vaults, silo and closure engineering.

Very little information could be found in the reviewed reports concerning the possibility of waste stack settlement and its treatment within the assessment. Similarly, none of the reports were found to cover the possibility of bitumen creeping/flowing out of failed containers due to loading by overlying stacks of containers or expansion of the bitumen. This latter process is, however, recognized as being potentially important.

We do not expect these mechanical processes, and the implications for coupled hydro-chemical processes, would markedly change the assessment results, if they were important. Nevertheless, these findings indicate there is scope to further assess

the mechanical evolution of the near-field, and the implications of this for barrier performance. The same conclusions are drawn regarding mechanical interactions between the vaults and the vaults/silo. It is noted that the review has not searched through the much wider suite of SR-PSU reports to see if these processes and couplings are further treated elsewhere.

7. References

NEA, 1997. Safety assessment of radioactive waste repositories – Systematic approaches to scenario development – An international database of Features, Events and Processes. Draft report (24/6/97) of the NEA working group on development of a Database of Features, Events and Processes relevant to the assessment of post-closure safety of radioactive waste repositories. Paris: OECD/NEA.

NEA, 2006. Electronic version 2.1 of the NEA FEP database developed on behalf of the Nuclear Energy Agency by Safety Assessment Management Ltd.

SKB, 2010a. Buffer, backfill and closure process report for the safety assessment SR-Site. SKB TR-10-47, Svensk Kärnbränslehantering AB.

SKB, 2010b. Geosphere process report for the safety assessment SR-Site. SKB TR-10-48, Svensk Kärnbränslehantering AB.

SKB, 2014a. FEP report for the safety assessment SR-PSU. SKB Report TR-14-07, Svensk Kärnbränslehantering AB.

SKB, 2014b. Radionuclide transport and dose calculations for the safety assessment SR-PSU. TR-14-09.

SKB, 2011. Long-term safety for the final repository for spent nuclear fuel at Forsmark. Main report of the SR-Site project. SKB TR-11-01, Svensk Kärnbränslehantering AB.

SKB, 2015. Safety analysis for SFR. Long-term safety. Main report for the safety assessment SR-PSU. SKB TR-14-01, Svensk Kärnbränslehantering AB.

Towler, T., Robinson, P., Watson C. and Penfold J.S. 2015. Review of radionuclide transport methodology in SR-PSU. Initial Review Phase Report to SSM, Call-off request number SSM2015-1019, Activity number: 3030014-1005 September 7th 2015.

Coverage of SKB reports

Following reports have been covered in the review.

Table A1-1: Coverage of SR-PSU reports.

Reviewed report	Reviewed sections	Comments
TR-14-02	All	None
TR-14-03	Sections relating to radionuclide transport	Also keyword search of the entire document
TR-14-04	Sections relating to radionuclide transport	Also keyword search of the entire document
TR-14-05	Sections relating to radionuclide transport	Also keyword search of the entire document

3

Authors: George Towler and James Penfold [1]
             [1]Quintessa Limited, Henley on Thames, UK

Consequence analysis review: importance of caissons in 2BMA

Abstract

The Swedish Radiation Safety Authority (SSM) received an application for the expansion of SKB's final repository for low and intermediate level waste at Forsmark (SFR) on 19 December 2014. SSM is tasked with the review of the application and will issue a statement to the government who will decide on the matter. An important part of the application is SKB's assessment of the long-term safety of the repository, which is documented in the safety analysis named SR-PSU.

SSM's review is divided into an initial review phase and a main review phase. This assignment contributes to the main review phase. In a study already undertaken as part of the main review phase, some of SKB's radionuclide transport models were reimplemented using the information provided in the SR-PSU documentation. The results were compared with the results of SKB's models, and model sensitivity and reasons for the differences were explored. The models reimplemented were SKB's near-field model for the proposed 2BMA vault, and SKB's model for the geosphere. SKB used the ECOLEGO code. The models were reimplemented using the AMBER code.

The concrete caissons were identified as a key feature for containment of radionuclides. The scope of the current assignment is to further understand the importance of the caissons and SKB's approach to modelling the caissons by:

a. reviewing and clarifying SKB's modelling approach for completely degraded concrete, including the assumptions made;
b. re-implementing the radionuclide transport models for the Accelerated Concrete Degradation Scenario in a suitable assessment code;
c. examining the sensitivity of the calculation results to the properties assumed for the wastes, and the grout used to fill around the waste packages in the caissons; and
d. implementing a case in which the caissons are assumed to be completely degraded at the start of the post-closure phase.

The key conclusions from the current assignment are as follows.

a. The Accelerated Concrete Degradation calculation case makes significantly cautious assumptions about the hydraulic properties of the concrete, consistent with SKB's classification of the scenario as a less probable scenario. The intact concrete is considered to have a hydraulic conductivity of 8.3E-10 m/s, the severely degraded concrete 1E-5 m/s and the completely degraded concrete 1E-3 m/s. A hydraulic conductivity of 1E-3 m/s is of the order that would be expected for a gravel, so this could be a cautious value. However, SSM have noted that cracks in the existing 1BMA caissons, result in areas of the 1BMA caisson walls having a hydraulic conductivity of this order. So, this is not an implausible value. (Remedial works are planned to be undertaken to reduce the hydraulic conductivity of the caissons in 1BMA prior to closure of the vault). The Accelerated Concrete Degradation calculation case assumes the chemical degradation of the concrete is identical to the Global Warming calculation case. However, the flows through the grout and wastes inside the caissons are significantly increased. This would increase the rate of cement alteration, so other SR-PSU near-field chemistry review area might consider whether this assumption is reasonable after thousands of years.

b. SKB's models were reimplemented for the proposed 2BMA vault using the AMBER code. The AMBER model of the Accelerate Concrete Degradation calculation case gives very similar results to the ECOLEGO model for radionuclides that are not sorbed or only weakly sorbed. This provides good confidence in the ECOLEGO implementation. However, there significant differences for radionuclides that are more strongly sorbed. Additional information on the configuration and parameterisation of SKB's models would be required to explore the reasons for these differences further. However, they only affect radionuclides that are of secondary importance for calculated biosphere doses, and the fluxes calculated by ECOLEGO are cautious (i.e. higher) relative to the fluxes calculated by AMBER.

c. The results of sensitivity cases show that the properties assumed for the wastes, and the grout used to fill around the waste packages in the caissons, affect the release of radionuclides that are more strongly sorbed. Changes to the parameter values used in the AMBER model, that affect radionuclide sorption, resulted in an improved fit against the ECOLEGO model results for radionuclides that are more strongly sorbed.

d. An extreme case in which the caissons are assumed to be fully degraded throughout the assessment timeframe could potentially result in higher doses than the Accelerated Concrete Degradation calculation case. However, this extreme case may not be realistic because it assumes the grout and waste packages inside the caissons are also highly permeable throughout the assessment timeframe, in addition to the walls of the caissons.

Contents

1 Introduction

The Swedish Radiation Safety Authority (SSM) has received an application for the expansion of SKB's final repository for low and intermediate level waste at Forsmark (SFR) on 19 December 2014. SSM is tasked with the review of the application and will issue a statement to the government who will decide on the matter. An important part of the application is SKB's assessment of the long-term safety of the repository, which is documented in the safety analysis named SR-PSU.

SSM's review is divided into an initial review phase and a main review phase. This assignment contributes to the main review phase. In the main review phase, Towler and Penfold (2017) reimplemented some of SKB's radionuclide transport models using the information provided in the SR-PSU documentation. The results were compared with the results of SKB's models, and model sensitivity and reasons for the differences were explored. Towler and Penfold (2017) reimplemented SKB's near-field model for the proposed 2BMA vault, and SKB's model for the geosphere. Towler and Penfold (2017) implemented the models using the AMBER code (Quintessa, 2016), while SKB used the ECOLEGO code[1].

The concrete caissons have been identified as a key feature for containment of radionuclides. The scope of this assignment is to further understand the importance of the caissons and SKB's approach to modelling the caissons by:

a. reviewing and clarifying SKB's modelling approach for completely degraded concrete, including the assumptions made;
b. re-implementing the radionuclide transport models for the Accelerated Concrete Degradation Scenario in a suitable assessment code;
c. examining the sensitivity of the calculation results to the properties assumed for the wastes, and the grout used to fill around the waste packages in the caissons; and
d. implementing a case in which the caissons are assumed to be completely degraded at the start of the post-closure phase.

Approach

The calculations presented in this report were undertaken using the AMBER model developed by Towler and Penfold (2017). On 28 October 2016, SKB gave a presentation to SSM on the radionuclide transport modelling for 1BMA and 2 BMA. The compartmental configuration used to represent the waste packages in ECOLEGO was not clearly described in SKB's SR-PSU documentation, and the SKB presentation revealed that the configuration used in the AMBER model was slightly different to that used in the ECOLEGO model. Tetramoulds were represented specifically in ECOLEGO, while in AMBER they were included with steel moulds (consistent with the description on page 197 of TR-14-09). Based on the results of the existing AMBER sensitivity calculations, the impact of this difference is expected to be small. Therefore, the AMBER model was not updated for this assignment. This approach maintains consistency with the early results of Towler and Penfold (2017), which is important when the AMBER results for the Accelerated Concrete Degradation Calculation Case (CCL_BC) are compared

---

[1] http://ecolego.facilia.se/ecolego/show/HomePage

against the existing AMBER results for the Global Warming Calculation Case (CCM_GW).

The Accelerated Concrete Degradation Calculation Case

The Accelerated Concrete Degradation Calculation Case (CCL_BC) is described in Section 4.2.3 of TR-14-09. The case assumes the concrete caissons physically degrade much more rapidly than in the CCM_GW. This leads to higher flow rates through the caissons, and hence the wastes and grout inside the caissons, at earlier times compared with the CCM_GW. However, accelerated chemical degradation is not considered, as the CCM_GW is already considered to cautiously overestimate the rate of chemical degradation.

We note that SKB make potentially cautious assumptions regarding the hydraulic conductivity of the concrete. The intact concrete is considered to have a hydraulic conductivity of 8.3E-10 m/s, the severely degraded concrete 1E-5 m/s and the completely degraded concrete 1E-3 m/s. A hydraulic conductivity of 1E-3 m/s is of the order that would be expected for a gravel, so this could be a cautious value. However, SSM have noted that cracks in the existing 1BMA caissons, result in areas of the 1BMA caisson walls having a hydraulic conductivity of this order. So, this is not an implausible value. (Remedial works are planned to be undertaken to reduce the hydraulic conductivity of the caissons in 1BMA prior to closure of the vault).

Table 4-7 in TR-14-09 shows that the CCL_BC assumes the concrete to be severely degraded from 3000 AD to 22,000 AD and completely degraded thereafter. In addition, the caissons are assumed to be fractured throughout the assessment timeframe. Under these conditions SKB assume radionuclides are transported by advection through the fractures without retardation by sorption.

The results of Towler and Penfold (2017) suggested there was a difference between the implementation of the fracture model in AMBER and ECOLEGO. On 5 May 2017, SKB issued complementary information (SKB, 2017) describing that a correction had been made to the implementation of the concrete fracture model in ECOLEGO. The note did not explain the nature of the correction, but presented updated calculated biosphere doses for the CCM_GW and CCL_BC cases, and compared them to the original results. Changes have not been made to the implementation of the fracture model in AMBER – it is consistent with the description in TR-14-09, so it is assumed to be correct.

Subsequent to issue of their complementary information (SKB, 2017), SKB have provided the following addition results to supported this review.
- Fluxes of selected radionuclides from the near-field to the geosphere, for the CCM_GW with corrected fracture flow model.
- Fluxes of selected radionuclides from the near-field to the geosphere, for the CCL_BC with corrected fracture flow model, and corrections to the waste volumes.

The original (SR-PSU) fluxes from the near-field to the geosphere for the CCL_BC were not available for this review.

Report Structure

This report is structured as follows.

- Section 2 discusses the results of the corrected CCM_GW and CCL_BC cases. The changes in the dose curves for the CCL_BC are used to infer the potential changes in the radionuclide fluxes from the near-field to the geosphere, and geosphere to the biosphere.
- Section 3 presents the results for the AMBER model of the CCL_BC.
- Section 4 presents the results of sensitivity cases.
- Section 5 presents the results of a calculation case where the caissons are assumed to be completely degraded from the start of the assessment.
- Section 6 presents the conclusions from this further review task.

2   Corrected SR-PSU Cases

Selected radionuclides fluxes from the near-field to the geosphere calculated by AMBER for the CCM_GW are compared with the original SR-PSU results (top) and the new corrected results from SKB (2017) (bottom) in Figure 1. The potential reasons for the differences between the AMBER results and SR-PSU results have been explored by Towler and Penfold (2017) and are not repeated here. Of note is the significant difference in the fluxes at 22,000 AD when the caissons are assumed to fracture. The fluxes calculated by AMBER exhibit a step increase at this time. The original SR-PSU results exhibit a smaller and more gradual increase. The corrected results exhibit a larger step increase in the fluxes, that is much more consistent with the AMBER results.

It is noted that the corrected ECOLEGO results result in significantly higher fluxes of C-14_inorg, Tc-99 and Pu-239 post-22,000 AD.

The calculated doses for the original and corrected CCM_GW cases are compared in Figure 2. Cl-36 and I-129 are not sorbed in the geosphere. In the corrected model there is a significant increase in the doses just after 22,000 AD, i.e. shortly after cracking of the caissons, when the fracture flow model is invoked for transport through the caissons. Cl and I are not sorbed in the geosphere (Table 8-6 in TR-14-10), hence a step increase in the releases from the caissons results in a step increase in biosphere doses only a short time later.

Mo is not sorbed in the geosphere either, and Figure 19 in Towler and Penfold (2017) shows that the Mo-93 fluxes from the geosphere to the biosphere calculated by AMBER exhibit a step increase at 22,000 AD. However, the doses due to Mo-93 decrease at 22,000 AD. The different responses of the calculated doses must be due to different behaviour of Mo compared with Cl and I in the biosphere.

The doses from Ni-59 are significantly increased beyond 22,000 AD compared with the original model. This is consistent with the results of the AMBER model, which showed a large step increase in fluxes from the near-field to the geosphere, and the geosphere to the biosphere at this time. Ni is only very weakly sorbed in the geosphere (Table 8-6 in TR-14-10), so in the AMBER model results the step increase in the flux from the near-field to the geosphere is not significantly attenuated when breakthrough at the geosphere-biosphere interface occurs (Figure

19 in Towler and Penfold, 2017). SKB's corrected dose calculations show a gradual increase in doses from Ni-59 post-22,000 AD. Figure 37 in Towler and Penfold (2017) shows that the AMBER and ECOLEGO geosphere models give near identical results for a range of radionuclides, including Ni-59. So the gradual increase in doses from Ni-59 post-22,000 AD must reflect the behaviour of Ni in the biosphere. This behaviour was discussed with experts from the biosphere review area, but the reason(s) for this behaviour could not be identified from the information available to the reviewers.

Figure 1. Comparison of radionuclides fluxes from the 2BMA vault to the geosphere calculated by AMBER (AMB) for the CCM_GW, compared with the original SR-PSU ECOLEGO (ECO) results (top) and the new corrected ECOLEGO (ECL) results (bottom)
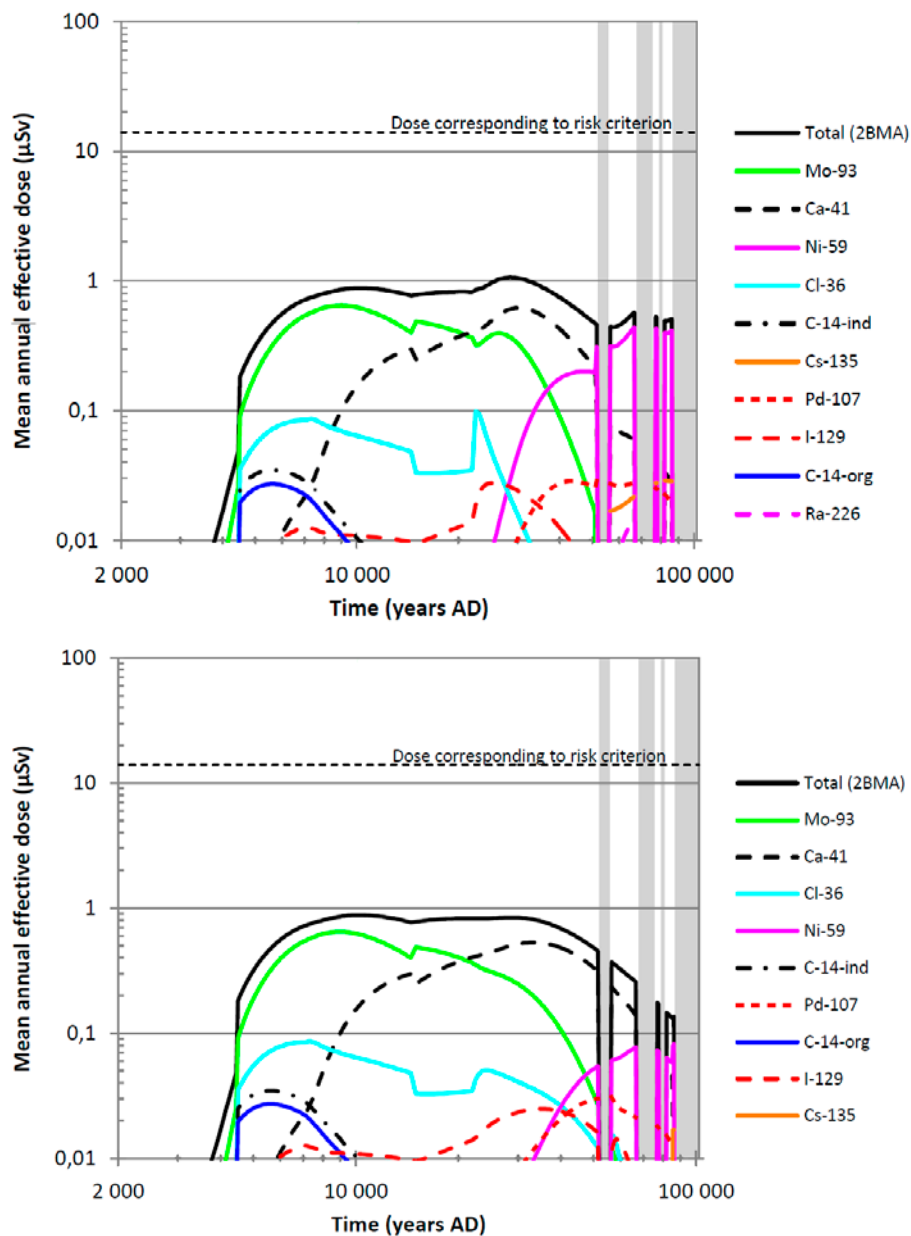
Figure 2. Corrected (top) and original (bottom) calculated doses from radionuclides released from the 2BMA vault for the CCM_GW calculation case (SKB, 2017)

The calculated doses for the original and corrected CCL_BC cases are compared in Figure 3. Comparison of the results shows:

- The original and corrected results show step increases in doses from Mo-93, Cl-36 and C-14_org at ~4,500 AD.
- The corrected results show step decreases in doses from Ni-59, Cl-36, Ca-41 and I-129 at 10,000 AD. This does not occur in the original results, although there is a smaller step decrease in the doses from Cl-36 and Ca-41 at ~12,000 AD.
- The corrected results show step increases in the doses from Ni-59 and I-129, and step decrease in doses from Ca-41 and Mo-93 at ~29,000 AD. These step changes are not present in the original results.

The original assessment calculations do not include any step changes in the near-field or geosphere flows or properties around 4,500 AD, 10,000 AD or 29,000 AD. From the complementary information provided by SKB, this should still be true for the corrected calculations. This is confirmed by the corrected radionuclide fluxes from the near-field to the geosphere calculated by ECOLEGO, which do not contain any step changes at these times.

The step change at ~4,500 AD coincides with a well becoming viable in biosphere object 157_2 (Table 4-1 in R-13-18). However, the reasons for the other step changes has not been identified. In addition, it is not known why at ~29,000 AD there are step increases in doses for some radionuclides, but step decreases for others.
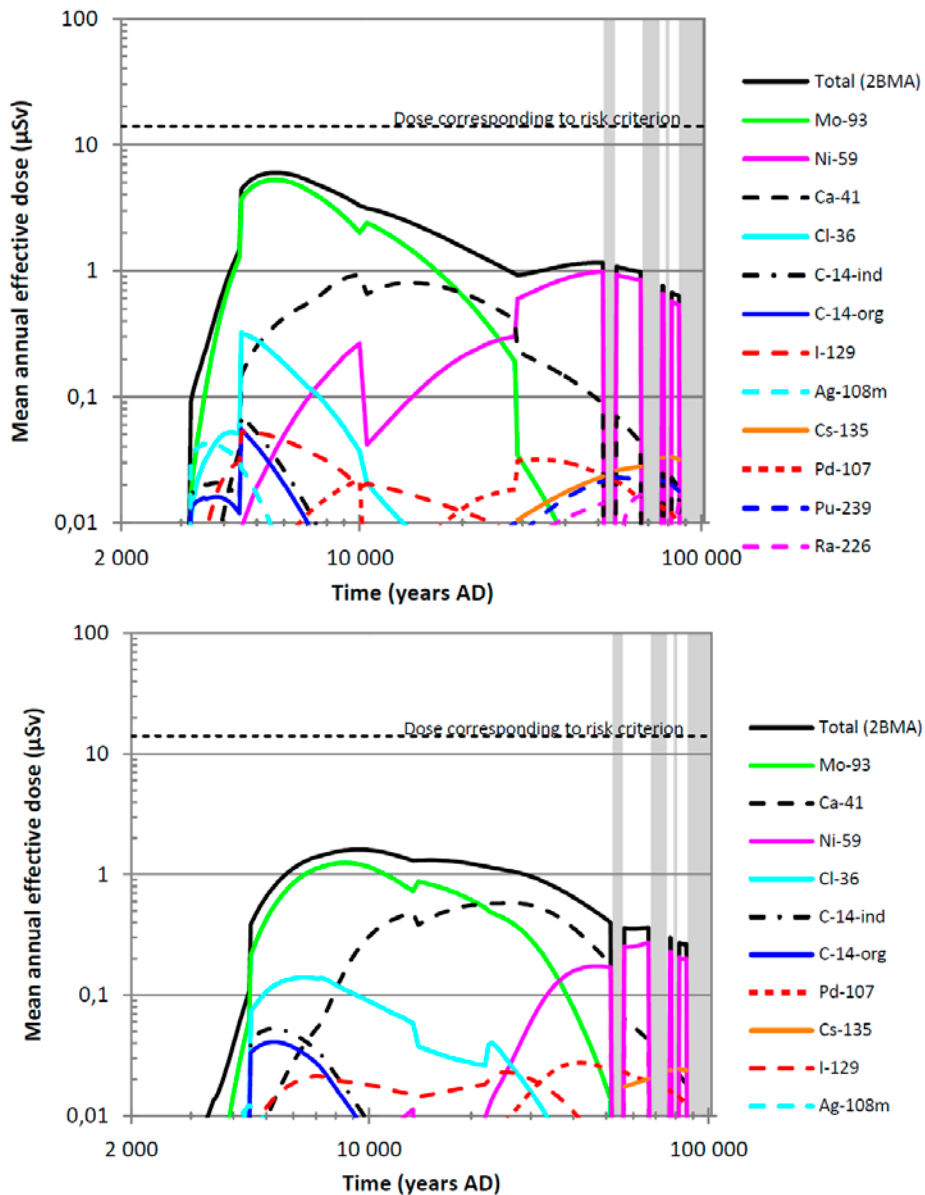
Figure 3. Corrected (top) and original (bottom) calculated doses from radionuclides released from the 2BMA vault for the CCL_BC calculation case (SKB, 2017)

3 Reimplementation of Radionuclide Transport Calculations for the Accelerated Concrete Degradation Scenario

The changes made to the AMBER model for the CCM_GW to implement the CCL_BC case were:

- flows through the near-field (Table 4-7 in TR-14-09);
- effective diffusivities (Table 4-8 in TR-14-09);
- porosities (Table 4-9 in TR-14-09); and
- the nature of the concrete - it is assumed to be fractured at all times (Table 4-7 in TR-14-09).

SKB had previously provided three spreadsheets that describe the flows through the near-field for the different shoreline positions at 2000 AD, 3000 AD and 5000 AD; and for each concrete degradation state at each shoreline position. The flows through the caissons and surrounding macadam were updated using data from the spreadsheets (SKBdoc 1595131), consistent with the pattern of flows described in Table 4-7 of TR-14-09.

Figure 4 shows that peak radionuclide fluxes are greater and occur earlier compared with the CCM_GW case. This is due to the greater flows through the caissons, and no sorption of radionuclides onto the caissons. This is reflected in the distribution of activity in the model (Figure 5), which shows a significant reduction in the amount of activity within the walls of the caissons before 22,000 AD, and a significant increase in the amount of activity released to the geosphere / biosphere. (Note in CCM_GW, the caissons fracture at 22,000 AD and there is no sorption onto the caissons beyond this time. Hence the amount of activity within the walls of the caissons decreases significantly at 22,000 AD as sorbed radionuclides are released).

The fluxes from the near-field to the geosphere calculated by AMBER and ECOLEGO are similar for C-14_org, Ni-59, Mo-93 and I-129 (Figure 6). However, the fluxes calculated by ECOLEGO are significantly greater than calculated by AMBER for radionuclides that are more strongly sorbed, i.e. C-14_inorg, Tc-99 and Pu-239. The ECOLEGO model results will therefore lead to higher calculated biosphere doses than the AMBER model results for these more strongly sorbed radionuclides. However, the calculated biosphere doses are dominated by radionuclides that are not sorbed, or are only weakly sorbed. These more strongly sorbed radionuclides are of secondary importance. The reasons for these differences are further explored in Section 4.
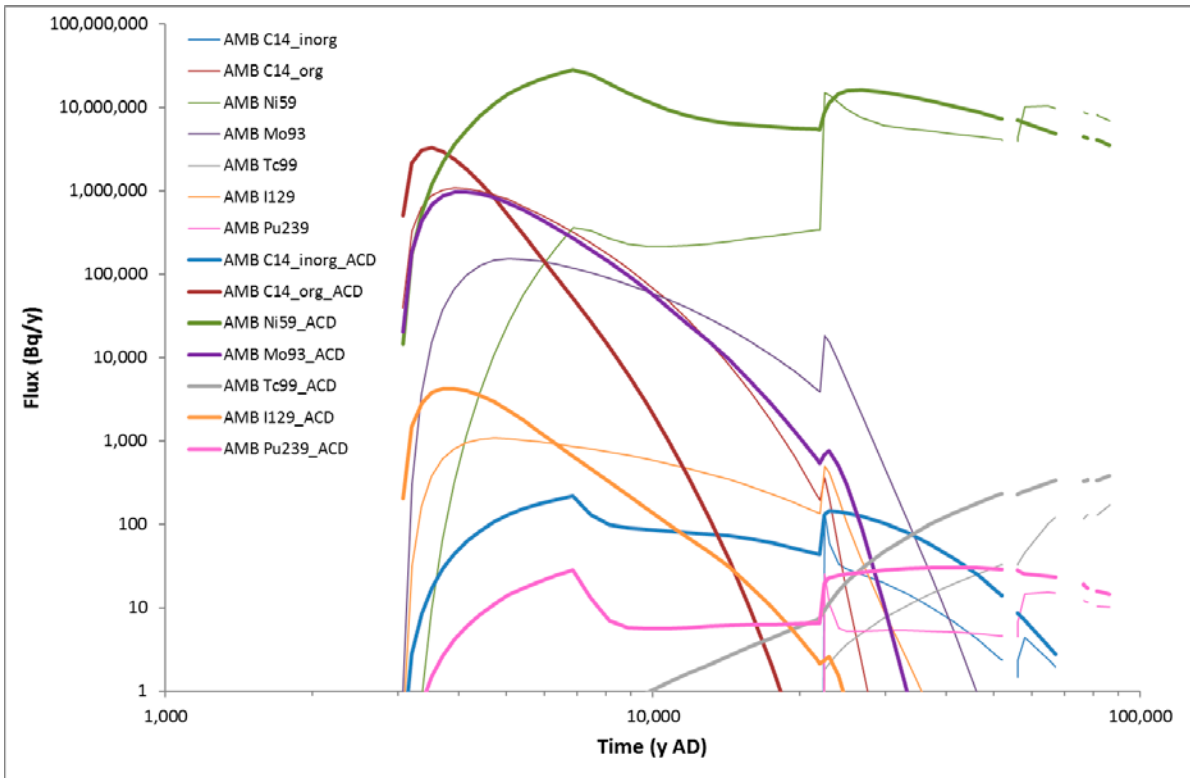
Figure 4. Comparison of radionuclide fluxes from the 2BMA vault to the geosphere calculated by AMBER for the global warming calculation case and accelerated concrete degradation calculation case (_ACD)

Figure 5. Comparison of the location of activity disposed to the 2BMA vault calculated by AMBER for the global warming calculation case (GW) and accelerated concrete degradation calculation case (ACD)
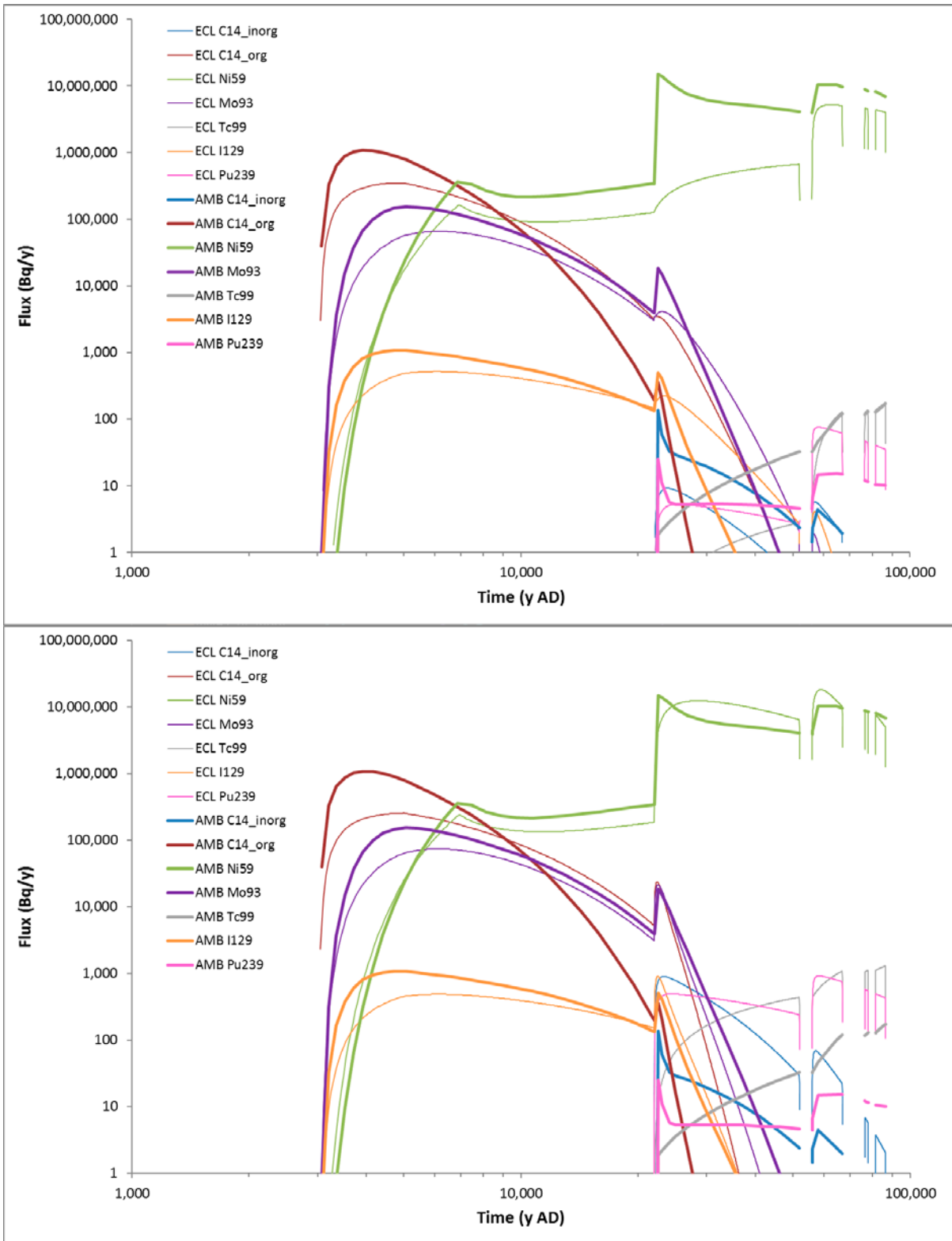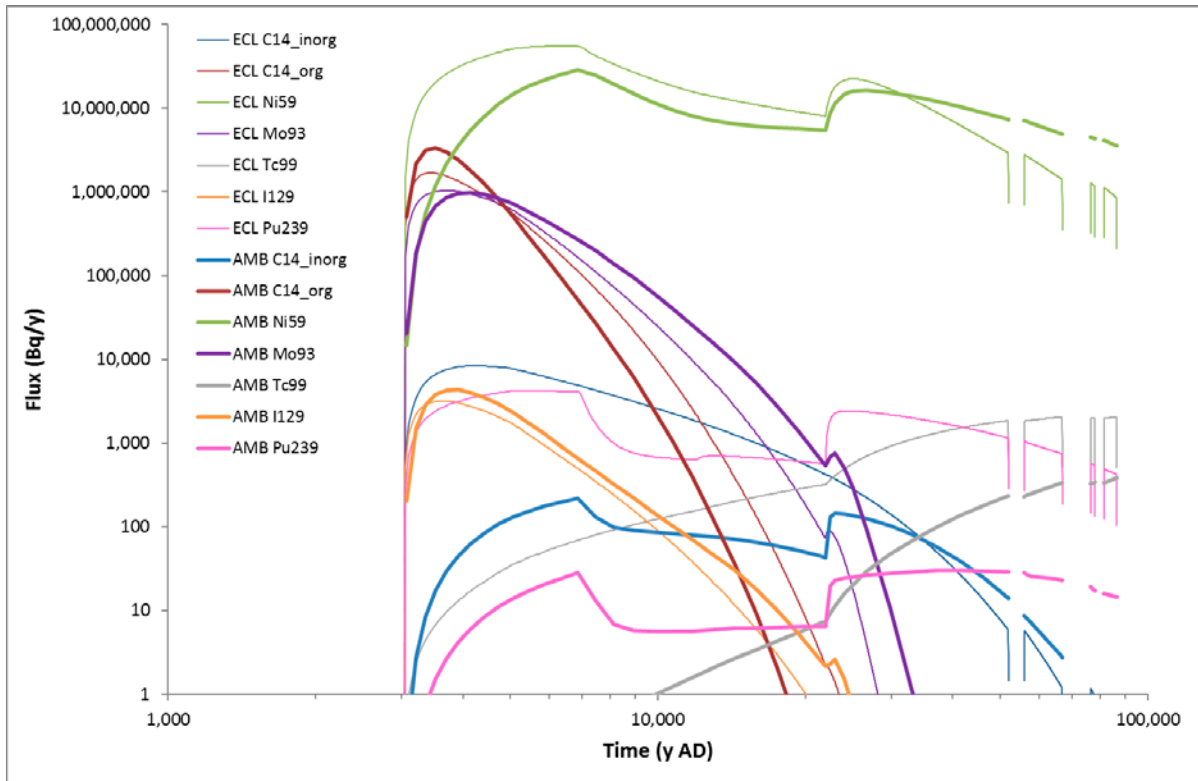
Figure 6. Comparison of radionuclide fluxes from the 2BMA vault to the geosphere calculated by AMBER (AMB) and the corrected fluxes calculated by ECOLEGO (ECL) for the accelerated concrete degradation calculation case

As noted previously, the AMBER and ECOLEGO geosphere models give very similar results for a range of radionuclides. Therefore, we would expect the fluxes of C-14_org, Ni-59 and Mo-93 from the geosphere to the biosphere calculated by ECOLEGO for the corrected CCL_BC to be very similar to the fluxes calculated by AMBER.

4 Sensitivity Cases

This section focuses on exploring the sensitivity of the accelerated concrete degradation calculation case results to different assumptions and parameter values.

Cases were run to test the sensitivity of the radionuclide fluxes from the near-field to the geosphere to the representation of, and properties assumed for, the wastes and the grout used to fill around the waste packages in the caissons. The choice of cases was informed by the results of the sensitivity cases presented by Towler and Penfold (2016).

In addition, a number of cases were run to explore the reasons for the significant differences in the fluxes from the near-field to the geosphere calculated by AMBER in comparison to ECOLEGO for radionuclides that are more strongly sobbed. It is noted that the ECOLEGO results are cautious compared with the AMBER results, and these radionuclides are of secondary importance for calculated biosphere doses.

The depth of analysis that has been undertaken to understand the reasons for the differences is proportionate to this context.

4.1 Fracturing of Moulds

The AMBER model includes the assumption that the concrete moulds fracture at the same time as the caissons. The same fracture transport model is used, i.e. there is no sorption onto the fractured moulds. A calculation was run where the moulds were assumed not to fracture. Figure 7 shows that the radionuclide fluxes from the near-field to the geosphere were not significantly changed so the results are not sensitive to this assumption. There was a change to the flux of Pu-239, but the flux is only ~10 Bq/y, which is very small.
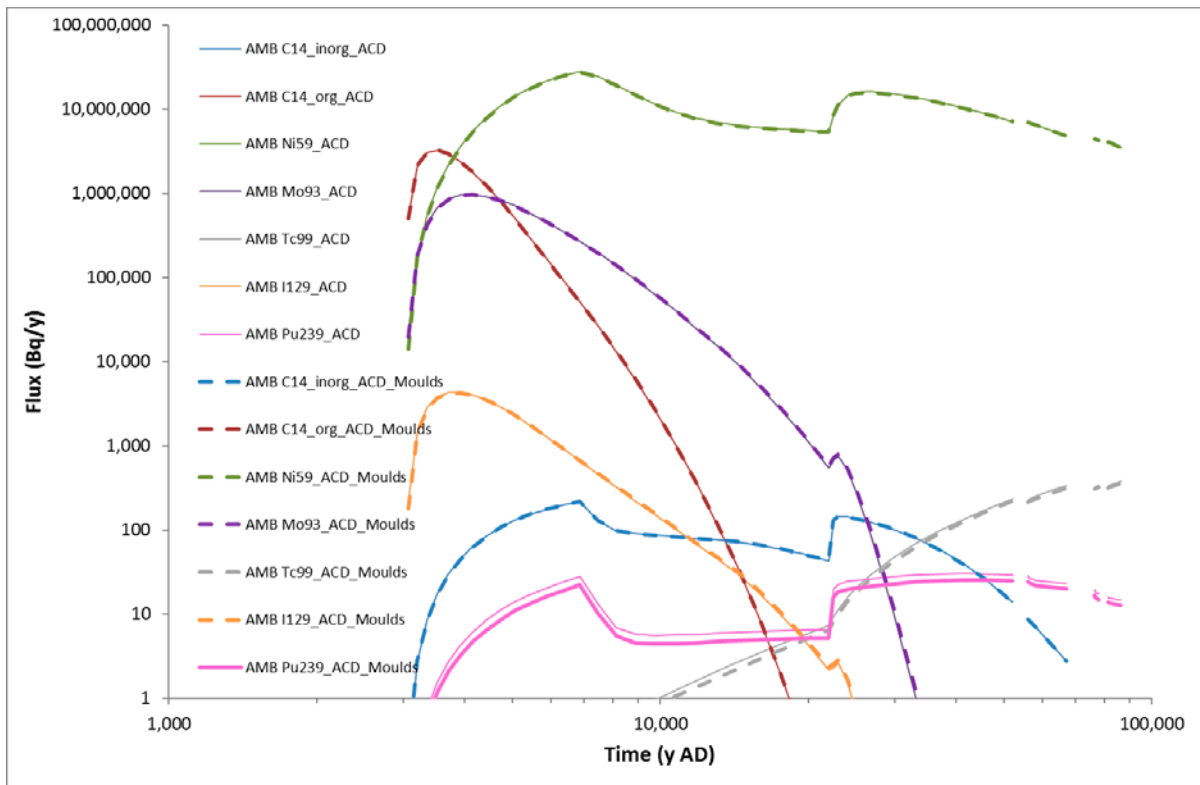
Figure 7. Comparison of radionuclide fluxes from the 2BMA vault to the geosphere calculated by AMBER for the accelerated concrete degradation case with cracking of the moulds (_ACD) and without cracking of the moulds (_ACD_Moulds)

4.2 Chemical Degradation

In the CCL_BC, it is assumed there is no additional chemical degradation of the cementitious components compared with the CCM_GW. In the CCM_GW, it was assumed that the concrete degradation state of all cementitious materials in 2BMA is state I to 7,000 AD, and state II thereafter (Table 4-4 in TR-14-09).

In CCL_BC there is no sorption onto the concrete caissons because they are assumed to be fractured, so this assumption only affects sorption onto the cementitious wastes and grout. Also, in the AMBER model, there is no sorption onto the concrete moulds which are also assumed to be fractured.

An important factor in the rate of concrete degradation is the flux of solutes in groundwater that are able to react with the concrete and degrade it. In CCM_GW the cumulative[2] flux of water through Caisson 1 between 3,000 AD and 7,000 AD is 32.6 m^3. In CCL_BC the cumulative flux over the same time period is 2309 m^3. Therefore, a variant of CCL_BC was run in which concrete degradation state II was assumed at all times. However, it is noted that with such high flow rates more advanced chemical degradation states (i.e. state IIIa or IIIb) might be reached within the assessment timeframe; although calculations to assess this possibility have not been undertaken as part of this radionuclide-transport review.

The calculated fluxes from the near-field to the geosphere are shown in Figure 8. This assumption either does not change the radionuclide fluxes or reduce the fluxes. This is because, for the radionuclides modelled in AMBER, there is no change in the sorption distribution coefficient (Kd) from state I to state II, or sorption increases. The SR-PSU near-field chemistry review area might consider whether this increase in sorption is realistic, or is an artefact of the distribution of values available.
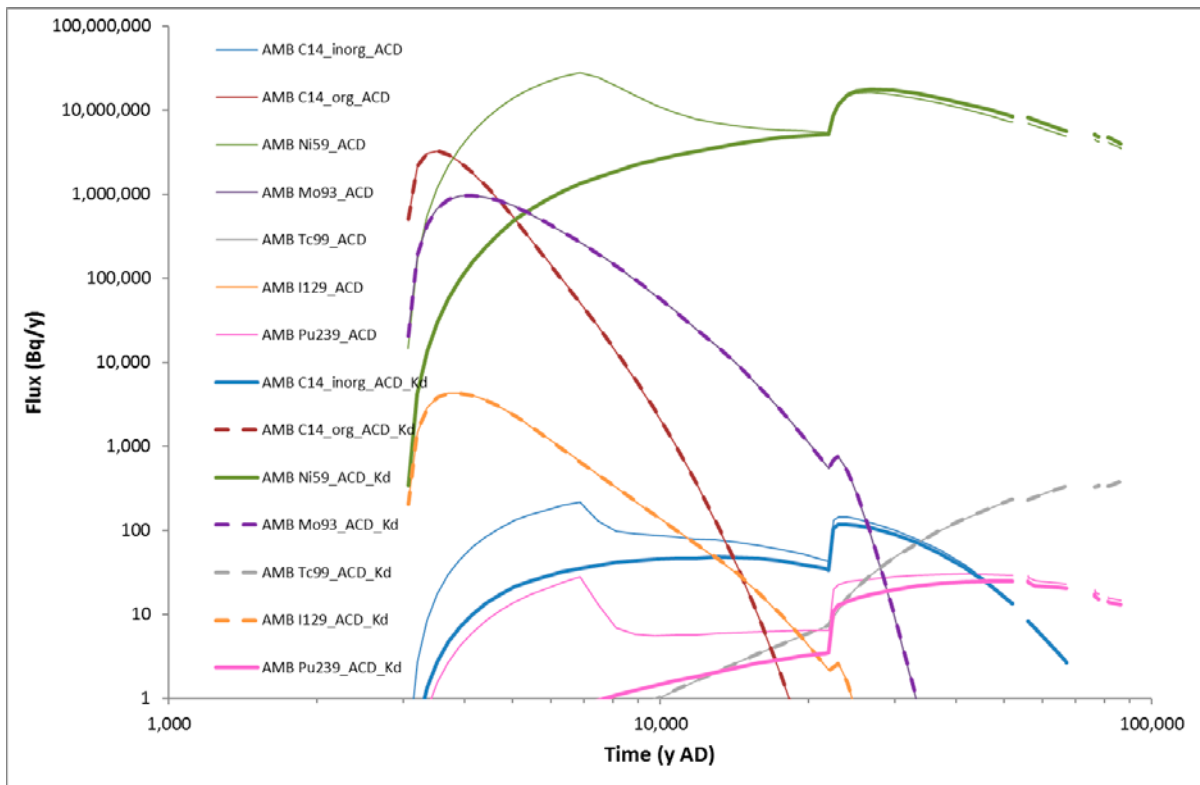
Figure 8. Comparison of radionuclide fluxes from the 2BMA vault to the geosphere calculated by AMBER for the accelerated concrete degradation calculation case (_ACD) and for the accelerated concrete degradation case assuming concrete degradation state II at all times (_ACD_Kd)

---

[2] Calculated as the integral of the flow-rate vs time curve.

4.3 Representation of the Caisson Walls

Variant Case 12 (NF_Var12) of Towler and Penfold (2016) explored sensitivity of the calculated radionuclide fluxes, from the near-field to the geosphere, to the discretisation of the caisson walls in the AMBER model for the CCM_GW case. In both the AMBER and ECOLEGO models the caisson walls are discretised into five compartments. In Variant Case 12, the discretisation of the caisson walls in AMBER was changed from compartments of uniform thickness to compartments of increasing thickness from the inside of the caisson to the outside. The changes affect the calculations of radionuclide diffusion through the caisson walls. The changes were found to give an improved match between ECOLEGO and AMBER for mobile radionuclides at early times for the CCM_GW case.

The same changes were implemented for the CCL_BC for the current study. The calculated radionuclide fluxes from the near-field (Figure 9) were negligibly changed compared with the original model (Figure 6). The fluxes are much less sensitive to the discretisation of the caissons in the CCL_BC than the CCM_GW because the flows through the caisson walls are greater. Therefore, diffusion is a less significant component of radionuclide transport.
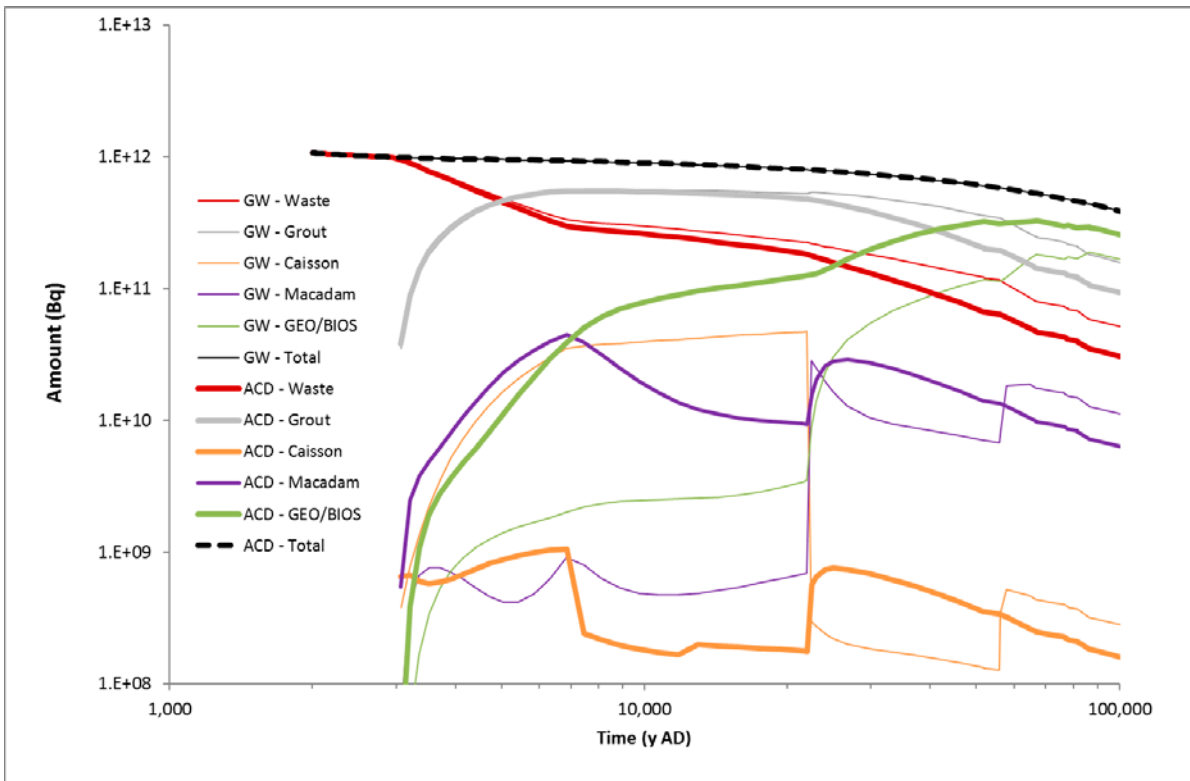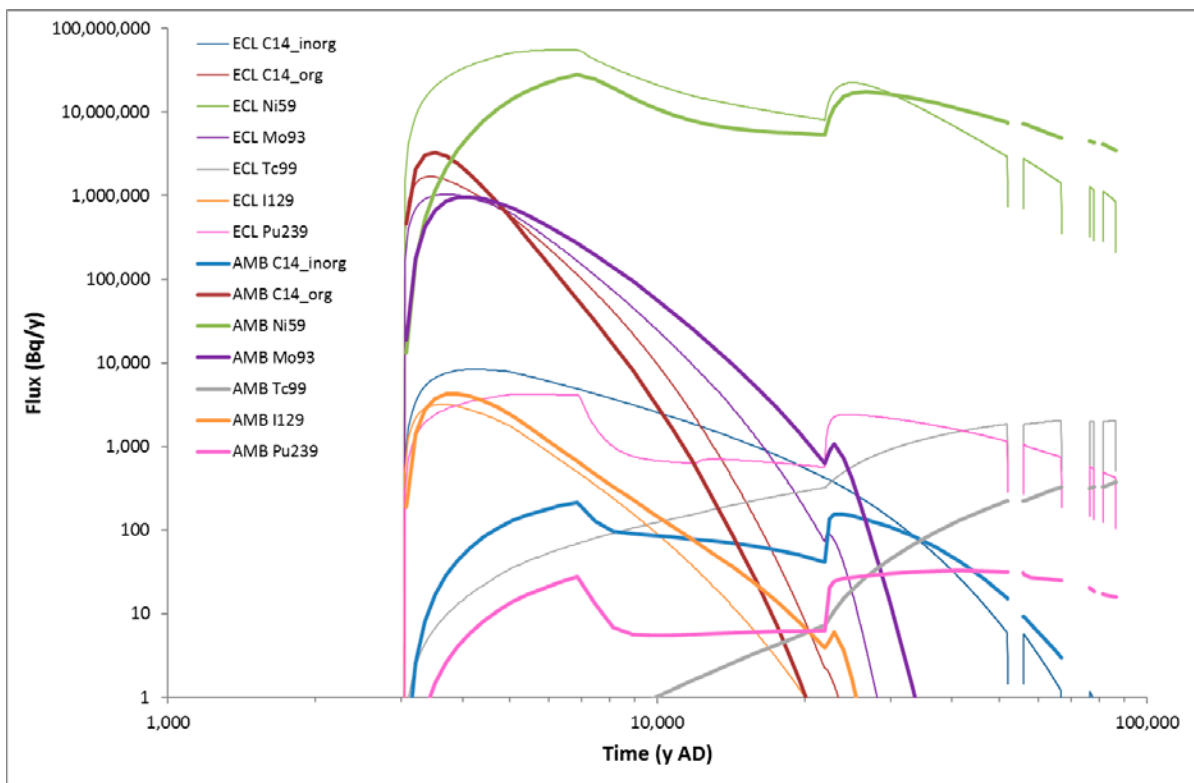

Figure 9. Comparison of radionuclide fluxes from the 2BMA vault to the geosphere calculated by ECOLEGO (ECL) and AMBER (AMB) for the accelerated concrete degradation calculation case, with changes to the discretisation of the caisson walls.

4.4 Representation of the Waste Packages

Towler and Penfold (2016) noted that the configuration of ECOLEGO to represent the waste packages was not clearly explained in the SR-PSU reports. Further the properties assumed for the waste packages (density, porosity, cement content, etc), and compartment dimensions used to represent the waste packages, were not reported. On 28 October 2016, SKB's safety assessment modelling sub-contractors gave a presentation to SSM where they provided more details on the configuration of the ECOLEGO near-field model (Åstrand, 2016).

Figure 10 shows the compartmental configuration used to represent the waste packages, in the 2BMA vault, in ECOLEGO. This configuration was implemented for a single caisson in AMBER. A similar variant case was explored by Towler and Penfold (2016), which was termed variant case 1 (NF_Var1). The parameterisation of the waste packages was taken from variant case 1 of Towler and Penfold (2016).
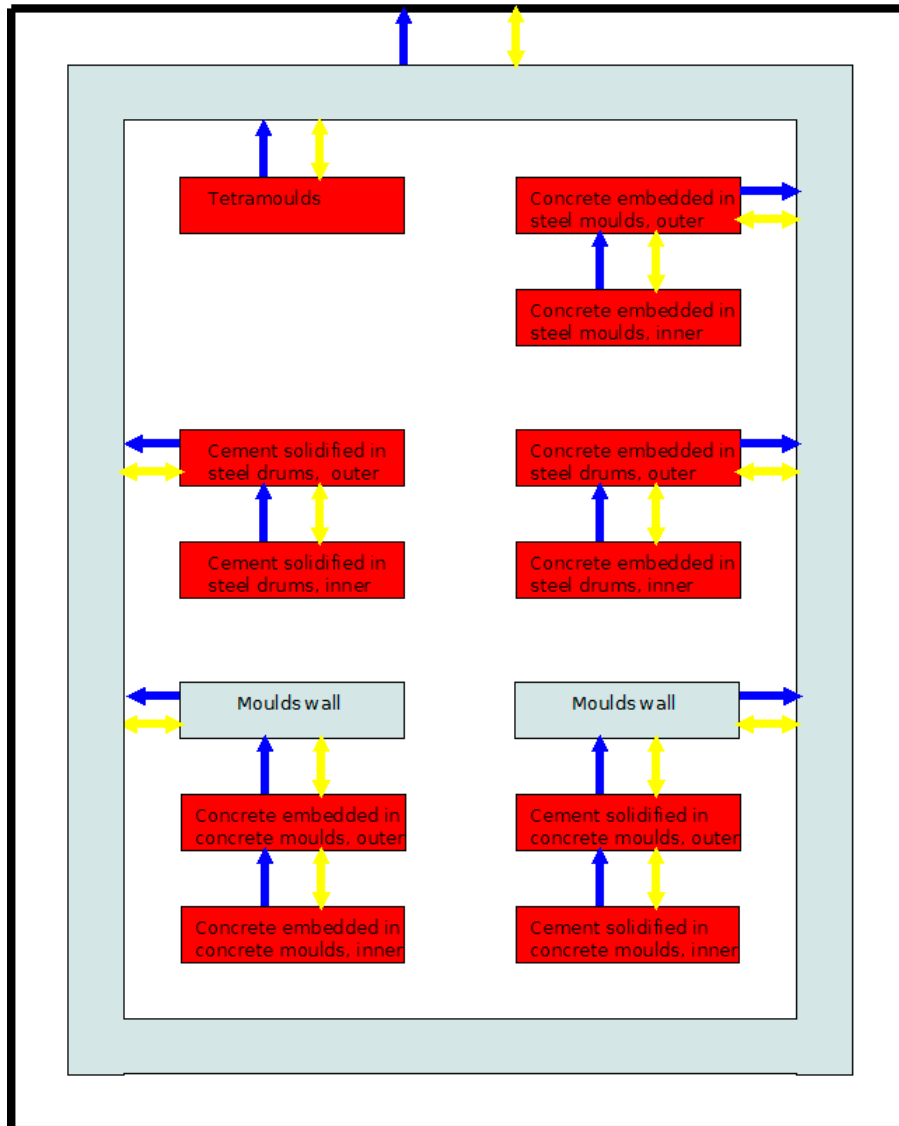
Figure 10. Representation of the waste packages in a caisson, in 2BMA, in ECOLEGO.

Variant case 1 of Towler and Penfold (2016) did not consider the Tetramoulds as a separate waste group (p197 in TR-14-09 states that tetramoulds are included under steel moulds). The AMBER model was further modified to represent the tetramoulds as a single compartment.

This required the Tetramoulds to be added to the AMBER model as a new package type, and the inventory to be recalculated. The recalculated waste package and radionuclide inventories are given in Table 1 and Table 2). The inventories were calculated using a spreadsheet provided by SKB which details the radionuclide inventory for each waste stream.

It is noted that the 2BMA inventory also includes:
- 2384 packages of wastes concrete embedded in steels drums, to which no inventory is assigned;
- 68 packages of steel moulds (waste stream R.15 in Appendix A of TR-14-02) that we assumed are cement solidified (because they are ion-exchange

resins), but this waste package type is not present in Figure 10, so it is not clear how they are represented in ECOLEGO.

Cement solidified wastes in steel drums are included in Figure 10, but there are no wastes of this type given in Appendix A of TR-14-02. Therefore they were not included in the AMBER model.

Table 1. Re-calculated numbers of waste packages, in the 2BMA vault, splitting out Tetramoulds from concrete embedded wastes in steel moulds (updated values highlighted in red)

Package Type	Number
Tetramoulds	1118
Cement solidified wastes in concrete moulds	192
Concrete embedded wastes in concrete moulds	967
Cement solidified wastes in steel moulds	68
Concrete embedded wastes in steel moulds	1107
Concrete embedded wastes in steel drums	2384

The following properties were used to represent the Tetramoulds:

- Height 1.2 m, Length 2.4 m, Width 2.4 m (Table 3-12 in TR-14-02).
- The wastes are concrete embedded (p197 in TR-14-09), so they were assumed to have the same properties of other concrete embedded wastes.

Table 2. Re-calculated waste inventory (Bq) in the 2BMA vault, splitting out Tetramoulds

	Cement solidified wastes in concrete moulds	Cement embedded wastes in concrete moulds	Solidified wastes in steel moulds	Embedded wastes in steel moulds	Embedded wastes in steel drums	Wastes in tetramoulds
Ac-227	0.00E+00	0.00E+00	0.00E+00	0.00E+00	0	0.00E+00
Ag-108m	2.34E+06	9.53E+08	3.26E+08	7.77E+09	0	3.16E+10
Am-241	5.01E+06	1.20E+10	7.68E+08	7.20E+08	0	2.78E+10
Am-242m	8.97E+03	2.22E+07	1.35E+06	2.35E+06	0	1.57E+08
Am-243	3.44E+04	8.70E+07	5.65E+06	9.49E+06	0	5.60E+08
Ba-133	1.66E+04	1.36E+07	1.33E+06	1.07E+06	0	1.27E+08
C-14-ind	0.00E+00	0.00E+00	0.00E+00	5.68E+07	0	5.03E+09
C-14-inorg	0.00E+00	0.00E+00	1.12E+10	6.51E+08	0	2.52E+09
C-14-org	0.00E+00	0.00E+00	2.97E+09	2.50E+07	0	9.65E+08
Ca-41	0.00E+00	0.00E+00	0.00E+00	0.00E+00	0	1.56E+10
Cd-113m	2.71E+05	4.28E+07	3.07E+07	1.11E+06	0	1.83E+07
Cl-36	2.53E+04	1.03E+07	3.84E+06	2.43E+06	0	1.86E+08
Cm-242	0.00E+00	0.00E+00	0.00E+00	0.00E+00	0	0.00E+00
Cm-243	6.91E+03	1.87E+07	8.09E+05	1.43E+06	0	8.18E+07
Cm-244	5.09E+05	1.48E+09	1.17E+07	1.65E+06	0	9.05E+09
Cm-245	3.44E+02	8.32E+05	5.65E+04	1.62E+05	0	9.06E+06
Cm-246	9.14E+01	2.22E+05	1.50E+04	5.85E+04	0	3.05E+06
Co-60	9.27E+07	3.27E+11	8.02E+09	7.04E+10	0	1.58E+12
Cs-135	5.18E+04	8.32E+06	1.93E+07	5.18E+05	0	2.51E+07
Cs-137	1.62E+09	2.27E+11	2.24E+11	8.33E+09	0	4.34E+11
Eu-152	2.86E+04	4.58E+06	3.22E+06	2.02E+05	0	1.33E+11
H-3	2.63E+05	1.82E+08	2.15E+07	1.94E+07	0	3.31E+12
Ho-166m	1.64E+05	6.67E+07	2.33E+07	1.46E+07	0	4.18E+08
I-129	1.56E+04	3.21E+06	3.08E+06	9.49E+04	0	1.27E+06
Mo-93	4.85E+04	3.37E+08	7.23E+06	3.47E+08	0	3.83E+09
Nb-93m	4.95E+06	2.85E+09	4.30E+08	5.60E+11	0	1.25E+13
Nb-94	4.22E+05	1.71E+08	6.05E+07	6.38E+09	0	8.46E+10
Ni-59	4.70E+08	1.69E+10	6.73E+10	1.49E+11	0	7.17E+11
Ni-63	4.30E+10	9.78E+11	5.49E+12	1.24E+13	0	7.34E+13
Np-237	5.26E+02	1.26E+06	8.98E+04	1.27E+05	0	6.21E+06
Pa-231	0.00E+00	0.00E+00	0.00E+00	0.00E+00	0	0.00E+00
Pb-210	0.00E+00	0.00E+00	0.00E+00	0.00E+00	0	0.00E+00
Pd-107	5.18E+03	7.21E+05	1.00E+06	2.55E+09	0	1.56E+06
Po-210	0.00E+00	0.00E+00	0.00E+00	0.00E+00	0	0.00E+00
Pu-238	3.07E+06	7.75E+09	1.90E+08	6.73E+08	0	3.56E+10
Pu-239	4.80E+05	1.16E+09	7.89E+07	1.00E+08	0	5.44E+09
Pu-240	6.76E+05	1.64E+09	1.10E+08	1.47E+08	0	7.31E+09
Pu-241	1.26E+07	3.85E+10	1.22E+09	2.03E+09	0	1.24E+11
Pu-242	3.46E+03	8.38E+06	5.68E+05	7.27E+05	0	4.05E+07
Ra-226	0.00E+00	0.00E+00	0.00E+00	0.00E+00	0	0.00E+00
Ra-228	0.00E+00	0.00E+00	0.00E+00	0.00E+00	0	0.00E+00
Se-79	2.07E+04	2.88E+06	4.01E+06	1.19E+05	0	2.53E+05
Sm-151	1.05E+07	1.44E+09	1.79E+09	1.22E+08	0	3.21E+10
Sn-126	2.59E+03	3.61E+05	5.01E+05	1.47E+05	0	1.65E+07
Sr-90	1.54E+08	2.06E+10	1.72E+10	6.75E+09	0	3.15E+11
Tc-99	6.45E+05	2.08E+08	1.30E+08	9.03E+07	0	9.92E+08
Th-228	0.00E+00	0.00E+00	0.00E+00	0.00E+00	0	0.00E+00
Th-229	0.00E+00	0.00E+00	0.00E+00	0.00E+00	0	0.00E+00
Th-230	0.00E+00	0.00E+00	0.00E+00	0.00E+00	0	0.00E+00
Th-232	0.00E+00	0.00E+00	0.00E+00	0.00E+00	0	0.00E+00
U-232	2.07E+01	5.25E+04	2.89E+03	2.41E+03	0	8.85E+04
U-233	0.00E+00	0.00E+00	0.00E+00	0.00E+00	0	0.00E+00
U-234	1.15E+03	2.79E+06	1.90E+05	5.35E+04	0	3.05E+03
U-235	2.30E+01	5.60E+04	3.79E+03	1.08E+03	0	1.72E+04
U-236	3.48E+02	8.38E+05	5.71E+04	9.62E+04	0	5.01E+06
U-238	4.61E+02	1.12E+06	7.55E+04	2.14E+04	0	1.31E+04
Zr-93	4.22E+04	1.71E+07	6.06E+06	4.22E+08	0	6.14E+08

Radionuclide fluxes out of the caisson calculated by AMBER for the accelerated concrete degradation case, and this variant case with a revised representation of the waste packages are compared in Figure 11. The fluxes of Ni-59, Mo-93, C-14_org, and I-129 decreased; while the fluxes of C-14_inorg and Tc-99 increased. The variation in the fluxes over time was very similar for all radionuclides.

Figure 11. Comparison of radionuclide fluxes from a caisson in the 2BMA vault, calculated by AMBER for the accelerated concrete degradation case and for the accelerated concrete degradation case with variant representation of waste packages (_VAR)

4.5 Properties of the Waste Packages

As noted in Section 4.4 and Towler and Penfold (2016), the properties assumed for the waste packages (density, porosity, cement content, etc) were not reported, so values had to be assumed. At the presentation given to SSM on 28 October 2016, some further information was given:

- the fraction of cement was set to 1; and
- an effective density was used to described the amount of sorbing material: 560 kg/m^3 for waste_cement and 75 kg/m^3 for waste_concrete.

The model described in Section 4.4 was updated using these properties. It was assumed 'waste_cement' maps to 'cement solidified wastes' and 'waste_concrete' maps to 'concrete embedded wastes'. Tetramoulds were assumed to be concrete embedded wastes (p197 in TR-14-09).

The porosities and effective diffusivities assigned to the wastes are still uncertain. However, this case is still a useful test of the sensitivity of the radionuclide fluxes to the properties assumed for the waste packages.

The fluxes of C-14_inorg, Tc-99 and Pu-239 out of the caisson were significantly increased compared with the base model for the accelerated concrete degradation case (Figure 12). This indicates that the differences between the fluxes of radionuclides that are more strongly sorbed calculated by AMBER and ECOLEGO (Figure 6) are largely due to the properties assumed for the waste.
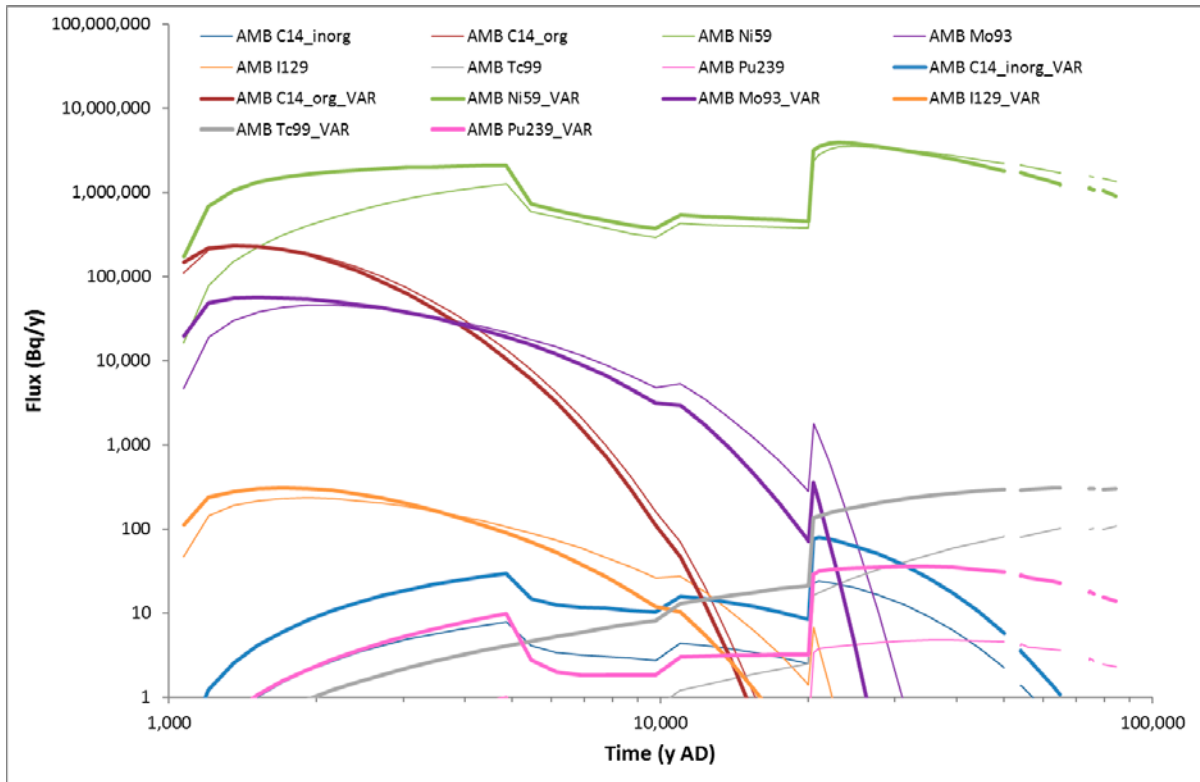
Figure 12. Comparison of radionuclide fluxes from a caisson in the 2BMA vault, calculated by AMBER for the accelerated concrete degradation case and for the accelerated concrete degradation case with variant representation of waste packages and waste properties (_VAR)

4.6 Summary

Overall, the AMBER near-field model for the CCL_BC gives very similar results to the ECOLEGO near-field model for radionuclides that are not sorbed or are only weakly sorbed. The differences are greater for radionuclides that are more strongly sorbed. The detailed configuration and parmeterisation of the waste packages in ECOLEGO are not clearly or fully described in the SR-PSU reports. SSM might wish to request further information from SKB to better understand the reasons for the differences, including the assumptions / basis for the effective parameters SKB have used, e.g. effective cement/concrete densities. However, the ECOLEGO results are cautious relative to AMBER and the radionuclides in question are only of secondary importance for calculated biosphere doses. So further exploration of these differences may not be necessary.

SSM might wish the SR-PSU near-field chemistry review area to consider the assumption that there is no additional chemical degradation in the accelerated concrete degradation case. For the Kds assumed by SKB, accelerated chemical degradation would lead to reduced fluxes of Ni-59 and C-14_inorg. SSM might wish the SR-PSU near-field chemistry review area to consider the selection of Kd values for key risk radionuclides at different stages of concrete degradation, at the same time as reviewing the assumption of no additional chemical degradation. The objective would be to confirm that accelerated chemical degradation is not likely to occur, and if it did occur whether it would lead to increased fluxes of key radionuclides.

5 Completely Degraded Case

A cautious case was run, in which it was assumed the caissons are fully degraded throughout the assessment timeframe. Effective diffusivities, porosities and chemical degradation states were not changed from the accelerated concrete degradation scenario. However, the near-field flows were changed using values from SKB's spreadsheets. This may be a cautious assumption because it assumes the caissons have a hydraulic conductivity of 1E-3 m/s, which is of the order expected for a gravel, throughout the assessment timeframe. However, as noted previously, it is not implausible given the current condition of the caissons in 1BMA. It also assumes the grout and waste packages inside the caissons are similarly permeable, which is also likely to be cautious. It results in significantly increased flows through the caissons at early times compared with the CCL_BC.

The peak fluxes are higher than in the CCL_BC. They occur a little earlier for radionuclides that are not sorbed or are weakly sorbed (Figure 13). The factors by which the peak fluxes are increased are given in Table 3.

Figure 3 shows that for the corrected CCL_BC, the highest doses for the 2BMA vault are from Mo-93. The calculated peak annual dose from Mo-93 is 5.3 µSv. Given that the AMBER and ECOLEGO models calculate similar fluxes of Mo-93 from the near-field to the geosphere (Figure 6), and the AMBER and ECOLEGO geosphere models give very similar results (Towler and Penfold, 2017), the dose from Mo-93 could increase to 5.3 µSv x 2.8 = 14.8 µSv for this completely degraded case. However, this scaling calculation does not take into account changes in the biosphere over time.

In Figure 3, there is a step increase in the dose from Mo-93 at 4,500 AD as a well becomes viable in biosphere object 157_2. At 4,500 AD, the flux of Mo-93 from the near-field to the geosphere is only slightly higher for this completely degraded case than the CCL_BC. The geosphere travel time for Mo-93 is very short. Therefore the calculated dose from Mo-93 is only slightly increased, given the assumption that a well is not viable in biosphere object 157_2 before 4,500 AD.
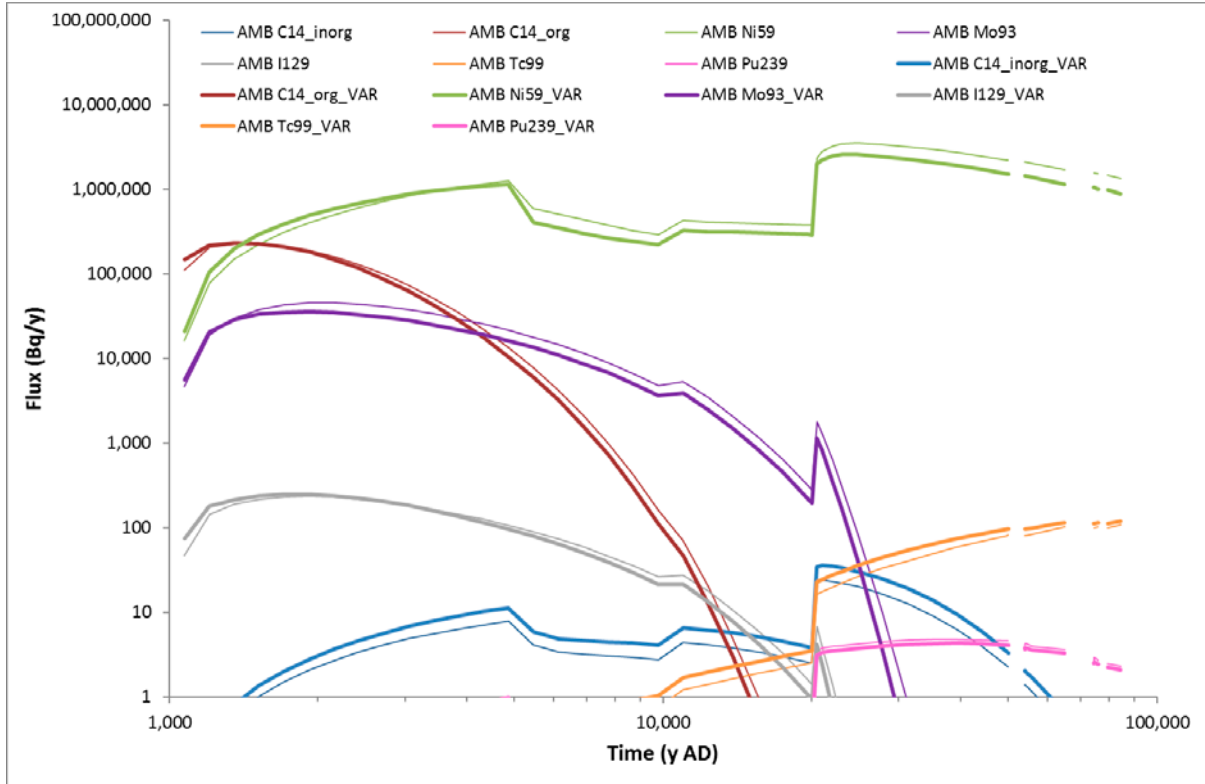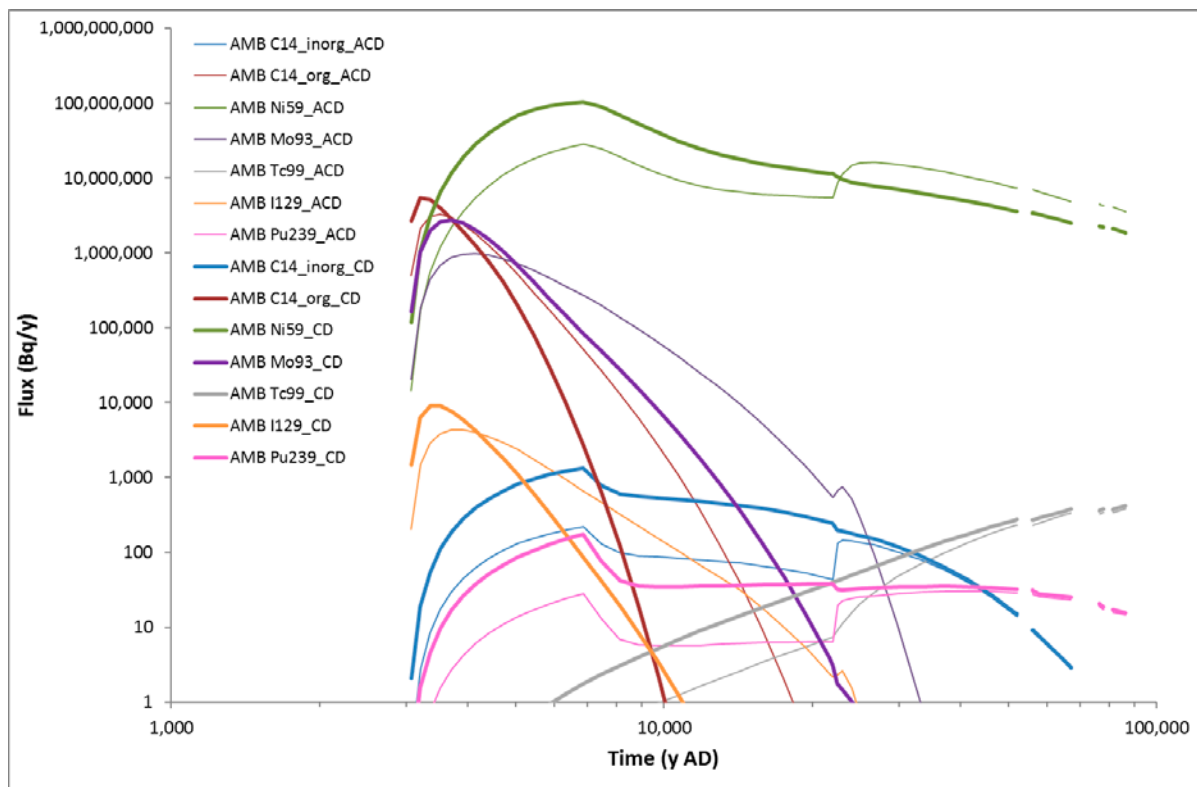
Figure 13. Comparison of radionuclide fluxes from the 2BMA vault to the geosphere calculated by AMBER for the accelerated concrete degradation calculation case (_ACD) and for the accelerated concrete degradation case assuming complete degradation of the concrete at all times (_CD)

Table 3. Factor of increase in the peak radionuclide flux from the 2BMA vault compared with CCL_BC

Radionuclide	Factor of increase in peak flux
C-14_inorg	6.2
C-14_org	1.7
Ni-59	3.7
Mo-93	2.8
I-129	2.1
Tc-99	1.1
Pu-239	5.7

6 Conclusions

The AMBER model of the CCL_BC gives very similar results to the corrected ECOLEGO model for radionuclides that are not sorbed or only weakly sorbed. This provides good confidence in the implementation of the CCL_BC case in ECOLEGO. However, there significant differences for radionuclides that are more strongly sorbed. Additional information on the configuration and parameterisation of SKB's models would be required to explore the reasons for these differences further. However, they only affect radionuclides that are of secondary importance for calculated biosphere doses, and the fluxes calculated by ECOLEGO are cautious

(i.e. higher) relative to the fluxes calculated by AMBER. This is further discussed in Section 4.6.

Corrections to the ECOLEGO near-field model have resulted in a number of changes in the calculated biosphere doses for the accelerated concrete degradation case that we have not been able to attribute to changes in the radionuclides fluxes from the near-field. Experts leading the biosphere review area were not able to identify the reason(s) for these changes using the information available to them, so they may need to be further considered in the wider SR-PSU review.

The CCL_BC makes significantly cautious assumptions about the hydraulic properties of the concrete, consistent with SKB's classification of the accelerated concrete degradation scenario as a less probable scenario. An extreme case in which the caissons are assumed to be fully degraded throughout the assessment timeframe could potentially result in higher doses than the CCL_BC. However, this extreme case may not be realistic because it assumes the grout and waste packages inside the caissons are also highly permeable throughout the assessment timeframe, in addition to the walls of the caissons.

The CCL_BC assumes the chemical degradation of the concrete is identical to the CCM_GW. However, the flows through the grout and wastes inside the caissons are significantly increased. This would increase the rate of cement alteration, so the SR-PSU near-field chemistry review area might consider whether this assumption is reasonable after thousands of years. Kd values chosen for key radionuclides would need to be reviewed at the same time (see discussion in Section 4.6).

7   References

Quintessa. 2016. AMBER Version 6.1.
https://www.quintessa.org/software/AMBER/index.html

TR-14-02: SKB. 2014a. Initial state report for the safety assessment SR-PSU. TR-14-02.

TR:14-09: SKB. 2014b. Radionuclide transport and dose calculations for the safety assessment SR-PSU. TR-14-09.

SKB. 2017. Corrected implementation of fracture model used for 1BMA and 2BMA in SR-PSU.

SKBdoc 1595131. Svar till SSM på begäran om komplttering av ansökan om utökad verksamhet vid SFR angående kod för transportmodeller.

Towler, G. and Penfold, J. 2017. SR-PSU Main Review Phase: Radionuclide Transport Modelling. QRS-1735D-ModellingReport_V1.1.

Åstrand, P. G. (2016). Implementation of SR-PSU near-field models in Ecolego. SSM2015-756-7.

Authors: Russell Walke[1], Laura Limer[1], George Shaw[3]
[1]Quintessa Limited, Henley on Thames, UK
[2]University of Nottingham, Nottingham, UK

4

Review of specific topics relating to the biosphere dose assessment for key radionuclides

1

Abstract

SKB has submitted an application to SSM for expansion of the final repository for low and intermediate level radioactive waste at Forsmark (SFR). SSM has contracted a number of organisations to support its review of SKB's safety analysis (SR-PSU), with each organisation contributing to the review of a different technical area. SSM has divided its review activities into an initial review phase and a main review phase which have already been undertaken and reported.

This report presents the findings of further review tasks associated with the main review phase aimed at addressing the following topics under the review of biosphere modelling for key radionuclides.

In the SR-PSU assessment, once C-14 has reached the biosphere, it is subject to a high loss rate to the atmosphere, especially from mire soils. Ingestion of C-14 in lake fish was a dominant exposure pathway in SKB's previous radiological assessment of the SFR facility. The potential for sub-surface horizontal groundwater flows (neglected in the SR-PSU assessment) to allow C-14 to be discharged to surface water without having been subject to high loss rates from the mire surface has been investigated. The results show that the small sub-surface horizontal flows estimated by SKB in its near-surface hydrogeological modelling have relatively little effect on the calculated maximum effective dose, which is dominated by contaminants other than C-14. However, the calculations have also shown that, if there is a strong sub-surface hydrological connection between the biosphere object that receives the discharge from the geosphere and the biosphere object that includes a lake immediately down-gradient from this location, then the maximum calculated dose increases by about a factor of two.

The importance of the SR-PSU modelling assumptions in determining C-14 doses has also been illustrated in further variant calculations, which show that:
- maximum calculated doses increase by about a factor of two if groundwater is discharged to biosphere object 157-1 (which includes a transition to a lake stage) rather than biosphere object 157-2 (which does not), this is due to ingestion of C-14 in fish;
- maximum calculated doses increase by about a factor of two if C-14 loss rates to the atmosphere from the mire and surface water are reduced by an order of magnitude, this is again due to ingestion of C-14 in fish; and
- reducing size of the hunter gatherer group from 30 to 10 individuals (consistent with the size of the drained mire and infield-outland farming groups) increases their peak calculated doses by a factor of about three (this would have an equivalent effect on the peak doses observed in the cases described above).

Two of the exposure groups represented in the SR-PSU assessment for the main scenario conservatively make use of a groundwater well either dug into the till, or drilled into the underlying rock. The capture fractions for the drilled well, which are defined for each separate component of the SFR facility, are very small, ranging from zero to 0.3%. The location of wells in the modelling used to support the capture fractions includes some arbitrary assumptions. The locations are relatively close to other wells considered within a "well interaction area" that exhibit capture fractions in excess of 10%. Variant calculations were undertaken by SSM's review team with capture fractions of 10%, which result in a factor of five increase in the maximum calculated doses, illustrating the importance of these assumptions.

Comparison of sorption coefficient (Kd) and concentration ratio (CR) distributions adopted in the SR-PSU assessment for the Forsmark area with those used in the SR-Site assessment for the same region highlights considerable changes (up to four orders of magnitude variation for some geometric means). The difference is, to some extent, explained by a greater preference for site-specific data in the SR-PSU assessment. Where data is lacking for some distributions, site-specific element analogue data is used in preference to element-specific literature data. The review highlights the significant uncertainty attributed to this approach, as is acknowledged in the SKB data compilations. The review also highlights examples where the choice of element analogue is poorly justified (notably for Tc, Np and Pa). Overall, the comparison of Kd and CR distributions between the SR-PSU and SR-Site assessments serves to highlight the significant uncertainty that can be attributed to these parameters. The magnitude of the variations in geometric means and parameter spreads mean that these uncertainties are not full captured in the probabilistic approach, especially where element and or media/species analogues are used.

The sensitivities discussed above should be interpreted within the context that the peak calculated dose for the global warming variant of the main scenario in the SR-PSU assessment, which relate to the drained mire group, is only a factor of about 2.5 lower than 14 μSv per year, which corresponds to the annual risk criterion of 10^{-6} for a representative individual in the group exposed to the greatest risk.

Contents

1. Introduction

SKB has submitted an application to SSM for expansion of the final repository for low and intermediate level radioactive waste at Forsmark (SFR). SSM has contracted a number of organisations to support its review of SKB's long-term safety analysis (SR-PSU), with each organisation contributing to the review of a different technical area. SSM has divided its review activities into an initial review phase and an in-depth review of key issues for the main review phase which have already been undertaken and reported.

Findings of the initial review phase for biosphere modelling in SR-PSU are described in SSM (2016) and those for the main review phase in Walke et al. (2017). In the initial review phase, the overall methodology adopted by SKB in its SR-PSU assessment was reviewed and an initial review of the biosphere modelling for key radionuclides was undertaken. Following-on from the initial review, specific attention was given to the following components of the SR-PSU assessment during the main review phase under the topic of reviewing biosphere modelling for key radionuclides:

- SKB's biosphere model (implemented in the Ecolego code[1]) was independently implemented in the AMBER compartment modelling code to verify results and gaining a thorough understanding of the modelling approach adopted;
- given its importance to the assessment, an in-depth review of the representation of C-14 in the biosphere within the SR-PSU assessment was undertaken; and
- the approach used to derive and justify parameter distributions for sorption coefficients (Kd) and concentration ratios (CR) was reviewed.

Topics that merited further consideration were identified as part of the main review phase. The current report presents the findings of further review tasks aimed at addressing the following topics.

- Variant calculations have been undertaken with the AMBER implementation of the SR-PSU biosphere model to explore the potential importance of sub-surface horizontal flows, amongst other factors, as described in Section 2.
- The Kd and (CR) values used in the SR-PSU assessment have been explicitly compared against those used in SKB's recent assessment for the potential deep disposal of spent nuclear fuel at the Forsmark site, as described in Section 3.

Conclusions relating to these further review tasks are brought together in Section 4. Detailed information supporting the work described in this report is presented in two appendices.

This report refers to the following SR-PSU reports:

- the Radionuclide Transport Report: TR-14-09 (SKB, 2014);
- the Biosphere Model Report: R-13-46 (Saetre et al., 2013);
- the Biosphere Parameter Report: R-13-18 (Grolander, 2013); and
- the Kd and CR Report: R-13-01 (Tröjbom et al., 2013).

---

[1] ecolego.facilia.se

2. Further Review of the SR-PSU Biosphere Model

Given the landscape evolution that is projected to occur at the site, SKB employ a relatively complicated biosphere model in support of the SR-PSU assessment that is implemented in the Ecolego code. As part of the main review phase for SR-PSU, SKB's biosphere model was independently implemented the AMBER compartment modelling code (Quintessa, 2016), with the objectives of:

- reviewing the completeness of the model specification;
- verifying the results presented by SKB; and
- developing a greater insight into the complex SR-PSU biosphere model.

To help facilitate the review, SKB provided the Ecolego calculation files for the SR-PSU assessment.

2.1. Conclusions from the Main Review Phase

The main review findings are reported in Walke et al. (2017). The exercise found that SKB's biosphere model and data are comprehensively documented and the independent implementation was able to largely reproduce the Ecolego results, achieving agreement to within about a factor of two. The exercise found some instances where the specification did not match the implementation in Ecolego and where parameter values were not available in the SR-PSU documentation, though these were relatively few in number.

A key conclusion that was drawn from the independent implementation was the extent to which the SR-PSU assessment represents a hybrid between a detailed fully probabilistic approach (e.g. there is a parameter distribution included for the width of a barley leaf) and a deterministic approach (important parameters, such as all water flows and the well interception fractions, are handled deterministically). There are also internal inconsistencies between aspects that are modelled probabilistically and others that are treated deterministically. These issues mean that the 'expectation value' presented as the results for the SR-PSU assessment does not fully reflect parameter uncertainties. The SR-PSU results should therefore be interpreted with these additional uncertainties in mind.

The independent implementation of the SR-PSU biosphere models also served to highlight the relatively low degree of occupancy and ingestion of potentially contaminated foods for several of the exposure groups. These assumptions included:

- drained mire and garden plot groups spend only 54 hours per year on potentially contaminated soils;
- the garden plot group obtains only 8% of their dietary carbon from the goods that they produce;
- the larger hunter-gatherer group is the only one that consumes fish, which was a key exposure pathway in previous SKB assessments; and
- the equivalent of 30 adult individuals used as a basis for the hunter-gatherer group effectively dilutes exposure in comparison to other groups such that

only 0.7% of dietary intake comes from the most contaminated biosphere object.

A further observation from the independent implementation was the extent to which C-14 is rapidly lost from the biosphere. C-14 was the radionuclide that dominated dose in the previous assessment iteration, SAR-08 (Bergström et al., 2008), where ingestion of lake fish was a key exposure pathway. In SR-PSU, the radionuclide releases to the biosphere are focused on biosphere 'object' 157-2, which does not include a transition to a lake stage. Potential sub-surface lateral groundwater flows are neglected in SR-PSU, such that radionuclides are transferred vertically upwards, through glacial clay, to the surface 'regolith'. C-14 is lost from the surface regolith to the atmosphere (and the model) at a fast rate (> 80 y^{-1}); a small fraction (less than 10%) is directed towards surface water.

One of the recommendations made during the main review phase was to review the importance of potential sub-surface lateral flows of water from biosphere object 157-2 (receiving contaminated groundwater discharges) to biosphere object 157-1 (down gradient and including a lake). This recommendation is addressed in this section, together with some further observations made in undertaking updated comparisons between the Ecolego and AMBER modelling.

2.2. Updated Comparisons

The objective of the AMBER implementation described in Walke et al. (2017) was to facilitate review of the complex biosphere modelling approach adopted by SKB, not to provide a full quantitative verification of SKB's biosphere modelling. The work described in Walke et al. (2017) achieved that objective. Further updates to the AMBER implementation necessary to facilitate the work described in the present report are described below.

The hunter gatherer representation was updated to allow the group to obtain food across all three biosphere objects represented (157-2, 157-1 and 116). This update was needed because the lateral flow modelling is of principal interest with regards to the ingestion of potentially contaminated fish from biosphere objects 157-1 and 116. Previously, the AMBER implementation (and the Ecolego output against which it was compared) focused on calculating potential doses solely from biosphere object 157-2, which receives the contaminated groundwater discharges.

Some modifications to the AMBER implementation for the garden plot group were also undertaken, following further inter-comparison of detailed results:
- a change was made to the fraction of peat fuel obtained by the garden plot group from the modelled region; and
- a change was made to the calculation of radionuclide concentrations in potatoes for the garden plot group.

An updated comparison of doses calculated with the AMBER implementation against those calculated with the Ecolego model with a groundwater discharge modelled to biosphere object 157-2 is shown in Figure 1. The simulation reflects a deterministic 'best estimate' calculation for the global warming case (CC1). The radionuclide fluxes to the biosphere are based on the original SR-PSU cases supplied by SKB and do not reflect any subsequent updates/corrections to the near-field and geosphere modelling made by SKB.

7

Figure 1 shows improved agreement[2] between the AMBER and Ecolego implementations for the garden plot group due to the corrections noted above.

The figure also shows improved agreement in the results for the hunter gatherer group on a 10,000 year time scale. The results during this period are expanded in Figure 2 for the hunter gatherer and drained mire farmer. The two 'spikes' in the hunter gatherer results arise from external irradiation from the upper regolith in 157-2 due to Ag-108m (peak at 3500 AD) and ingestion of C-14 in lake fish from biosphere objects 157-1 and 116 (peak at 4600 AD).
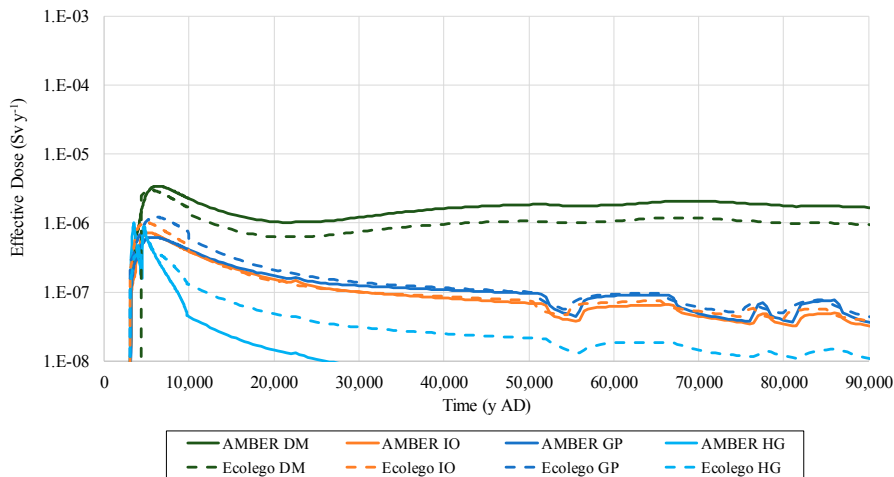
Figure 1: Total calculated effective doses to 90,000 AD for drained mire farmers (DM), infield-outland farmers (IO) and garden plot group (GP) based on biosphere object 157-2 and for hunter gatherers (HG).

Figure 2: Total calculated effective doses to 10,000 AD for drained mire farmers in biosphere object 157-2 (DM) and hunter gatherers (HG).

Focus on the time scale to 10,000 AD also highlights that the Ecolego drained mire farmer exposure only occurs from 4350 AD, whereas in the AMBER implementation, it occurs as soon as biosphere object 157-2 begins to emerge from the sea. Examination of the Ecolego case shows that drained mire doses only begin after biosphere object 157-2 has completely emerged from the sea. This was not implemented in the AMBER model because the 'switch' is not described in any of

---

[2] Compare against Figure 7 in the report on the main phase review findings relating to biosphere modelling for specific radionuclides included in SSM (2017).

the equations for the drained mire dose calculations in SKB's Biosphere Model Report (Saetre et al., 2013). The introductory text to Section 7.2 of the Biosphere Model Report notes that drained mire "cultivation is considered feasible only after the wetland area has emerged sufficiently above the sea level". The Biosphere Model Report then refers to further discussion concerning "threshold agriculture" in Chapter 9 of the Biosphere Parameters Report; however, discussion of this parameter cannot be found in that report.

2.3. Sub-surface Horizontal Groundwater Flows

The calculation of near-surface and surface water flows in support of the SR-PSU is described in Werner et al. (2013). The report describes how landscape modelling is used to support snapshots of the biosphere objects at 3000 AD (largely submerged), 5000 AD (some lakes present) and 11,000 AD (no lakes present). Water balance calculations are then performed with the MIKE SHE catchment-scale hydrological modelling code[3] for each biosphere object at each of these times. The MIKE SHE flows are normalised with respect of the biosphere object areas (see Figure 3, for example). The resulting water flows are mapped onto the compartment structure used for the radionuclide transport modelling in the biosphere. Differences between the vertical stratification used in the MIKE SHE modelling and that adopted in the radionuclide transport modelling mean that 'adjustments' are needed in the mapping of flows between the two. The water flows are interpolated between the modelled times and extrapolated beyond the modelled times in the Ecolego modelling.

---

[3] www.mikepoweredbydhi.com/products/mike-she
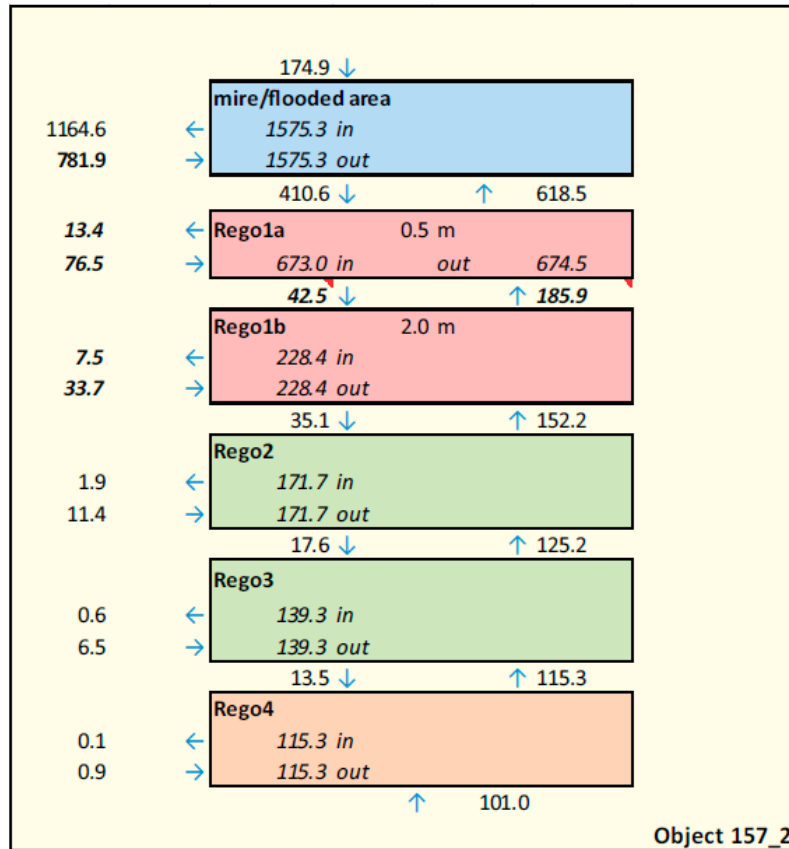
Figure 3: Water balance for biosphere object 157-2 at 5000 AD based on MIKE SHE modelling, prior to abstraction for use in the SR-PSU radionuclide transport modelling (Figure A1-42 of Werner et al., 2013).

As with any modelling on such extended time scales, the hydrological and hydrogeological modelling in support of the SR-PSU assessment is not an exact science. Undertaking the calculations based on the landscape evolution projections is a logical approach and the water balance checks provide some confidence that the modelling is not unphysical. The calculated water flows are, however, uncertain, not least in the way that they need to be adjusted, mapped, normalised, interpolated and extrapolated. These uncertainties are not explicitly represented either in the hydrological and hydrogeological modelling itself nor in the way that the resulting deterministic water flows are used in the probabilistic SR-PSU assessment.

One aspect of the representation of water flows within the SR-PSU assessment that was considered to merit further review was the way in which sub-surface water flows are neglected in mapping MIKE SHE results to the radionuclide transport modelling. Whilst the calculated subsurface water flows are small[4] in comparison to calculated groundwater discharge to the surface regolith layer, they may represent an important pathway to surface water for C-14, which is subject to very high losses from the surface regolith.

The current review focuses on potential sub-surface flows between biosphere object 157-2, which is represented by SKB as receiving 100% of the potentially

---

[4] Figure A1-42 of Werner et al. (2013) indicates that sub-surface flows are equivalent to about 4% of the flow reaching the surface mire.

contaminated groundwater flows, and the down-stream biosphere object 157-1, which includes a transition to a lake stage (Figure 4 shows the biosphere objects). In practice, the potential for sub-surface flows between these two biosphere objects will depend on the detailed sub-surface topography and stratigraphy, which is uncertain. Groundwater is represented as discharging to a till layer that is adjacent to the bedrock. The till is significantly more hydrologically conductive than the glacial clay that overlies it. The till itself is significantly anisotropic, with a horizontal hydraulic conductivity that is 30 times greater than the vertical hydraulic conductivity. There are also indications that the horizontal hydraulic conductivity is even higher at the rock-regolith interface than in the till itself.
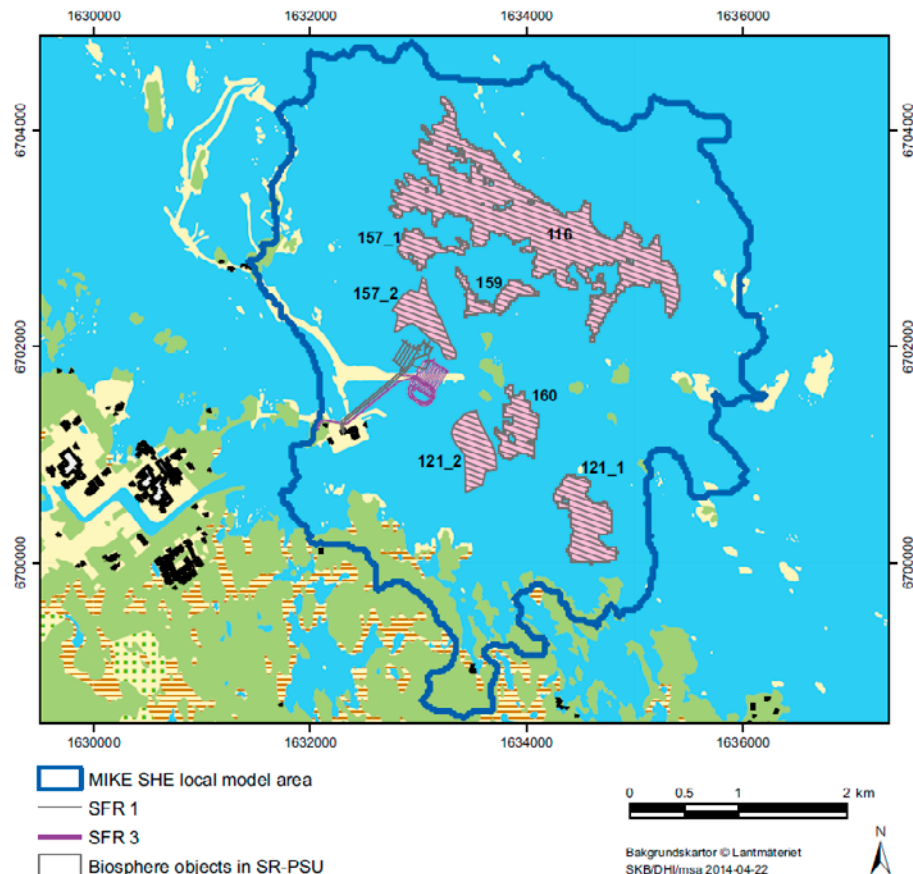
Figure 4: Local area used for MIKE SHE modelling, highlighting the biosphere object locations and SFR in the context of the present-day landscape configuration (Figure 3-2 from Werner et al., 2013).

The landscape evolution and hydrological modelling is subject to separate review task as part of the scrutiny of the SR-PSU assessment. Alternative sets of groundwater flow numbers have been produced as part of that task, including explicit representation of potential sub-surface horizontal flows between biosphere objects 157-2 and 157-1 (Kłos, 2017). The following two sets of alternative numbers have been produced.

- Flow Case 1: Based on the same flow numbers used in support of the SR-PSU assessment, but with the sub-surface flow values reinstated.
- Flow Case 2: Assuming that there is preferential horizontal flow from the till.

The variant set of flow numbers used in the AMBER modelling is reproduced in Appendix A. These provide values for sub-surface horizontal groundwater flow from the till, glacial clay, post-glacial deposits and peat, as illustrated in Figure 5.
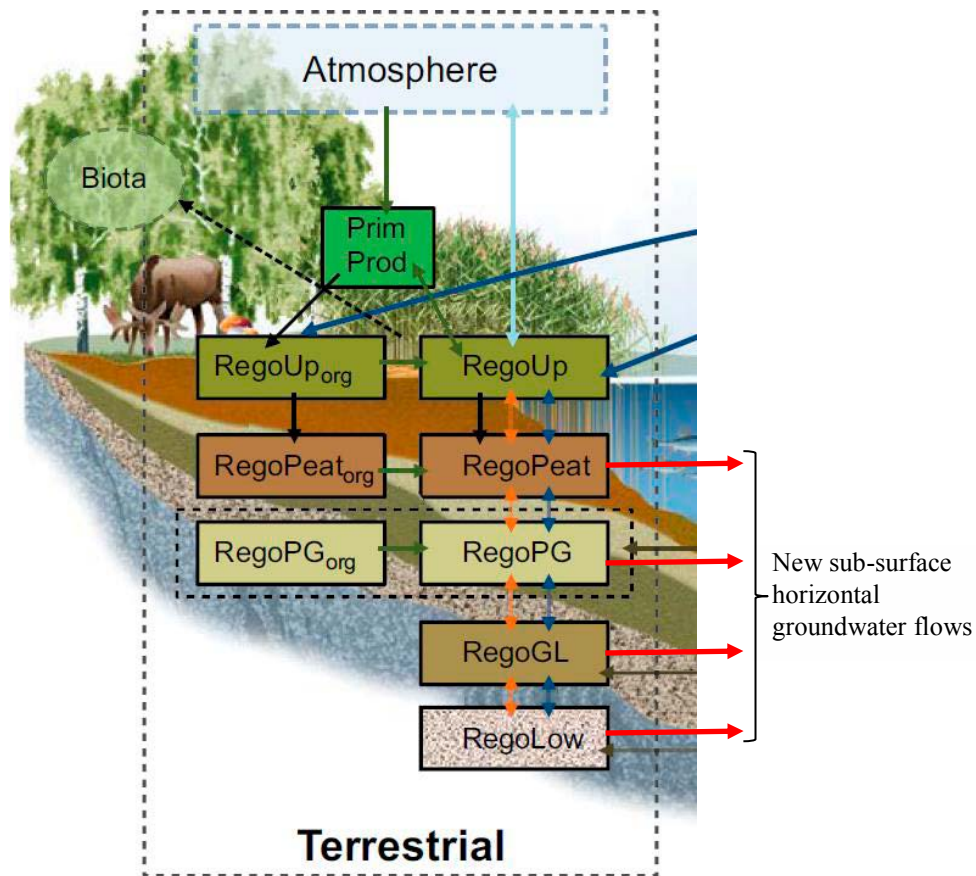
Figure 5: Compartment structure for terrestrial stage of biosphere object 157-1 with the additional sub-surface horizontal groundwater flows highlighted with red arrows (based on Figure 3-1 of the Biosphere Model Report).

Figure 4 shows that biosphere objects 157-2 and 157-1 are not immediately adjacent – they are separated by a distance of c. 75 m (a short distance relative to the size of the biosphere objects). For the purpose of the variant calculations, the potential complexities of sub-surface lithostratigraphy and water flows within this unmodeled region are neglected. Two options for the sub-surface horizontal groundwater transfers are instead considered for each of the two variant flow cases.

- Regolith to regolith: Flow from each regolith layer in biosphere object 157-2 is directed to the equivalent terrestrial regolith compartment in biosphere object 157-1.
- Regolith to water: Flow from each regolith layer in biosphere object 157-2 is directed to surface water in biosphere object 157-1 (analogous to the flow discharging to surface between the two biosphere objects).

The total calculated effective doses to the drained mire farmer and hunter gatherer groups for Flow Case 1 are shown in Figure 6 and compared against the results for the original SR-PSU flow assumptions. The figure shows that, when the small proportion of sub-surface horizontal flow is included and directed to the terrestrial regolith in the down-stream biosphere object 157-1 ("Flow Case 1 regolith" in Figure 6), then there is negligible effect on the calculated doses. When the sub-

surface horizontal flow is modelled as discharging to surface water between biosphere object 157-2 and 157-1, then there is a 30% increase in the calculated dose to the hunter gatherer. This increase is due to increased C-14 reaching the lake in the relatively small additional sub-surface horizontal water flows before it has had an opportunity to be released to the atmosphere via the high loss rates from the mire surface.
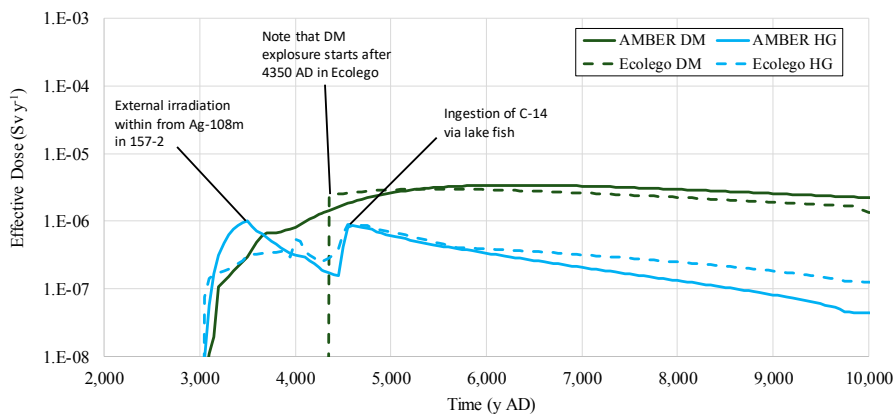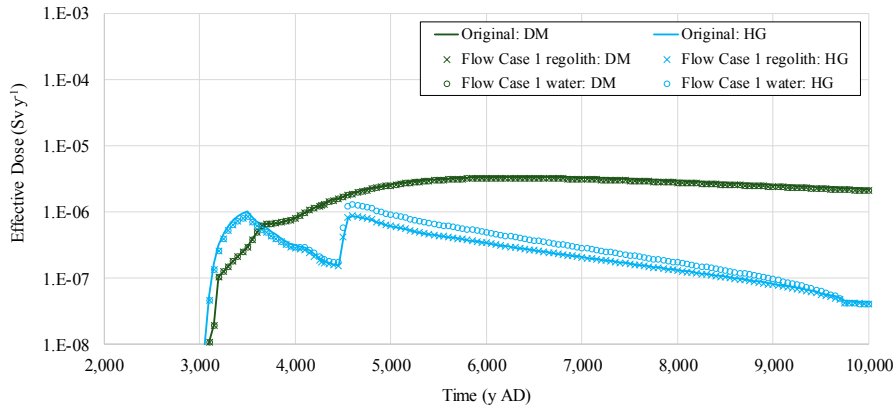

Figure 6: Total calculated effective doses to 10,000 AD for drained mire farmers in biosphere object 157-2 (DM) and hunter gatherers (HG) for Flow Case 1 compared to the original results.

When higher sub-surface horizontal water flows are included, as in Flow Case 2, there is a more marked difference in the calculated results for the biosphere. Figure 7 shows that increased sub-surface horizontal groundwater flows from biosphere object 157-2, decrease the drained mire dose in biosphere object 157-2. In addition, the figure shows that, when the flows are directed to the terrestrial regolith in the downstream biosphere object 157-1 ("Flow Case 2 regolith" in Figure 7), there is little effect on the hunter gatherer dose. However, the figure also shows that the calculated hunter gatherer doses increase by about an order of magnitude and exceed the original drained mire dose if the higher sub-surface flows from biosphere object 157-2 are modelled as discharging to water ("Flow Case 2 water in Figure 7). As in Flow Case 1, this increase is due to C-14 reaching fish before it has had an opportunity to be lost to the atmosphere from the mire.
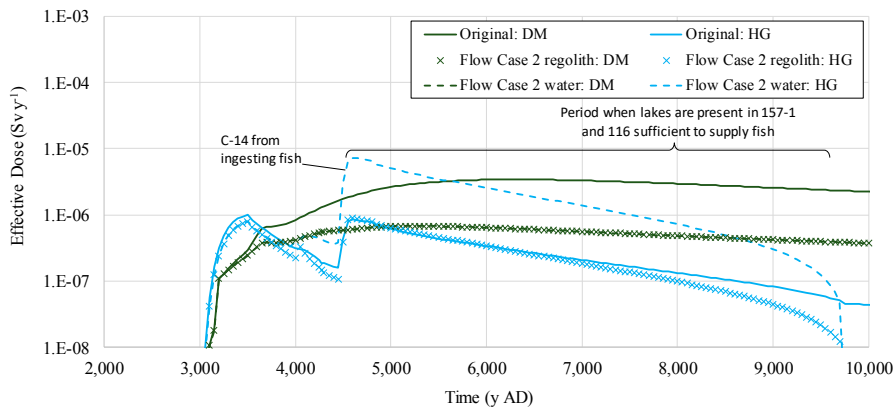
Figure 7: Total calculated effective doses to 10,000 AD for drained mire farmers in biosphere object 157-2 (DM) and hunter gatherers (HG) for Flow Case 2 compared to the original results.

13

The result for the sub-surface flow variant calculations, especially those with greater sub-surface flow discharging to surface water between biosphere objects 157-2 (where the discharge occurs) and 157-1 (where there is a lake), highlight the importance of assumptions regarding flow routing and the potential for releases to lakes to result in greater radiological impacts.

2.4. Further Variant Calculations

In addition to the further comparisons and variant calculations described in the preceding sections, additional "what if" style calculations have been undertaken with the AMBER implementation of the SR-PSU biosphere model to help provide further understanding of the importance of specific assumptions and processes. These calculations are described in the sub-sections below.

2.4.1. Release to Biosphere Object 157-1

A calculation has been undertaken with the radionuclide flux from the geosphere released to the till beneath biosphere object 157-1, rather than 157-2. The calculated effective doses are compared in Figure 8. The figure shows that the highest calculated dose across the two exposure groups increases by about a factor of two. The hunter gatherer group becomes the most exposed in this situation, due to ingestion of C-14 contaminated fish in the lake.
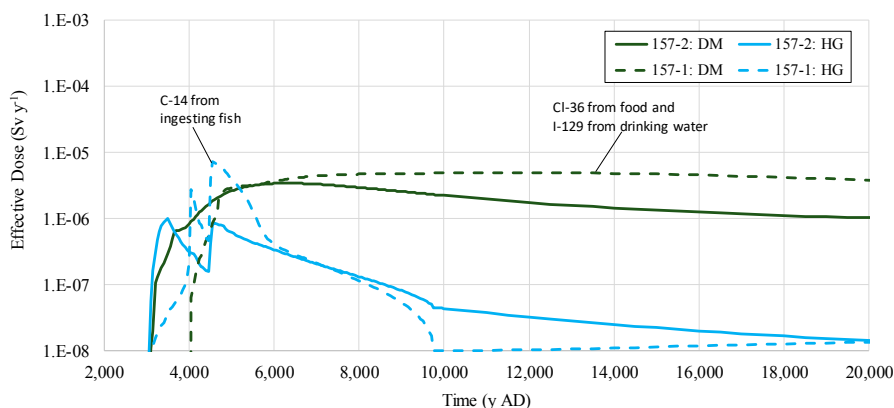
Figure 8: Total calculated effective doses to 20,000 AD for drained mire farmers in biosphere object 157-1 (DM) and hunter gatherers (HG) with a geosphere release to biosphere object 157-1, compared against the SR-PSU case with releases to 157-2.

2.4.2. Reduced C-14 Loss Rates to Atmosphere

The high rate loss rate for C-14 from mire soils was noted in the main review (Walke et al., 2017). As with other aspects of the assessment, the assumptions surrounding the behaviour of C-14 in mire soils are uncertain. A case was therefore set up to explore the sensitivity of the results to assumptions about C-14 loss rates to the atmosphere by reducing the terrestrial and aquatic piston velocities by an order of magnitude. The results are shown in Figure 9. The figure shows that the peak calculated dose rate for the hunter gatherer group from ingestion of C-14 fish increases by about an order of magnitude when the loss rate for C-14 from mire and surface water is reduced by the same extent.
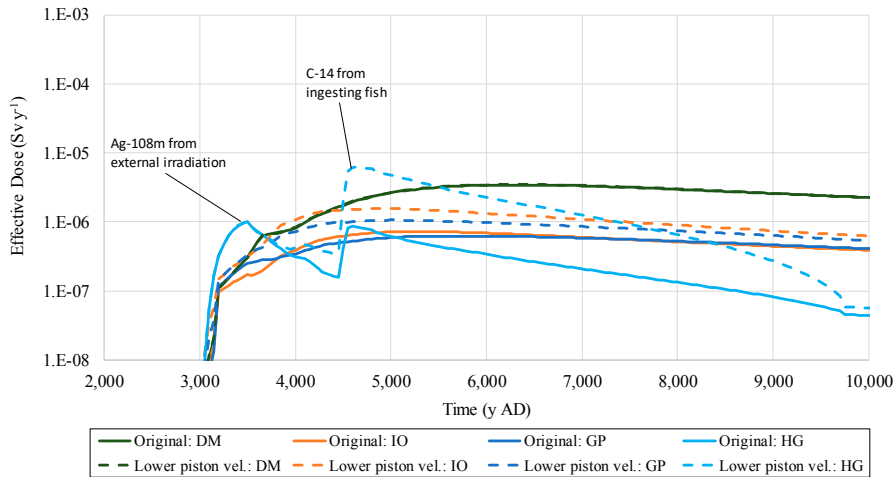
Figure 9: Total calculated effective doses to 10,000 AD for drained mire farmers (DM), infield-outland farmers (IO) and garden plot group (GP) based on biosphere object 157-2 and for hunter gatherers (HG) with lower loss rates for C-14 to the atmosphere compared to the original results.

2.4.3. Smaller Hunter-Gatherer Group

The hunter gatherer is the only potentially exposed group in the SR-PSU assessment that consumes fish (a key exposure pathway in SKB's SAR-08 assessment). The hunter gatherer group is also the only group that numbers 30 individuals; the drained mire and inland-outfield farmers are both 10 individuals and the garden plot group is 5 individuals. If the size of the hunter gatherer group was set to 10 individuals, then the fraction of their carbon intake that may derive from lake fish in biosphere object 157-1 is increased by a factor of three. The effect of this alternative assumption is illustrated in Figure 10; note that the first peak in the hunter gatherer dose is unaffected because it arises due to external irradiation from Ag-108m while occupying biosphere object 157-2. The peak in the hunter gatherer dose that is associated with eating C-14 in lake fish is increased by about a factor of three.
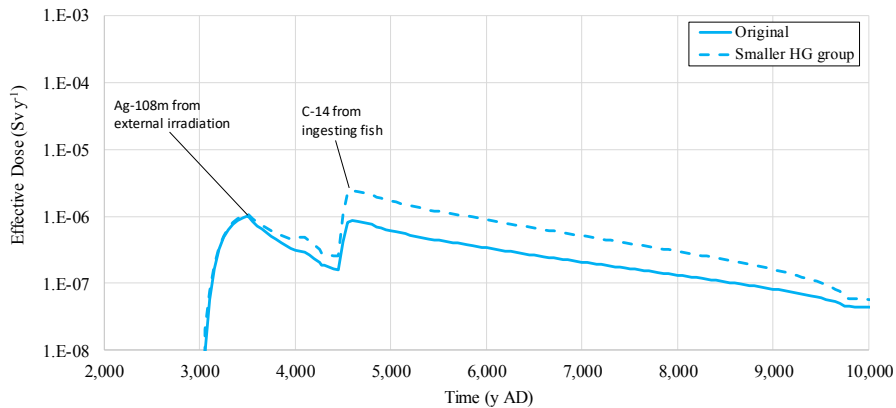
Figure 10: Total calculated effective doses to 10,000 AD for hunter gatherers (HG) with the original (30 person) and smaller (10 person) group sizes.

15

2.4.4. Drained Mire Group Consuming Fish

A calculation has also been undertaken to explore the potential effect of including consumption of lake fish from biosphere objects 157-1 and 116 in the diet of the drained mire farmer in biosphere object 157-2. This has been implemented by assigning 10% of carbon intake to lake fish and reducing the fraction of dietary carbon from milk from 25% to 15%. The 10% dietary carbon from fish is then apportioned between biosphere objects 157-1 and 116, depending on their capacity to supply fish to the ten person drained mire group, favouring fish from biosphere object 157-1, which will have the higher calculated radionuclide concentrations.

The resulting total calculated doses for the drained mire farmer including fish consumption are shown in Figure 11 and compared against the results without fish consumption. The figure shows that including fish consumption results in a relatively small increase in calculated doses at around 4500 AD. The reason that the effect is relatively small is because the lake in biosphere object 157-1, which is subject to the least degree of dilution, can only supply up to 2% of the dietary carbon to the ten person drained mire group (see Figure 12). The main contributor to the original calculated dose is Mo-93 from ingestion of cereals grown on the drained mire in biosphere object 157-2.
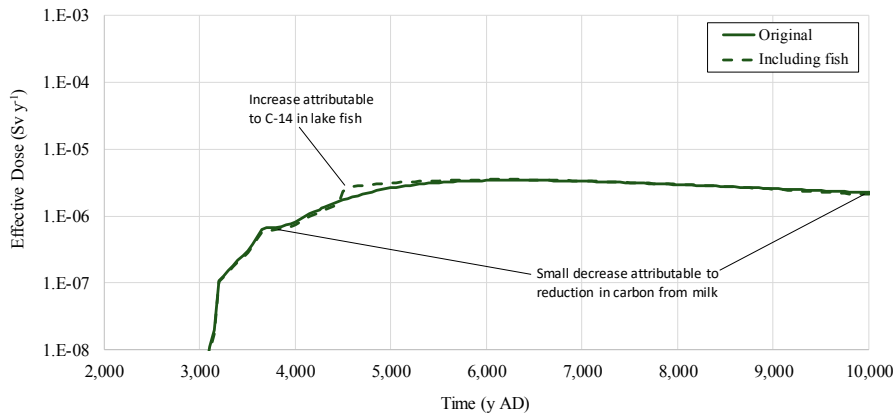
Figure 11: Total calculated effective doses to 10,000 AD for the drained mire farmer in biosphere object 157-2, including potential to receive up to 10% of dietary carbon from fish in biosphere objects 157-1 and 116.
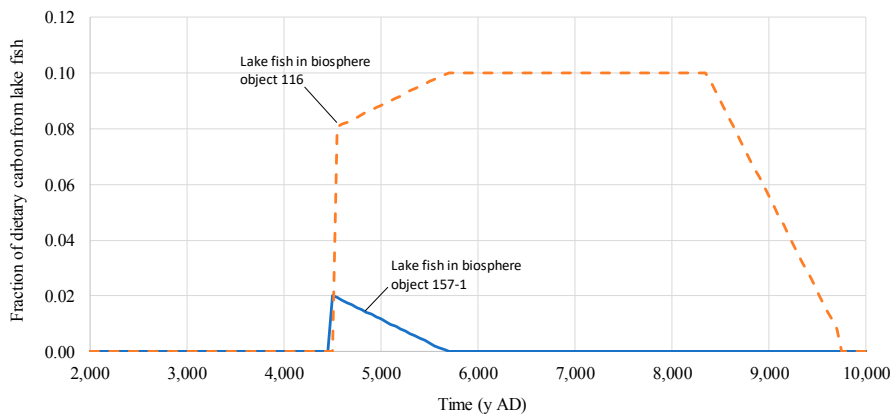
Figure 12: Fraction of drained mire group dietary carbon obtained from fish in biosphere objects 157-1 and 116.

16

2.4.5. Increased Well Capture Fractions

As noted in the initial review phase, the capture fractions for wells drilled into the bedrock are extremely small in the main calculation cases for the SR-PSU assessment (see Table 1). The capture fractions are significantly uncertain (although they are only assigned an uncertainty factor of two in the SR-PSU assessment).

Table 1: Capture fractions used in SR-PSU for wells drilled into rock for agricultural groups (Table 12-4 of Werner et al., 2013).

SFR Component	Capture fraction	SFR Component	Capture fraction
BLA1	0%	BMA2	0.2%
BLA2	0.2%	BTF1	0.004%
BLA3	0.3%	BTF2	0.002%
BLA4	0.2%	BRT	0.2%
BLA5	0.1%	Silo	0.02%
BMA1	0%		

In the SR-PSU assessment modelling, the concentration in well water is conservatively modelled using the higher calculated radionuclide concentration from a drilled well, and a well dug into the till. With the very small capture fractions listed in Table 1, the dug well typically dominates over the drilled well in terms of calculated concentrations and therefore contributes towards the calculated doses, especially for the key radionuclides for the drinking water pathway (notably I-129, U-238 and C-14).

To explore the potential consequence of higher well capture fractions, a variant "what if" style calculation has been undertaken with the AMBER implementation with the capture fraction set to 10% across all parts of the model. This is more representative of a well drilled within the "well interaction area", but does not appear unreasonable if wells were drilled within a few hundred metres of the more suitable agricultural soils, indeed some of the modelled capture fractions in this region exceed this value[5]. The effect on the calculated effective dose for the drained mire farmer and garden plot groups is shown in Figure 13 (neither the infield-outland nor hunter gatherer groups makes use of the drilled well). The figure shows that the maximum dose to the drained mire group increases by about a factor of five and that for the garden plot group by about a factor of twenty (both groups consume 2 L of well water per person per day). The increase in calculated doses is entirely attributable to their consumption well water, where Pu-239/240, Ac-227 and I-129 are the key contributors.

---

[5] See wells 23 and 26 in Figure 6-13 and in Tables A3-2 and A3-3 of Werner et al. (2013).
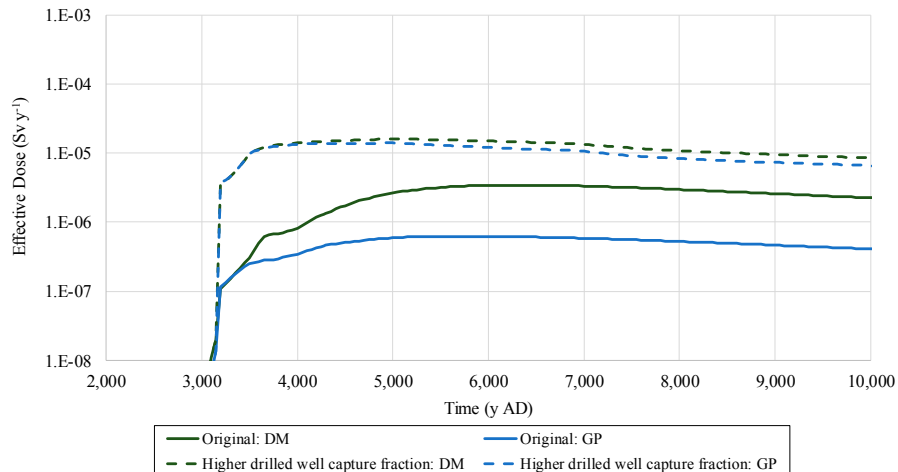
Figure 13: Total calculated effective doses to 10,000 AD for the drained mire farmer (DM) and garden plot (GP) groups with the SR-PSU (original) and increased well capture fractions.

2.4.6. Increased Occupancies

The exposure calculations for the drained mire farmer and garden plot exposure groups in the SR-PSU assessment are based on both only spending 54 hours per year in the potentially contaminated region. This duration is low considering that:

- the drained mire exposure group obtains all of its dietary carbon from this area; and
- the water used by the garden plot exposure group for irrigating the vegetable plot soils will likely be used for watering other parts of its garden.

A side calculation has been undertaken with the AMBER implementation, increasing the duration of occupancy for the drained mire farmer and garden plot groups to from 54 hours per year to 1000 hours per year (equivalent to eight hours per day, five days per week for half of the year). The resulting effect on the calculated doses is shown in Figure 14. The figure shows increased calculated doses, with the increases peaking at about 3500 AD due to external irradiation from Ag-108m. The increase for the drained mire farmer is not sufficient to alter their maximum calculated dose, which arises after about 6000 AD due to ingestion of Mo-93 in crops. However, the increase is sufficient to change the maximum calculated dose to the garden plot group by about a factor of three; their dose was previously dominated by I-129, C-14 and U-238 in drinking water at about 5800 AD.

18
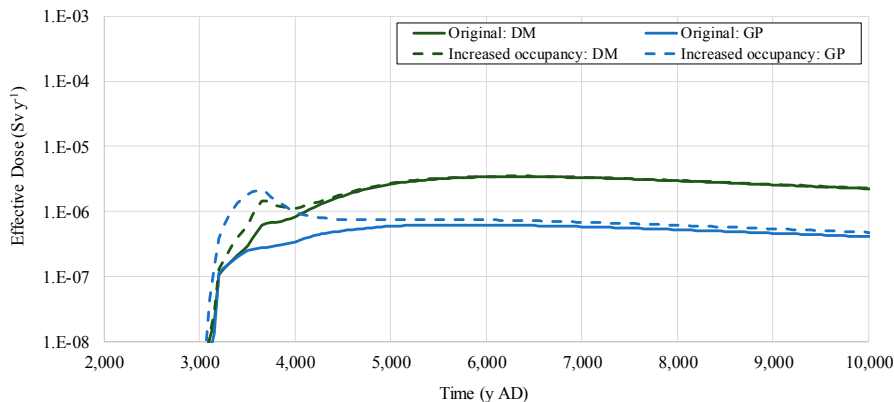
Figure 14: Total calculated effective doses to 10,000 AD for the drained mire farmer (DM) and garden plot (GP) groups with the SR-PSU (original) and increased occupancy assumptions.

2.4.7. Conclusions from Further Variant Calculations

The further variant calculations described above have highlighted the following points with regards to the SR-PSU biosphere modelling.

- The maximum calculated impacts of radionuclide releases to biosphere object 157-1 (which includes a transition to a lake stage), are about a factor of two greater than those where the release occurs to biosphere object 157-2 (which transitions direct from a marine to a terrestrial state).

- The results are sensitive to the high loss rates assumed for C-14 from mire sediments and from water. Reducing the loss rate by an order of magnitude results in an approximate order of magnitude increase in the calculated dose to the hunter gatherer, due to ingestion of fish. This is sufficient for the hunter gatherer to receive the highest calculated dose, which is about a factor of two greater than the original maximum, which was associated with the drained mire farmer in biosphere object 157-2.

- Decreasing the size of the hunter gatherer group from 30 to 10 individuals increases their maximum calculated dose by about a factor of three, although this remains below the highest dose received by the drained mire group.

- Introducing fish from biosphere object 157-1 into the diet of the drained mire farmer in biosphere object 157-2 has little effect on the calculated doses because the additional exposure is insufficient to exceed the peak that they receive from ingesting crops.

- The calculated results for the drained mire and garden plot groups are sensitive to assumptions about the well capture fraction for drilled wells. Increasing the capture fraction to be consistent with those within the "well interaction area", which does not seem unreasonable based on discussion in the supporting SR-PSU report, increases the maximum calculated dose by about a factor of five.

- Increasing the degree of occupancy of potentially contaminated area by the drained mire farmer does not increase the maximum calculated dose, which is dominated by ingestion of crops.

- Increasing the degree of occupancy of the garden plot exposure group increases their maximum calculated dose by about a factor of three, although it does not exceed the original maximum calculated dose for the drained mire farmer.

19

3. Further Review of Kd and CR Values Used in SR-PSU Biosphere Model

The purpose of this review was to compare the Kd and CR distributions used in the SR-PSU assessment directly with those used in the SR-Site assessment. Note that a different modelling approach was adopted in SR-PSU for C-14 that did not involve Kd and CR, so it is therefore excluded from the following discussion.

Of the 31 elements modelled with Kd and CR in SR-PSU, 29 were also considered in SR-Site (neither Ba nor Co were considered in SR-Site). Therefore, the values for these two elements used in the SR-PSU assessment have been compared with the wider literature (typically, IAEA collations). Where conversion of units between the literature and SR-PSU is required, the dry matter content and carbon content data listed in Appendix F of the Kd and CR Report (Tröjbom et al., 2013) have been used.

This review seeks to compare the best estimate (BE), geometric mean (GM) and geometric standard deviation (GSD) assumed for the distributions between the two assessments, or to compare with the wider literature in the case of Ba and Co. The following sub-sections consider in turn:
- Kd distributions (Section 3.1);
- terrestrial CR distributions (Section 3.2); and
- aquatic CR distributions (Section 3.3).

Tables comparing the SR-PSU values with those used in the SR-Site assessment are included in Appendix B. The following sub-sections discuss the comparisons.

3.1. Kd Distributions

The eleven Kd parameters used in the SR-PSU assessment are compared with their equivalents in the SR-Site assessment in Appendix B.1. The comparisons are provided for the following media (SR-PSU parameter name given in brackets):
- till (kd_regoLow);
- glacial clay (kd_regoGL);
- post-glacial deposits (kd_regoPG);
- peat (kd_regoPeat);
- cultivated clayey till and glacial clay (kd_regoUp_io and kd_regoUp_garden);
- drained mire (kd_regoUp_drain);
- upper oxic layer of terrestrial regolith (peat) (kd_regoUp_ter);
- upper aquatic regolith (both lake and sea) (kd_regoUp_aqu);
- suspended particulate matter in lakes (kd_PM_lake); and
- suspended particulate matter in the sea (kd_PM_sea).

To highlight overall differences in the magnitudes of Kds used in both assessments, the median values of the SR-PSU/SR-Site ratios (based on GM values for each parameter) are plotted for each element in Figure 15, along with the minimum and maximum ratios calculated for each element. Ratios close to 1 indicate parity in parameter value selection between each assessment while deviation either above or below 1 indicates that a higher or lower (respectively) GM Kd has been selected in SR-PSU than in SR-Site. The black symbols indicate elements of particular interest

in this review, based on eight elements identified as being important from the perspective of potential doses in the initial review phase (SSM, 2016), plus two further elements (Tc and Np) that demonstrate the largest differences between the two assessments.

Figure 15: Distribution of median ratios between GM Kd values adopted in SR-PSU and SR-Site across a range of media (black symbols highlight the elements of particular interest; elements ranked by highest to lowest median ratio).

Whilst most elements have ratios of GMs ranging over less than three orders of magnitude, for Tc, Pu and Po the variability is approximately five orders of magnitude. Over the 29 elements shown in Figure 15, 13 of the highest ratio values are associated with Kd value assumed for glacial clay, and eight of the lowest ratios are associated with Kd assumed for suspended particulate matter at sea.

Considering specific elements, Figure 15 shows that median GM Kd values for Tc, Np, Pd, Ac and Ca have increased between about one to two orders of magnitude in SR-PSU, compared with SR-Site. For Tc and Np, for which the increases in selected GM of Kd values were greatest, it is notable that element analogues (EA) have been used in SR-PSU. The Kd and CR Report notes that EA are used:

> *"when data for an element are not available but data for an element with similar biogeochemical properties are available. In general, elements of the same group of the periodic table have similar chemical properties since they have the same number of outer electrons that can participate in chemical reactions."*

The analogue elements chosen for Tc were rhenium (Re) and zirconium (Zr). In the absence of any naturally-occurring isotopes of Tc, Re has previously been proposed as an analogue (Brookins, 1986). Both elements occupy the same group within the transition metals of the periodic table. Scrutiny of the Pourbaix (Eh-pH) diagrams (Figure 16) of each element show similarities, notably the dominance of Tc(VII) (pertechnetate) and Re(VII) (perrhenate) at values of Eh and pH which are likely to be encountered in oxic soils and sediments. In anaerobic soils and sediments, Tc is known to be reduced to Tc(IV) (TcO_2 in Figure 16a), which results in a marked

SSM 2017:30

increase in its Kd. The analogous species for Re is ReO_2, which has a much smaller stability field with respect to Eh and pH (Figure 16b).

Experimental evidence (Figure 17) indicates that, under increasingly reducing conditions, Kd values for both Tc and Re increase according to an exponential function, though the slope of increase in Kd with decreasing Eh is much greater for Tc than for Re. It can be concluded that the two elements show qualitatively similar sorption behaviour in soils but, quantitatively, the absolute Kd values for each element can be as much as two orders of magnitude different.
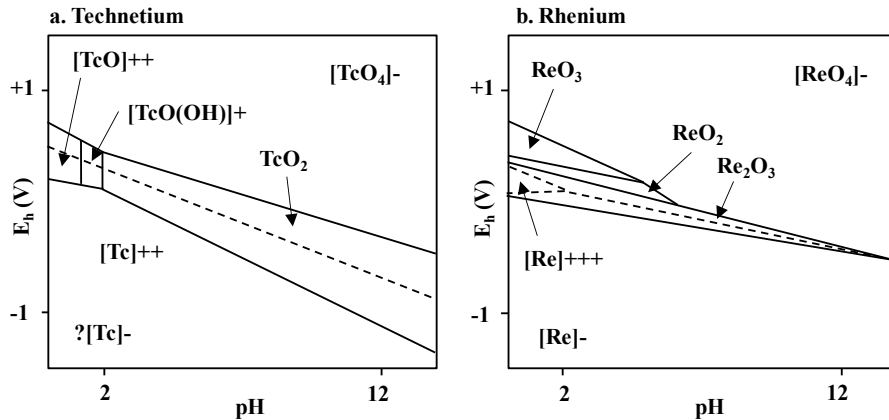
Figure 16: Pourbaix (Eh-pH) diagrams for technetium and rhenium.
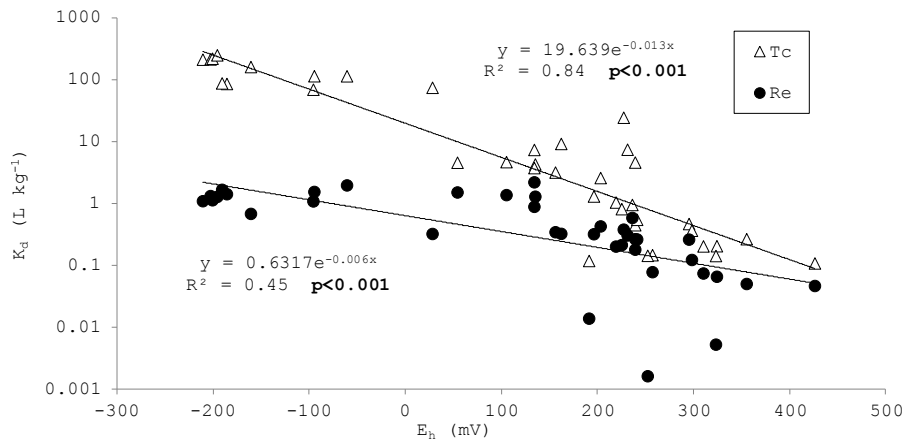
Figure 17: Kd values for Tc and Re in soils over a wide range of oxidation-reduction potentials (Eh) (Gould, 2012).

Zirconium (Zr) has also been used in SR-PSU as an elemental analogue for Tc. Both elements occur within the same period in the transition metals, though examination of the Pourbaix diagram for Zr (Figure 18a) indicates little qualitative similarity between the chemistries of Tc and Zr. The Pourbaix diagram of molybdenum (Mo) is also presented (Figure 18b), and shows greater qualitative similarity with Tc. Molybdenum is adjacent to Tc in period 5 within the transition metals and may provide a better analogue for Tc than either Re or Zr, though rigorous experimental data are lacking. Despite SKB's recent interest in molybdenum (Lidman et al., 2017) no consideration seems to have been made of the potential for this element as an analogue for Tc.

(a) Zirconium   (b) Molybdenem
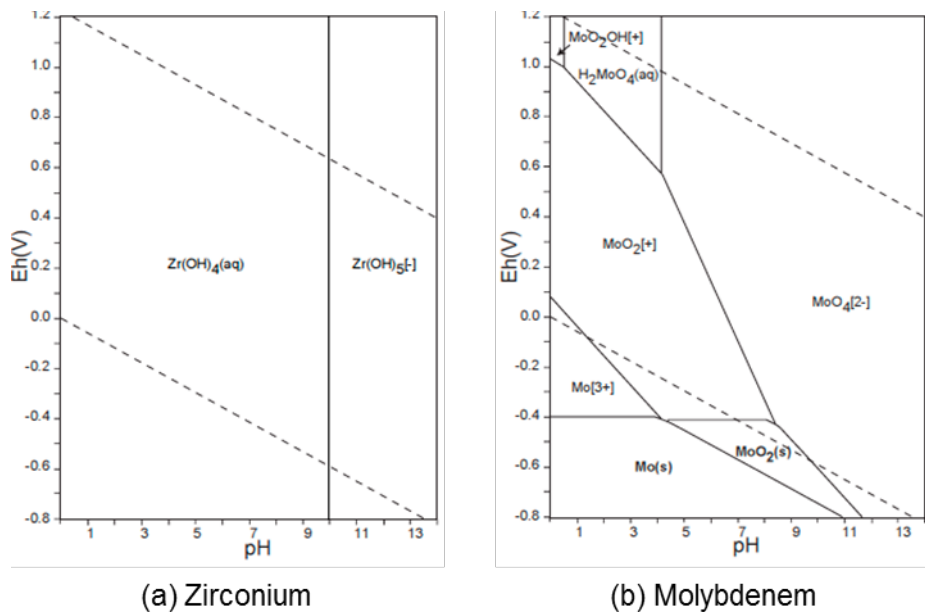
Figure 18: Pourbaix (Eh-pH) diagrams for zirconium and molybdenum (from Takeno, 2005).

The analogue elements chosen for Np were thorium (Th) and samarium (Sm). The Pourbaix diagrams for each of these elements are given in Figure 19. Neptunium can exist in valence states III, IV, V and IV. Under oxic conditions its most common species is NpO_2^+ (valence V), which can be seen as a dominant stability field in Figure 19a. Thorium has a single valency of VI while samarium, as a lanthanide element, has a single valency of III. While both of these elements exhibit a range of hydroxy species at different pH (and Th can form complexes with carbonates), their chemistries are much simpler than that of Np, so their use as elemental analogues for Np seems to be <u>poorly justified</u>.

a) Neptunium   b) Thorium   c) Samarium (3+)
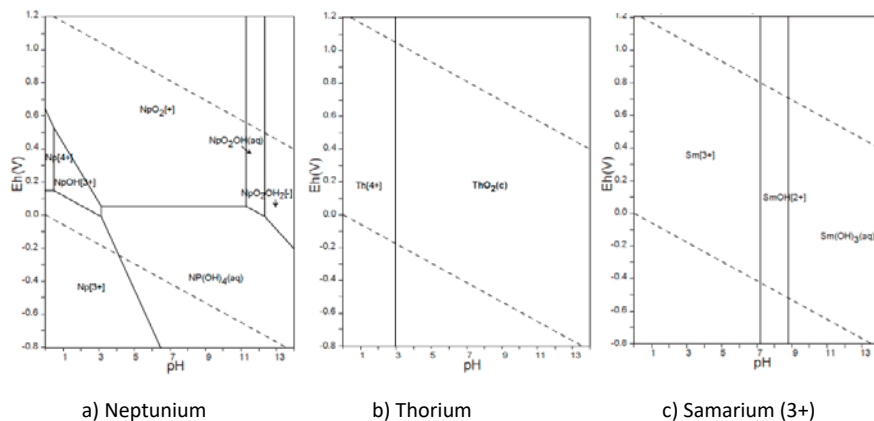
Figure 19: Pourbaix (Eh-pH) diagrams for neptunium, thorium and samarium (from Takeno, 2005).

Overall, the basic approach used to define the Kd distributions for the SR-PSU assessment differs fundamentally to that used in the SR-Site assessment. Rather

than combining site and literature data to generate the distributions, or using element-specific literature data in the absence of any site-specific data, site data relating to the element of interest, or an element analogue, is used in preference to any literature data. A preference for site-specific Kd data has previously been strong recommended by SSM (Xu et al., 2008).

As a result of the new approach, the GM of the Kd distributions has typically increased in the SR-PSU assessment in comparison to the SR-Site assessment. The effect of this change will vary, depending on exposure pathways of importance for each radionuclide discharged to the biosphere and their decay chains. However, the increase can generally be considered to be cautious, e.g. increasing retention of radionuclides in those layers that vegetation, biota and humans might be exposed to.

3.2. Terrestrial CR Distributions

Distributions for the eight terrestrial CR and transfer coefficient parameters used in SR-PSU are compared to their equivalents in the SR-Site assessment in Appendix B.2. The eight parameters are given below (SR-PSU parameter names given in brackets):

- terrestrial primary producer CRs (cR_Ter_pp);
- cereal CRs (cR_agri_cereal);
- agricultural vegetable CRs (cR_agri_veg);
- edible tuber CRs (cR_agri_tuber);
- mushroom CRs (cR_Ter_mush);
- meat transfer coefficients (TC_meat);
- milk transfer coefficients (TC_milk); and
- primary producer to herbivore CRs (cR_food_herbiv).

As with the Kd distributions, to highlight the differences in the magnitudes of terrestrial CRs used in both assessments, the median values of the SR-PSU/ SR-Site ratios (based on GM values for each parameter) are plotted for each element in Figure 20, along with the minimum and maximum ratios calculated. In general, the variability is between one and four orders of magnitude. Note that the ratio for nickel is highlighted in Figure 20 as a square plot symbol – the transfer coefficient to meat for this element was 32 times higher in SR-PSU than in SR-Site, though for other organisms/pathways the CR values in both assessments were similar.
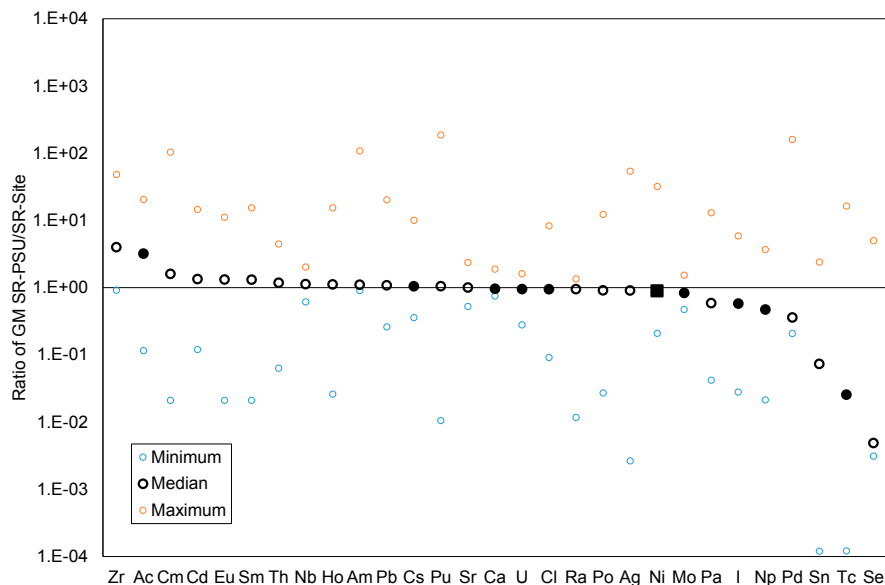
Figure 20: Distribution of median ratios between GM terrestrial CR and transfer coefficient values adopted in SR-PSU and SR-Site across a range of plants and animals (black symbols highlight the elements of particular interest; elements ranked by highest to lowest ratio).

Looking at the CR distributions assumed for Ba and Co, the GM assumed in the SR-PSU assessment typically varies within one order of magnitude to the GM of the distribution reported in the literature. The one exception is the tuber CR for Ba, see Table B15. No site data was available and so SKB took the parameter distribution from the literature. As IAEA (2010) reports only a single measurement of a Ba CR for tubers, SKB turned to element analogues. In Section 2.7.1 of the Kd and CR Report (Tröjbom et al., 2013), it is stated that "*the use of analogues among the alkaline earth metals has been restricted to Ca and Sr, and, Ba and Ra (Jaremalm et al., 2014)*". However, in the SR-PSU assessment, SKB used Sr as an analogue for Ba for this parameter, not Ra, despite there being plentiful samples for each (106 and 45 samples for Sr and Ra, respectively). As can be seen from Table 2, the distribution for Sr would give a more conservative estimate as to the uptake of Ba into tubers, but the use of Sr is inconsistent with the combination of analogues that SKB state that they use.

Table 2: Properties of tuber CR distributions for Ra, Sr and Ba, as reported in IAEA (2010) [kg dw plant kg dw^{-1} soil].

Element	N	BE/Mean	GSD	Minimum	Maximum
Ra	45	1.1E-2	6.8	2.4E-4	3.9E+0
Sr	106	1.6E-1	3.0	7.4E-3	1.6E+0
Ba	1	5.0E-3	-	-	-

Figure 20 shows that, of the elements of specific interest to this review, the terrestrial CR for actinium (Ac) increased most in the SR-PSU assessment while the terrestrial CR for Tc decreased most significantly. In the Kd and CR Report (Tröjbom et al., 2013), SKB state that:

> "*Am, Cm and Ac always lack site data and site data for a selected lanthanide are preferred over reported literature data (the lanthanide with the highest reported sample number is chosen as [an element analogue]).*"

The use of trivalent lanthanide elements as analogues for Ac is reasonably well justified on the basis that Ac is also a trivalent element. However, as in the case of soil geochemistry of Tc and Re, it should be borne in mind that qualitative similarity in the chemistry of an element and its analogue is no guarantee of a quantitative similarity in parameter values for K_d and CR.

As noted in Appendix F of the Radionuclide Transport Report (SKB, 2014), the transfer coefficient to meat (TC_meat) is one of three key parameters in determining the peak dose from Ni-59 in the main scenario (CCM_GW) of the SR-PSU assessment. Table B17 shows that the best estimate and geometric means of the distributions used in the SR-Site and SR-PSU assessments differ by a factor of 32, with the higher values being used in the SR-PSU assessment. The value used as a geometric mean in the SR-Site assessment (5.0E-3) is the best estimate from the SAFE and SR-97 assessments, as reported in Karlsson and Bergstrom (2002). Karlsson and Bergström (2002) cite the data as having been taken from IAEA (1994), with a log-triangular distribution taking lower and upper limits of 5.0E-4 and 5.0E-2, respectively. The distribution used in SR-PSU is for the element analogue Zn. The properties of the three distributions are shown in Table 3.

Table 3: Properties of the Ni transfer coefficient to meat distributions used in SKB assessments.

Assessment	Distribution	BE	GM	GSD	Minimum	Maximum
SAFE and SR-97	Log-triangular	5.0E-3	-	-	5.0E-4	5.0E-2
SR-Site	Log-normal	5.0E-3	5.0E-3	3.2	-	-
SR-PSU	Log-normal	1.6E-1	1.6E-1	4	1.6E-2	1.6E0

3.3. Aquatic CR Distributions

Distributions for aquatic CRs used in SR-PSU are compared to their equivalents in the SR-Site assessment in Appendix B.3. The nine parameters are given below (SR-PSU parameter names given in brackets):
- limnic phytoplankton CRs (cR_lake_pp_plank);
- limnic microphytobenthos CRs (cR_lake_pp_micro);
- limnic macroalgae and macrophyte CRs (cR_lake_pp_macro);
- limnic crayfish CRs (cR_lake_cray);
- limnic fish CRs (cR_lake_fish);
- marine pelagic phytoplankton (cR_sea_pp_plank);
- marine microphytobenthos CRs (cR_sea_pp_micro);
- marine primary producers (cR_sea_pp_macro); and
- marine fish (cR_sea_fish).

In the absence of sufficient site-specific data for both limnic and marine microphytobenthos, CRs for macroalgae were adopted in the SR-PSU assessment.

To highlight the differences in the magnitudes of aquatic CRs used in both assessments, the median values of the SR-PSU/ SR-Site ratios (based on GM values for each parameter) are plotted for each element in Figure 21.
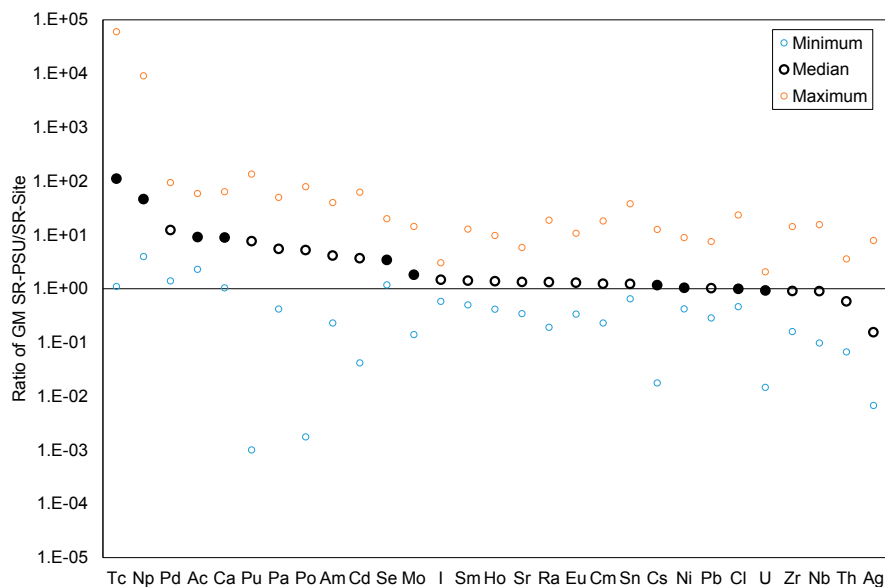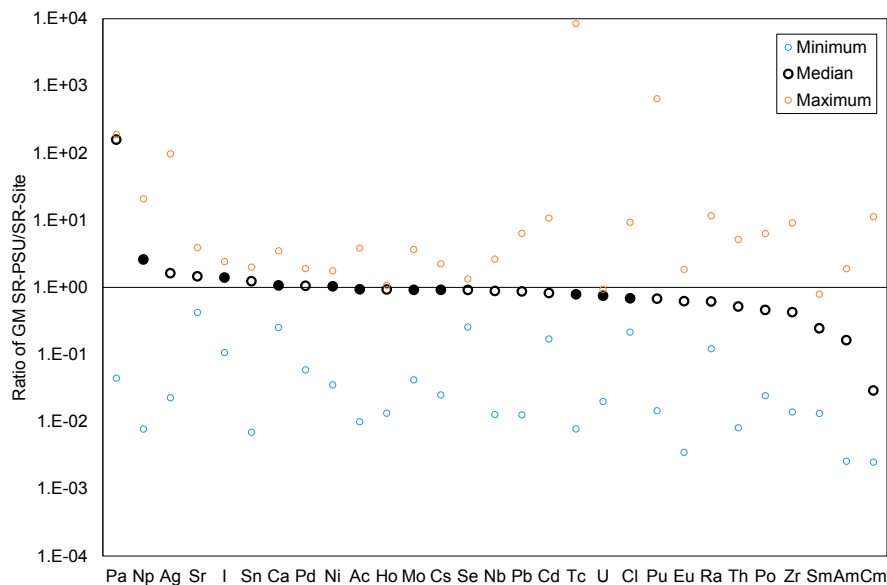
Figure 21: Distribution of median ratios between GM aquatic CR values adopted in SR-PSU and SR-Site across a range of organisms (black symbols highlight the elements of particular interest; elements ranked by highest to lowest median ratio).

One of the stand-out features of Figure 21 and the tables in Appendix B.3 is that the CR values adopted for protactinium (Pa) in the SR-PSU assessment are skewed such that the GM values assumed in the SR-PSU assessment are typically two orders of magnitude greater than those assumed in the SR-Site assessment. These higher values are all associated with the primary producers (freshwater and marine).

In the SR-PSU assessment, data for La was used as an element analogue for Pa for fish (both freshwater and marine) and freshwater primary producers. In the SR-PSU assessment, Nd was used as an element analogue for Pa for the three marine primary producers. Pa can exist in valence states II, III, IV and IV, although, like Np, it is most commonly present in oxidation state V, as stated in the Kd and CR Report. Curiously, however, in the Kd and CR Report SKB also state that:

> "*other trivalent actinides or lanthanides are utilised as analogues for Pa*"

which is justified on the basis that Pa is "*less particle reactive than Th in sea water*". This seems to be a weak justification for the choice of trivalent analogues for a predominantly pentavalent element.

3.4. Summary of Review Findings

The basic approach used to define the Kd and CR distributions in the SR-PSU assessment differs fundamentally to that used in the SR-Site assessment. Rather than combining site and literature data to generate the distributions, or using element specific literature data in the absence of any site-specific data, site data relating to the element of interest, or an element analogue, is used in preference to any literature data in the SR-PSU assessment.

The changes in the geometric mean values assumed for the Kd and CR parameters between SR-Site and SR-PSU for eight radionuclides identified as being important from a perspective of potential doses in SSM (2016) is given in Table 4.

Table 4: Comparison of Kd and CR geometric means for eight radionuclides identified as being important from the perspective of potential doses in the SR-PSU assessment (ratio of SR-PSU value to SR-Site value).

Parameter	Element							
	Ac	Ca	Cl	Cs	I	Mo	Ni	U
kd_RegoLow	9.2	8.5	1.2	0.33	2.0	0.14	0.44	0.015
kd_RegoGL	59	63	0.46	13	0.96	0.46	8.9	0.068
kd_regoPG	2.3	2.8	0.76	1.5	2.0	6.9	0.42	0.92
kd_RegoPeat	5.9	25	2.5	0.018	3.0	8.1	1.4	2.1
kd_regoIO and kd_regoGar	9.4	9.3	0.53	7.7	0.83	0.38	1.2	0.068
kd_regoUp_drain	3.2	7.3	1.9	0.42	0.58	1.5	0.44	0.94
kd_regoUp_ter	7.1	21	1.9	0.018	0.83	9.2	1.0	1.6
kd_regoUp_aqu	35	11	0.62	1.3	1.3	1.9	6.8	0.86
kd_PM_lake	9.1	1.6	23	1.0	1.6	1.8	1.1	1.3
kd_PM_sea	46	1.0	0.64	1.7	1.6	14	1.0	1.0
CR_ter_PP	3.2	0.75	8.3	1.6	0.19	1.4	0.78	0.71
CR_cereal	20	0.92	0.091	0.36	0.10	0.67	0.27	0.28
CR_veg	0.12	0.91	0.90	0.89	0.028	1.0	0.21	0.90
CR_tuber	0.22	1.2	0.56	1.3	0.11	0.47	0.36	1.2
CR_mush	3.2	0.85	8.3	1.1	0.97	0.53	1.0	0.69
TC_meat (d kg_{fw}^{-1})	6.5	1.0	1.0	1.0	1.0	1.0	32	1.0
TC_milk (d L^{-1})	0.21	1.0	0.49	1.0	1.0	0.55	1.0	1.0

28

Parameter	Element							
	Ac	Ca	Cl	Cs	I	Mo	Ni	U
CR_herbivore	Not in SR-Site	1.9	4.6	10	5.9	1.5	4.8	1.6
CR_lake_plank	1.1	1.1	0.22	0.92	1.4	0.73	1.0	0.74
CR_lake_ubent	1.1	3.5	9.3	0.31	1.4	0.042	1.0	0.020
CR_lake_macro	1.1	1.1	0.22	0.92	1.4	0.73	1.0	0.74
CR_lake_cray	3.8	3.0	1.0	1.3	1.3	1.6	1.1	0.94
CR_lake_fish	0.010	1.1	0.69	0.77	1.5	3.7	0.28	0.52
CR_sea_plank	0.94	2.6	0.30	0.15	2.4	0.92	0.86	0.75
CR_sea_ubent	0.94	0.25	0.39	0.025	0.11	0.044	0.035	0.75
CR_sea_macro	0.94	0.80	1.3	2.2	1.3	1.7	1.8	0.75
CR_sea_fish	0.058	0.78	0.86	1.0	1.7	1.2	0.73	0.84

Colour-coding used in Table 4:

Value from SR-PSU more than 1 order of magnitude lower than the value from SR-Site.

Value from SR-PSU less than 1 order of magnitude lower than the value from SR-Site.

Value from SR-PSU equal to or less than 1 order of magnitude higher than the value from SR-Site.

Value from SR-PSU between 1 and 2 orders of magnitude higher than the value from SR-Site.

29

A summary of the assumptions made to support the choice of Kd and CR distributions are listed below.

- Ac: element analogues are used in SR-PSU (either La, Sm, Am or Nd).
- Ca, Cl, Cs, I, Ni and U: site data used where possible, potentially with some prior data from SR-Site. Occasional use of environmental media/biota analogue, but not element analogue.
- Mo: site data used where possible, potentially with some prior data from SR-Site. Occasional use of environmental media/biota analogue. In one instance, cR_Ter_mush, Cr was used as an element analogue.

It is noticeable that, with the exception of Ac and Mo, no element analogues have been used in the derivation of the Kd and CR distributions.

Whilst it was shown in Appendix F of the Radionuclide Transport Report (SKB,2014) that higher values of Kd in the glacial clay, and higher CR values, would likely lead to higher doses associated with those radionuclides affected if the flux from the geosphere remained unaltered, this does not hold for all Kd values. A higher Kd in the till (regoLow) might be expected to lead to a lower dose due to the retention of radionuclide away for the parts of the biosphere with which vegetation, humans and non-human biota interact. The implications of Kd and CR assumptions on the calculated dose for a given radionuclide will also depend upon the dominant exposure pathways for that radionuclide (e.g. increased CR for Nb-94 is unlikely to affect dose, since the dominant exposure from Nb-94 is via external radiation).

Several other elements also of specific interest to dose calculations in SR-PSU have shown significant changes in Kd and CR values compared with the parameter values previously used in SR-Site. The common characteristic linking these particular elements appears to be that element analogues have been used to bolster the data set on which best estimates, geometric means and maxima and minima have been determined. Judicious selection of element analogues can certainly provide qualitative clues as to the likely behaviour of specific radionuclides in sediment-soil-plant-animal systems. However, as illustrated by the case of Tc and Re Kd, caution must be applied in extrapolating quantitative parameter values from one element to another, even when the chemistry of these elements is demonstrably similar; SKB acknowledge this in the Kd and CR Report (Tröjbom et al., 2013):

> "even if elements are chemically similar their behaviour in natural environments can differ, which is especially true for uptake in biota. Thus, an analogue can for example be used to describe element mobility of a certain element although (at the same time) be unusable to describe uptake."

One commonly used radionuclide-analogue pairs is caesium (Cs) and potassium (K). It is widely acknowledged that there are qualitative similarities in the chemical and biological behaviour of these elements, yet the quantitative differences in Kd and CR values for these elements are in the order of factors of 10 to 100.

Several of the selections of element analogues in SR-PSU have involved choices which are not particularly well justified, which likely contributes to why such large discrepancies have arisen between some of the parameter distributions used in SR-PSU and SR-Site; element analogues were not used in SR-Site. In the Kd and CR Report (Tröjbom et al., 2013), SKB state that:

> "[element analogues] are utilised in the parameterisation when element-specific data are missing or as supporting data for comparison and evaluation of data. The [element analogue] approach always

implies an increased level of uncertainty compared to the situation when the data of the proper element are available (IAEA 2010)."

The conclusion to be drawn from this is that, given a lack of direct quantitative estimates of Kd and CR values in SR-PSU, the use of element analogues has involved a sacrifice in the form of decreased precision on these parameters. From the examples discussed in the review of Kd distributions, it is clear that the use of this method can lead to assumed distributions that are questionable at best, and sometimes poorly justified given consideration of the chemical behaviour of the element of interest and the analogue selected.

4. Conclusions of the Further Reviews

Two specific topics relating to the SR-PSU assessment have been subject to further review in this report. Conclusions for each topic are summarised in the sub-sections below.

The sensitivities discussed below should be interpreted within the context that the peak calculated dose for the global warming variant of the main scenario in the SR-PSU assessment, which relate to the drained mire group, is only a factor of about 2.5 lower than 14 μSv per year, which corresponds to the annual risk criterion of 10^{-6} for a representative individual in the group exposed to the greatest risk.

4.1. Biosphere Modelling Review

An independent implementation of the SR-PSU biosphere model in the AMBER code has been updated, improving comparison against SKB's implementation for an exposure group that originally exhibited some differences. The updated calculations highlight that assumptions concerning when the mire in the biosphere object modelled as receiving 100% of the contaminated discharge from the geosphere can feasibly be drained and used for agriculture are not well documented or discussed in the SR-PSU reports. The drained mire farming group receives the highest calculated effective doses for the main scenario in SR-PSU.

In the SR-PSU assessment, C-14 is subject to a high loss rate to the atmosphere, especially from mire soils. Ingestion of C-14 in lake fish was a dominant exposure pathway SKB's previous radiological assessment of the SFR facility. The potential for sub-surface horizontal groundwater flows (neglected in the SR-PSU assessment) to allow C-14 to be discharged to surface water without having been subject to high loss rates from the mire surface has been investigated. The results show that the small sub-surface horizontal flows estimated by SKB in its near-surface hydrogeological modelling have relatively little effect on the calculated maximum effective dose, which is dominated by contaminants other than C-14. However, the calculations have also shown that, if there is a strong sub-surface hydrological connection between the biosphere object that receives the discharge from the geosphere and the biosphere object that includes a lake immediately down-gradient from this location, then the maximum calculated dose increases by about a factor of two.

The importance of the SR-PSU modelling assumptions in determining C-14 doses has also been illustrated in further variant calculations, which show that:
- maximum calculated doses increase by about a factor of two if groundwater is discharged to biosphere object 157-1 (which includes a transition to a lake stage) rather than biosphere object 157-2 (which does not), this is due to ingestion of C-14 in fish;
- maximum calculated doses increase by about a factor of two if C-14 loss rates to the atmosphere from the mire and surface water are reduced by an order of magnitude, this is again due to ingestion of C-14 in fish; and
- reducing size of the hunter gatherer group from 30 to 10 individuals (consistent with the size of the drained mire and infield-outland farming groups) increases their peak calculated doses by a factor of about three (this would have an equivalent effect on the peak doses observed in the cases described above).

Two of the exposure groups represented in the SR-PSU assessment for the main scenario conservatively make use of a groundwater well either dug into the till, or drilled into the underlying rock. The capture fractions for the drilled well, which are defined for each separate component of the SFR facility, are very small, ranging from zero to 0.3%. The location of wells in the modelling used to support the capture fractions includes some arbitrary assumptions. The locations are close to other wells considered within the "well interaction area" that exhibit capture fractions in excess of 10%. Variant calculations were undertaken with capture fractions of 10%, which result in a factor of five increase in the maximum calculated doses, illustrating the importance of these assumptions.

4.2. Consistency of Kd and CR Between Assessments

Comparison of Kd and CR distributions adopted in the SR-PSU assessment for the Forsmark area with those used in the SR-Site assessment for the same region highlights considerable changes (up to four orders of magnitude variation for some geometric means). The difference is, to some extent, explained by a greater preference for site-specific data in the SR-PSU assessment, which is welcomed. However, where data is lacking for some distributions, site-specific element analogue data is used in preference to element-specific literature data. The review highlights the significant uncertainty attributed to this approach, as is acknowledged in the SKB data compilations. The review also highlights examples where the choice of element analogue is poorly justified (notably for Tc, Np and Pa).

As a result of the new approach, Kd values have typically increased in the SR-PSU assessment in comparison to the SR-Site assessment, which can generally be considered to be cautious, e.g. increasing retention of radionuclides in those layers that vegetation, biota and humans might be exposed to. For CR distributions, the result of the new approach is more mixed, with average uptake values increasing for some elements and decreasing for others.

Overall, the comparison of Kd and CR distributions between the SR-PSU and SR-Site assessments serves to highlight the significant uncertainty that can be attributed to these parameters. The large magnitude of the changes in geometric means results in little overlap in the parameter distributions for some parameters and elements between the two assessments.

5. References

References quoted in the main report and in the appendices are listed below.

Avila R., 2006. The ecosystem models used for dose assessments in SR-Can. SKB R-06-81, Svensk Kärnbränslehantering AB.

Beresford N.A., Brown J., Copplestone D., Garnier-Laplace J., Howard B., Larsson C.M., Oughton D., Pröhl G., Zinger I. (eds), 2007. D-ERICA: An integrated approach to the assessment and management of environmental risk from ionising radiation. Description of purpose, methodology and application. EC contract number FI6R-CT-2004-508847, European Commission, Brussels.

Bergström U, Avila R, Ekström P-A, de la Cruz I, 2008. Dose assessments for SFR 1. SKB R-08-15, Svensk Kärnbränslehantering AB.

Brookins D., 1986. Rhenium as analog for fissiogenic technetium: Eh-pH diagram (25°C, 1 bar) constraints. Applied Geochemistry, 1(4), 513-517.

Gould O.J.P., 2012. Bacterial control of *in situ* sorption of technetium and rhenium in oxic and anoxic soils. PhD thesis, University of Nottingham, UK.

Grolander S., 2013. Biosphere parameters used in radionuclide transport modelling and dose calculations in SR-PSU. SKB R-13-18, Svensk Kärnbränslehantering AB.

Hosseini A., Thørring H., Brown J.E., Saxen R., Ilus E., 2008. Transfer of radionuclides in aquatic ecosystems – Default concentration ratios for aquatic biota in the Erica Tool. Journal of Environmental Radioactivity 99, 1408–1429.

IAEA, 1994. Handbook of parameter values for prediction of radionuclide transfer in temperate environments. Technical Report Series No 364, International Atomic Energy Agency, Vienna, Austria.

IAEA, 2004. Sediment Distribution Coefficients and Concentration Factors for Biota in the Marine Environment. Technical Report Series, 422. International Atomic Energy Agency, Vienna, Austria.

IAEA, 2010. Handbook of parameter values for the prediction of radionuclide transfer in terrestrial and freshwater environments. Technical Reports Series, 472. International Atomic Energy Agency, Vienna, Austria.

IAEA, 2013. Handbook of parameter values for the prediction of radionuclide transfer to wildlife. Technical Reports Series, 479. International Atomic Energy Agency, Vienna, Austria.

Jaremalm M., Lidman F., Köhler S., 2014. Precipitation of barite and its consequences for the mobility of Ra. SKB TR-13-28, Svensk Kärnbränslehantering AB.

Karlson S., Bergström U., 2002. Element specific parameter values used in the biosphere models of the safety assessments SR 97 and SAFE. SKB R-02-28, Svensk Kärnbränslehantering AB.

Kłos R., 2017. Interpretation of hydrology of object 157 in the future Forsmark landscape. SSM Dnr. 2016-3261-7.

Lidman F., Källström K., Kautsky U., 2017. Mo-93 from the grave to the cradle. SKB Report, P-16-22, 30 pp.

Nordén S., Avila R., de la Cruz I., Stenberg K., Grolander S., 2010. Element-specific and constant parameters used for dose calculations in SR-Site, Svensk Kärnbränslehantering AB technical report TR-10-07, updated 2013-12.

Quintessa, 2016. AMBER 6.1 Reference Manual. Quintessa Limited report QE-AMBER-1, Version 6.1.

Robens E., Hauschild J., Aumann D.C., 1988. Iodine-129 in the environment of a Nuclear Fuel Reprocessing Plant: III Soil To Plant Concentration Factors for Iodine-129 and Iodine-127 and there Transfer Factors to milk, egg and pork. Journal of Environmental Radioactivity Volume 8, Issue 1, pp 37–52.

Saetre P, Nordén S, Keesmann S, Ekström P-A, 2013. The biosphere model for radionuclide transport and dose assessment in SR-PSU. SKB R-13-46, Svensk Kärnbränslehantering AB.

Sheppard S., Long J., Sanipelli B., Sohlenius G., 2009. Solid/liquid partition coefficients (Kd) for selected soils and sediments at Forsmark and Laxemar-Simpevarp. SKB R-09-27, Svensk Kärnbränslehantering AB.

SKB, 2014. Radionuclide transport and dose calculations for the safety assessment SR-PSU, SKB TR-14-09, Svensk Kärnbränslehantering AB.

SSM, 2016. SSM's external experts' reviews of SKB's safety assessment SR-PSU – radionuclide transport, dose assessment, and safety analysis methodology: Initial review phase. Strålsäkerhetsmyndigheten (SSM) report 2016:09.

Takeno N., 2005. Atlas of Eh-pH diagrams - intercomparison of thermodynamic databases. Geological Survey of Japan Open File Report No.419. National Institute of Advanced Industrial Science and Technology Research Center for Deep Geological Environments, Japan.

Tröjbom M., Grolander S., Rensfeldt V., Nordén S., 2013. Kd and CR used for transport calculation in the biosphere in SR-PSU. SKB R-13-01, Svensk Kärnbränslehantering AB.

Veselý J., Majer V., Kučera J., Havránek V., 2001. Solid-water partitioning of elements in Czech freshwaters. Applied Geochemistry, 16, pp 437–450.

Walke R., Limer L., Shaw G., 2017. In-depth review of key issues for the main review phase regarding biosphere models for specific radionuclides in SR-PSU. SSM Dnr. 2016-3262-3

Werner K., Sassner M., Johansson E., 2013. Hydrology and near-surface hydrogeology at Forsmark – synthesis for the SR-PSU project. SKB R-13-19, Svensk Kärnbränslehantering AB.

Xu S., Wörman A., Dverstorp B., Klos R., Shaw G., Marklund L., 2008. SSI's independent consequence calculations in support of the regulatory review of the SR-Can safety assessment. SSI Rapport 2008:08.

Appendix A: Variant Water Flows

Water flow data used in variant AMBER calculations exploring the potential significance of sub-surface hydrological connection between biosphere object 157-2 and 157-1 are presented in this appendix, as described in Section 2.3. Two variants are considered.

- Flow Case 1: Based on the same flow numbers used in support of the SR-PSU assessment, but with the sub-surface flow values reinstated.
- Flow Case 2: Assuming that there is preferential horizontal flow from the till.

Note that the flow values have been derived as part of a separate review task. They are considered appropriate to support associated exploratory calculations (e.g. the flow values for biosphere object 157-1 have not been adjusted).

Table A1: Inter-compartmental water flows for biosphere object 157-2 for the two variant cases with differences from the original values highlighted in red.

Parameter	SR-PSU	Flow Case 1	Flow Case 2
q_low_gl_sea	2.83E-02	2.83E-02	2.83E-02
q_gl_low_sea	2.13E-02	2.13E-02	2.13E-02
q_gl_pg_sea	2.93E-02	2.93E-02	2.93E-02
q_pg_gl_sea	2.23E-02	2.23E-02	2.23E-02
q_pg_up_sea	3.09E-02	3.09E-02	3.09E-02
q_up_pg_sea	2.38E-02	2.38E-02	2.38E-02
q_up_wat_sea	3.09E-02	3.09E-02	3.09E-02
q_wat_up_sea	2.38E-02	2.38E-02	2.38E-02
q_low_gl_lake	1.84E-01	1.84E-01	0.00E+00
q_gl_low_lake	4.20E-02	4.20E-02	0.00E+00
q_gl_pg_lake	2.21E-01	2.21E-01	0.00E+00
q_pg_gl_lake	7.20E-02	7.20E-02	0.00E+00
q_pg_up_lake	4.97E-01	4.97E-01	3.08E-01
q_up_pg_lake	3.08E-01	3.08E-01	3.08E-01
q_up_wat_lake	6.56E-01	6.56E-01	4.32E-01
q_wat_up_lake	4.11E-01	4.11E-01	4.11E-01
q_downstream_iso	1.16E+00	1.16E+00	1.16E+00
q_low_gl_ter_iso	1.84E-01	1.84E-01	0.00E+00
q_gl_low_ter_iso	4.20E-02	4.20E-02	0.00E+00
q_gl_pg_ter_iso	2.21E-01	2.21E-01	0.00E+00
q_pg_gl_ter_iso	7.20E-02	7.20E-02	0.00E+00
q_up_wat_ter_iso	1.16E+00	1.16E+00	1.16E+00
q_wat_up_ter_iso	0.00E+00	0.00E+00	0.00E+00
q_pg_peat_ter_iso	4.97E-01	4.97E-01	3.08E-01

Parameter	SR-PSU	Flow Case 1	Flow Case 2
q_peat_pg_ter_iso	3.08E-01	3.08E-01	3.08E-01
q_peat_up_ter_iso	6.56E-01	6.56E-01	4.32E-01
q_up_peat_ter_iso	4.11E-01	4.11E-01	4.11E-01
q_low_downstream_iso	0.00E+00	7.71E-03	1.49E-01
q_GL_downstream_iso	0.00E+00	1.56E-03	8.31E-03
q_PG_downstream_iso	0.00E+00	8.60E-03	4.89E-02
q_peat_downstream_iso	0.00E+00	3.76E-03	3.76E-03
q_downstream_end	1.25E+00	1.25E+00	1.25E+00
q_low_gl_ter_end	2.22E-01	2.22E-01	0.00E+00
q_gl_low_ter_end	4.83E-02	4.83E-02	0.00E+00
q_gl_pg_ter_end	2.44E-01	2.44E-01	0.00E+00
q_pg_gl_ter_end	6.25E-02	6.25E-02	0.00E+00
q_up_wat_ter_end	1.25E+00	1.25E+00	1.25E+00
q_wat_up_ter_end	0.00E+00	0.00E+00	0.00E+00
q_pg_peat_ter_end	5.34E-01	5.34E-01	2.76E-01
q_peat_pg_ter_end	2.76E-01	2.76E-01	2.76E-01
q_peat_up_ter_end	6.94E-01	6.94E-01	4.35E-01
q_up_peat_ter_end	3.93E-01	3.93E-01	3.93E-01
q_low_downstream_end	0.00E+00	5.83E-03	1.80E-01
q_GL_downstream_end	0.00E+00	1.06E-03	8.71E-03
q_PG_downstream_end	0.00E+00	9.82E-03	8.53E-02
q_peat_downstream_end	0.00E+00	5.38E-03	5.38E-03

Appendix B: Kd and CR Comparisons

In each table in the following sub-sections the ratio of the BE and GM values assumed for a given parameter in the SR-PSU assessment are divided by the equivalent value from the SR-Site Assessment. The following colour coding has been used across all the tables to show the differences.

Table B1: Explanation of colour coding in comparison tables.

Colour	Explanation
	Value from SR-PSU more than 1 order of magnitude lower than the value from SR-Site / wider literature.
	Value from SR-PSU less than 1 order of magnitude lower than the value from SR-Site / wider literature.
	Value from SR-PSU equal to or less than 1 order of magnitude higher than the value from SR-Site / wider literature.
	Value from SR-PSU between 1 and 2 orders of magnitude higher than the value from SR-Site / wider literature.
	Value from SR-PSU more than 2 orders of magnitude higher than the value from SR-Site / wider literature.

B.1 Kd Comparisons

Kd data used for the till in SR-PSU (Table 5-3 of the Kd and CR Report) is compared with the Kd for inorganic deposits from SR-Site (Table 3-1 of Nordén et al., 2010), or IAEA (2010) in Table B2.

Table B2: Comparison of BE, GM and GSD for Kd in the till (kd_regoLow); the ratio reflects SR-PSU:SR-Site.

Element	Ratio of BE values	Ratio of GM values	Ratio of GSD values	Notes
Ac	9.2E0	9.2E0	1.5E0	1
Ag	7.9E0	7.9E0	1.0E0	2
Am	4.2E0	4.2E0	5.0E-1	1
Ba	8.4E-2	8.4E-2	Not in SR-Site	3
Ca	8.5E0	8.5E0	1.8E0	4
Cd	4.6E0	4.6E0	1.0E0	4
Cl	1.2E0	1.2E0	6.4E-1	5
Cm	1.2E0	1.2E0	7.5E-1	1
Co	5.2E0	5.2E0	Not in SR-Site	6
Cs	3.3E-1	3.3E-1	7.3E-1	4
Eu	8.3E-1	8.3E-1	5.5E-1	4
Ho	1.1E0	1.1E0	3.1E-1	5
I	2.0E0	2.0E0	5.9E-1	5
Mo	1.4E-1	1.4E-1	9.1E-1	4
Nb	1.6E+1	1.6E+1	5.7E-1	5
Ni	2.6E0	4.4E-1	7.5E-1	4
Np	1.2E+3	1.2E+3	7.5E-1	7
Pa	7.9E0	7.9E0	1.5E0	1
Pb	2.2E0	2.2E0	5.6E-1	4
Pd	5.6E0	5.6E0	1.5E0	8
Po	7.1E+1	7.9E+1	7.2E-1	9
Pu	1.5E+1	1.5E+1	7.5E-1	1
Ra	5.6E-1	1.9E-1	1.4E0	10
Se	6.4E0	6.4E0	1.2E0	4
Sm	2.2E0	2.2E0	2.3E-1	5
Sn	3.8E+1	3.8E+1	1.5E0	2
Sr	3.4E-1	3.4E-1	1.0E0	4
Tc	6.0E+4	6.0E+4	7.5E-1	11
Th	7.5E-1	7.5E-1	2.0E-1	4
U	1.5E-2	1.5E-2	9.4E-1	4
Zr	7.7E0	7.7E0	1.9E0	4

Notes:
1. SR-Site distribution was taken from IAEA (2010). In SR-PSU, site data for the element analogue, Sm, was used.
2. SR-Site distribution was taken from IAEA (2010). In SR-PSU, site data used.

3. In SR-PSU, site data was used. This is compared against data from IAEA (2010) for Ra as an element analogue for "All soils", as only a single value reported for Ba.
4. SR-Site distribution based on a prior from the population. In SR-PSU, site data was used.
5. SR-Site distribution based on a prior from the subpopulation. In SR-PSU, site data was used.
6. In SR-PSU, site data was used. This is compared against data from IAEA (2010) for "All soils".
7. SR-Site distribution was taken from IAEA (2010). In SR-PSU, site data for the element analogue, Th, was used.
8. SR-Site distribution was taken from IAEA (2010). In SR-PSU, site data for the element analogue, Ni, was used.
9. SR-Site distribution was taken from IAEA (2010). In SR-PSU, site data for the element analogue, Bi, was used.
10. SR-Site distribution based on site data. In SR-PSU, site data was used also.
11. SR-Site distribution was taken from IAEA (2010). In SR-PSU, site data for the element analogue, Zr, was used.

41

Kd data used for glacial clay in SR-PSU (Table 5-5 of the Kd and CR Report) is compared with the Kd for organic deposits from SR-Site (Table 3-2 of Nordén et al., 2010) in Table B3.

Table B3: Comparison of BE, GM and GSD for glacial clay (kd_regoGL); the ratio reflects SR-PSU:SR-Site.

Element	Ratio of BE values	Ratio of GM values	Ratio of GSD values	Notes
Ac	5.9E+1	5.9E+1	1.0E0	1
Ag	5.6E-3	6.7E-3	8.6E-1	2
Am	4.0E+1	4.0E+1	6.2E-1	1
Ba	2.8E0	2.8E0	Not in SR-Site	3
Ca	1.5E+1	6.3E+1	6.0E-1	4
Cd	4.0E0	7.1E0	1.6E-1	5
Cl	5.1E-1	4.6E-1	8.6E-1	2
Cm	1.1E+1	1.1E+1	7.8E-1	1
Co	9.7E+2	9.7E+2	Not in SR-Site	6
Cs	1.3E+1	1.3E+1	1.4E0	2
Eu	1.1E+1	1.1E+1	1.1E0	7
Ho	6.7E0	9.8E0	6.4E-1	4
I	3.2E-1	9.6E-1	3.9E-1	4
Mo	2.0E-1	4.6E-1	5.2E-1	4
Nb	3.8E0	3.8E0	7.9E-1	2
Ni	5.7E0	9.0E0	7.0E-1	4
Np	1.1E+2	1.1E+2	2.3E0	8
Pa	5.0E+1	5.0E+1	1.0E0	1
Pb	4.9E0	7.5E0	5.2E-1	4
Pd	9.4E+1	9.4E+1	1.5E0	9
Po	2.0E+1	2.0E+1	6.0E-1	10
Pu	1.4E+2	1.4E+2	7.8E-1	1
Ra	4.0E0	4.3E0	1.4E0	7
Se	1.7E0	4.0E0	1.6E0	4
Sm	9.1E0	1.3E+1	5.8E-1	4
Sn	1.6E0	1.6E0	8.3E-1	2
Sr	5.8E0	5.8E0	1.1E0	2
Tc	1.8E+4	1.8E+4	1.0E0	11
Th	2.2E0	2.2E0	8.1E-1	2
U	6.5E-02	6.8E-2	2.5E0	2
Zr	9.6E0	9.6E0	1.9E-1	2

Notes:
1. SR-Site distribution was taken from IAEA (2010). In SR-PSU, site data for the element analogue, Sm, was used.
2. SR-Site distribution based on a prior from the population. In SR-PSU, site data was used.

3. In SR-PSU site data was used. This is compared against data from IAEA (2010) for Ra as an element analogue for "Organic" soil, as only a single value reported for Ba.
4. SR-Site distribution based on a prior from the subpopulation. In SR-PSU, site data was used.
5. SR-Site distribution based on a prior from the subpopulation. In SR-PSU, site data for the element analogue, Zn, was used.
6. In SR-PSU site data was used. This is compared against data from IAEA (2010) for "Organic" soil.
7. In both assessments, site data was used.
8. SR-Site distribution was taken from IAEA (2010). In SR-PSU, site data for the element analogue, Th, was used.
9. SR-Site distribution was taken from IAEA (2010). In SR-PSU, site data for the element analogue, Ni, was used.
10. SR-Site distribution was taken from IAEA (2010). In SR-PSU, site data for the element analogue, Bi, was used.
11. SR-Site distribution was taken from IAEA (2010). In SR-PSU, site data for the element analogue, Zr, was used.

Kd data used for post-glacial deposits in SR-PSU (Table 5-7 of the Kd and CR Report) is compared with the Kd for organic deposits from SR-Site (Table 3-2 of Nordén et al., 2010) or IAEA (2010) in Table B4.

Table B4: Comparison of BE, GM and GSD for post-glacial deposits (kd_regoPG); the ratio reflects SR-PSU:SR-Site.

Element	Ratio of BE values	Ratio of GM values	Ratio of GSD values	Notes
Ac	2.1E0	2.3E0	1.0E0	1
Ag	6.6E-2	7.9E-2	1.2E0	2
Am	1.4E0	1.6E0	6.0E-1	1
Ba	1.5E0	3.2E-1	Not in SR-Site	3
Ca	5.9E-1	2.8E0	6.0E-1	4
Cd	1.7E-2	4.2E-2	1.6E-1	5
Cl	8.4E-1	7.6E-1	8.6E-1	2
Cm	3.8E-1	4.2E-1	7.5E-1	1
Co	1.5E+1	9.1E0	Not in SR-Site	6
Cs	1.7E0	1.5E0	1.4E0	2
Eu	4.4E-1	4.2E-1	5.9E-1	7
Ho	2.5E-1	4.1E-1	6.4E-1	4
I	6.8E-1	2.0E0	3.9E-1	4
Mo	3.1E0	6.9E0	6.3E-1	4
Nb	7.8E-1	6.3E-1	7.9E-1	2
Ni	3.7E-1	4.2E-1	7.2E-1	4
Np	1.6E+1	1.6E+1	2.3E0	8
Pa	1.8E0	2.0E0	1.0E0	1
Pb	1.8E-1	3.5E-1	5.2E-1	4
Pd	6.1E0	4.4E0	1.6E0	9
Po	5.6E0	5.6E0	6.0E-1	10
Pu	4.7E0	5.3E0	7.5E-1	1
Ra	1.0E0	1.1E0	1.4E0	7
Se	2.8E0	1.5E0	1.1E0	4
Sm	3.2E-1	5.0E-1	5.7E-1	4
Sn	3.4E0	3.4E0	2.7E0	2
Sr	4.8E-1	4.8E-1	1.1E0	2
Tc	1.4E+3	7.0E+2	1.4E0	11
Th	3.1E-1	3.1E-1	8.1E-1	2
U	5.8E-1	9.2E-1	8.8E-1	2
Zr	7.3E-1	3.8E-1	2.7E-1	2

Notes:
1. SR-Site distribution was taken from IAEA (2010). In SR-PSU, site data for the element analogue, Sm, was used.
2. SR-Site distribution based on a prior from the population. In SR-PSU, site data was used.

3. In SR-PSU site data was used. This is compared against data from IAEA (2010) for Ra as an element analogue for "Organic" soil, as only a single value reported for Ba.
4. SR-Site distribution based on a prior from the subpopulation. In SR-PSU, site data was used.
5. SR-Site distribution based on a prior from the subpopulation. In SR-PSU, site data for the element analogue, Zn, was used.
6. In SR-PSU site data was used. This is compared against data from IAEA (2010) for "Organic" soil.
7. In both assessments, site data was used.
8. SR-Site distribution was taken from IAEA (2010). In SR-PSU, site data for the element analogue, Th, was used.
9. SR-Site distribution was taken from IAEA (2010). In SR-PSU, site data for the element analogue, Ni, was used.
10. SR-Site distribution was taken from IAEA (2010). In SR-PSU, site data for the element analogue, Bi, was used.
11. SR-Site distribution was taken from IAEA (2010). In SR-PSU, site data for the element analogue, Zr, was used.

Kd data used for peat in SR-PSU (Table 5-9 of the Kd and CR Report) is compared with the Kd for organic deposits from SR-Site (Table 3-2 of Nordén et al., 2010) or IAEA (2010) in Table B5.

Table B5: Comparison of BE, GM and GSD for peat (kd_regoPeat); the ratio reflects SR-PSU:SR-Site.

Element	Ratio of BE values	Ratio of GM values	Ratio of GSD values	Notes
Ac	5.9E0	5.9E0	1.0E0	1
Ag	4.2E-2	5.0E-2	8.6E-1	2
Am	4.0E0	4.0E0	6.0E-1	1
Ba	4.3E-1	4.3E-1	Not in SR-Site	3
Ca	6.0E0	2.5E+1	6.0E-1	4
Cd	4.0E0	7.1E0	3.7E-1	4
Cl	2.7E0	2.5E0	1.1E0	2
Cm	1.1E0	1.1E0	7.5E-1	1
Co	3.4E+1	3.4E+1	Not in SR-Site	5
Cs	1.8E-2	1.8E-2	1.4E0	2
Eu	1.5E0	1.5E0	1.1E0	6
Ho	1.1E0	1.6E0	6.4E-1	4
I	1.0E0	3.0E0	3.9E-1	4
Mo	3.5E0	8.1E0	3.4E-1	4
Nb	3.0E-1	3.0E-1	7.9E-1	2
Ni	8.7E-1	1.4E0	7.0E-1	4
Np	4.0E0	4.0E0	2.6E0	7
Pa	5.0E0	5.0E0	1.0E0	1
Pb	3.3E-1	5.0E-1	5.2E-1	4
Pd	2.4E+1	2.4E+1	3.0E0	8
Po	2.3E0	2.3E0	6.0E-1	9
Pu	1.4E+1	1.4E+1	7.5E-1	1
Ra	8.4E-1	9.1E-1	1.4E0	7
Se	8.3E-1	1.9E0	1.6E0	4
Sm	9.1E-1	1.3E0	5.7E-1	4
Sn	1.3E0	1.3E0	9.7E-1	2
Sr	3.3E0	3.3E0	1.1E0	2
Tc	8.7E+2	8.7E+2	1.0E0	10
Th	7.6E-2	7.6E-2	9.2E-1	2
U	2.0E0	2.1E0	9.1E-1	2
Zr	4.6E-1	4.6E-1	1.9E-1	2

Notes:
1. SR-Site distribution was taken from IAEA (2010). In SR-PSU, site data for the element analogue, Sm, was used.
2. SR-Site distribution based on a prior from the population. In SR-PSU, site data was used.

3. In SR-PSU site data was used. This is compared against data from IAEA (2010) for Ra as an element analogue for "Organic" soil, as only a single value reported for Ba.
4. SR-Site distribution based on a prior from the subpopulation. In SR-PSU, site data was used.
5. In SR-PSU site data was used. This is compared against data from IAEA (2010) for "Organic" soil.
6. In both assessments, site data was used.
7. SR-Site distribution was taken from IAEA (2010). In SR-PSU, site data for the element analogue, Th, was used.
8. SR-Site distribution was taken from IAEA (2010). In SR-PSU, site data was used.
9. SR-Site distribution was taken from IAEA (2010). In SR-PSU, site data for the element analogue, Bi, was used.
10. SR-Site distribution was taken from IAEA (2010). In SR-PSU, site data for the element analogue, Zr, was used.

Kd data used for cultivated clayey till and glacial clay in SR-PSU (Table 5-11 of the Kd and CR Report) is compared with the Kd for organic deposits from SR-Site (Table 3-2 of Nordén et al., 2010) or IAEA (2010) in Table B6.

Table B6: Comparison of BE, GM and GSD for cultivated clayey till and glacial clay (kd_regoUp_io and kd_regoUp_garden); the ratio reflects SR-PSU:SR-Site.

Element	Ratio of BE values	Ratio of GM values	Ratio of GSD values	Notes
Ac	1.2E+1	9.4E0	1.4E0	1
Ag	4.2E-2	5.0E-2	5.7E-1	2
Am	8.4E0	6.4E0	8.4E-1	1
Ba	8.5E-1	6.2E-1	Not in SR-Site	3
Ca	1.9E0	9.3E0	4.6E-1	4
Cd	1.6E0	1.8E0	3.1E-1	4
Cl	5.8E-1	5.3E-1	5.7E-1	2
Cm	2.3E0	1.7E0	1.1E0	1
Co	1.3E+2	1.0E+2	Not in SR-Site	5
Cs	9.6E0	7.7E0	2.1E0	2
Eu	2.0E0	1.4E0	9.3E-1	6
Ho	1.3E0	1.6E0	7.7E-1	4
I	2.8E-1	8.3E-1	2.6E-1	4
Mo	1.5E-1	3.8E-1	2.3E-1	4
Nb	5.5E-1	4.5E-1	1.1E0	2
Ni	8.7E-1	1.2E0	4.7E-1	4
Np	2.6E+1	2.0E+1	3.2E0	1
Pa	1.1E+1	8.0E0	1.4E0	1
Pb	1.4E0	1.6E0	1.2E0	4
Pd	2.6E+1	2.6E+1	3.0E0	7
Po	4.8E0	4.8E0	9.6E-1	8
Pu	5.1E-1	5.8E-1	5.0E-1	9
Ra	2.4E0	2.6E0	1.4E0	7
Se	1.8E0	2.9E0	8.9E-1	4
Sm	1.9E0	2.1E0	7.9E-1	4
Sn	1.0E0	1.0E0	6.1E-1	2
Sr	1.0E0	1.3E0	8.9E-1	2
Tc	3.7E+1	3.7E+1	6.7E-1	10
Th	6.0E-1	5.2E-1	1.3E0	2
U	5.8E-2	6.8E-2	5.9E-1	2
Zr	3.9E-1	3.4E-1	1.7E-1	2

Notes:
1. SR-Site distribution was taken from IAEA (2010). In SR-PSU, site data for the element analogue, Sm, was used.
2. SR-Site distribution based on a prior from the population. In SR-PSU, site data was used.

3. In SR-PSU site data was used. This is compared against data from IAEA (2010) for Ra as an element analogue for "Organic" soil, as only a single value reported for Ba.

4. SR-Site distribution based on a prior from the subpopulation. In SR-PSU, site data was used.

5. In SR-PSU site data was used. This is compared against data from IAEA (2010) for "Organic" soil.

6. In both assessments, site data was used.

7. SR-Site distribution was taken from IAEA (2010). In SR-PSU, site data was used.

8. SR-Site distribution was taken from IAEA (2010). In SR-PSU, site data for the element analogue, Bi, was used.

9. SR-Site distribution was taken from IAEA (2010). In SR-PSU, site data for the element analogue, U, was used.

10. SR-Site distribution was taken from IAEA (2010). In SR-PSU, site data for the element analogue, Re, was used.

Kd data used for drained mire in SR-PSU (Table 5-13 of the Kd and CR Report) is compared with the Kd for organic deposits from SR-Site (Table 3-2 of Nordén et al., 2010) or IAEA (2010) in Table B7.

Table B7: Comparison of BE, GM and GSD for drained mire (kd_regoUp_drain); the ratio reflects SR-PSU:SR-Site.

Element	Ratio of BE values	Ratio of GM values	Ratio of GSD values	Notes
Ac	3.2E0	3.2E0	1.1E0	1
Ag	4.5E-2	5.4E-2	7.1E-1	2
Am	2.2E0	2.2E0	6.6E-1	1
Ba	6.2E-1	6.2E-1	Not in SR-Site	3
Ca	1.7E0	7.3E0	5.8E-1	4
Cd	4.4E-1	7.9E-1	3.8E-1	4
Cl	2.1E0	1.9E0	7.7E-1	2
Cm	5.9E-1	5.9E-1	8.3E-1	1
Co	9.2E0	9.2E0	Not in SR-Site	5
Cs	4.2E-1	4.2E-1	1.6E0	2
Eu	3.4E-1	3.4E-1	6.5E-1	6
Ho	3.7E-1	5.4E-1	7.4E-1	4
I	2.0E-1	5.8E-1	3.6E-1	4
Mo	6.7E-1	1.5E0	3.6E-1	4
Nb	9.8E-2	9.8E-2	7.6E-1	2
Ni	2.8E-1	4.4E-1	5.8E-1	4
Np	6.8E0	6.8E0	2.5E0	1
Pa	2.8E0	2.8E0	1.1E0	1
Pb	1.9E-1	2.9E-1	6.6E-1	4
Pd	3.6E0	3.6E0	3.0E0	7
Po	1.1E0	1.1E0	6.8E-1	8
Pu	8.0E0	8.0E0	8.5E-1	9
Ra	8.4E-1	9.1E-1	9.5E-1	7
Se	2.5E0	5.7E0	7.9E-1	4
Sm	5.0E-1	7.1E-1	6.2E-1	4
Sn	6.9E-1	6.9E-1	6.7E-1	2
Sr	1.2E0	1.2E0	9.3E-1	2
Tc	2.2E+1	2.2E+1	2.5E0	10
Th	9.5E-2	9.5E-2	7.8E-1	2
U	8.9E-1	9.4E-1	1.0E0	2
Zr	1.6E-1	1.6E-1	2.8E-1	2

Notes:
1. SR-Site distribution was taken from IAEA (2010). In SR-PSU, site data for the element analogue, Sm, was used.
2. SR-Site distribution based on a prior from the population. In SR-PSU, site data was used.

3. In SR-PSU site data was used. This is compared against data from IAEA (2010) for Ra as an element analogue for "Organic" soil, as only a single value reported for Ba.
4. SR-Site distribution based on a prior from the subpopulation. In SR-PSU, site data was used.
5. In SR-PSU site data was used. This is compared against data from IAEA (2010) for "Organic" soil.
6. In both assessments, site data was used.
7. SR-Site distribution was taken from IAEA (2010). In SR-PSU, site data was used.
8. SR-Site distribution was taken from IAEA (2010). In SR-PSU, site data for the element analogue, Bi, was used.
9. SR-Site distribution was taken from IAEA (2010). In SR-PSU, site data for the element analogue, U, was used.
10. SR-Site distribution was taken from IAEA (2010). In SR-PSU, site data for the element analogue, Re, was used.

Kd data used for the upper oxic layer of terrestrial regolith (peat) in SR-PSU (Table 5-15 of the Kd and CR Report) is compared with the Kd for organic deposits from SR-Site (Table 3-2 of Nordén et al., 2010) or IAEA (2010) in Table B8.

Table B8: Comparison of BE, GM and GSD for upper layer of terrestrial regolith (kd_regoUp_ter); the ratio reflects SR-PSU:SR-Site.

Element	Ratio of BE values	Ratio of GM values	Ratio of GSD values	Notes
Ac	7.1E0	7.1E0	1.0E0	1
Ag	1.9E-1	2.3E-1	8.6E-1	2
Am	4.8E0	4.8E0	6.0E-1	1
Ba	6.3E-1	6.3E-1	Not in SR-Site	3
Ca	4.9E0	2.1E+1	6.0E-1	4
Cd	3.0E0	5.4E0	2.9E-1	4
Cl	2.1E0	1.9E0	8.6E-1	2
Cm	1.3E0	1.3E0	7.5E-1	1
Co	2.0E+1	2.0E+1	Not in SR-Site	5
Cs	1.8E-2	1.8E-2	1.4E0	2
Eu	4.7E-1	4.7E-1	1.1E0	6
Ho	8.0E-1	1.2E0	6.4E-1	4
I	2.8E-1	8.3E-1	3.9E-1	4
Mo	4.0E0	9.2E0	3.4E-1	4
Nb	1.8E-1	1.8E-1	7.9E-1	2
Ni	6.3E-1	1.0E0	7.0E-1	4
Np	1.5E+1	1.5E+1	2.3E0	1
Pa	6.0E0	6.0E0	1.0E0	1
Pb	4.2E-1	6.4E-1	5.5E-1	4
Pd	1.1E+1	1.1E+1	1.5E0	7
Po	1.8E0	1.8E0	6.0E-1	8
Pu	1.4E+1	1.4E+1	7.5E-1	9
Ra	8.4E-1	9.1E-1	1.4E0	7
Se	1.9E0	4.3E0	1.6E0	4
Sm	1.1E0	1.5E0	5.7E-1	4
Sn	6.5E-1	6.5E-1	1.1E0	2
Sr	2.7E0	2.7E0	1.1E0	2
Tc	1.4E+2	1.4E+2	1.0E0	10
Th	6.7E-2	6.7E-2	8.1E-1	2
U	1.5E0	1.6E0	8.8E-1	2
Zr	4.1E-1	4.1E-1	1.9E-1	2

Notes:
1. SR-Site distribution was taken from IAEA (2010). In SR-PSU, site data for the element analogue, Sm, was used.
2. SR-Site distribution based on a prior from the population. In SR-PSU, site data was used.

3. In SR-PSU site data was used. This is compared against data from IAEA (2010) for Ra as an element analogue for "Organic" soil, as only a single value reported for Ba.
4. SR-Site distribution based on a prior from the subpopulation. In SR-PSU, site data was used.
5. In SR-PSU site data was used. This is compared against data from IAEA (2010) for "Organic" soil.
6. In both assessments, site data was used.
7. SR-Site distribution was taken from IAEA (2010). In SR-PSU, site data for the element analogue, Ni, was used.
8. SR-Site distribution was taken from IAEA (2010). In SR-PSU, site data for the element analogue, Bi, was used.
9. SR-Site distribution was taken from IAEA (2010). In SR-PSU, site data for the element analogue, U, was used.
10. SR-Site distribution was taken from IAEA (2010). In SR-PSU, site data for the element analogue, Re, was used.

Kd data used for the upper layer of aquatic regolith in SR-PSU (Table 5-17 of the Kd and CR Report) is compared with the Kd for organic deposits from SR-Site (Table 3-2 of Nordén et al., 2010) or IAEA (2010) in Table B9.

Table B9: Comparison of BE, GM and GSD for the upper layer of aquatic regolith (kd_regoUp_aqu); the ratio reflects SR-PSU:SR-Site.

Element	Ratio of BE values	Ratio of GM values	Ratio of GSD values	Notes
Ac	5.2E+1	3.5E+1	1.0E0	1
Ag	4.5E-1	1.1E0	8.9E-1	2
Am	3.5E+1	2.4E+1	6.0E-1	1
Ba	2.5E0	2.7E0	Not in SR-Site	3
Ca	2.4E0	1.1E+1	6.0E-1	4
Cd	1.5E+1	6.3E+1	1.8E-1	4
Cl	9.0E-1	6.2E-1	1.1E0	2
Cm	9.5E0	6.3E0	7.5E-1	1
Co	1.8E+2	1.7E+2	Not in SR-Site	5
Cs	1.8E0	1.3E0	1.4E0	2
Eu	9.2E0	6.4E0	5.6E-1	6
Ho	5.1E0	5.4E0	6.4E-1	4
I	4.9E-1	1.3E0	3.9E-1	4
Mo	5.4E-1	1.9E0	3.4E-1	4
Nb	3.8E0	3.0E0	7.9E-1	2
Ni	4.7E0	6.8E0	7.0E-1	4
Np	1.1E+2	7.3E+1	2.3E0	1
Pa	4.4E+1	3.0E+1	1.0E0	1
Pb	3.5E0	6.1E0	5.2E-1	4
Pd	7.8E+1	7.2E+1	1.5E0	7
Po	8.5E0	6.2E0	6.0E-1	8
Pu	6.1E0	7.3E0	7.5E-1	9
Ra	1.3E0	1.5E0	1.4E0	10
Se	8.3E0	2.0E+1	1.1E0	4
Sm	8.0E0	7.6E0	5.7E-1	4
Sn	1.2E0	1.2E0	8.3E-1	2
Sr	1.2E0	1.4E0	1.1E0	2
Tc	6.0E+1	6.0E+1	2.0E0	11
Th	5.0E0	3.6E0	8.1E-1	2
U	6.8E-1	8.6E-1	8.8E-1	2
Zr	1.6E+1	1.4E+1	2.5E-1	2

Notes:
1. SR-Site distribution was taken from IAEA (2010). In SR-PSU, site data for the element analogue, Sm, was used.
2. SR-Site distribution based on a prior from the population. In SR-PSU, site data was used.

3. In SR-PSU site data was used. This is compared against data from IAEA (2010) for Ra as an element analogue for "Organic" soil, as only a single value reported for Ba.
4. SR-Site distribution based on a prior from the subpopulation. In SR-PSU, site data was used.
5. In SR-PSU site data was used. This is compared against data from IAEA (2010) for "Organic" soil.
6. In both assessments, site data was used.
7. SR-Site distribution was taken from IAEA (2010). In SR-PSU, site data for the element analogue, Ni, was used.
8. SR-Site distribution was taken from IAEA (2010). In SR-PSU, site data for the element analogue, Bi, was used.
9. SR-Site distribution was taken from IAEA (2010). In SR-PSU, site data for the element analogue, U, was used.
10. In SR-Site, site data was used. In SR-PSU, site data for the element analogue, Ba, was used.
11. SR-Site distribution was taken from IAEA (2010). In SR-PSU, site data for the element analogue, Re, was used.

Kd data used for suspended particulate matter in the lakes in SR-PSU (Table 5-19 of the Kd and CR Report) is compared with the same parameter from SR-Site (Table 3-4 of Nordén et al., 2010) or IAEA (2010) in Table B10.

Table B10: Comparison of BE, GM and GSD for suspended particulate matter in lakes (kd_PM_lake); the ratio reflects SR-PSU:SR-Site.

Element	Ratio of BE values	Ratio of GM values	Ratio of GSD values	Notes
Ac	7.7E0	9.1E0	9.4E-1	1
Ag	3.9E-1	3.9E-1	2.2E0	2
Am	6.4E-1	7.6E-1	5.3E-1	3
Ba	3.2E0	6.0E0	Not in SR-Site	4
Ca	1.2E0	1.6E0	9.4E-1	5
Cd	3.8E0	2.8E0	7.5E-1	6
Cl	6.2E+1	2.3E+1	1.6E-1	7
Cm	1.5E+1	1.8E+1	3.1E-1	3
Co	1.5E0	2.0E0	Not in SR-Site	8
Cs	7.4E-1	1.0E0	9.4E-1	6
Eu	9.0E-1	1.3E0	1.0E0	6
Ho	3.3E-1	4.7E-1	1.4E0	2
I	2.5E0	1.6E0	8.1E-1	6
Mo	1.6E0	1.8E0	5.7E-1	6
Nb	7.0E-1	1.2E0	9.4E-1	6
Ni	1.6E0	1.1E0	1.3E0	6
Np	7.7E+3	9.1E+3	6.1E-1	3
Pa	7.7E-1	9.1E-1	9.4E-1	1
Pb	1.2E0	1.0E0	1.0E0	6
Pd	2.1E+1	1.4E+1	9.4E-1	9
Po	1.4E+2	3.5E+1	1.6E0	10
Pu	6.3E-3	3.5E-2	1.0E0	11
Ra	8.6E-1	1.6E0	9.7E-1	12
Se	1.0E0	1.2E0	1.4E0	5
Sm	5.5E-1	6.5E-1	8.3E-1	6
Sn	1.2E0	2.7E0	1.7E0	13
Sr	7.9E-1	1.2E0	1.0E0	2
Tc	1.3E+2	8.6E+1	6.5E-1	14
Th	5.0E-1	6.3E-1	6.5E-1	6
U	2.4E-1	1.3E0	7.4E-1	6
Zr	1.0E0	1.5E0	6.8E-1	6

Notes:
1. SR-Site distribution from Karlsson and Bergström (2002). In SR-PSU, site data for the element analogue, Sm, was used.
2. SR-Site distribution based on a prior from the subpopulation. In SR-PSU, site data was used.

3. SR-Site distribution from IAEA (2010). In SR-PSU, site data for the element analogue, Sm, was used.
4. In SR-PSU site data was used. This is compared against data from IAEA (2010).
5. In both assessments, site data was used.
6. SR-Site distribution based on a prior from the population. In SR-PSU, site data was used.
7. SR-Site distribution from Veselý et al. (2001). In SR-PSU, site data for the element analogue, Br, was used.
8. In SR-PSU site data was used. This is compared against data from IAEA (2010), specifically the field measurements of Kd.
9. SR-Site distribution from Karlsson and Bergström (2002). In SR-PSU, site data for the element analogue, Ni, was used.
10. SR-Site distribution from Karlsson and Bergström (2002). In SR-PSU, site data for the element analogue, Bi, was used.
11. SR-Site distribution from IAEA (2010). In SR-PSU, site data for the element analogue, U, was used.
12. SR-Site distribution from IAEA (2010). In SR-PSU, site data for the element analogue, Ba, was used.
13. SR-Site distribution from Karlsson and Bergström (2002). In SR-PSU, site data for the element analogue, Zr, was used.
14. SR-Site distribution from IAEA (2010). In SR-PSU, site data for the element analogue, Re, was used.

Kd data used for suspended particulate matter in the sea in SR-PSU (Table 5-21 of the Kd and CR Report) is compared with the same parameter from SR-Site (Table 3-3 of Nordén et al., 2010) or IAEA (2004) in Table B11.

Table B11: Comparison of BE, GM and GSD for suspended particulate matter in the sea (kd_PM_sea); the ratio reflects SR-PSU:SR-Site.

Element	Ratio of BE values	Ratio of GM values	Ratio of GSD values	Notes
Ac	8.1E+1	4.6E+1	9.4E-1	1
Ag	3.6E0	3.6E0	2.2E0	2
Am	4.1E-1	2.3E-1	5.3E-1	3
Ba	3.0E+2	3.8E+1	Not in SR-Site	4
Ca	3.1E0	1.0E0	1.1E0	5
Cd	5.2E0	2.6E0	7.3E-1	6
Cl	6.4E-1	6.4E-1	2.0E-1	7
Cm	4.1E-1	2.3E-1	3.1E-1	3
Co	5.0E-1	2.3E-1	Not in SR-Site	4
Cs	7.1E0	1.7E0	6.0E-1	6
Eu	1.5E0	1.3E0	1.2E0	6
Ho	5.4E0	3.3E0	5.9E-1	6
I	1.7E0	1.6E0	1.4E0	6
Mo	3.9E+1	1.4E+1	6.0E-1	6
Nb	5.5E0	1.9E0	6.4E-1	6
Ni	1.1E0	1.0E0	2.1E0	6
Np	8.1E+2	4.6E+2	1.0E0	3
Pa	7.4E-1	4.2E-1	9.4E-1	8
Pb	8.4E-1	1.0E0	1.1E0	6
Pd	1.5E0	1.4E0	9.4E-1	9
Po	3.9E-3	1.8E-3	9.4E-1	10
Pu	1.5E-3	1.0E-3	2.0E-1	11
Ra	1.5E+2	1.9E+1	1.5E+1	12
Se	1.8E0	2.6E0	1.9E-1	13
Sm	1.9E0	1.1E0	1.4E0	6
Sn	1.0E0	1.0E0	1.9E0	6
Sr	4.8E0	4.9E0	1.4E-1	13
Tc	1.1E0	1.1E0	6.5E-1	14
Th	2.7E0	7.8E-1	6.7E-1	6
U	1.5E0	1.0E0	1.1E0	6
Zr	3.8E0	1.3E0	7.0E-1	6

Notes:
1. SR-Site distribution from Karlsson and Bergström (2002). In SR-PSU, site data for the element analogue, Sm, was used.
2. SR-Site distribution from Beresford et al. (2007). In SR-PSU, the value of kd_PM_lake was used.

3. SR-Site distribution from Beresford et al. (2007). In SR-PSU, site data for the element analogue, Sm, was used.
4. In SR-PSU site data was used. This is compared against data from IAEA (2004), specifically the ocean margin value. This is consistent with the approach adopted in Beresford et al. (2007), which is the literature data considered in Table 5-20 of the Kd and CR Report.
5. In both assessments, site data was used.
6. SR-Site distribution based on a prior from the population. In SR-PSU, site data was used.
7. SR-Site distribution from IAEA (2010). In SR-PSU, site data was used.
8. SR-Site distribution from Sheppard et al. (2009). In SR-PSU, site data for the element analogue, Sm, was used.
9. SR-Site distribution from Karlsson and Bergström (2002). In SR-PSU, site data for the element analogue, Ni, was used.
10. SR-Site distribution from Beresford et al. (2007). In SR-PSU, site data for the element analogue, Bi, was used.
11. SR-Site distribution from Sheppard et al. (2009). In SR-PSU, site data for the element analogue, U, was used.
12. SR-Site distribution from IAEA (2010). In SR-PSU, site data for the element analogue, Ba, was used.
13. SR-Site distribution based on a prior from the subpopulation. In SR-PSU, site data was used.
14. SR-Site distribution from Beresford et al. (2007). In SR-PSU, site data for the element analogue, Re, was used.

B.2   Terrestrial CR Comparisons

Terrestrial primary producer CR data used in SR-PSU (Table 6-8 of the Kd and CR Report) is compared with the same parameter from SR-Site (Table 4-2 of Nordén et al., 2010) or IAEA (2010) in Table B12.

Table B12: Comparison of BE, GM and GSD CR values for terrestrial primary producers (cR_Ter_pp); the ratio reflects SR-PSU:SR-Site.

Element	Ratio of BE values	Ratio of GM values	Ratio of GSD values	Notes
Ac	2.0E0	3.2E0	1.4E0	1
Ag	3.8E-2	4.3E-2	2.3E0	2
Am	6.9E-1	1.1E0	1.4E0	3
Ba	1.8E-1	2.0E-1	Not in SR-Site	4
Ca	4.7E-1	7.5E-1	1.2E0	5
Cd	7.6E-1	7.7E-1	8.8E-1	5
Cl	1.1E+1	8.3E0	1.1E0	6
Cm	1.0E0	1.6E0	2.3E0	3
Co	3.0E-1	4.2E-1	Not in SR-Site	7
Cs	1.8E0	1.6E0	1.7E0	5
Eu	1.8E0	1.8E0	1.5E0	5
Ho	2.2E0	2.2E0	1.6E0	5
I	2.9E-1	1.9E-1	1.2E0	5
Mo	1.6E0	1.4E0	1.3E0	5
Nb	2.0E0	2.0E0	1.2E0	8
Ni	6.7E-1	7.8E-1	1.1E0	5
Np	1.7E-2	2.7E-2	2.1E0	3
Pa	3.0E-1	4.8E-1	1.8E0	1
Pb	1.6E0	1.6E0	1.3E0	5
Pd	2.7E-1	3.2E-1	9.4E-1	9
Po	2.7E-2	2.7E-2	1.7E0	10
Pu	9.1E-1	1.1E0	1.9E0	11
Ra	4.3E-1	4.3E-1	8.7E-1	5
Se	1.3E-3	4.7E-3	2.9E0	2
Sm	1.1E0	1.3E0	8.7E-1	8
Sn	2.8E0	2.4E0	1.9E0	8
Sr	1.7E0	5.2E-1	1.2E0	6
Tc	4.3E-4	4.3E-4	2.3E0	12
Th	6.3E-2	6.3E-2	1.3E0	13
U	5.9E-1	7.1E-1	1.4E0	5
Zr	8.0E0	4.8E+1	1.0E0	6

Notes:

1.   SR-Site distribution from Karlsson and Bergström (2002). In SR-PSU, site data for the element analogue, La, was used.

2. SR-Site distribution from Karlsson and Bergström (2002). In SR-PSU, the value of cR_agri_cereal was used.
3. SR-Site distribution from IAEA (2010). In SR-PSU, site data for the element analogue, La, was used.
4. In SR-PSU site data was used. This is compared against data from IAEA (2010), specifically grass for "All soils".
5. SR-Site distribution based on a prior from the population. In SR-PSU, site data was used.
6. SR-Site distribution based on a prior from the subpopulation. In SR-PSU, site data was used.
7. In SR-PSU site data was used. This is compared against data from IAEA (2010), specifically pasture for "All soils".
8. In both assessments, site data was used.
9. SR-Site distribution from Karlsson and Bergström (2002). In SR-PSU, site data for the element analogue, Ni, was used.
10. SR-Site distribution from IAEA (2010). In SR-PSU, site data for the element analogue, Bi, was used.
11. SR-Site distribution from IAEA (2010). In SR-PSU, site data for the element analogue, U, was used.
12. SR-Site distribution from IAEA (2010). In SR-PSU, site data for the element analogue, Re, was used.
13. SR-Site distribution from IAEA (2010). In SR-PSU, site data was used.

Cereal CR data used in SR-PSU (Table 6-19 of the Kd and CR Report) is compared with the same parameter from SR-Site (Table 4-3 of Nordén et al., 2010) or IAEA (2010) in Table B13.

Table B13: Comparison of BE, GM and GSD CR values for cereal (cR_agri_cereal); ratio reflects Sr-PSU:SR-Site.

Element	Ratio of BE values	Ratio of GM values	Ratio of GSD values	Notes
Ac	5.3E0	2.0E+1	2.0E0	1
Ag	4.2E-2	4.7E-2	1.0E0	2
Am	1.1E+2	1.1E+2	5.9E-1	3
Ba	7.2E0	7.2E0	Not in SR-Site	4
Ca	9.2E-1	9.2E-1	1.3E0	5
Cd	1.2E-1	1.2E-1	1.5E0	5
Cl	9.1E-2	9.1E-2	1.9E0	6
Cm	1.0E+2	1.0E+2	2.0E0	3
Co	5.7E-1	5.7E-1	Not in SR-Site	7
Cs	3.6E-1	3.6E-1	1.9E0	5
Eu	1.1E+1	1.1E+1	2.2E0	2
Ho	1.5E+1	1.5E+1	1.7E0	2
I	1.0E-1	1.0E-1	1.1E0	8
Mo	6.7E-1	6.7E-1	2.3E-1	5
Nb	3.2E-1	6.1E-1	3.3E0	6
Ni	2.7E-1	2.7E-1	1.1E0	5
Np	8.2E-1	8.2E-1	1.3E0	9
Pa	6.9E-1	6.9E-1	2.0E0	1
Pb	2.6E-1	2.6E-1	8.3E-1	5
Pd	2.1E-1	2.1E-1	9.7E-1	10
Po	1.2E+1	1.2E+1	3.0E0	5
Pu	1.9E+2	1.9E+2	1.6E0	5
Ra	1.0E0	1.0E0	1.0E0	5
Se	1.1E-3	4.3E-3	1.7E0	2
Sm	1.5E+1	1.5E+1	2.0E0	2
Sn	3.7E-2	1.4E-1	9.4E-1	2
Sr	1.1E0	1.1E0	1.1E0	5
Tc	2.2E-2	2.2E-2	1.4E0	11
Th	1.7E0	1.7E0	1.9E0	5
U	2.8E-1	2.8E-1	1.4E0	5
Zr	3.4E+1	3.4E+1	2.6E-1	5

Notes:
1. SR-Site distribution from Karlsson and Bergström (2002). In SR-PSU, site data for the element analogue, La, was used.
2. SR-Site distribution from Karlsson and Bergström (2002). In SR-PSU, site data was used.

3. SR-Site distribution from IAEA (2010). In SR-PSU, site data for the element analogue, La, was used.
4. In SR-PSU site data was used. This is compared against data from IAEA (2010), using Ra as analogue as only one value of Ba reported. All soils considered.
5. SR-Site distribution from IAEA (2010). In SR-PSU, site data was used.
6. SR-Site distribution based on a prior from the population. In SR-PSU, site data was used.
7. In SR-PSU site data was used. This is compared against data from IAEA (2010), using data for "All Soils".
8. SR-Site distribution from Robens et al. (1988). In SR-PSU, site data was used.
9. SR-Site distribution based on a prior from the population. In SR-PSU, site data for the element analogue, La, was used.
10. SR-Site distribution from Karlsson and Bergström (2002). In SR-PSU, site data for the element analogue, Ni, was used.
11. SR-Site distribution from IAEA (2010). In SR-PSU, site data for the element analogue, Zr, was used.

Vegetable CR data used in SR-PSU (Table 6-21 of the Kd and CR Report) is
compared with the same parameter from SR-Site (Table 4-5 of Nordén et al., 2010)
or IAEA (2010) in Table B14.

Table B14: Comparison of BE, GM and GSD CR values for vegetables
(cR_agri_veg); ratio reflects SR-PSU:SR-Site.

Element	Ratio of BE values	Ratio of GM values	Ratio of GSD values	Notes
Ac	1.2E-1	1.2E-1	8.7E-1	1
Ag	9.1E-1	9.1E-1	1.2E0	2
Am	9.0E-1	9.0E-1	1.2E0	2
Ba	1.0E0	1.0E0	Not in SR-Site	3
Ca	9.1E-1	9.1E-1	1.0E0	4
Cd	3.8E-1	3.8E-1	1.3E0	5
Cl	9.0E-1	9.0E-1	2.4E0	2
Cm	9.0E-1	9.0E-1	1.0E0	2
Co	1.0E0	1.0E0	Not in SR-Site	6
Cs	8.9E-1	8.9E-1	1.0E0	2
Eu	1.5E-1	1.5E-1	1.3E0	1
Ho	1.5E-1	1.5E-1	1.3E0	1
I	2.8E-2	2.8E-2	1.1E0	7
Mo	1.0E0	1.0E0	5.8E0	2
Nb	1.1E0	1.1E0	5.4E0	2
Ni	1.8E-1	2.1E-1	2.2E0	8
Np	9.0E-1	9.0E-1	1.3E0	2
Pa	1.5E0	1.5E0	1.3E0	1
Pb	8.8E-1	8.8E-1	1.0E0	2
Pd	1.8E-1	2.1E-1	2.2E0	9
Po	9.1E-1	9.1E-1	1.0E0	2
Pu	9.2E-1	9.2E-1	1.5E0	2
Ra	8.9E-1	8.9E-1	1.0E0	2
Se	8.4E-4	3.1E-3	2.9E0	10
Sm	1.5E-1	1.5E-1	1.3E0	1
Sn	1.9E-3	9.7E-4	1.9E0	11
Sr	9.1E-1	9.1E-1	1.0E0	2
Tc	1.2E-4	1.2E-4	5.0E-1	12
Th	9.1E-1	9.1E-1	1.0E0	2
U	9.0E-1	9.0E-1	5.2E-1	2
Zr	9.2E-1	9.2E-1	5.0E-1	2

Notes:
1. SR-Site distribution from Karlsson and Bergström (2002). In SR-PSU, site
   data for the element analogue, La, was used.
2. SR-Site distribution from IAEA (2010). In SR-PSU, site data was used.

3. In SR-PSU, data for the element analogue, Ra, for leafy vegetables from IAEA (2010) was used ("All soils"). This is the considered a sensible approach given IAEA (2010) reports only a single value for Ba.

4. SR-Site distribution from IAEA (2010). In SR-PSU, site data for the element analogue, Sr, was used.

5. SR-Site distribution from Karlsson and Bergström (2002). In SR-PSU, site data for the element analogue, Zn, was used.

6. In SR-PSU, data for leafy vegetables from IAEA (2010) was used, for "All soils". In the absence of site data, this is considered a sensible approach.

7. SR-Site distribution from Robens et al. (1988). In SR-PSU, site data was used.

8. SR-Site distribution from Karlsson and Bergström (2002). In SR-PSU, the value of cR_Ter_pp was used.

9. SR-Site distribution from Karlsson and Bergström (2002). In SR-PSU, site data for the element analogue, Ni, was used.

10. SR-Site distribution from Karlsson and Bergström (2002). In SR-PSU, the value of cR_agri_cereal was used.

11. SR-Site distribution from Karlsson and Bergström (2002). In SR-PSU, site data for the element analogue, Th, was used.

12. SR-Site distribution from IAEA (2010). In SR-PSU, site data for the element analogue, Re, was used.

Tuber CR data used in SR-PSU (Table 6-23 of the Kd and CR Report) is compared with the same parameter from SR-Site (Table 4-4 of Nordén et al., 2010) or IAEA (2010) in Table B15.

Table B15: Comparison of BE, GM and GSD CR values for tubers (cR_agri_tuber); ratio reflects SR-PSU:SR-Site.

Element	Ratio of BE values	Ratio of GM values	Ratio of GSD values	Notes
Ac	1.9E0	2.2E-1	8.2E-1	1
Ag	1.9E-3	2.6E-3	1.5E0	2
Am	1.2E0	1.2E0	1.0E0	3
Ba	1.5E+1	1.5E+1	Not in SR-Site	4
Ca	1.2E0	1.2E0	1.3E0	5
Cd	2.4E-1	2.4E-1	2.9E-1	6
Cl	5.9E-1	5.6E-1	1.0E0	2
Cm	1.2E0	1.2E0	1.1E0	3
Co	9.9E-1	9.9E-1	Not in SR-Site	7
Cs	1.3E0	1.3E0	1.3E0	3
Eu	1.6E0	1.6E0	1.3E0	1
Ho	1.1E0	1.1E0	1.3E0	1
I	1.1E-1	1.1E-1	2.1E-1	3
Mo	4.7E-1	4.7E-1	2.2E0	2
Nb	1.2E0	1.2E0	5.0E-1	3
Ni	3.1E-1	3.6E-1	2.2E0	8
Np	1.2E0	1.2E0	1.6E0	3
Pa	1.6E-1	1.6E-1	1.3E0	1
Pb	1.2E0	1.2E0	1.0E0	3
Pd	3.1E-1	3.6E-1	2.2E0	9
Po	1.2E0	1.2E0	1.0E0	3
Pu	1.2E0	1.2E0	1.0E0	3
Ra	1.4E0	1.4E0	1.0E0	3
Se	1.4E-3	5.1E-3	2.9E0	10
Sm	2.4E0	2.4E0	1.3E0	1
Sn	8.4E-4	5.1E-4	3.1E0	11
Sr	1.2E0	1.2E0	1.3E0	3
Tc	1.2E0	1.2E0	1.1E0	3
Th	1.2E0	1.2E0	1.0E0	3
U	1.2E0	1.2E0	1.0E0	3
Zr	5.9E0	6.8E0	5.0E-1	12

Notes:
1. SR-Site distribution from Karlsson and Bergström (2002). In SR-PSU, site data for the element analogue, La, was used.
2. SR-Site distribution from Karlsson and Bergström (2002). In SR-PSU, site data was used.

3. SR-Site distribution from IAEA (2010). In SR-PSU, site data was used.
4. In SR-PSU data for the element analogue, Sr, from IAEA (2010) was used. This is compared against data from IAEA (2010), using Ra as analogue as only one value of Ba reported. All soils considered.
5. SR-Site distribution from IAEA (2010). In SR-PSU, site data for the element analogue, Sr, was used.
6. SR-Site distribution from IAEA (2010). In SR-PSU, site data for the element analogue, Zn, was used.
7. In SR-PSU data from IAEA (2010) was used. This is compared against data from IAEA (2010), using data for "All Soils".
8. SR-Site distribution from Karlsson and Bergström (2002). In SR-PSU, the value of cR_Ter_pp was used.
9. SR-Site distribution from Karlsson and Bergström (2002). In SR-PSU, site data for the element analogue, Ni, was used.
10. SR-Site distribution from Karlsson and Bergström (2002). In SR-PSU, the value of cR_agri_cereal was used.
11. SR-Site distribution from Karlsson and Bergström (2002). In SR-PSU, site data for the element analogue, Th, was used.
12. SR-Site distribution from IAEA (2010). In SR-PSU, the value of cR_Ter_pp was used.

Mushroom CR data used in SR-PSU (Table 6-25 of the Kd and CR Report) is compared with the same parameter from SR-Site (Table 4-6 of Nordén et al., 2010) or IAEA (2010) in Table B16.

Table B16: Comparison of BE, GM and GSD CR values for mushrooms (cR_Ter_mush); ratios reflect SR-PSU:SR-Site.

Element	Ratio of BE values	Ratio of GM values	Ratio of GSD values	Notes
Ac	2.0E0	3.2E0	1.8E0	1
Ag	5.3E0	5.9E0	9.7E-1	2
Am	6.9E-1	1.1E0	1.7E0	3
Ba	5.3E0	5.3E0	Not in SR-Site	4
Ca	8.5E-1	8.5E-1	1.0E0	5
Cd	1.4E+1	1.4E+1	1.0E0	6
Cl	1.0E+1	8.3E0	1.8E0	7
Cm	1.0E0	1.6E0	2.9E0	8
Co	1.1E0	1.1E0	Not in SR-Site	9
Cs	1.1E0	1.1E0	7.2E-1	10
Eu	1.8E0	1.8E0	2.6E0	7
Ho	2.2E0	2.2E0	2.8E0	7
I	9.7E-1	9.7E-1	1.3E0	5
Mo	5.3E-1	5.3E-1	1.3E0	11
Nb	2.0E0	2.0E0	2.0E0	7
Ni	1.0E0	1.0E0	1.3E0	5
Np	1.3E-2	2.1E-2	2.6E0	3
Pa	3.0E-1	4.8E-1	2.2E0	1
Pb	1.2E0	1.2E0	1.3E0	5
Pd	7.5E-1	7.5E-1	9.4E-1	12
Po	2.7E-2	2.7E-2	1.7E0	13
Pu	2.0E0	2.0E0	3.3E0	14
Ra	1.2E-2	1.2E-2	7.0E-1	15
Se	1.3E-3	4.7E-3	2.9E0	16
Sm	1.1E0	1.3E0	1.6E0	7
Sn	2.0E-1	2.0E-1	1.9E0	17
Sr	7.6E-1	7.6E-1	9.4E-1	5
Tc	2.9E-2	2.9E-2	2.3E0	18
Th	1.2E0	1.2E0	1.3E0	5
U	6.9E-1	6.9E-1	1.1E0	5
Zr	9.6E0	4.8E+1	2.1E0	7

Notes:
1. SR-Site distribution for pasture from Karlsson and Bergström (2002). In SR-PSU, site data for the element analogue, La, was used.
2. SR-Site distribution for pasture from Karlsson and Bergström (2002). In SR-PSU, site data for the element analogue, Cu, was used.

3. SR-Site distribution from Avila (2006). In SR-PSU, site data for the element analogue, La, was used.
4. In SR-PSU, site data for the element analogue, Sr, was used. This is compared against data from IAEA (2010), using Sr as an element analogue.
5. In both assessments, site data was used.
6. In SR-Site, site data based on green vegetation was used for the distribution. In SR-PSU, site data was used.
7. In SR-Site, site data based on green vegetation was used for the distribution. In SR-PSU, the value of cR_Ter_pp was used.
8. SR-Site distribution for pasture from IAEA (2010). In SR-PSU, site data for the element analogue, La, was used.
9. In SR-PSU, site data was used. Consistent with SKB's approach, this was compared against the distribution for cR_Ter_pp(Co).
10. SR-Site distribution based on a prior from the population. In SR-PSU, site data was used.
11. In SR-Site, site data based on green vegetation was used for the distribution. In SR-PSU, site data for the element analogue, Cr, was used.
12. SR-Site distribution for pasture from Karlsson and Bergström (2002). In SR-PSU, site data for the element analogue, Ni, was used.
13. SR-Site distribution for pasture from IAEA (2010). In SR-PSU, site data for the element analogue, Bi, was used.
14. SR-Site distribution from Avila (2006). In SR-PSU, site data for the element analogue, U, was used.
15. SR-Site distribution from Avila (2006). In SR-PSU, site data for the element analogue, Sr, was used.
16. SR-Site distribution for pasture from Karlsson and Bergström (2002). In SR-PSU, the value of cR_agri_cereal was used.
17. In SR-Site, site data based on green vegetation was used for the distribution. In SR-PSU, site data for the element analogue, Th, was used.
18. SR-Site distribution from Avila (2006). In SR-PSU, site data for the element analogue, Re, was used.

The transfer coefficient data for meat used in SR-PSU (Table 6-15 of the Kd and CR Report) is compared with the same parameter from SR-Site (Table 4-8 of Nordén et al., 2010) or IAEA (2010) in Table B17.

Table B17: Comparison of BE, GM and GSD transfer coefficients to meat (TC_meat); ratios reflect SR-PSU:SR-Site.

Element	Ratio of BE values	Ratio of GM values	Ratio of GSD values	Notes
Ac	6.5E0	6.5E0	2.2E0	1
Ag	5.3E+1	4.6E+1	3.1E0	2
Am	1.0E0	1.0E0	8.9E-1	3
Ba	1.0E0	1.0E0	Not in SR-Site	4
Ca	1.0E0	1.0E0	5.9E0	3
Cd	1.5E+1	1.5E+1	2.4E0	5
Cl	1.0E0	1.0E0	8.9E-1	3
Cm	6.5E0	6.5E0	2.2E0	1
Co	1.0E0	1.0E0	Not in SR-Site	4
Cs	1.0E0	1.0E0	1.8E0	3
Eu	2.2E-2	2.2E-2	2.2E0	1
Ho	2.6E-2	2.6E-2	2.2E0	1
I	1.0E0	1.0E0	1.9E0	3
Mo	1.0E0	1.0E0	2.2E0	5
Nb	1.0E0	1.0E0	8.9E-1	3
Ni	3.2E+1	3.2E+1	1.3E0	2
Np	1.3E-1	1.0E0	2.2E0	1
Pa	1.3E+1	1.3E-1	2.2E0	1
Pb	1.0E0	1.3E+1	2.4E0	3
Pd	1.6E+2	1.0E0	1.3E0	2
Po	1.4E-1	1.6E+2	2.4E0	6
Pu	1.0E0	4.1E-1	3.1E0	3
Ra	1.0E0	1.0E0	8.9E-1	3
Se	4.7E-1	1.0E0	1.8E0	7
Sm	2.6E-2	5.0E0	2.2E0	1
Sn	1.2E-4	2.6E-2	2.2E0	8
Sr	1.0E0	1.2E-4	1.5E0	3
Tc	1.2E-2	1.0E0	2.2E0	8
Th	1.0E0	1.2E-2	1.8E0	3
U	1.0E0	1.0E0	5.4E0	3
Zr	1.0E0	1.0E0	8.9E-1	3

Notes:
1. SR-Site distribution from Karlsson and Bergström (2002). In SR-PSU, IAEA (2010) data for the element analogue, La, was used.
2. SR-Site distribution from Karlsson and Bergström (2002). In SR-PSU, IAEA (2010) data for the element analogue, Zn, was used.

3. IAEA (2010) used in both assessments.
4. IAEA (2010) used in SR-PSU. This is considered a sensible approach.
5. SR-Site distribution from Karlsson and Bergström (2002). In SR-PSU, IAEA (2010) data was used.
6. SR-Site distribution from Karlsson and Bergström (2002). In SR-PSU, IAEA (2010) data for the element analogue, Pb, was used.
7. SR-Site distribution from Karlsson and Bergström (2002). In SR-PSU, IAEA (2010) data for the element analogue, Te, was used.
8. SR-Site distribution from Karlsson and Bergström (2002). In SR-PSU, IAEA (2010) data for the element analogue, Te, was used.

The transfer coefficient data for milk used in SR-PSU (Table 6-17 of the Kd and CR Report) is compared with the same parameter from SR-Site (Table 4-7 of Nordén et al., 2010) or IAEA (2010) in Table B18.

Table B18: Comparison of BE, GM and GSD for the transfer coefficient to milk (TC_milk); ratios reflect SR-PSU:SR-Site.

Element	Ratio of BE values	Ratio of GM values	Ratio of GSD values	Notes
Ac	2.1E-1	2.1E-1	2.2E0	1
Ag	5.4E+1	5.4E+1	1.3E0	2
Am	1.0E0	1.0E0	1.2E0	3
Ba	1.0E0	1.0E0	Not in SR-Site	4
Ca	1.0E0	1.0E0	2.5E0	3
Cd	1.9E0	1.9E0	4.7E0	5
Cl	3.2E-1	4.9E-1	3.6E0	6
Cm	2.1E-2	2.1E-2	2.2E0	1
Co	1.0E0	1.0E0	Not in SR-Site	4
Cs	1.0E0	1.0E0	1.2E0	3
Eu	2.1E-2	2.1E-2	2.2E0	1
Ho	1.7E-1	1.4E-1	2.2E0	1
I	1.0E0	1.0E0	1.4E0	3
Mo	5.5E-1	5.5E-1	1.3E0	4
Nb	1.0E0	1.0E0	1.2E0	3
Ni	1.0E0	1.0E0	1.2E0	3
Np	8.4E-2	8.4E-2	2.2E0	1
Pa	8.4E-3	4.2E-2	2.2E0	1
Pb	1.0E0	1.0E0	1.1E0	3
Pd	9.5E-1	9.5E-1	2.2E0	7
Po	1.0E0	1.0E0	2.9E0	3
Pu	1.0E0	1.0E0	1.2E0	3
Ra	1.0E0	1.0E0	2.0E0	3
Se	1.0E0	1.0E0	2.2E0	3
Sm	2.1E-2	2.1E-2	2.2E0	1
Sn	3.6E-3	3.6E-3	1.3E0	8
Sr	1.0E0	1.0E0	2.1E0	3
Tc	1.8E-1	3.6E-2	1.3E0	1
Th	7.2E-1	1.2E0	7.4E-1	1
U	1.0E0	1.0E0	3.7E0	3
Zr	1.0E0	1.0E0	1.8E0	3

Notes:
1. SR-Site distribution from Karlsson and Bergström (2002). In SR-PSU, IAEA (2010) data for the element analogue, Am, was used.
2. SR-Site distribution from Karlsson and Bergström (2002). In SR-PSU, IAEA (2010) data for the element analogue, Zn, was used.

3. IAEA (2010) used in both assessments.
4. IAEA (2010) used in SR-PSU. This is considered a sensible approach.
5. SR-Site distribution from Karlsson and Bergström (2002). In SR-PSU, IAEA (2010) was used.
6. SR-Site distribution from Karlsson and Bergström (2002). In SR-PSU, IAEA (2010) data for the element analogue, I, was used.
7. SR-Site distribution from IAEA (2010). In SR-PSU, IAEA (2010) data for the element analogue, Ni, was used.
8. SR-Site distribution from Karlsson and Bergström (2002). In SR-PSU, IAEA (2010) data for the element analogue, Zr, was used.

Herbivore feed CR data used in SR-PSU (Table 6-13 of the Kd and CR Report) is compared with the same parameter from SR-Site (Table 4-10 of Nordén et al., 2010) or IAEA (2010) in Table B19.

Table B19: Comparison of BE, GM and GSD CR values for herbivore feed (cR_food_herbiv); ratio reflects SR-PSU:SR-Site.

Element	Ratio of BE values	Ratio of GM values	Ratio of GSD values	Notes
Ac	8.3E0	Not in SR-Site	Not in SR-Site	1
Ag	8.1E-5	Not in SR-Site	Not in SR-Site	2
Am	5.0E+1	2.1E+1	6.4E0	1
Ba	5.9E-1	5.4E-1	Not in SR-Site	3
Ca	3.1E0	1.9E0	1.5E0	4
Cd	7.9E0	4.7E0	1.7E0	4
Cl	4.2E0	4.6E0	2.0E0	5
Cm	1.3E+1	6.7E0	6.4E0	1
Co	2.1E+1	9.0E0	Not in SR-Site	6
Cs	7.8E0	1.0E+1	1.5E0	4
Eu	1.0E0	1.0E0	1.5E0	5
Ho	1.1E0	1.1E0	1.5E0	5
I	4.0E0	5.9E0	6.2E0	2
Mo	1.4E0	1.5E0	1.8E0	5
Nb	1.9E0	1.3E0	1.2E0	5
Ni	2.2E+1	4.8E0	1.7E0	4
Np	8.1E0	3.7E0	6.4E0	1
Pa	1.3E+1	6.7E0	6.4E0	1
Pb	8.9E+1	2.0E+1	7.3E-1	4
Pd	5.8E0	Not in SR-Site	Not in SR-Site	7
Po	2.9E-3	Not in SR-Site	Not in SR-Site	2
Pu	8.3E-3	1.1E-2	5.3E0	2
Ra	3.8E-1	2.0E-1	5.7E0	2
Se	3.0E-1	3.1E-1	3.3E0	2
Sm	8.5E0	2.0E0	8.2E-1	5
Sn	1.4E0	2.1E0	6.4E-1	5
Sr	4.4E0	2.4E0	1.4E0	4
Tc	1.0E+1	1.6E+1	2.1E0	8
Th	4.4E0	4.4E0	3.0E0	4
U	1.5E0	1.6E0	1.9E0	4
Zr	1.4E0	1.1E0	9.5E-1	5

Notes:

1. SR-Site distribution estimated from model given in Section 2.4 of Nordén et al. (2010). In SR-PSU, site data for the element analogue, La, was used.
2. SR-Site distribution estimated from model given in Section 2.4 of Nordén et al. (2010). In SR-PSU, site data was used.
3. Site data used in SR-PSU. This is compared against data from IAEA (2010), using Sr as an element analogue in generic meat.
4. Site-specific data was used in both assessments.
5. Site-specific data was used in both assessments, although the SR-Site value is based on vegetation only.
6. Site data used in SR-PSU. This is compared against data from IAEA (2010), for generic meat.
7. SR-Site distribution estimated from model given in Section 2.4 of Nordén et al. (2010). In SR-PSU, site data for the element analogue, Ni, was used.
8. SR-Site distribution estimated from model given in Section 2.4 of Nordén et al. (2010). In SR-PSU, site data for the element analogue, Zr, was used.

B.3 Aquatic CR Comparisons

CR data used for lake plankton in SR-PSU (Table 7-6 of the Kd and CR Report) is compared with the same parameter from SR-Site (Table 5-2 of Nordén et al., 2010) or IAEA (2013) in Table B20.

Table B20: Comparison of BE, GM and GSD for CR to lake plankton (cR_lake_pp_plank); ratios reflect SR-PSU:SR-Site.

Element	Ratio of BE values	Ratio of GM values	Ratio of GSD values	Notes
Ac	8.0E-1	1.1E0	2.2E0	1
Ag	9.7E+1	9.7E+1	6.4E0	2
Am	5.3E-2	1.6E-1	8.4E-1	3
Ba	1.0E0	1.1E0	Not in SR-Site	4
Ca	1.2E0	1.1E0	1.9E0	5
Cd	8.5E-1	4.3E-1	1.1E0	5
Cl	7.3E-2	2.2E-1	9.9E-1	5
Cm	1.1E-1	Not in SR-Site	Not in SR-Site	3
Co	4.3E0	5.7E0	Not in SR-Site	6
Cs	9.2E-1	9.2E-1	1.3E0	5
Eu	3.2E0	9.5E-1	1.3E0	5
Ho	3.3E0	9.3E-1	1.5E0	5
I	2.2E0	1.4E0	2.1E0	5
Mo	6.1E-1	7.3E-1	2.1E0	5
Nb	1.7E0	5.2E-1	2.1E0	5
Ni	1.6E0	1.0E0	2.3E0	5
Np	5.3E-2	8.6E-2	6.4E0	3
Pa	6.3E+2	1.8E+2	2.2E0	1
Pb	2.8E0	8.7E-1	1.3E0	5
Pd	3.4E-1	2.6E-1	2.6E0	7
Po	4.6E-1	4.6E-1	3.3E0	8
Pu	4.6E-1	4.6E-1	2.0E0	8
Ra	7.3E-1	6.2E-1	1.4E0	9
Se	1.2E0	9.1E-1	4.7E0	5
Sm	1.8E0	5.5E-1	1.1E0	5
Sn	4.3E0	2.0E0	2.2E0	10
Sr	1.1E0	7.1E-1	1.8E0	5
Tc	4.8E-1	6.9E-1	1.4E0	11
Th	1.2E0	5.2E-1	1.4E0	5
U	9.6E-1	7.4E-1	2.3E0	5
Zr	9.1E-1	4.3E-1	1.8E0	5

Notes:
1. SR-Site distribution for marine water plants from Karlsson and Bergström (2002). In SR-PSU, site data for the element analogue, La, was used.

2.   In SR-Site, site-specific data for marcophytes used. In SR-PSU, data from ERICA used (Hosseini et al., 2008).
3.   SR-Site distribution from Beresford et al. (2007). In SR-PSU, site data for the element analogue, La, was used.
4.   In SR-PSU, the value for cR_lake_pp_macro was used. This is compared against data from IAEA (2013), specifically for vascular plants.
5.   In SR-Site, site-specific data for marcophytes used. In SR-PSU, the value for cR_lake_pp_macro was used.
6.   In SR-PSU, the value for cR_lake_pp_macro was used. This is compared against data from IAEA (2013), specifically for phytoplankton.
7.   SR-Site distribution for marine water plants from Karlsson and Bergström (2002). In SR-PSU, site data for the element analogue, Ni, was used.
8.   SR-Site distribution from Beresford et al. (2007). In SR-PSU, data from ERICA used (Hosseini et al., 2008).
9.   In SR-Site, site-specific data for marcophytes used. In SR-PSU, site data for the element analogue, Ba, was used.
10. SR-Site distribution for marine water plants from Karlsson and Bergström (2002). In SR-PSU, site data for the element analogue, Zr, was used.
11. SR-Site distribution from Beresford et al. (2007). In SR-PSU, data from ERICA used (Hosseini et al., 2008).

CR data used for lake microalgae in SR-PSU (Table 7-3 of the Kd and CR Report) is compared with the same parameter from SR-Site (Table 5-3 of Nordén et al., 2010) or IAEA (2013) in Table B21.

Table B21: Comparison of BE, GM and GSD for CR to lake microalgae (cR_lake_pp_micro); ratio reflects SR-PSU:SR-Site.

Element	Ratio of BE values	Ratio of GM values	Ratio of GSD values	Notes
Ac	8.0E-1	1.1E0	2.2E0	1
Ag	2.6E0	2.6E0	6.4E0	2
Am	5.3E-2	1.6E-1	8.3E-1	3
Ba	1.0E0	1.1E0	Not in SR-Site	4
Ca	3.8E0	3.5E0	1.1E0	5
Cd	4.0E-1	2.0E-1	6.1E-1	5
Cl	3.2E0	9.3E0	9.9E-1	5
Cm	1.1E-1	3.2E-2	Not in SR-Site	3
Co	4.3E0	5.7E0	Not in SR-Site	6
Cs	3.1E-1	3.1E-1	7.5E-1	5
Eu	1.1E-1	3.3E-2	1.1E0	5
Ho	4.7E-2	1.3E-2	1.5E0	5
I	2.1E0	1.4E0	1.2E0	5
Mo	3.6E-2	4.2E-2	1.8E0	5
Nb	4.2E-2	1.3E-2	2.1E0	5
Ni	3.0E-1	1.0E0	1.3E0	5
Np	5.3E-2	8.6E-2	6.3E0	3
Pa	6.6E+2	1.9E+2	2.2E0	1
Pb	1.4E-1	8.7E-1	9.4E-1	5
Pd	3.4E-1	2.6E-1	1.5E0	7
Po	3.2E-2	3.2E-2	3.3E0	8
Pu	5.0E0	5.0E0	7.0E0	9
Ra	7.3E-1	6.2E-1	8.2E-1	10
Se	1.2E0	9.1E-1	2.7E0	5
Sm	4.3E-2	1.3E-2	1.1E0	5
Sn	4.3E0	2.0E0	1.4E0	11
Sr	6.4E0	3.9E0	1.1E0	5
Tc	6.1E-1	8.8E-1	1.4E0	9
Th	1.9E-2	8.4E-3	1.3E0	5
U	2.6E-2	2.0E-2	1.6E0	5
Zr	4.5E-2	2.1E-2	1.2E0	5

Notes:
1. SR-Site distribution for marine water plants from Karlsson and Bergström (2002). In SR-PSU, site data for macrophytes for the element analogue, La, was used.

2. In SR-Site, site-specific data for macrophytes used. In SR-PSU, data from ERICA used (Hosseini et al., 2008).
3. SR-Site distribution for phytoplankton from Beresford et al. (2007). In SR-PSU, site data for macrophytes for the element analogue, La, was used.
4. In SR-PSU, the value for cR_lake_pp_macro was used. This is compared against data from IAEA (2013), specifically for vascular plants.
5. In both assessments, site-specific data used. In SR-Site this was the singular microbenthos observation, with the GSD derived from the cR_lake_pp_macro for the same element. In SR-PSU, the site data from macrophytes were used to define the distribution.
6. In SR-PSU, the value for cR_lake_pp_macro was used. This is compared against data from IAEA (2013), specifically for phytoplankton.
7. SR-Site distribution for marine water plants from Karlsson and Bergström (2002). In SR-PSU, site data for the element analogue, Ni, was used.
8. SR-Site distribution from for phytoplankton Beresford et al. (2007). In SR-PSU, data from ERICA used (Hosseini et al., 2008).
9. SR-Site distribution from for phytoplankton Beresford et al. (2007). In SR-PSU, data from IAEA (2010) used.
10. In SR-Site, site-specific data for macrophytes used. In SR-PSU, site data for the element analogue, Ba, was used.
11. SR-Site distribution for marine water plants from Karlsson and Bergström (2002). In SR-PSU, site data for the element analogue, Zr, was used.

CR data used for lake macroalgae in SR-PSU (Table 7-3 of the Kd and CR Report) is compared with the same parameter from SR-Site (Table 5-4 of Nordén et al., 2010) or IAEA (2013) in Table B22.

Table B22: Comparison of BE, GM and GSD for CR to lake macroalgae (cR_lake_pp_macro); ratio reflects SR-PSU:SR-Site.

Element	Ratio of BE values	Ratio of GM values	Ratio of GSD values	Notes
Ac	8.0E-1	1.1E0	2.2E0	1
Ag	2.6E0	2.6E0	6.4E0	2
Am	1.2E0	3.5E-1	8.3E-1	3
Ba	1.0E0	1.1E0	Not in SR-Site	4
Ca	1.2E0	1.1E0	1.1E0	5
Cd	8.5E-1	4.3E-1	6.1E-1	6
Cl	7.3E-2	2.2E-1	9.9E-1	6
Cm	3.9E+1	1.1E+1	2.7E0	7
Co	4.3E0	5.7E0	Not in SR-Site	8
Cs	9.2E-1	9.2E-1	7.5E-1	9
Eu	3.2E0	9.5E-1	1.1E0	5
Ho	3.3E0	9.3E-1	1.5E0	5
I	2.2E0	1.4E0	1.2E0	6
Mo	6.1E-1	7.3E-1	1.8E0	5
Nb	1.7E0	5.2E-1	2.1E0	5
Ni	1.6E0	1.0E0	1.3E0	6
Np	6.4E-1	1.8E-1	6.3E0	3
Pa	6.3E+2	1.8E+2	2.2E0	1
Pb	2.8E0	8.7E-1	9.4E-1	6
Pd	3.4E-1	2.6E-1	1.5E0	10
Po	7.3E-1	7.3E-1	1.5E0	11
Pu	1.8E0	1.8E0	1.0E0	12
Ra	7.3E-1	6.2E-1	8.2E-1	13
Se	1.2E0	9.1E-1	2.7E0	9
Sm	1.8E0	5.5E-1	1.1E0	5
Sn	4.3E0	2.0E0	1.4E0	14
Sr	1.1E0	7.1E-1	1.1E0	6
Tc	7.8E-3	7.8E-3	1.4E0	15
Th	1.2E0	5.2E-1	1.3E0	6
U	9.6E-1	7.4E-1	1.6E0	6
Zr	9.1E-1	4.3E-1	1.2E0	5

Notes:
1. SR-Site distribution for marine water plants from Karlsson and Bergström (2002). In SR-PSU, site data for the element analogue, La, was used.
2. In SR-Site, site-specific data was used. In SR-PSU, data from ERICA used (Hosseini et al., 2008).

3. SR-Site distribution from IAEA (2010). In SR-PSU, site data for the element analogue, La, was used.
4. In SR-PSU, site data was used. This is compared against data from IAEA (2013), specifically for vascular plants.
5. In both assessments, site-specific data was used.
6. SR-Site distribution based on a prior from the subpopulation. In SR-PSU, site data was used.
7. SR-Site distribution from Beresford et al. (2007). In SR-PSU, site data for the element analogue, La, was used.
8. In SR-PSU, site data was used. This is compared against data from IAEA (2013), specifically for phytoplankton.
9. SR-Site distribution based on a prior from the population. In SR-PSU, site data was used.
10. SR-Site distribution for marine water plants from Karlsson and Bergström (2002). In SR-PSU, site data for the element analogue, Ni, was used.
11. SR-Site distribution from Beresford et al. (2007). In SR-PSU, data from ERICA used (Hosseini et al., 2008).
12. IAEA (2010) used for both assessments.
13. SR-Site distribution based on a prior from the subpopulation. In SR-PSU, site for the element analogue, Ba, was used.
14. SR-Site distribution for marine water plants from Karlsson and Bergström (2002). In SR-PSU, site data for the element analogue, Zr, was used.
15. SR-Site distribution from Beresford et al. (2007). In SR-PSU, data from IAEA (2010) was used.

CR data used for lake crayfish in SR-PSU (Table 7-18 of the Kd and CR Report) is compared with the same parameter from SR-Site (Table 5-5 of Nordén et al., 2010) or IAEA (2010) in Table B23.

Table B23: Comparison of BE, GM and GSD CR for lake crayfish (cR_lake_cray); ratios reflect SR-PSU:SR-Site.

Element	Ratio of BE values	Ratio of GM values	Ratio of GSD values	Notes
Ac	2.1E0	3.8E0	1.6E0	1
Ag	1.6E0	1.6E0	2.2E-1	2
Am	8.3E-1	1.5E0	7.1E-1	3
Ba	4.4E+1	5.9E+1	Not in SR-Site	4
Ca	1.7E0	3.0E0	7.4E-1	2
Cd	1.7E0	1.1E0	1.9E0	5
Cl	3.8E-1	1.0E0	8.2E-1	2
Cm	2.1E-1	3.8E-1	4.5E0	3
Co	3.0E+2	2.1E+2	Not in SR-Site	4
Cs	8.5E-1	1.3E0	1.1E0	5
Eu	2.1E0	1.9E0	5.3E-1	2
Ho	5.9E-1	9.5E-1	8.6E-1	6
I	2.0E0	1.3E0	1.4E0	5
Mo	8.6E-1	1.6E0	1.3E0	5
Nb	1.4E0	1.0E0	2.2E0	2
Ni	1.4E0	1.1E0	2.1E0	5
Np	1.8E0	3.3E0	5.0E0	7
Pa	2.1E+1	3.8E+1	1.6E0	1
Pb	2.2E0	1.2E0	1.1E0	5
Pd	1.2E0	1.1E0	1.6E0	8
Po	7.0E-1	7.0E-1	4.2E0	9
Pu	6.8E-1	6.8E-1	3.3E0	9
Ra	4.0E+1	8.1E-1	2.0E0	10
Se	1.1E0	1.0E0	4.2E0	5
Sm	4.1E-1	7.9E-1	4.5E-1	2
Sn	2.5E-1	3.4E-1	4.2E0	11
Sr	1.1E0	1.5E0	1.5E0	2
Tc	3.4E-1	3.4E-1	5.1E-1	12
Th	3.8E-1	5.0E-1	9.6E-1	2
U	1.7E-1	9.4E-1	1.2E0	2
Zr	1.0E0	1.4E0	1.2E0	5

Notes:
1. SR-Site distribution from Karlsson and Bergström (2002). In SR-PSU, site data for the element analogue, La, was used.
2. SR-Site distribution based on site data for a filter feeder, using a prior from a subpopulation. In SR-PSU, the value for cR_lake_bivalve_NHB was used, which is based on site data.

3. SR-Site distribution from IAEA (2010). In SR-PSU, site data for the element analogue, La, was used.
4. In SR-PSU, site data was used. This is compared against data from IAEA (2010), specifically freshwater invertebrates.
5. SR-Site distribution based on site data for a filter feeder, using a prior from a population. In SR-PSU, the value for cR_lake_bivalve_NHB was used, which is based on site data.
6. SR-Site distribution based on site data for a filter feeder. In SR-PSU, the value for cR_lake_bivalve_NHB was used, which is based on site data.
7. SR-Site distribution from Beresford et al. (2007). In SR-PSU, site data for the element analogue, La, was used.
8. SR-Site distribution from Karlsson and Bergström (2002). In SR-PSU, site data for the element analogue, Ni, was used.
9. SR-Site distribution from Beresford et al. (2007). In SR-PSU, data from ERICA was used (Hosseini et al., 2008).
10. SR-Site distribution based on site data for a filter feeder, using a prior from a subpopulation. In SR-PSU, data from ERICA was used (Hosseini et al., 2008).
11. SR-Site distribution based on site data for a filter feeder. In SR-PSU, site data for the element analogue, Zr, was used.
12. SR-Site distribution from IAEA (2010). In SR-PSU, data from ERICA was used (Hosseini et al., 2008).

CR data used for lake fish in SR-PSU (Table 7-20 of the Kd and CR Report) is compared with the same parameter from SR-Site (Table 5-6 of Nordén et al., 2010) or IAEA (2010) in Table B24.

Table B24: Comparison of BE, GM and GSD CR for lake fish (cR_lake_fish); ratios reflect SR-PSU:SR-Site.

Element	Ratio of BE values	Ratio of GM values	Ratio of GSD values	Notes
Ac	1.2E-2	1.0E-2	1.4E0	1
Ag	7.8E-1	7.8E-1	4.1E-1	2
Am	6.8E-3	2.6E-3	4.1E-1	3
Ba	4.9E-2	1.1E-1	Not in SR-Site	4
Ca	6.9E-1	1.1E0	1.2E0	5
Cd	1.4E0	1.4E0	4.1E-1	6
Cl	6.6E-1	6.9E-1	7.8E-1	5
Cm	1.1E-2	4.1E-3	4.1E-1	7
Co	2.7E-1	3.7E-1	Not in SR-Site	4
Cs	4.6E-1	7.7E-1	1.9E0	5
Eu	9.3E-3	3.5E-3	6.1E-1	3
Ho	3.6E-1	3.6E-1	1.6E0	8
I	2.2E0	1.5E0	1.1E0	5
Mo	4.0E0	3.7E0	1.3E0	5
Nb	4.2E-1	3.7E-1	4.1E-1	5
Ni	2.8E-1	2.8E-1	2.6E0	9
Np	2.1E-2	7.8E-3	6.8E-1	6
Pa	1.2E-1	4.5E-2	9.4E-1	1
Pb	7.8E-1	7.8E-1	1.0E0	2
Pd	5.9E-2	5.9E-2	1.6E0	10
Po	1.6E-1	1.6E-1	2.0E0	11
Pu	6.4E+2	6.4E+2	1.4E0	11
Ra	5.5E-1	2.2E-1	5.5E-1	12
Se	1.9E-1	2.6E-1	1.0E0	8
Sm	7.9E-2	7.9E-2	1.6E0	8
Sn	1.7E-2	7.0E-3	9.4E-1	13
Sr	8.5E-1	1.1E0	7.0E-1	14
Tc	7.9E-1	7.9E-1	6.8E-1	6
Th	7.9E-1	7.9E-1	1.0E0	6
U	1.3E-1	5.2E-1	7.9E-1	5
Zr	4.1E0	1.6E0	8.3E-1	5

Notes:
1. SR-Site distribution from Karlsson and Bergström (2002). In SR-PSU, site data for the element analogue, La, was used.
2. IAEA (2010) data used for both assessments.
3. SR-Site distribution from IAEA (2010). In SR-PSU, site data for the element analogue, La, was used.

4. In SR-PSU, site data was used. This is compared against data from IAEA (2013), specifically all fish.
5. SR-Site distribution using a prior from a subpopulation. In SR-PSU, site data was used.
6. SR-Site distribution from Beresford et al. (2007). In SR-PSU, ERICA data was used (Hosseini et al., 2008).
7. SR-Site distribution from Beresford et al. (2007). In SR-PSU, site data for the element analogue, La, was used.
8. SR-Site distribution from Karlsson and Bergström (2002). In SR-PSU, site data was used.
9. SR-Site distribution from IAEA (2010). In SR-PSU, site data was used.
10. SR-Site distribution from Karlsson and Bergström (2002). In SR-PSU, site data for the element analogue, Ni, was used.
11. SR-Site distribution from Beresford et al. (2007). In SR-PSU, IAEA (2010) was used.
12. SR-Site distribution using a prior from a subpopulation. In SR-PSU, site data for the element analogue, Ba, was used.
13. SR-Site distribution from Karlsson and Bergström (2002). In SR-PSU, site data for the element analogue, Zr, was used.
14. SR-Site distribution using a prior from a subpopulation. In SR-PSU, site data was used.

CR data used for sea plankton in SR-PSU (Table 8-6 of the Kd and CR Report) is compared with the same parameter from SR-Site (Table 5-7 of Nordén et al., 2010) or IAEA (2004) in Table B25.

Table B25: Comparison of BE, GM and GSD CR for sea plankton (cR_sea_pp_plank); ratios reflect SR-PSU:SR-Site.

Element	Ratio of BE values	Ratio of GM values	Ratio of GSD values	Notes
Ac	8.9E-2	9.4E-1	2.3E0	1
Ag	4.5E-1	4.5E-1	1.3E0	2
Am	1.6E-3	3.5E-3	3.2E0	3
Ba	2.2E0	1.3E0	Not in SR-Site	4
Ca	2.3E0	2.6E0	4.5E0	5
Cd	1.0E+1	8.8E0	1.9E0	6
Cl	3.8E-1	3.0E-1	5.0E0	5
Cm	1.2E-3	2.5E-3	3.7E0	3
Co	1.5E+1	5.4E0	Not in SR-Site	4
Cs	2.1E+1	1.5E-1	3.8E0	6
Eu	2.4E-1	6.2E-1	6.0E-1	7
Ho	2.6E-1	1.1E0	6.8E-1	7
I	3.4E0	2.4E0	3.1E0	5
Mo	1.3E0	9.2E-1	4.5E0	5
Nb	2.6E0	2.6E0	1.5E0	7
Ni	1.3E0	8.6E-1	3.8E0	5
Np	1.9E0	4.1E0	4.9E0	3
Pa	7.4E+1	1.6E+2	2.3E0	1
Pb	1.6E-2	1.3E-2	1.5E0	6
Pd	1.4E0	1.4E0	1.9E0	8
Po	4.4E-1	4.4E-1	1.1E0	2
Pu	4.5E-1	4.5E-1	1.2E0	2
Ra	1.0E0	6.4E-1	2.4E0	9
Se	5.4E-1	5.7E-1	9.8E-1	6
Sm	5.1E-2	1.9E-1	2.1E0	7
Sn	1.2E0	1.2E0	1.4E0	7
Sr	2.1E0	2.1E0	1.9E0	7
Tc	4.5E-1	4.5E-1	1.0E0	2
Th	1.3E-1	2.5E-2	4.0E0	6
U	7.5E-1	7.5E-1	2.4E0	7
Zr	8.7E-1	2.1E-1	3.0E0	6

Notes:
1. SR-Site distribution for marine water plants from Karlsson and Bergström (2002). In SR-PSU, site data for the element analogue, Nd, was used.
2. SR-Site distribution from Beresford et al. (2007). In SR-PSU, ERICA data was used (Hosseini et al., 2008).

3. SR-Site distribution from Beresford et al. (2007). In SR-PSU, site data for the element analogue, Nd, was used.
4. In SR-PSU, the value for cR_sea_pp_macro was used. This is compared against data from IAEA (2004), specifically phytoplankton.
5. In SR-Site, site-specific data were used. In SR-PSU, the value for cR_sea_pp_macro was used.
6. In SR-Site, site-specific data were used, with a prior from the subpopulation. In SR-PSU, the value for cR_sea_pp_macro was used.
7. In SR-Site, site-specific data for macrophytes were used. In SR-PSU, the value for cR_sea_pp_macro was used.
8. SR-Site distribution for marine water plants from Karlsson and Bergström (2002). In SR-PSU, site data for the element analogue, Ni, was used.
9. SR-Site distribution from Beresford et al. (2007). In SR-PSU, site data for the element analogue, Ba, was used.

87

CR data used for sea microalgae in SR-PSU (Table 8-3 of the Kd and CR Report) is compared with the same parameter from SR-Site (Table 5-8 of Nordén et al., 2010) or IAEA (2004) in Table B26.

Table B26: Comparison of BE, GM and GSD CR for sea microalgae (cR_sea_pp_micro); ratios reflect SR-PSU:SR-Site.

Element	Ratio of BE values	Ratio of GM values	Ratio of GSD values	Notes
Ac	8.9E-2	9.4E-1	2.3E0	1
Ag	2.3E-2	2.3E-2	1.3E0	2
Am	1.6E-3	3.5E-3	3.2E0	3
Ba	2.5E+1	1.5E+1	Not in SR-Site	4
Ca	2.2E-1	2.5E-1	2.7E0	5
Cd	2.0E-1	1.7E-1	2.4E0	5
Cl	5.0E-1	3.9E-1	Not in SR-Site	5
Cm	1.2E-3	2.5E-3	3.7E0	3
Co	4.9E0	1.8E0	Not in SR-Site	4
Cs	8.4E-2	2.5E-2	4.4E0	5
Eu	9.1E-2	2.8E-1	3.5E0	5
Ho	9.4E-2	3.8E-1	5.6E0	5
I	1.5E-1	1.1E-1	1.9E0	5
Mo	6.0E-2	4.4E-2	1.9E0	5
Nb	2.6E0	2.6E0	1.5E0	6
Ni	5.2E-2	3.5E-2	2.1E0	5
Np	1.9E0	4.1E0	4.9E0	3
Pa	7.4E+1	1.6E+2	2.3E0	1
Pb	5.2E-2	4.2E-2	1.2E0	5
Pd	1.4E0	1.4E0	1.1E0	1
Po	2.4E-2	2.4E-2	1.1E0	7
Pu	1.5E-2	1.5E-2	1.2E0	2
Ra	1.0E0	6.4E-1	1.8E0	8
Se	2.9E-1	3.1E-1	2.1E0	5
Sm	6.4E-2	2.5E-1	8.0E0	5
Sn	1.2E0	1.2E0	1.4E0	6
Sr	2.1E0	2.1E0	1.9E0	6
Tc	8.4E+3	8.4E+3	1.0E0	2
Th	4.3E-2	8.1E-3	7.5E0	5
U	7.5E-1	7.5E-1	2.4E0	6
Zr	5.7E-2	1.4E-2	5.9E0	5

Notes:
1. SR-Site distribution for marine water plants from Karlsson and Bergström (2002). In SR-PSU, site data for the element analogue, Nd, was used.
2. SR-Site distribution for phytoplankton from Beresford et al. (2007). In SR-PSU, ICRP (2011) data was used.

3. SR-Site distribution for phytoplankton from Beresford et al. (2007). In SR-PSU, site data for the element analogue, Nd, was used.
4. In SR-PSU, site data was used. This is compared against data from IAEA (2004), specifically macroalgae.
5. In both assessments, site-specific data used.
6. In both assessments, site-specific data used. In SR-Site, the site data related to macrophytes.
7. SR-Site distribution for phytoplankton from Beresford et al. (2007). In SR-PSU, ERICA data was used (Hosseini et al., 2008).
8. SR-Site distribution from Beresford et al. (2007). In SR-PSU, site data for the element analogue, Ba, was used.

89

CR data used for sea macroalgae in SR-PSU (Table 8-3 of the Kd and CR Report) is compared with the same parameter from SR-Site (Table 5-9 of Nordén et al., 2010) or IAEA (2004) in Table B27.

Table B27: Comparison of BE, GM and GSD CR for sea macroagae (cR_sea_pp_macro); ratios reflect SR-PSU:SR-Site.

Element	Ratio of BE values	Ratio of GM values	Ratio of GSD values	Notes
Ac	8.9E-2	9.4E-1	2.3E0	1
Ag	1.7E0	1.7E0	1.4E0	2
Am	8.9E-1	1.9E0	2.7E0	3
Ba	2.5E+1	1.5E+1	Not in SR-Site	4
Ca	7.0E-1	8.0E-1	9.1E-1	5
Cd	1.6E0	1.1E+1	9.7E-1	6
Cl	1.7E0	1.3E0	1.7E0	7
Cm	5.4E-2	1.2E-1	3.2E0	3
Co	4.9E0	1.8E0	Not in SR-Site	4
Cs	7.6E0	2.2E0	1.1E0	7
Eu	2.4E-1	6.2E-1	6.0E-1	6
Ho	2.6E-1	1.1E0	6.8E-1	5
I	1.8E0	1.3E0	1.4E0	7
Mo	2.3E0	1.7E0	1.3E0	7
Nb	2.6E0	2.6E0	1.5E0	6
Ni	2.6E0	1.8E0	1.5E0	7
Np	9.7E0	2.1E+1	4.1E0	3
Pa	7.4E+1	1.6E+2	2.3E0	1
Pb	4.1E0	6.4E0	2.1E0	6
Pd	1.4E0	1.4E0	1.1E0	8
Po	8.5E-1	8.5E-1	1.5E0	9
Pu	1.1E0	1.1E0	8.6E-1	2
Ra	1.9E+1	1.2E+1	2.2E0	10
Se	1.3E0	1.3E0	1.4E0	7
Sm	5.1E-2	1.9E-1	2.1E0	5
Sn	1.2E0	1.2E0	1.4E0	7
Sr	2.1E0	2.1E0	1.9E0	6
Tc	1.3E0	1.3E0	1.6E0	2
Th	1.3E+1	5.2E0	1.6E0	6
U	7.5E-1	7.5E-1	2.4E0	7
Zr	9.5E0	9.1E0	1.9E0	6

Notes:
1. SR-Site distribution from Karlsson and Bergström (2002). In SR-PSU, site data for the element analogue, Nd, was used.
2. SR-Site distribution from Beresford et al. (2007). In SR-PSU, ICRP (2011) data was used.

3. SR-Site distribution from Beresford et al. (2007). In SR-PSU, site data for the element analogue, Nd, was used.
4. In SR-PSU, site data was used. This is compared against data from IAEA (2004), specifically macroalgae.
5. In both assessments, site-specific data used.
6. SR-Site distribution based on a prior from the subpopulation. In SR-PSU, site data was used.
7. SR-Site distribution based on a prior from the population. In SR-PSU, site data was used.
8. SR-Site distribution from Karlsson and Bergström (2002). In SR-PSU, site data for the element analogue, Ni, was used.
9. SR-Site distribution from Beresford et al. (2007). In SR-PSU, ERICA data was used (Hosseini et al., 2008).
10. SR-Site distribution from Beresford et al. (2007). In SR-PSU, site data for the element analogue, Ba, was used.

CR data used for sea fish in SR-PSU (Table 8-17 of the Kd and CR Report) is compared with the same parameter from SR-Site (Table 5-10 of Nordén et al., 2010) or IAEA (2004) in Table B28.

Table B28: Comparison of BE, GM and GSD CR for sea fish (cR_sea_fish); ratios reflect SR-PSU:SR-Site.

Element	Ratio of BE values	Ratio of GM values	Ratio of GSD values	Notes
Ac	2.6E-2	5.8E-2	2.4E0	1
Ag	8.2E-1	8.2E-1	1.0E0	2
Am	7.0E-2	7.0E-2	1.9E0	3
Ba	1.8E0	1.0E0	Not in SR-Site	4
Ca	3.5E0	7.8E-1	2.1E0	5
Cd	2.4E0	8.2E-1	4.6E-1	6
Cl	7.1E-1	8.6E-1	1.6E0	7
Cm	2.6E-2	2.6E-2	8.2E-1	3
Co	3.2E-1	1.1E-1	Not in SR-Site	4
Cs	9.5E-1	1.0E0	1.5E0	7
Eu	2.6E-2	2.6E-2	1.6E0	1
Ho	8.7E-2	8.7E-2	1.6E0	1
I	2.0E0	1.7E0	1.4E0	5
Mo	1.8E0	1.2E0	1.5E0	7
Nb	8.8E-1	8.8E-1	2.4E0	7
Ni	1.9E0	7.3E-1	6.1E-1	6
Np	2.6E0	2.6E0	8.2E-1	3
Pa	2.6E-1	2.6E-1	1.6E0	1
Pb	1.3E0	1.4E0	1.0E0	5
Pd	1.9E0	1.9E0	9.4E-1	8
Po	6.3E0	6.3E0	1.5E0	2
Pu	3.6E-1	3.6E-1	1.0E0	9
Ra	2.1E-1	1.2E-1	1.1E0	10
Se	8.1E-1	7.3E-1	1.6E0	6
Sm	7.0E-1	7.0E-1	1.4E0	7
Sn	1.0E0	1.0E0	2.0E0	7
Sr	4.2E-1	4.2E-1	1.5E0	7
Tc	8.7E-1	8.7E-1	1.0E0	2
Th	6.3E0	3.0E0	9.1E-1	7
U	8.4E-1	8.4E-1	2.4E0	7
Zr	3.9E0	2.7E0	7.3E-1	6

Notes:
1. SR-Site distribution for brackish water fish from Karlsson and Bergström (2002). In SR-PSU, site data for the element analogue, La, was used.
2. SR-Site distribution from Beresford et al. (2007). In SR-PSU, ERICA data was used (Hosseini et al., 2008).

3. SR-Site distribution from Beresford et al. (2007). In SR-PSU, site data for the element analogue, La, was used.
4. In SR-PSU, site data was used. This is compared against data from IAEA (2004), specifically surface fish.
5. In both assessments, site-specific data used.
6. SR-Site distribution based on a prior from the subpopulation. In SR-PSU, site data was used.
7. SR-Site distribution based on a prior from the population. In SR-PSU, site data was used.
8. SR-Site distribution for brackish water fish from Karlsson and Bergström (2002). In SR-PSU, site data for the element analogue, Ni, was used.
9. SR-Site distribution from Beresford et al. (2007). In SR-PSU, ICRP (2011) data was used.
10. SR-Site distribution from Beresford et al. (2007). In SR-PSU, site data for the element analogue, Ba, was used.

93

2017:30

The Swedish Radiation Safety Authority has a comprehensive responsibility to ensure that society is safe from the effects of radiation. The Authority works to achieve radiation safety in a number of areas: nuclear power, medical care as well as commercial products and services. The Authority also works to achieve protection from natural radiation and to increase the level of radiation safety internationally.

The Swedish Radiation Safety Authority works proactively and preventively to protect people and the environment from the harmful effects of radiation, now and in the future. The Authority issues regulations and supervises compliance, while also supporting research, providing training and information, and issuing advice. Often, activities involving radiation require licences issued by the Authority. The Swedish Radiation Safety Authority maintains emergency preparedness around the clock with the aim of limiting the aftermath of radiation accidents and the unintentional spreading of radioactive substances. The Authority participates in international co-operation in order to promote radiation safety and finances projects aiming to raise the level of radiation safety in certain Eastern European countries.

The Authority reports to the Ministry of the Environment and has around 300 employees with competencies in the fields of engineering, natural and behavioural sciences, law, economics and communications. We have received quality, environmental and working environment certification.